

## **General Disclaimer**

### **One or more of the Following Statements may affect this Document**

- This document has been reproduced from the best copy furnished by the organizational source. It is being released in the interest of making available as much information as possible.
- This document may contain data, which exceeds the sheet parameters. It was furnished in this condition by the organizational source and is the best copy available.
- This document may contain tone-on-tone or color graphs, charts and/or pictures, which have been reproduced in black and white.
- This document is paginated as submitted by the original source.
- Portions of this document are not fully legible due to the historical nature of some of the material. However, it is the best reproduction available from the original submission.

CR 151008

MCDONNELL DOUGLAS TECHNICAL SERVICES CO.  
HOUSTON ASTRONAUTICS DIVISION

SPACE SHUTTLE ENGINEERING AND OPERATIONS SUPPORT

DESIGN NOTE NO. 1.4-4-8

ORBITER ENTRY TRAJECTORY CORRIDORS -  
32,000 POUND PAYLOAD, 67.5% CENTER OF GRAVITY

MISSION PLANNING, MISSION ANALYSIS AND SOFTWARE FORMULATION

9 JULY 1975

This Design Note is Submitted to NASA Under Task Order  
No. D0303, Task Assignment 1.4-4-A in Fulfillment of  
Contract NAS 9-13970.

PREPARED BY: J. H. Treybig  
J. H. Treybig  
Engineer  
488-5660, Ext. 243

APPROVED BY: J. M. Hiott  
J. M. Hiott  
Task Manager  
488-5660, Ext. 243

APPROVED BY: W. W. Hinton, Jr.  
W. W. Hinton, Jr.  
FPB Work Package Manager  
488-5660, Ext. 240

APPROVED BY: W. E. Hayes  
W. E. Hayes  
Project Manager  
Mission Planning,  
Mission Analysis, and  
Software Formulation  
488-5660, Ext. 266

OCT 1976  
RECEIVED  
NASA STI FACILITY  
INPUT BRANCH

(NASA-CR-151008) ORBITER ENTRY TRAJECTORY  
CORRIDORS: 32000 POUND PAYLOAD, 67.5  
PERCENT CENTER OF GRAVITY (McDonnell-Douglas  
Technical Services) 150 p HC \$6.00 CSCI 22A

N76-33234

Unclas  
G3/13 05730



## 1.0 SUMMARY

This design note presents plots of Orbiter thermal and equilibrium glide boundaries in the drag/mass-relative velocity ( $D/M-V$ ), dynamic pressure-relative velocity ( $\bar{q}-V$ ), and altitude-relative velocity ( $h-V$ ) planes for an Orbiter having a 32,000 pound payload and a 67.5% center of gravity (cg) location. These boundaries were defined for control points 1 through 4 of the Shuttle Orbiter for  $40^\circ$ - $30^\circ$  and  $38^\circ$ - $28^\circ$  ramped angle of attack entry profiles and  $40^\circ$ ,  $38^\circ$ ,  $35^\circ$ ,  $30^\circ$ ,  $28^\circ$ , and  $25^\circ$  constant angle of attack entry profiles each at  $20^\circ$ ,  $15^\circ$ , and  $10^\circ$  constant body flap settings.

## 2.0 INTRODUCTION

Thermal and equilibrium glide boundaries are used to analyze and/or design Shuttle Orbiter entry trajectories. The boundaries presented in this note were used by the Flight Performance Branch (FPB) of the NASA for trajectory profile shaping of entry trajectories corresponding to a vehicle weight of 193,000 pounds (32,000 pound payload) and a 67.5% cg location. These conditions are consistent with a 28.5° inclination Eastern Test Range (ETR) mission and were used by the FPB to evaluate an ETR mission in support of Thermal Protection System (TPS) design.

### 3.0 DISCUSSION

Plots of thermal and equilibrium glide boundaries in the D/M-V (Figures 2-49),  $\bar{q}$ -V (Figures 50-97), and h-V (Figures 98-145) planes are presented for the 40°-30° and 38°-28° ramped angle of attack profiles and the 40°, 38°, 35°, 30°, 28°, and 25° constant angle of attack profiles each at 20°, 15°, and 10° constant body flap settings. The 40°-30° and 38°-28° ramped angle of attack profiles are presented in Figure 1.

The data presented in the note were generated using the Thermal Boundary Analysis Program (TBAP) (Reference 1) which uses simplified heating models in defining thermal boundaries. Revisions to TBAP for this study include a more sophisticated method in determining the normal shock viscosity coefficient (Reference 2), updates to the transition criteria on control point 2 by representing the normal shock Reynold's number as a function of angle of attack and body flap deflection angle (Reference 3), and updated transition criteria for control point 4 (Reference 4).

The equilibrium glide boundaries were generated using a digital program to solve the equilibrium glide equation:

$$D/M = \frac{g}{\frac{L}{D} \cos \phi} \left( 1 - \frac{V_I^2}{V_{sat}^2} \right) \quad (3-1)$$

- D = drag force (lbs)  
M = mass (slugs)  
 $V_I$  = inertial velocity (ft/sec)  
g = gravitational acceleration (ft/sec<sup>2</sup>)  
L/D = lift-to-drag ratio (-)  
 $\phi$  = roll angle  
 $V_{sat}$  = satellite velocity (ft/sec)

It should be noted, in equation (3-1), that data for the equilibrium glide boundaries in the D/M-V planes were calculated as a function of inertial velocity ( $V_I$ ) but were plotted versus relative velocity (V) as though  $V = V_I$ . Therefore, for the data to be meaningful, a transformation from inertial to relative velocity must be applied. In the D/M-V plane this can be done by shifting the data by the difference in the inertial and relative velocities for the trajectory of interest. An approximate transformation is

$$V = V_I - \omega R \cos i \quad (3-2)$$

where

- $\omega$  = earth rotation rate (radians/sec)  
R = earth radius (ft)  
and  $i$  = orbit inclination (radians).

Equation (3-2) is least accurate for polar orbits, exhibiting a maximum error of about 45 ft/sec. On the D/M-V boundary figures

presented in this note a 45 ft/sec. error is negligible. Hence, equation (3-2) can be used to adjust the equilibrium glide boundaries to account for orbit inclination.

The equilibrium glide boundaries in the  $\bar{q}$ -V and h-V planes can be determined from the drag equation:

$$D/M = \frac{\rho V^2 C_D S}{2M} \quad (3-3)$$

where D/M is determined from equation 3-2 and

$C_D$  = aerodynamic drag coefficient (-)

S = reference area (ft<sup>2</sup>)

$\rho$  = free stream density (slug/ft<sup>3</sup>)

that is

$$\bar{q} = \frac{1}{2} \rho V^2 = \left( \frac{D}{M} \right) \frac{M}{C_D S} \quad (3-4)$$

and h = function of  $\rho$

$$\text{where } \rho = \left( \frac{D}{M} \right) \frac{2M}{V^2 C_D S} \quad (3-5)$$

The solution of (3-4) and (3-5) requires an iteration on altitude since  $C_D$  is a function of altitude through the Mach number and since h is not easily represented as a direct function of  $\rho$  for the 1962 standard atmosphere.

The data for the equilibrium glide boundaries in the  $\bar{q}$ -V and h-V planes are accurate only for 90° orbit inclinations (i.e. orbits for which  $V \approx V_I$ ). Unlike the equilibrium glide boundaries in the D/M-V plane, a simple "shifting" of the boundaries in the  $\bar{q}$ -V and h-V planes is not possible. Determination of the boundaries in these planes requires independent generation of the data for each orbit inclination of interest. Note, however, that the analytic drag control entry guidance software operates in the D/M-V plane and the data presented in that plane can be adjusted for orbit inclination thus providing all the information required for profile shaping for any orbit inclination.

#### 4.0 REFERENCES

1. Evans, M. E.: "Thermal Boundaries Analysis Program Document", MDTSCO, SSEOS Design Note No. 1.4-4-5, 30 April 1975.
2. Greenschlag, S. N.: "An Improvement in Normal Shock Viscosity Estimates", Rockwell International Internal Letter SAS-AA&T-75-102, 24 March 1975.
3. Haney, J. W.: "Revision to Control Point 2 of the Entry Flight Mode Optimization Program", Rockwell International Internal Letter SAS-AA&T-75-042, 14 February 1975.
4. Haney, J. W.: "Revision to Control Point 4 of the Entry Flight Mode Optimization Program", Rockwell International Internal Letter ASA-AA&T-74-072, 5 March 1975.

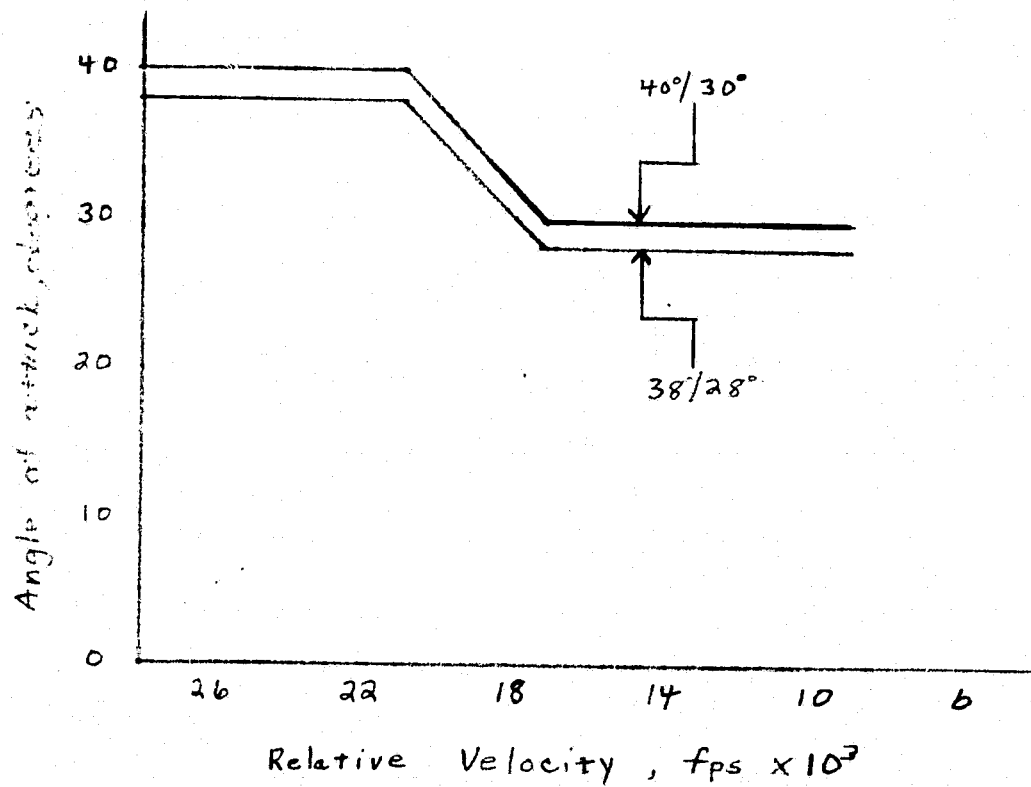


Figure 1

RAMPED ANGLE-OF-ATTACK PROFILES AS A FUNCTION OF RELATIVE VELOCITY



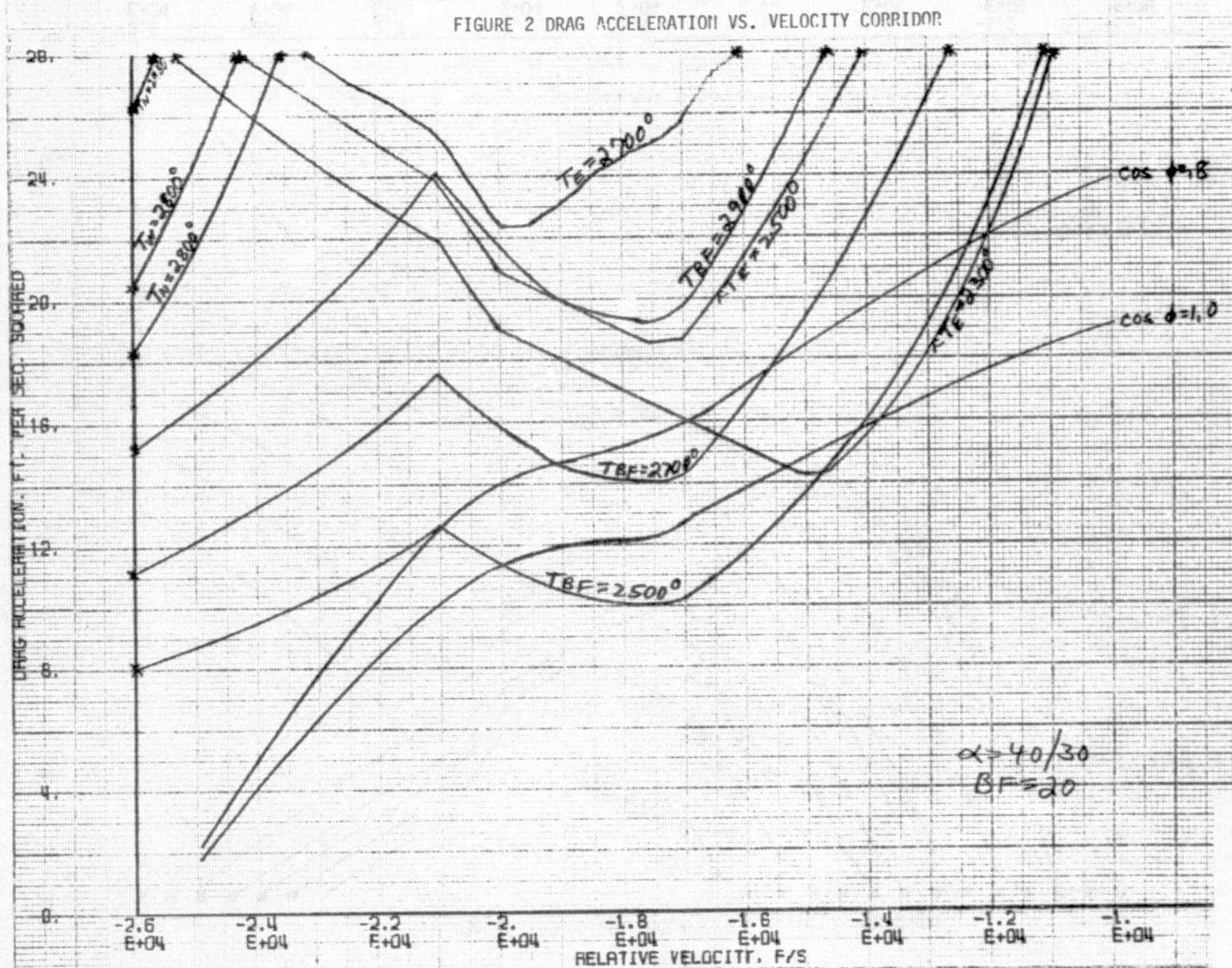


FIGURE 3 DRAG ACCELERATION VS. VELOCITY CORRIDOR

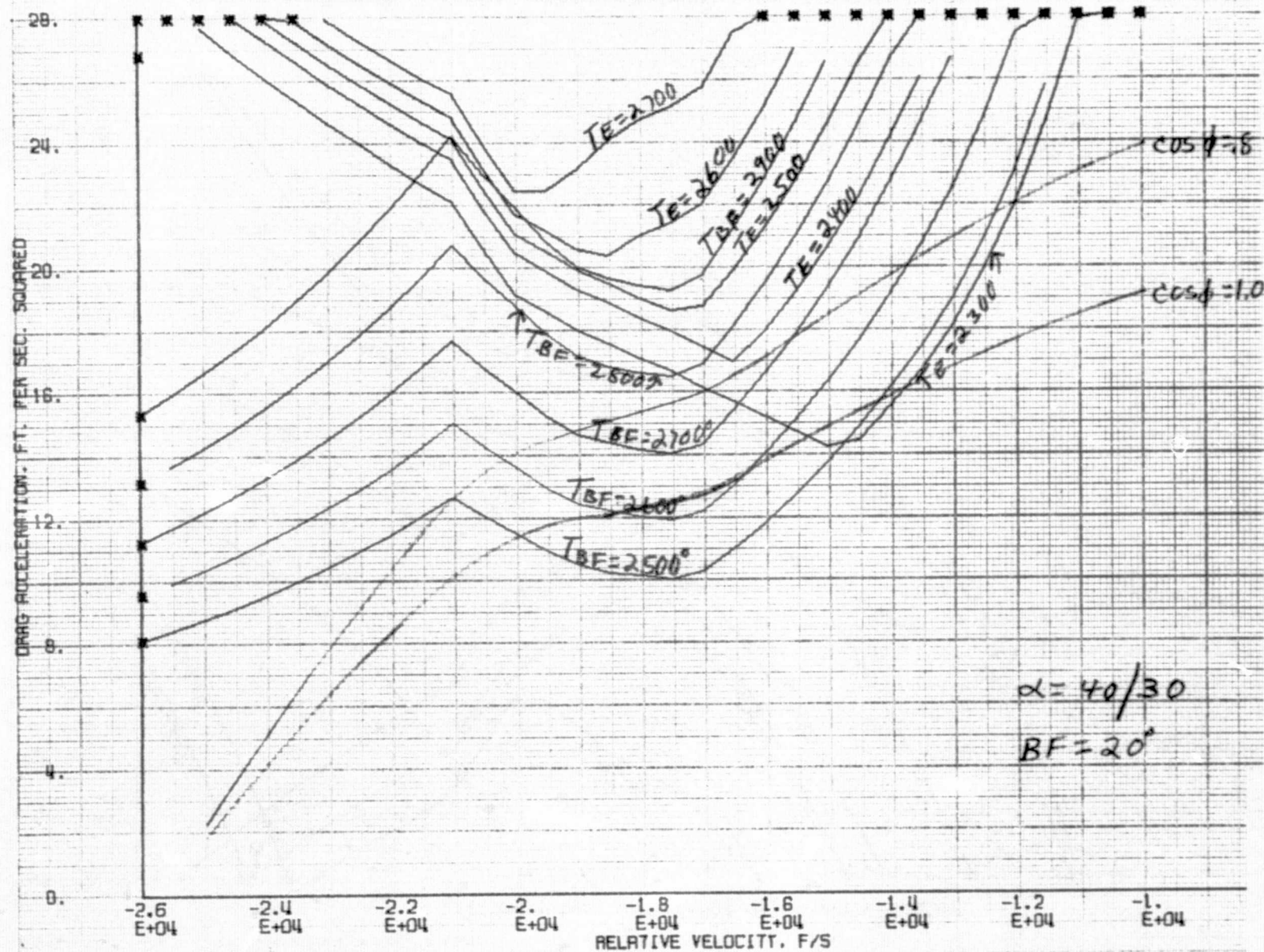




FIGURE 4 DRAG ACCELERATION VS. VELOCITY CORRIDOR

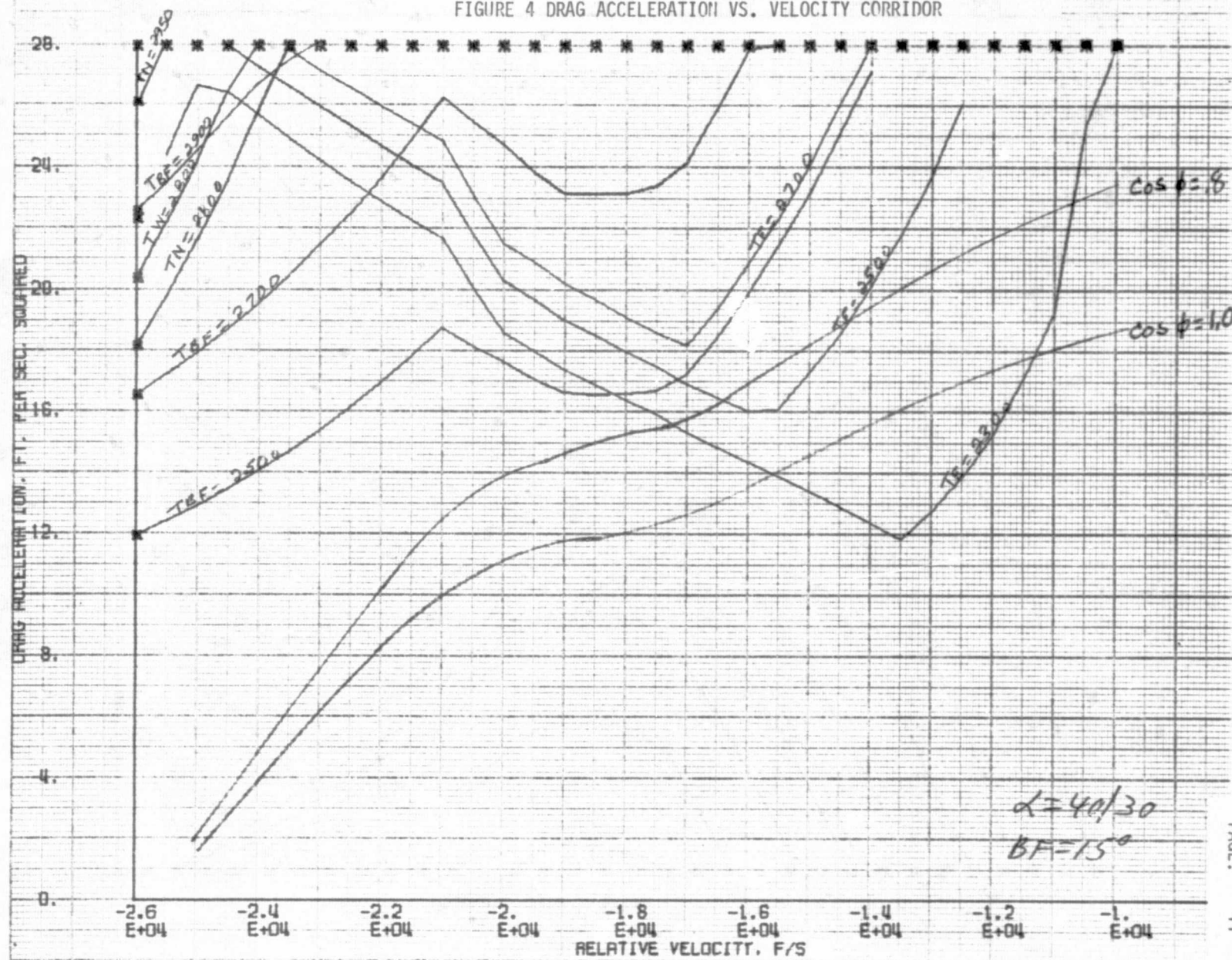
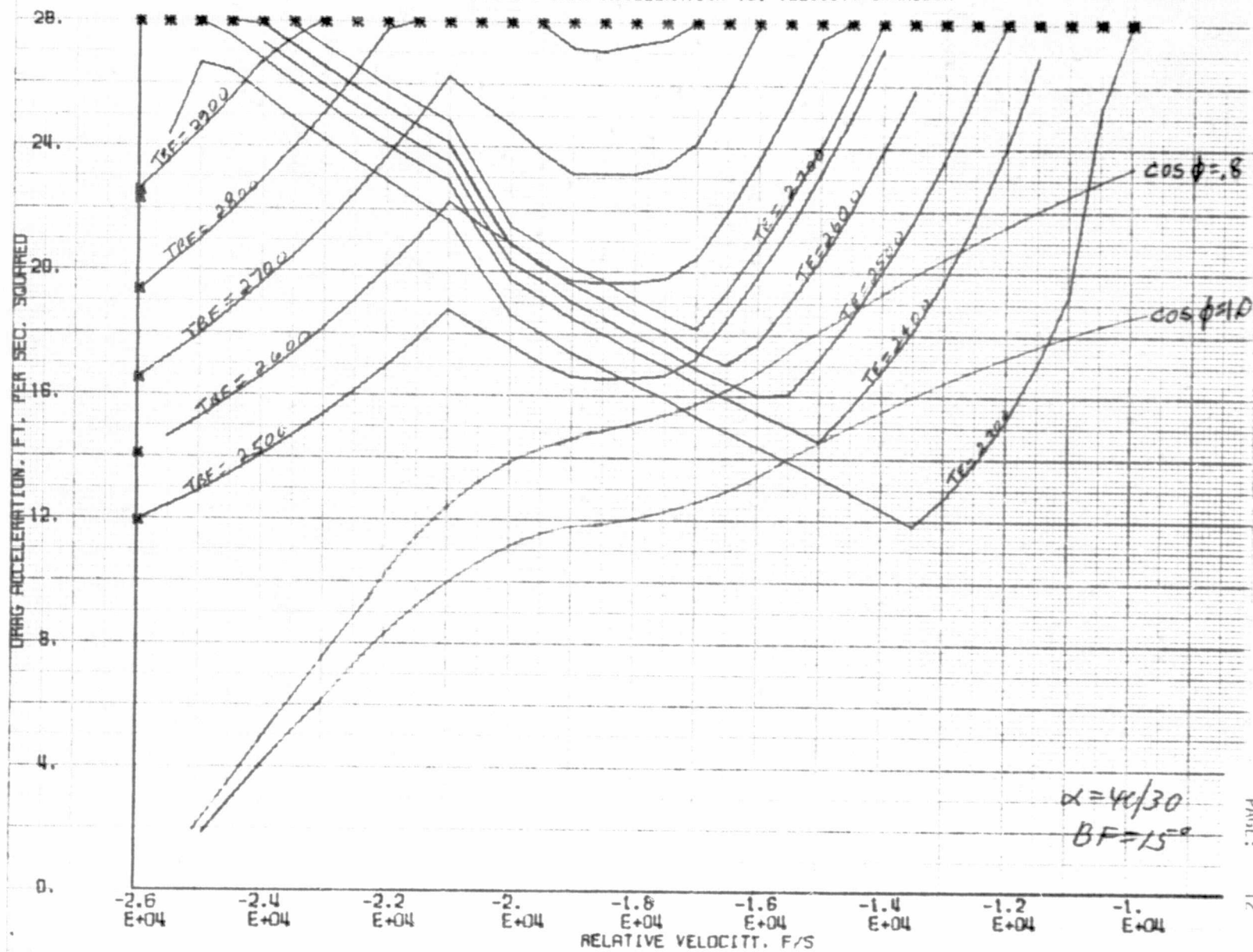


FIGURE 5 DRAG ACCELERATION VS. VELOCITY CORRIDOR



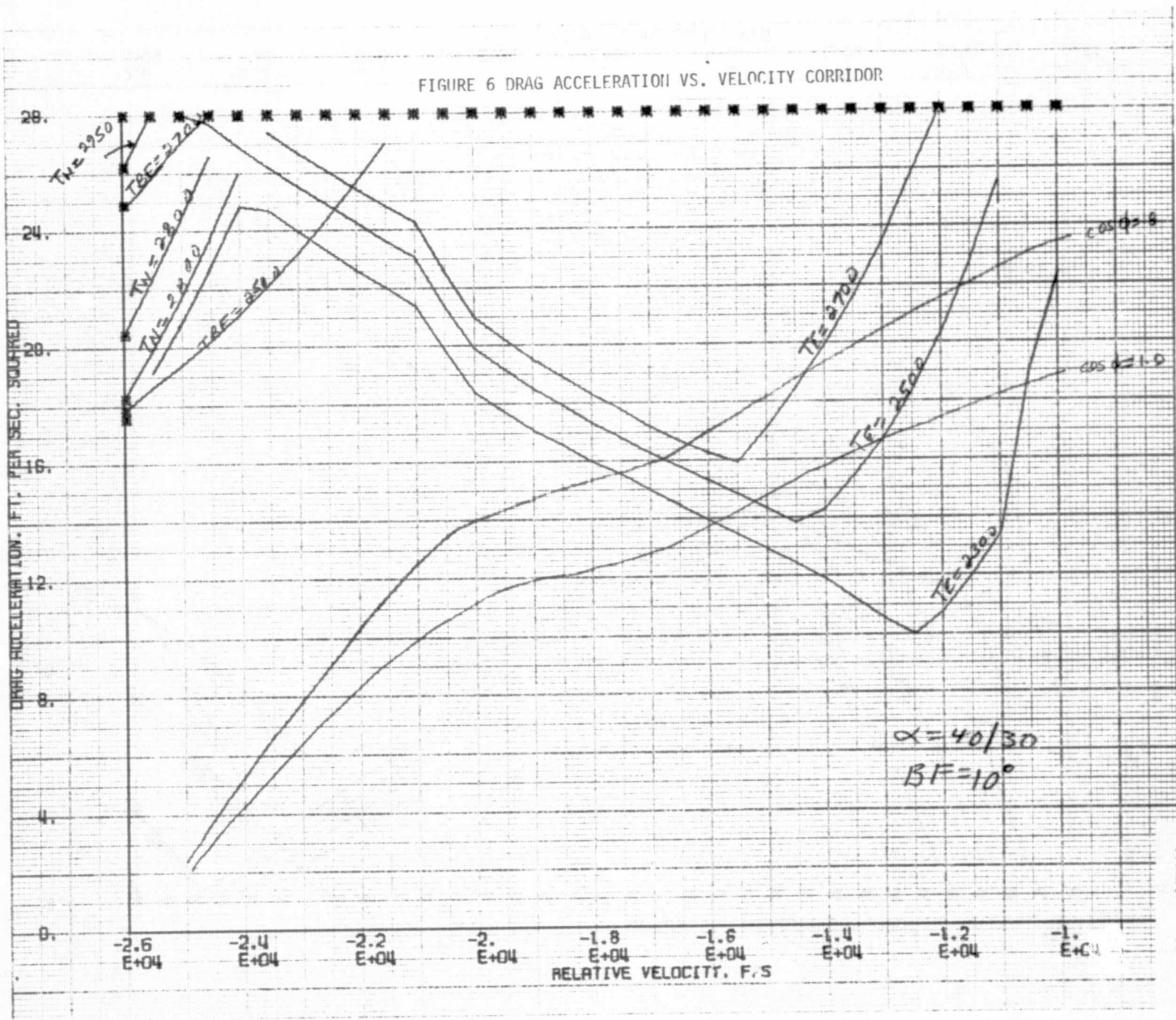




FIGURE 7 DRAG ACCELERATION VS. VELOCITY CORRIDOR

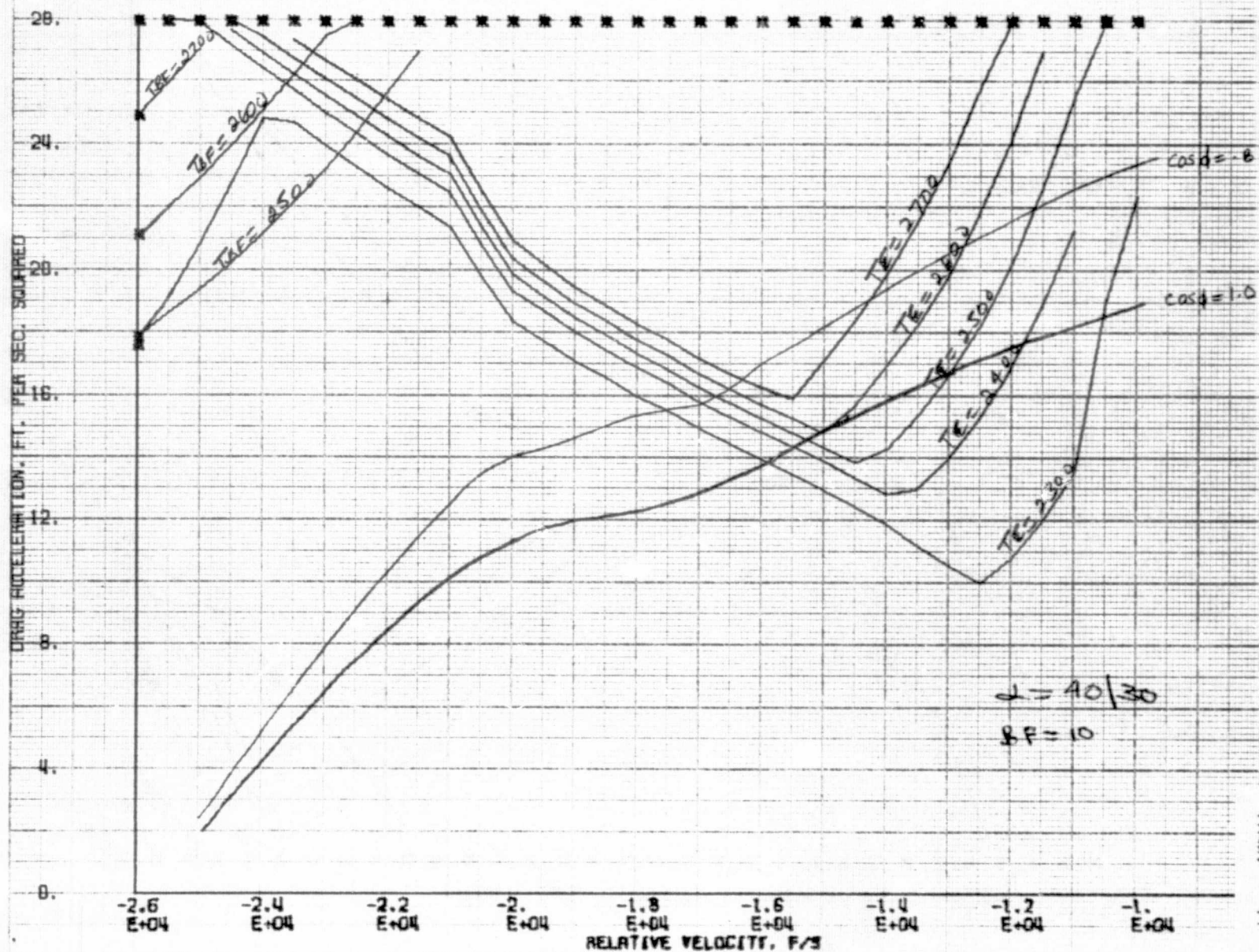


FIGURE 8 DRAG ACCELERATION VS. VELOCITY CORRIDOR

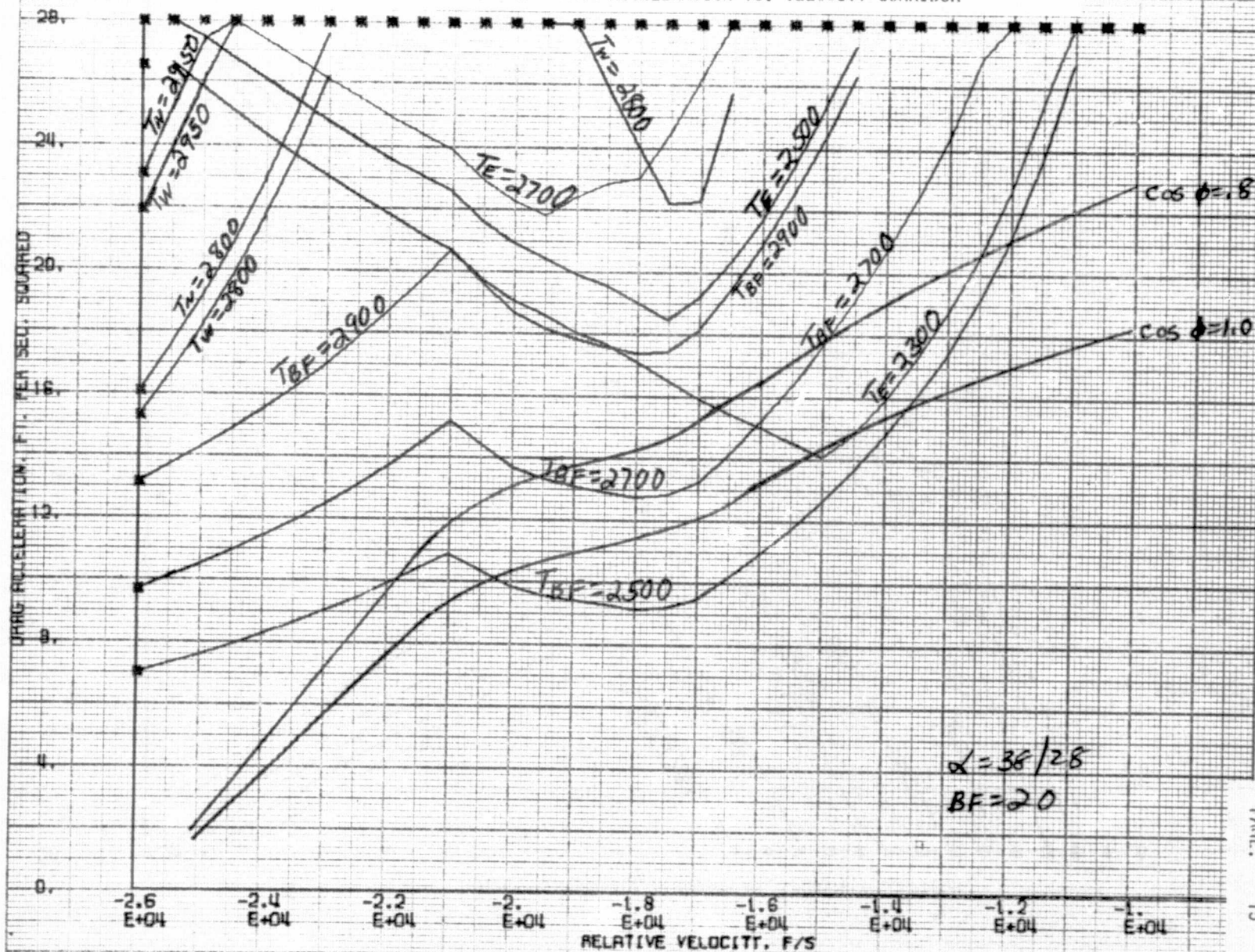




FIGURE 9 DRAG ACCELERATION VS. VELOCITY CORRIDOR

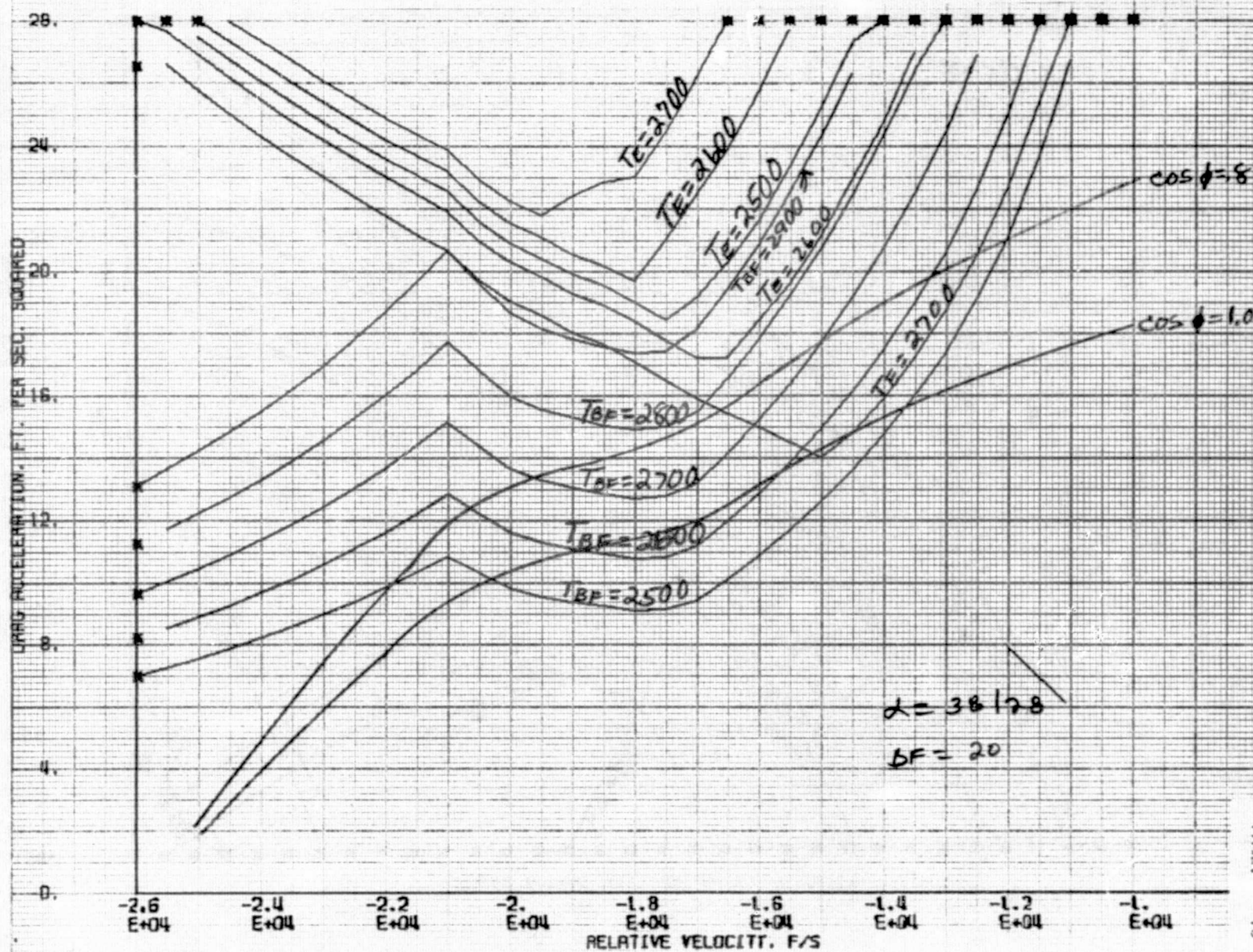




FIGURE 10 DRAG ACCELERATION VS. VELOCITY CORRIDOR

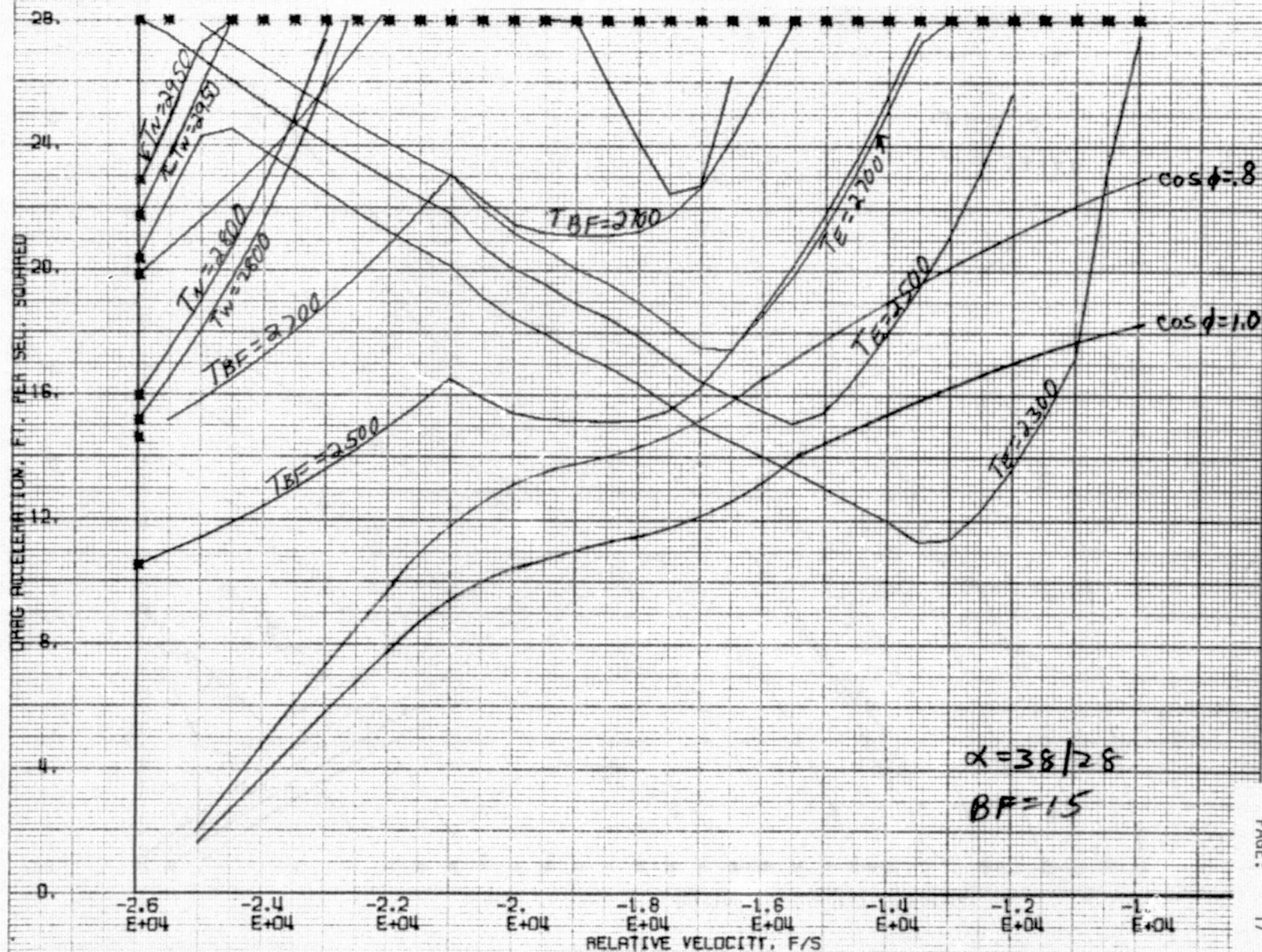
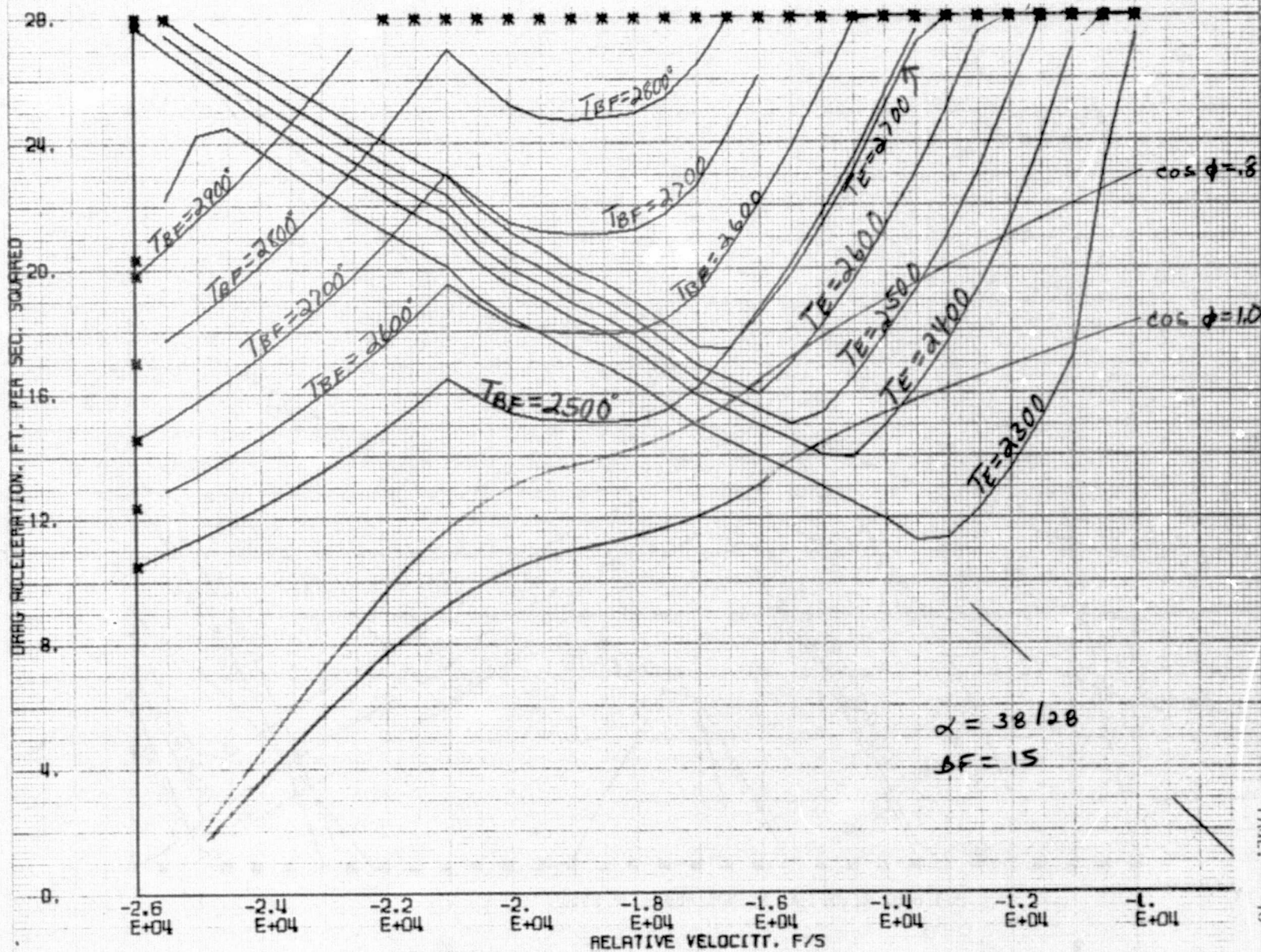


FIGURE 11 DRAG ACCELERATION VS. VELOCITY CORRIDOR





REPRODUCIBILITY OF THE  
ORIGINAL PAGE IS POOR

FIGURE 12 DRAG ACCELERATION VS. VELOCITY CORRIDOR

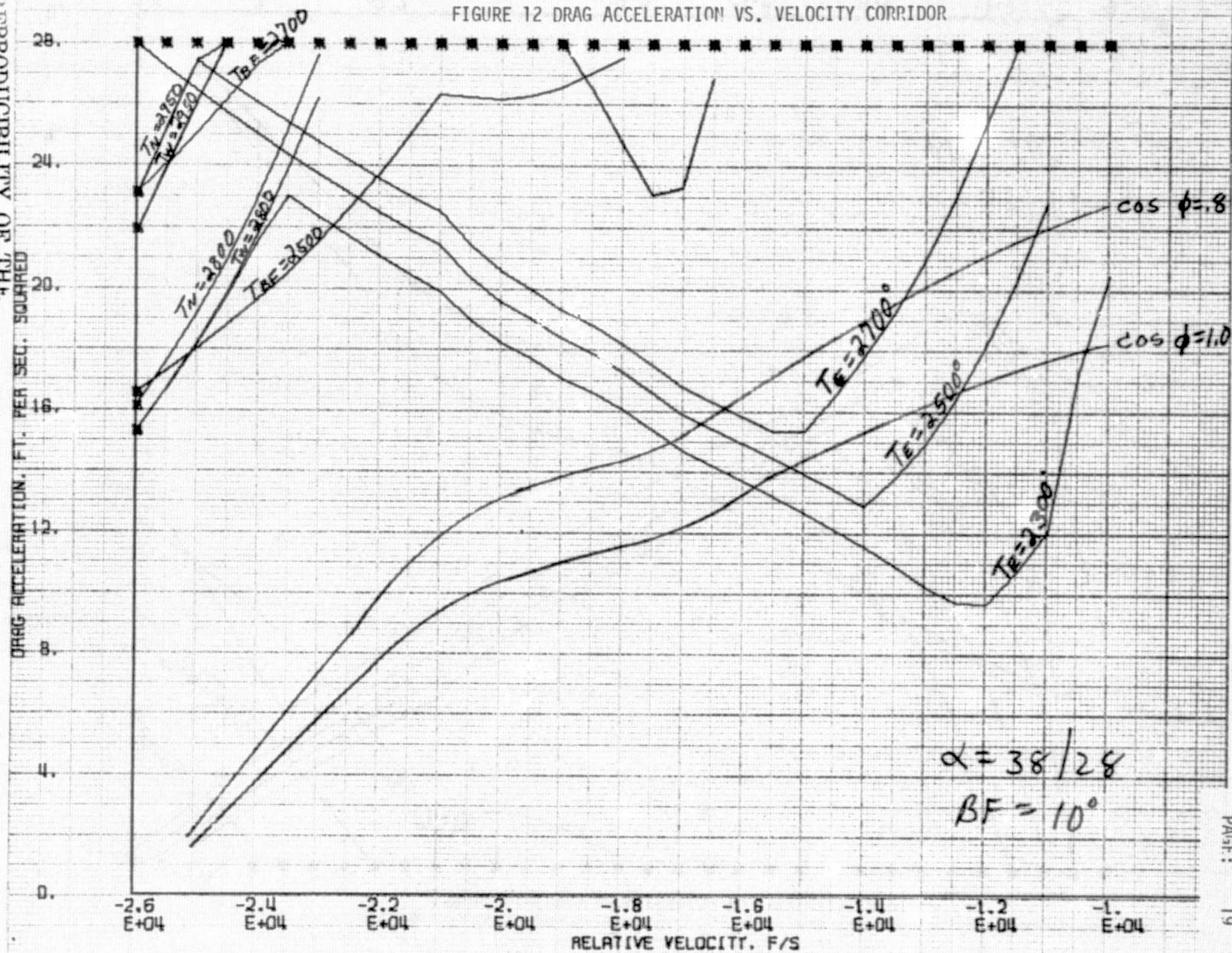


FIGURE 13 DRAG ACCELERATION VS. VELOCITY CORRIDOR

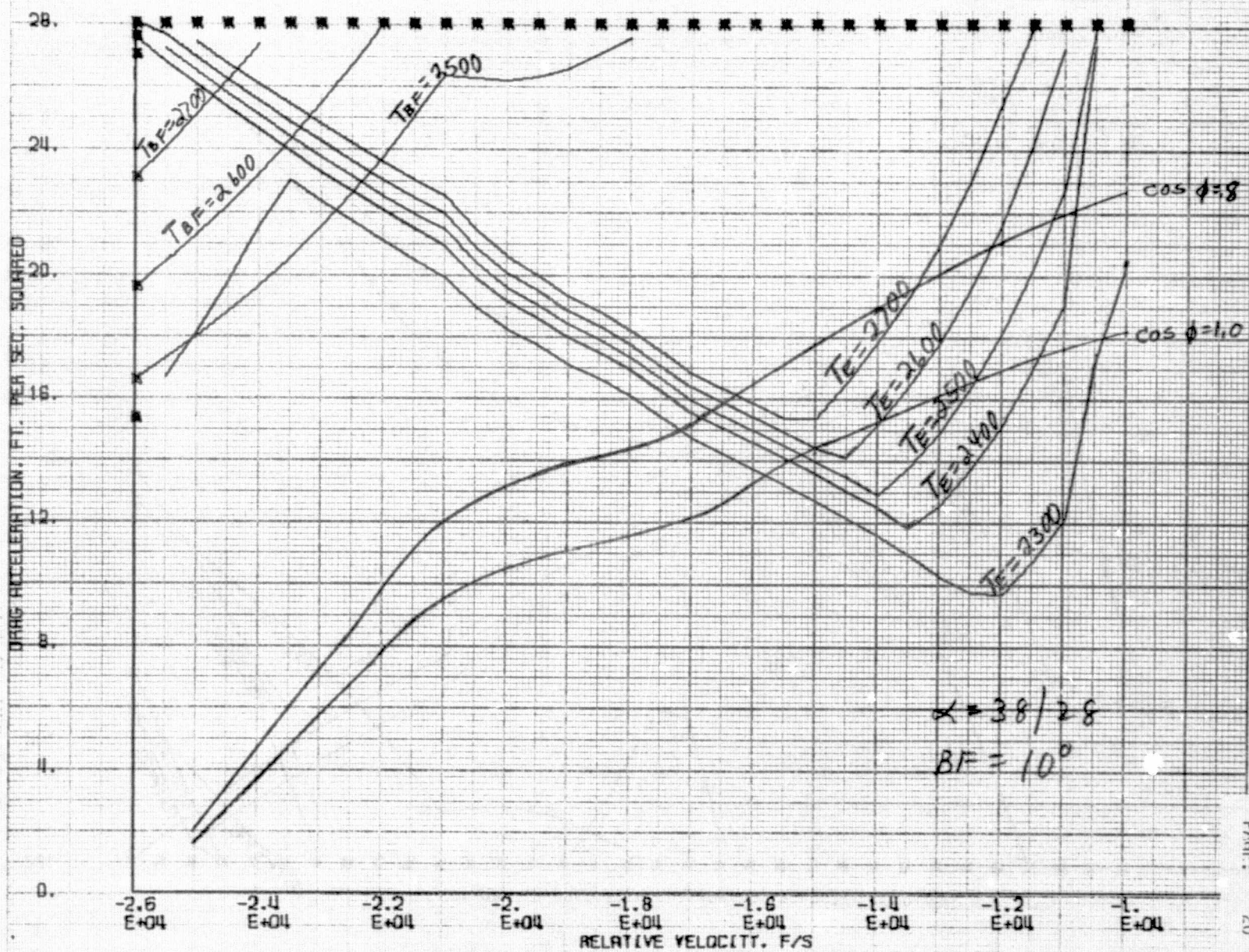




FIGURE 14 DRAG ACCELERATION VS. VELOCITY CORRIDOR

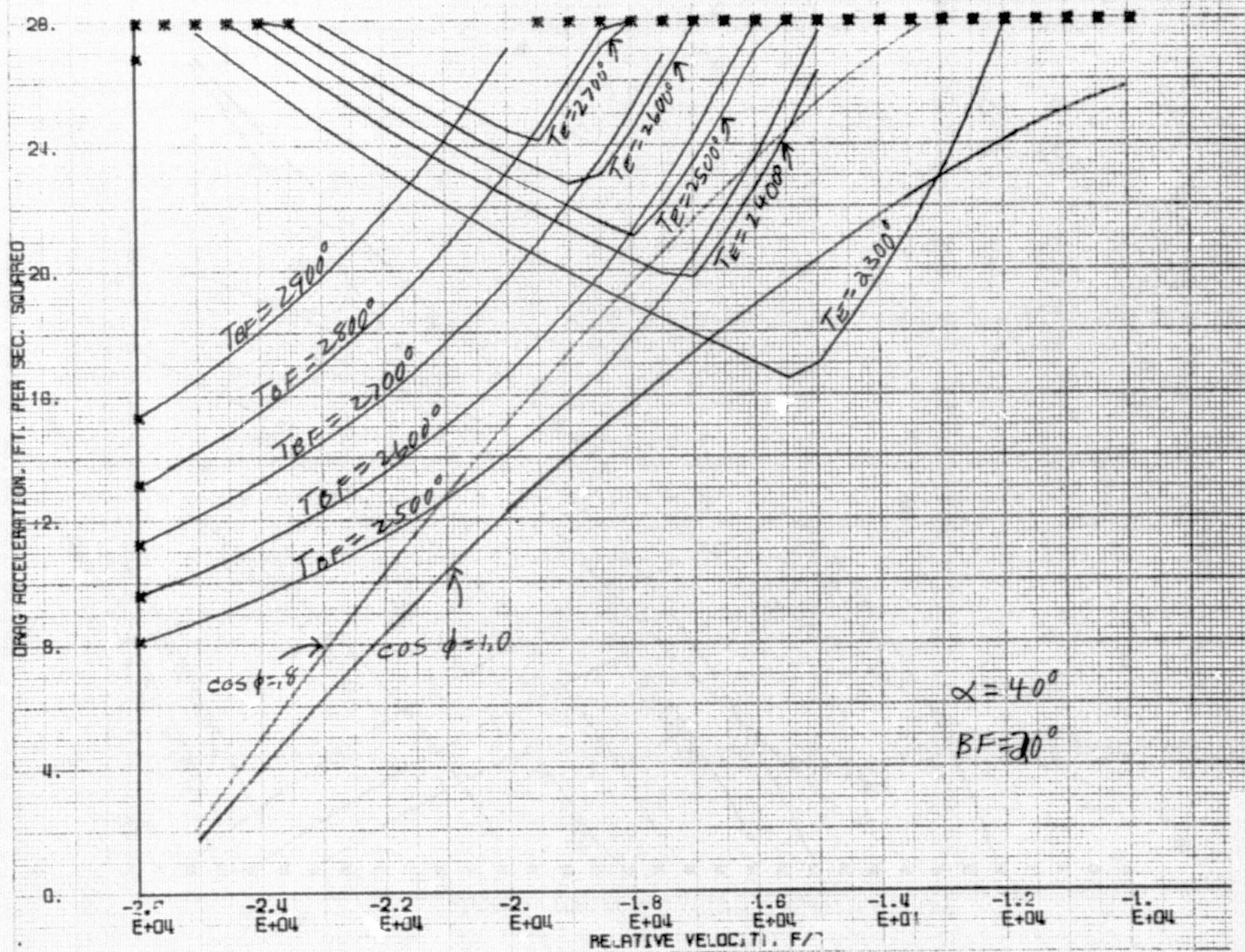


FIGURE 15 DRAG ACCELERATION VS. VELOCITY CORRIDOR

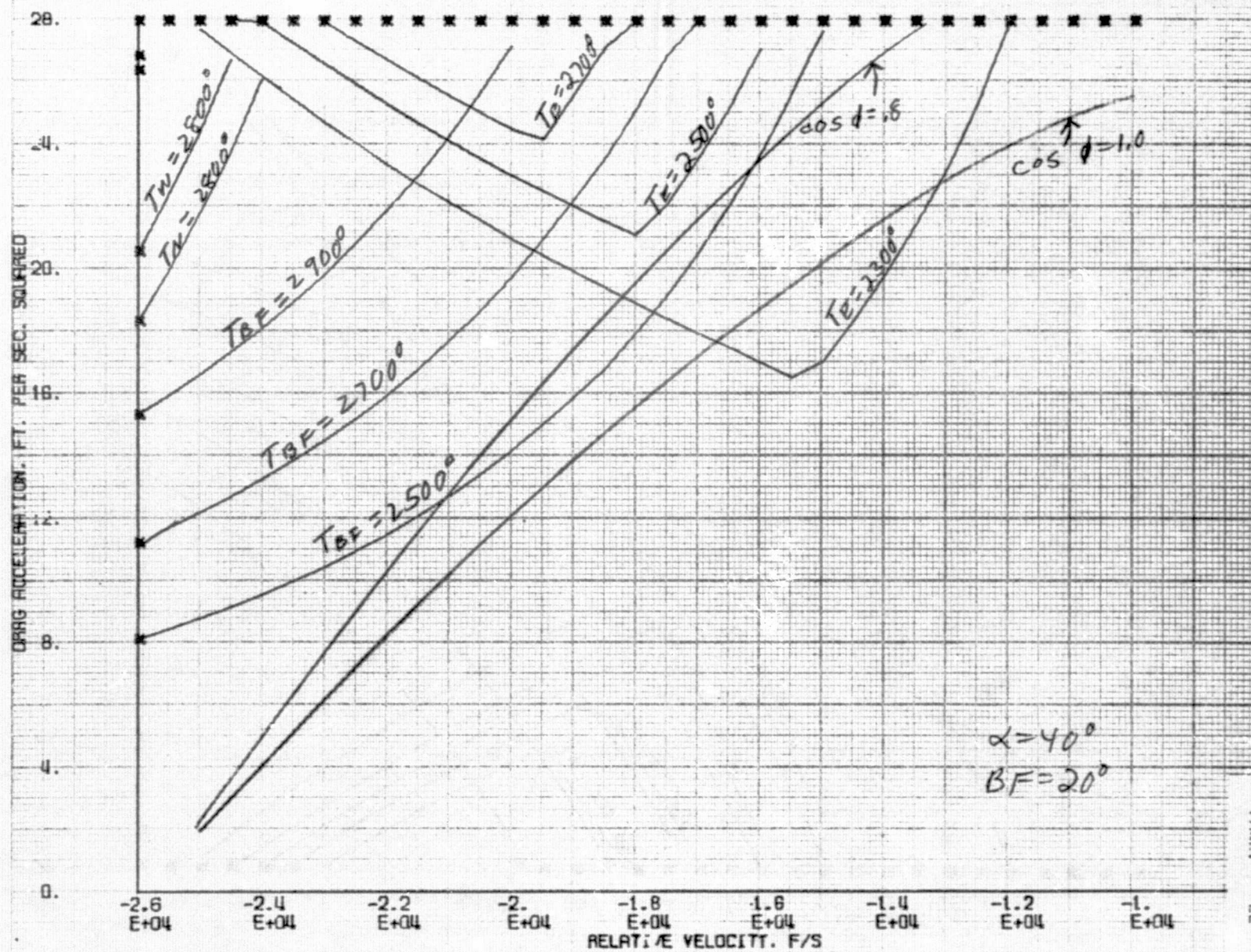




FIGURE 16 DRAG ACCELERATION VS. VELOCITY CORRIDOR

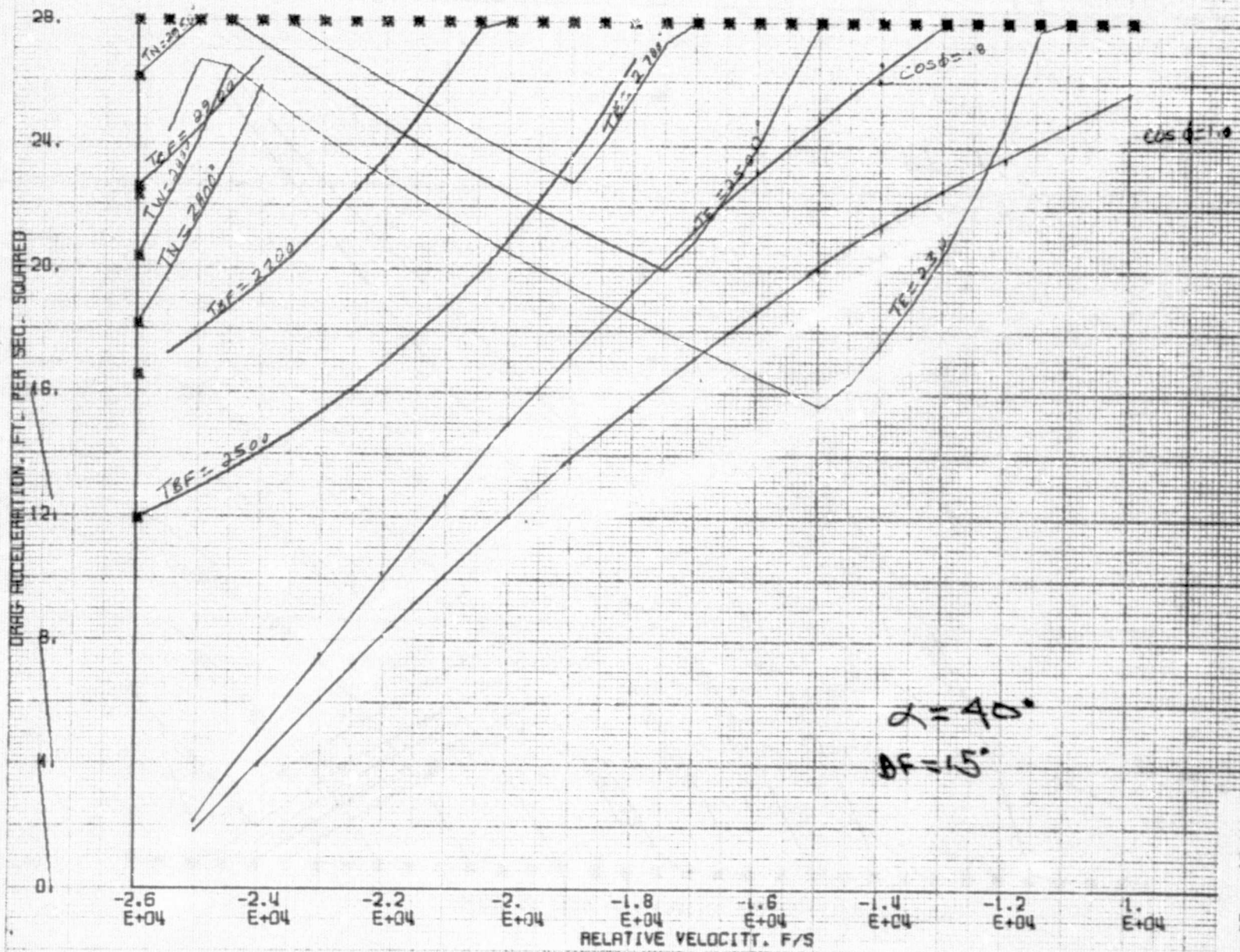
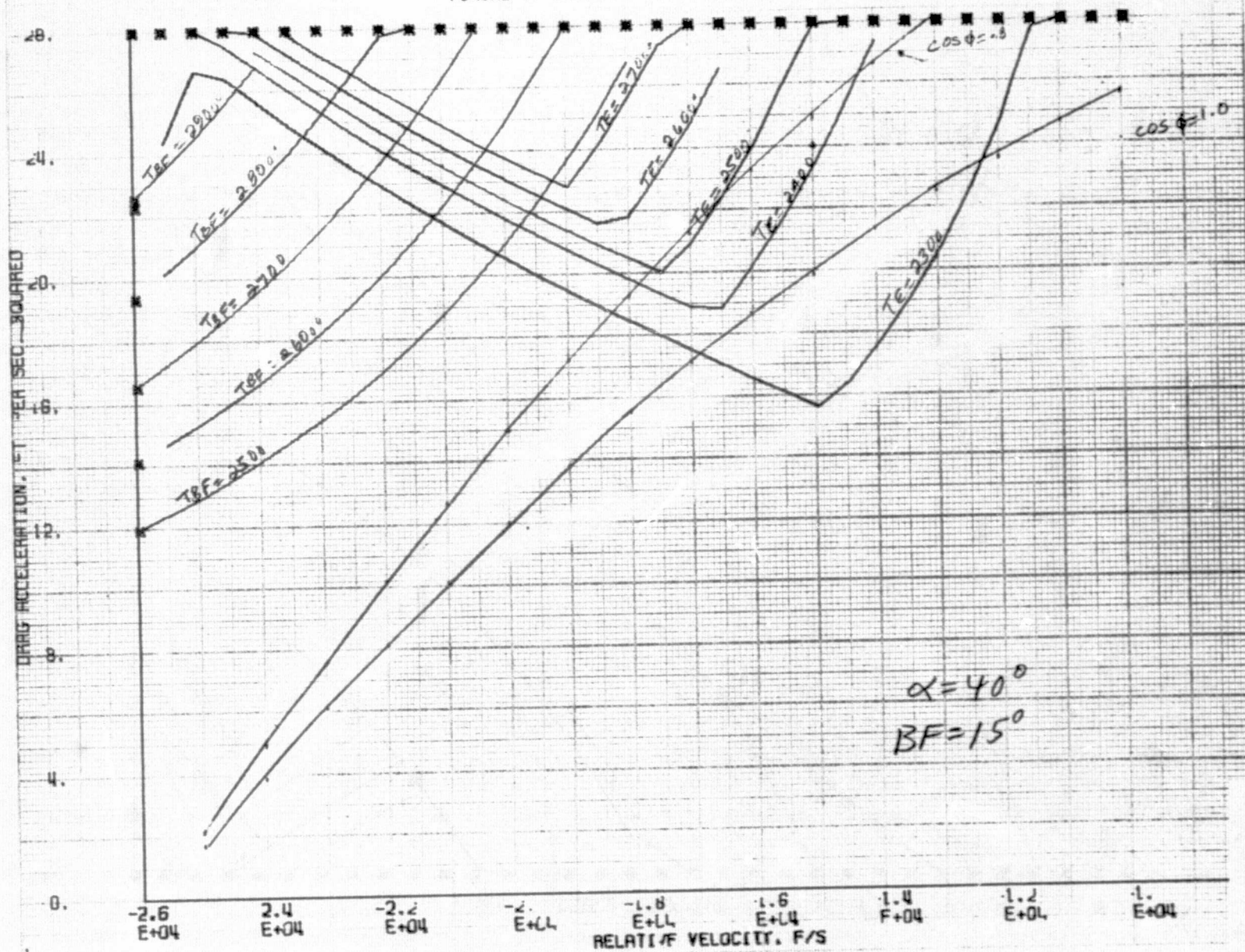


FIGURE 17 DRAG ACCELERATION VS. VELOCITY CORRIDOR





REPRODUCIBILITY OF THIS  
ORIGINAL PAGE IS POOR

FIGURE 18 DRAG ACCELERATION VS. VELOCITY CORRIDOR

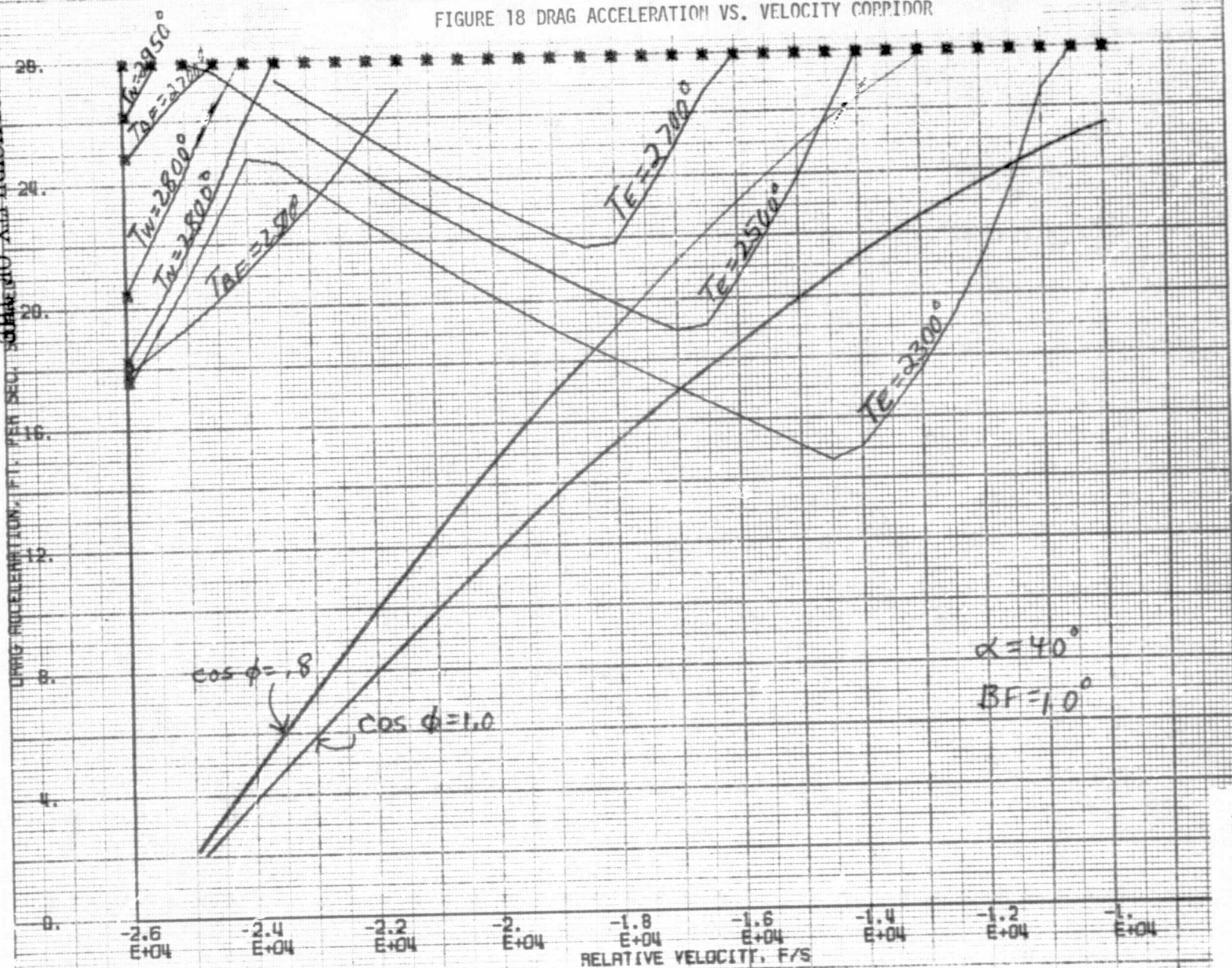


FIGURE 19 DRAG ACCELERATION VS. VELOCITY CORRIDOR

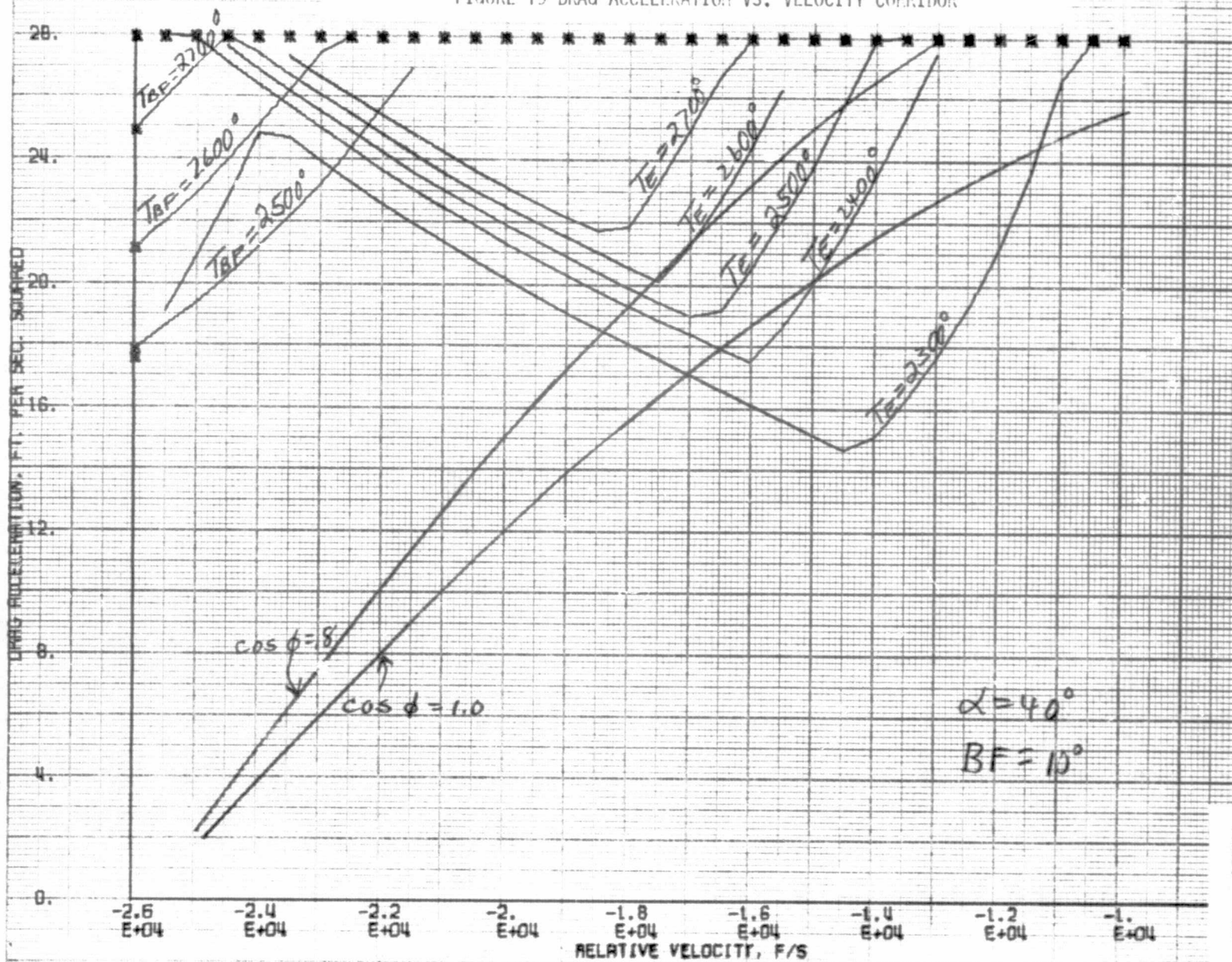




FIGURE 20 DRAG ACCELERATION VS. VELOCITY CORRIDOR

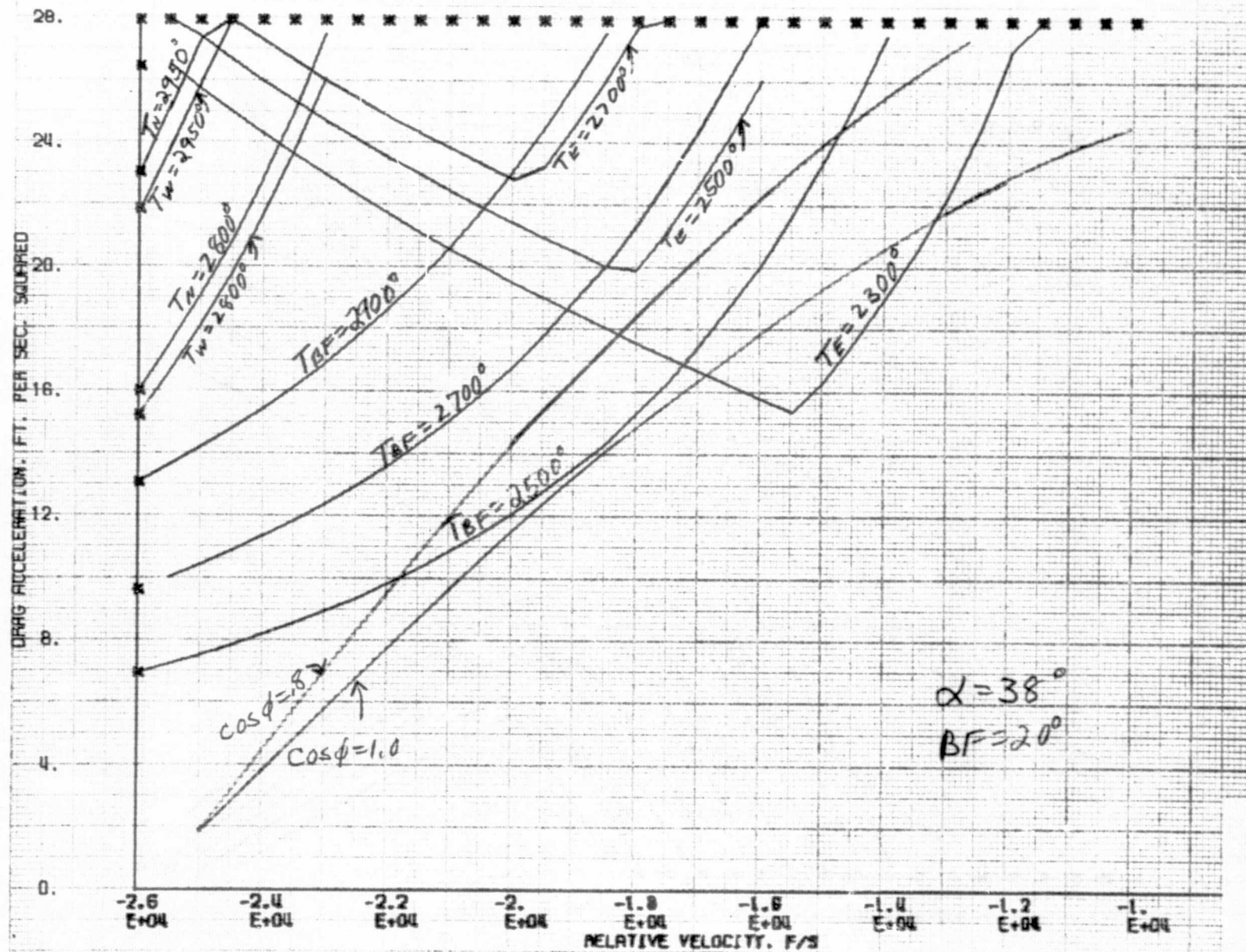


FIGURE 21 DRAG ACCELERATION VS. VELOCITY CORRIDOR

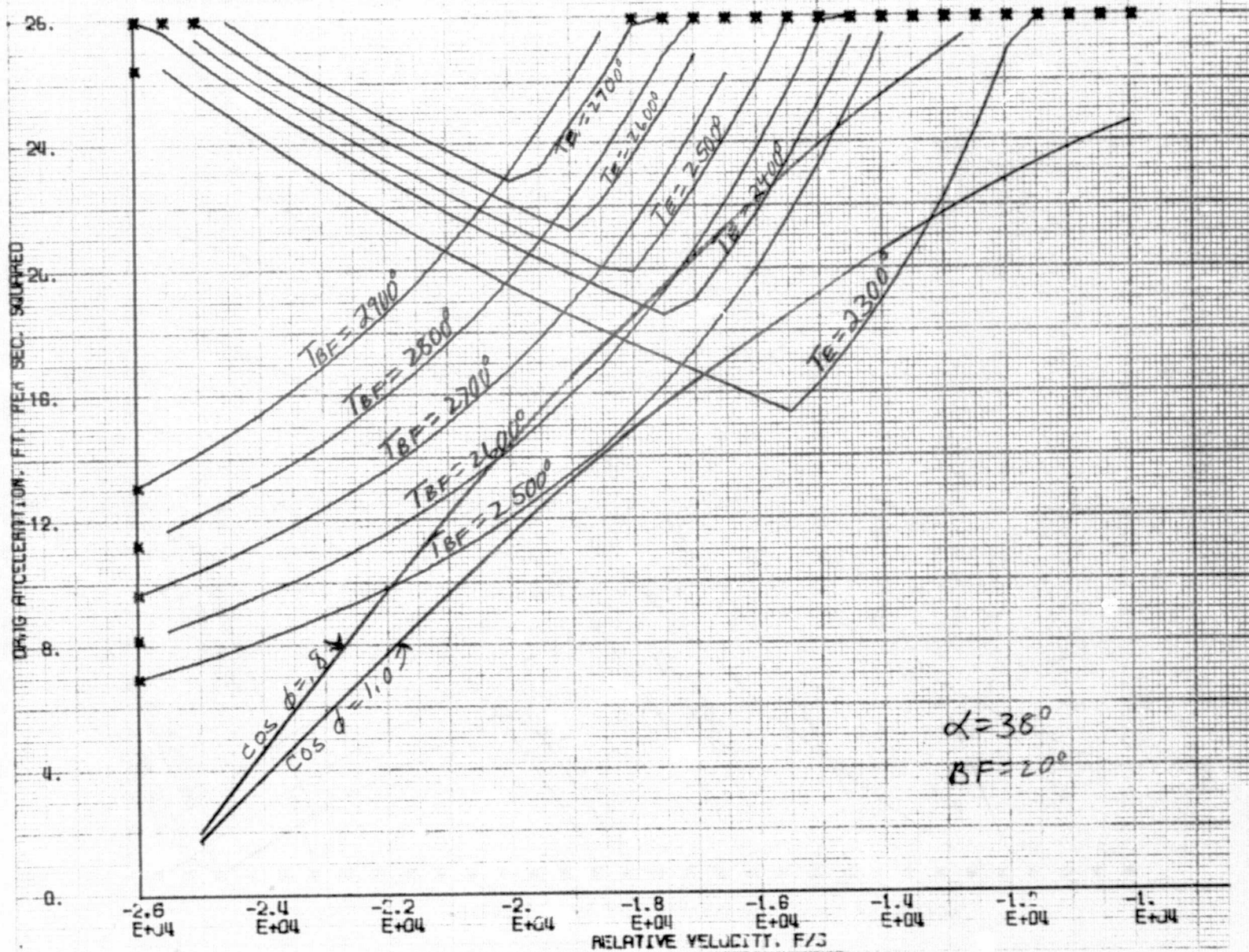




FIGURE 22 DRAG ACCELERATION VS. VELOCITY CORRIDOR

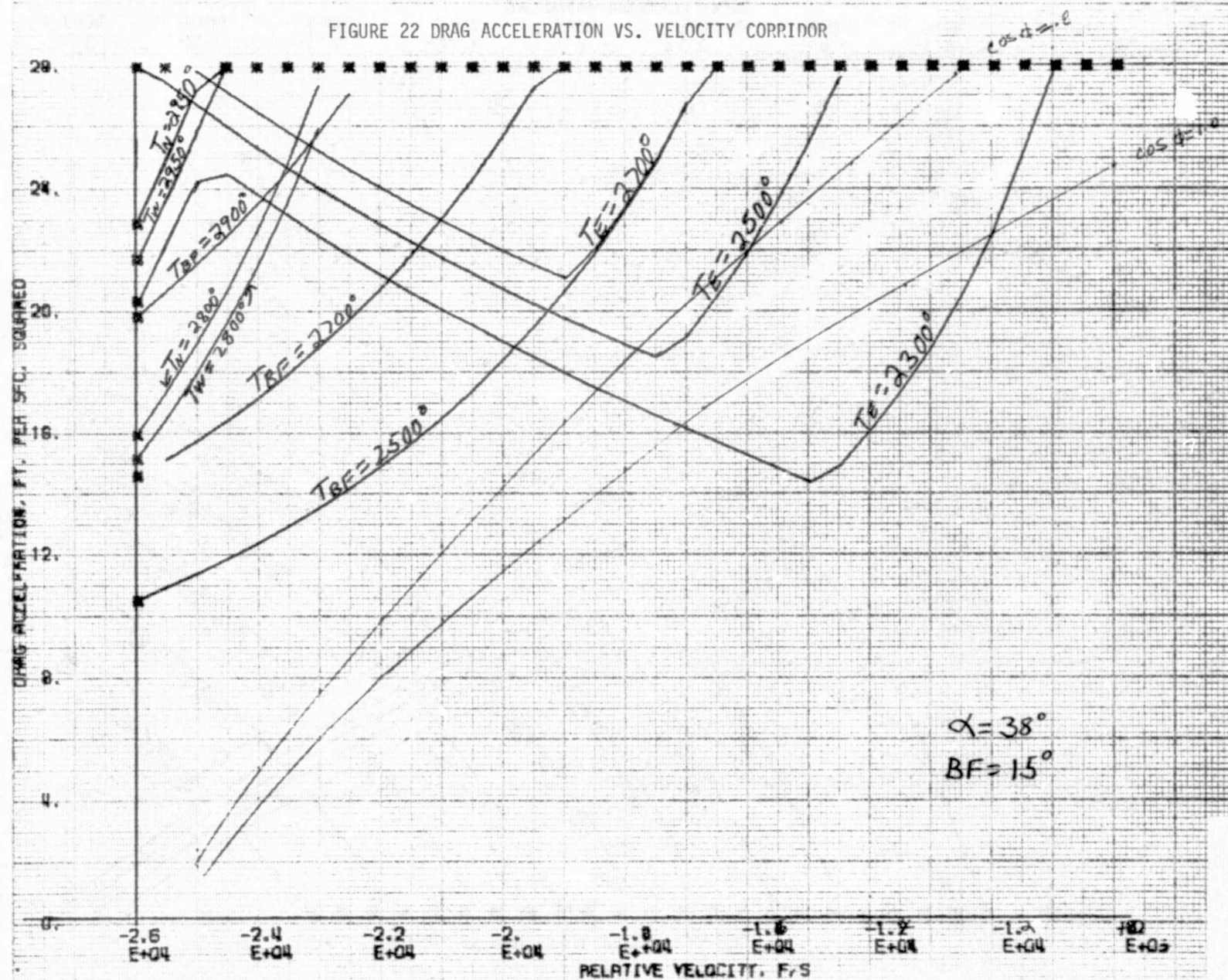
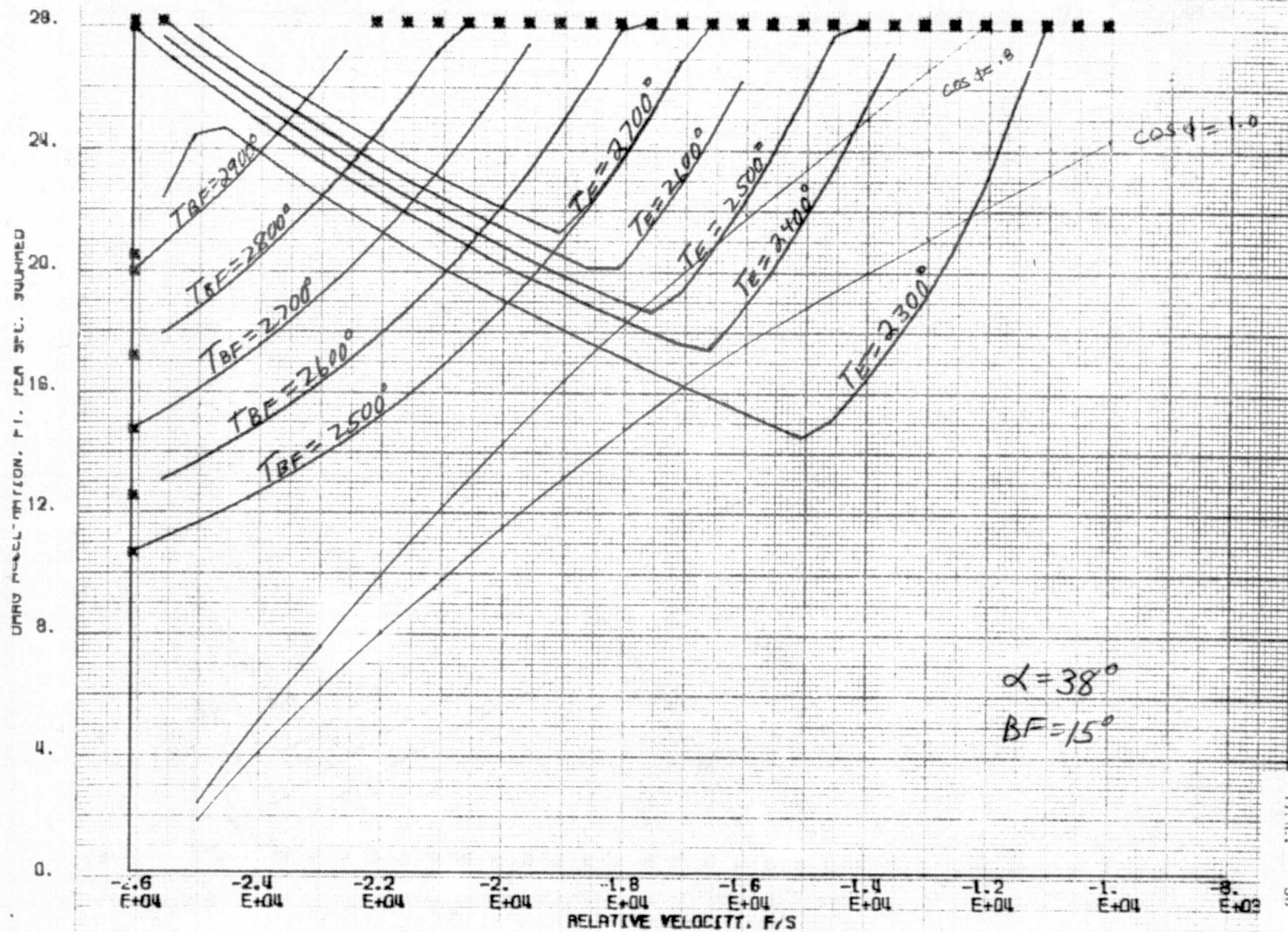


FIGURE 23 DRAG ACCELERATION VS. VELOCITY CORRIDOR





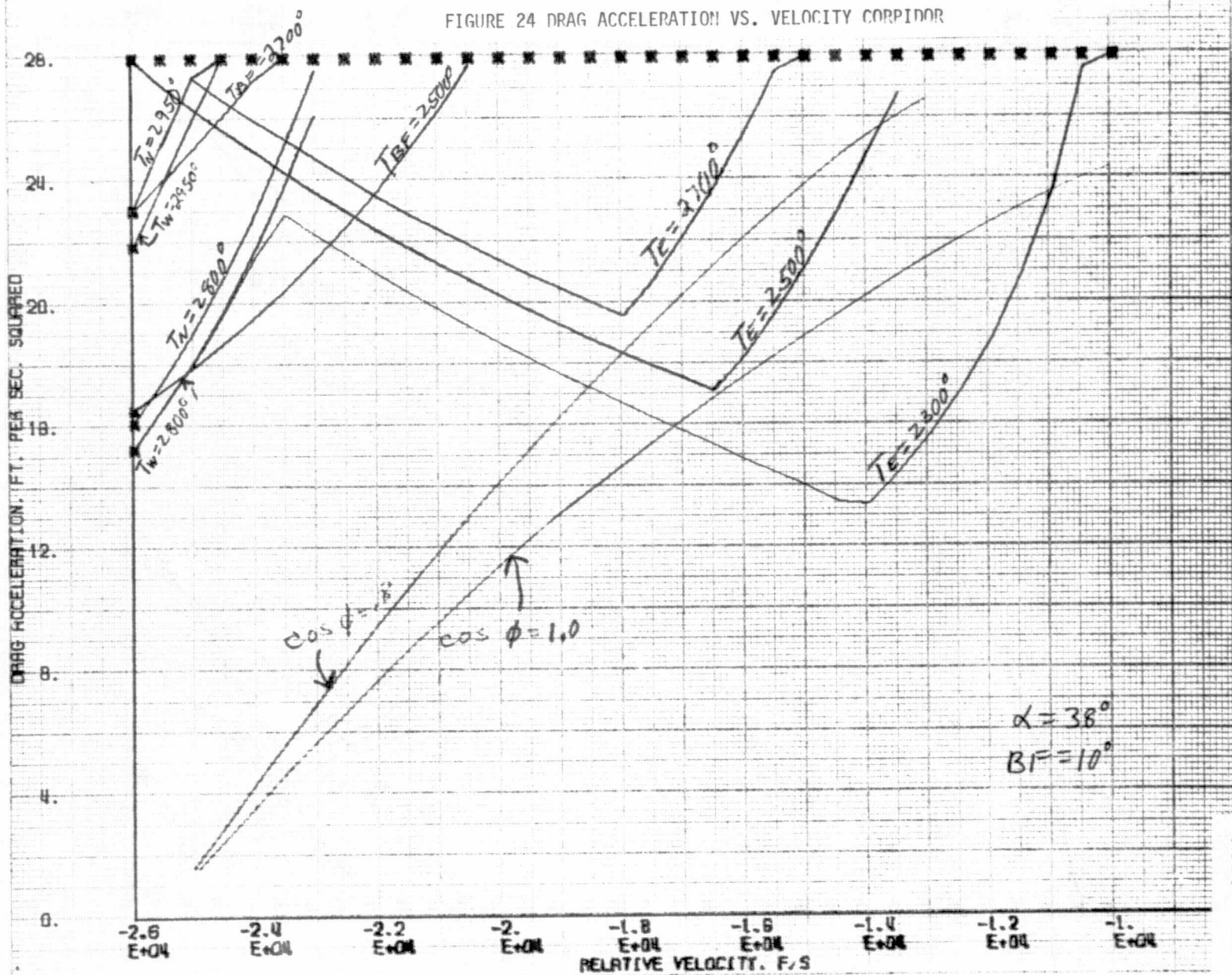


FIGURE 25 DRAG ACCELERATION VS. VELOCITY CORRIDOR

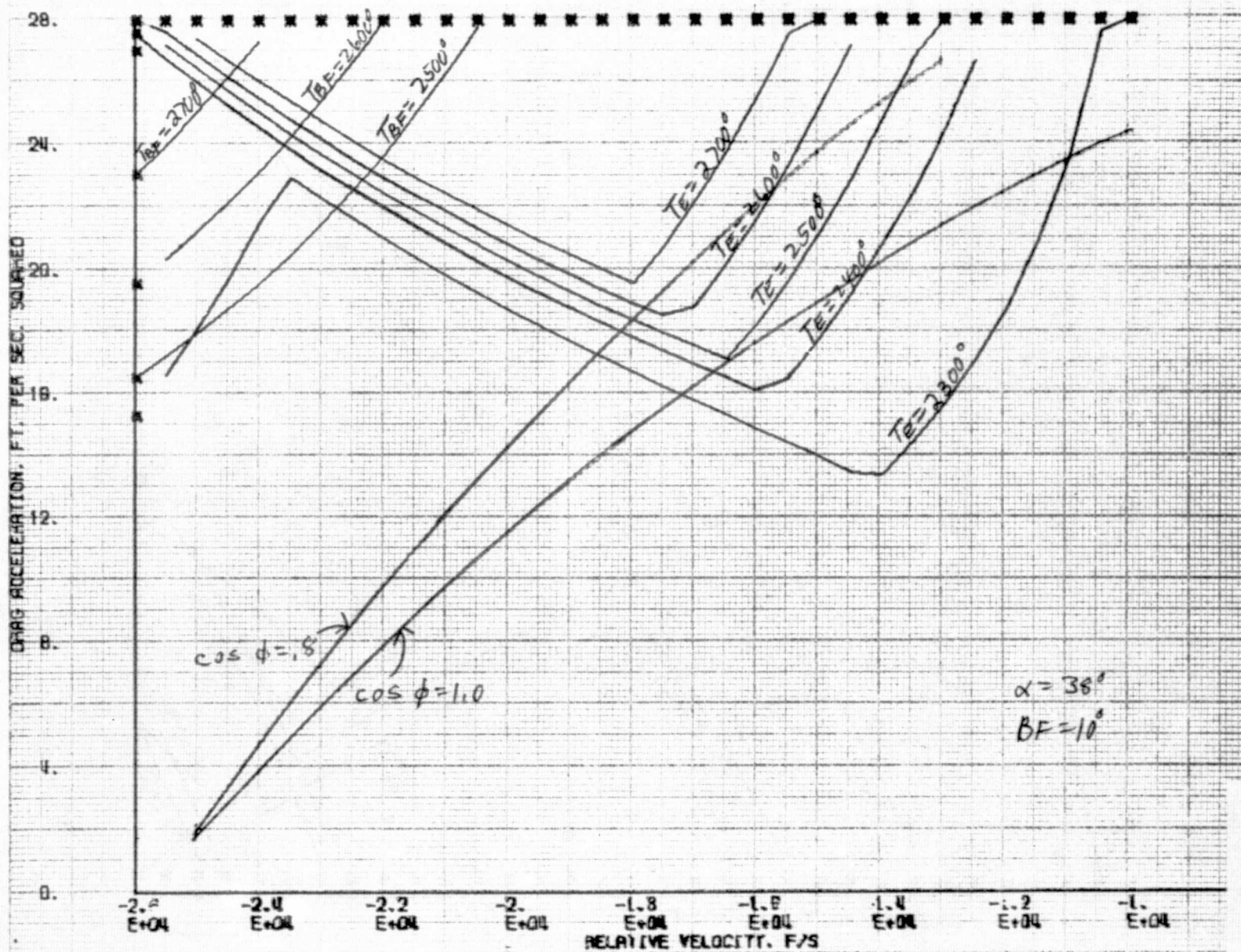




FIGURE 26 DRAG ACCELERATION VS. VELOCITY CORRIDOR

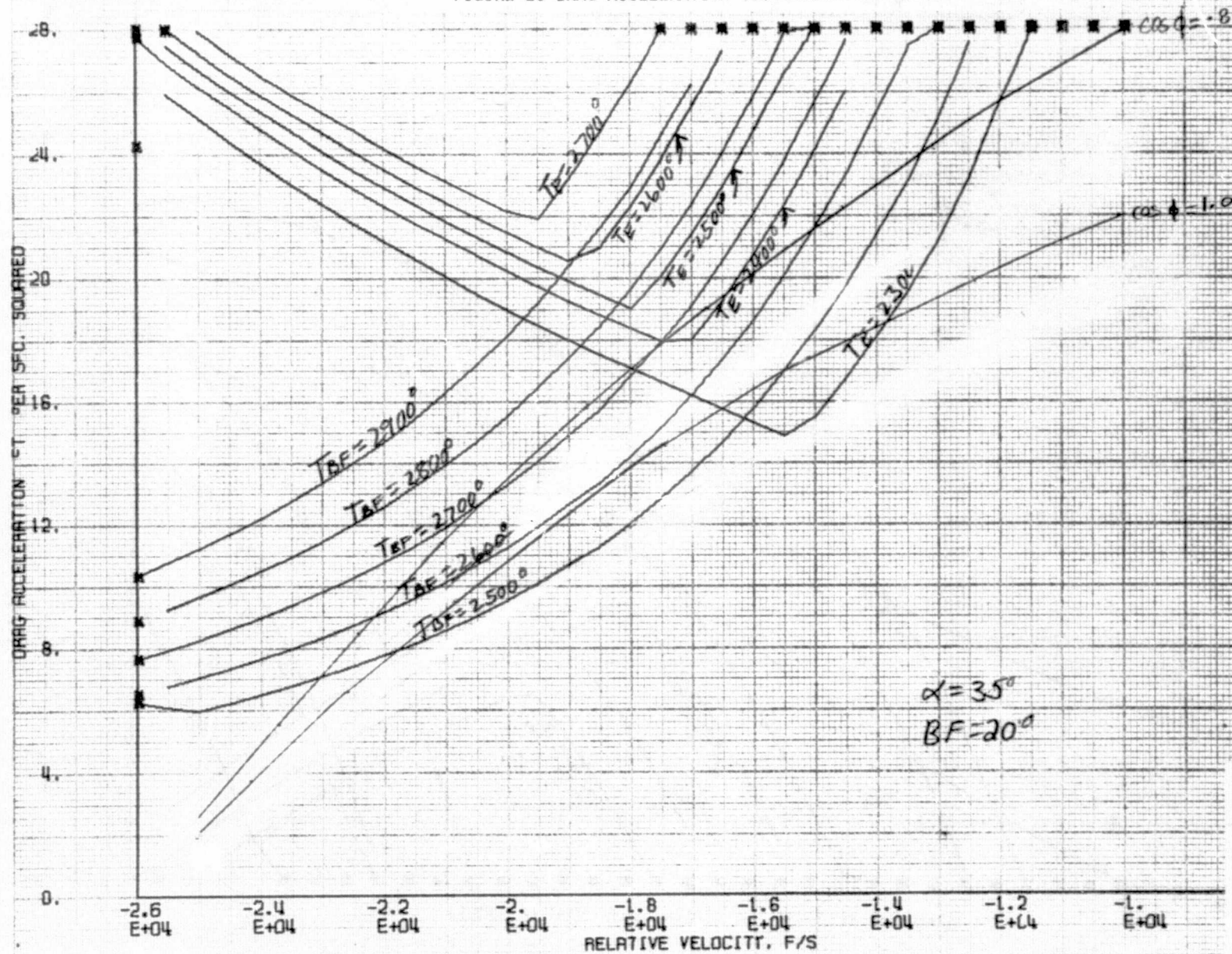


FIGURE 27 DRAG ACCELERATION VS. VELOCITY CORRIDOR

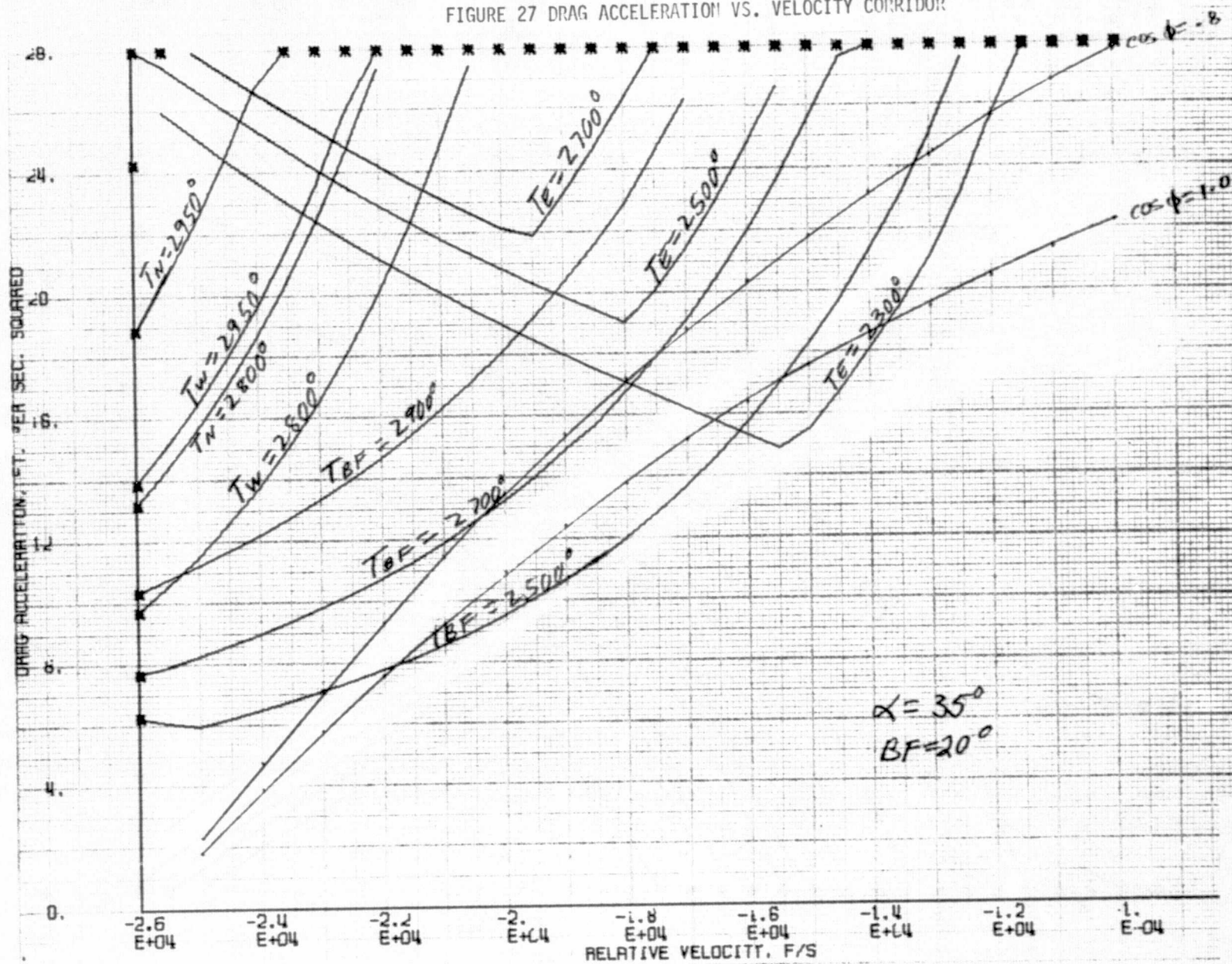




FIGURE 28 DRAG ACCELERATION VS. VELOCITY CORRIDOR

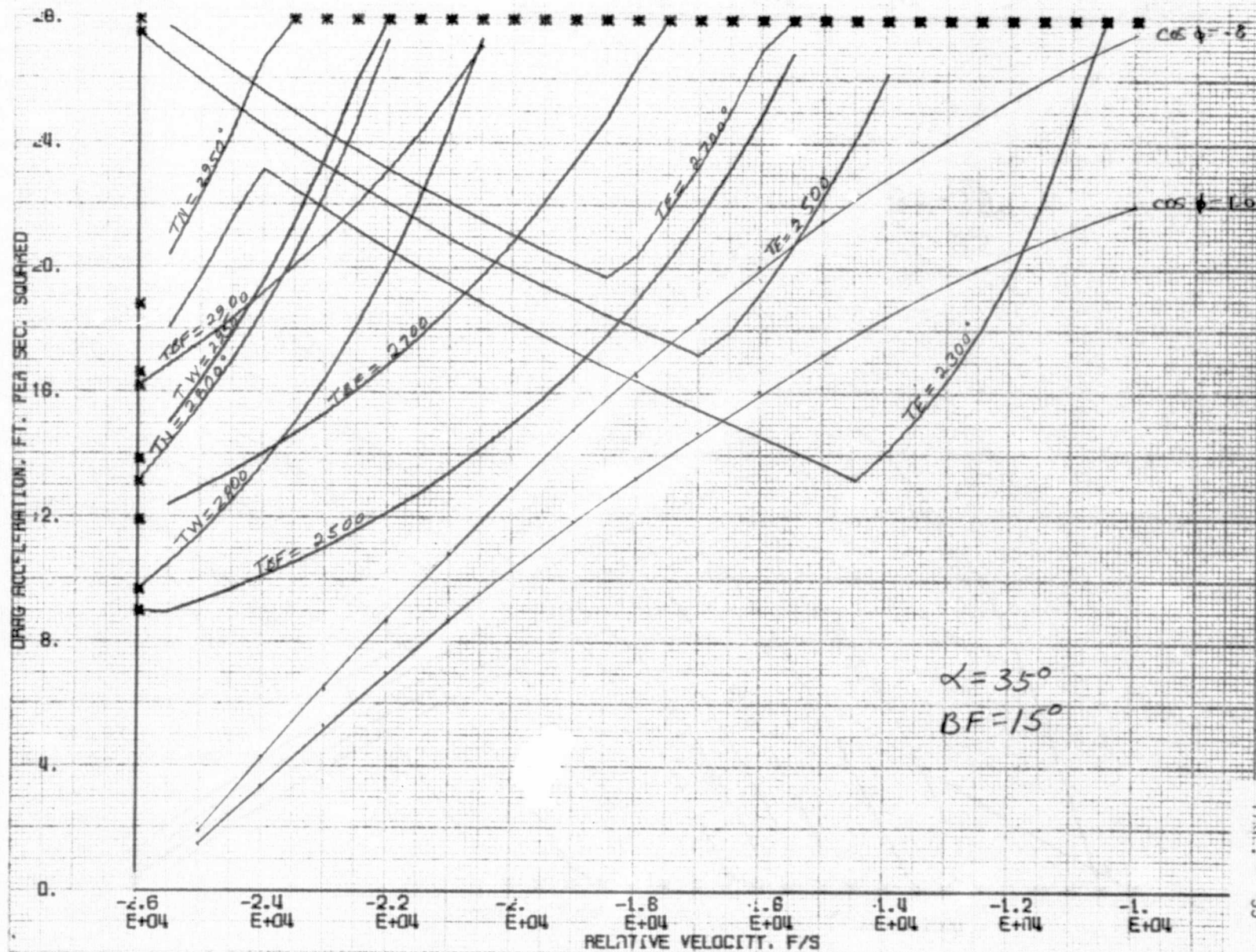


FIGURE 29 DRAG ACCELERATION VS. VELOCITY CORRIDOR

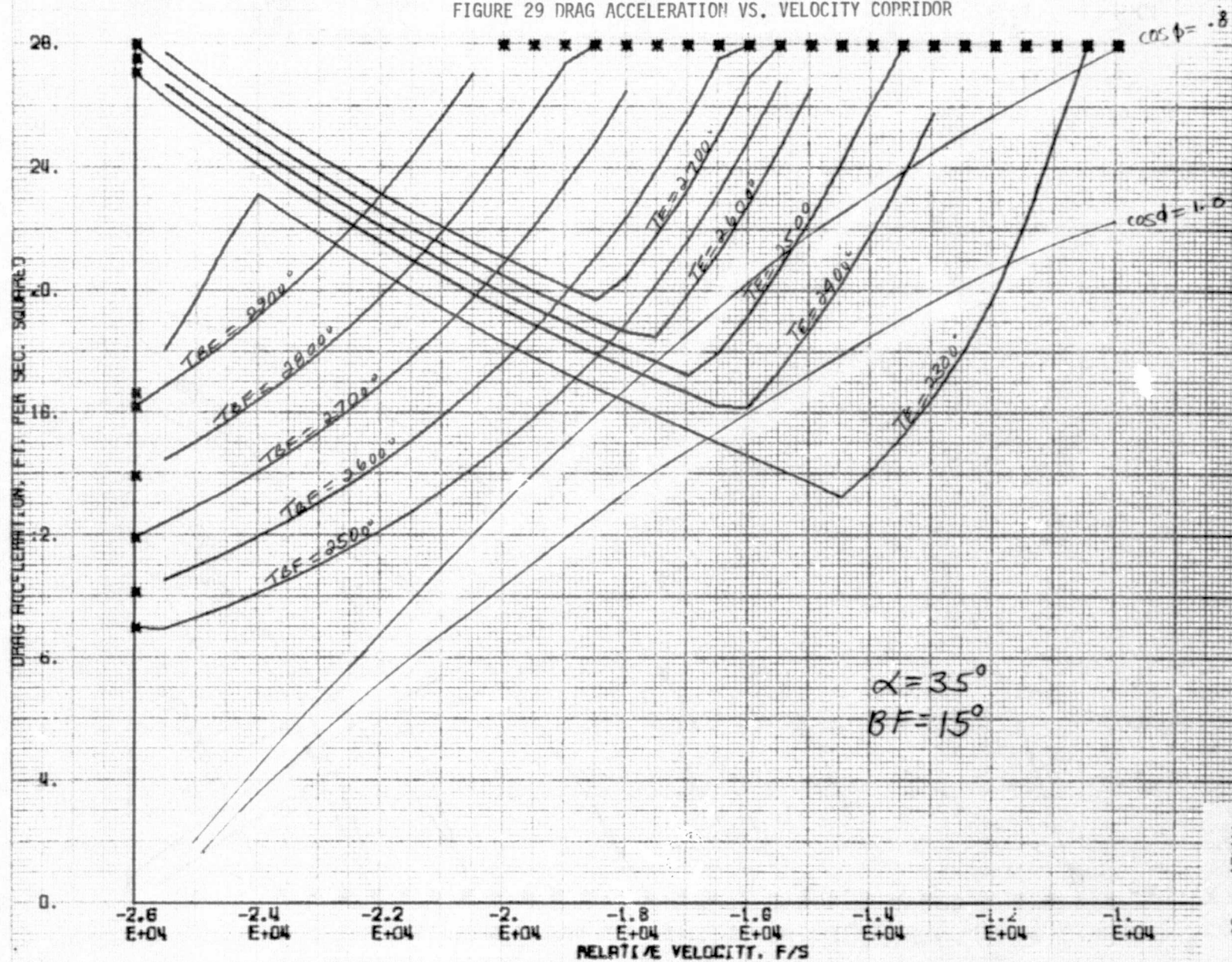




FIGURE 30 DRAG ACCELERATION VS. VELOCITY CORRIDOR

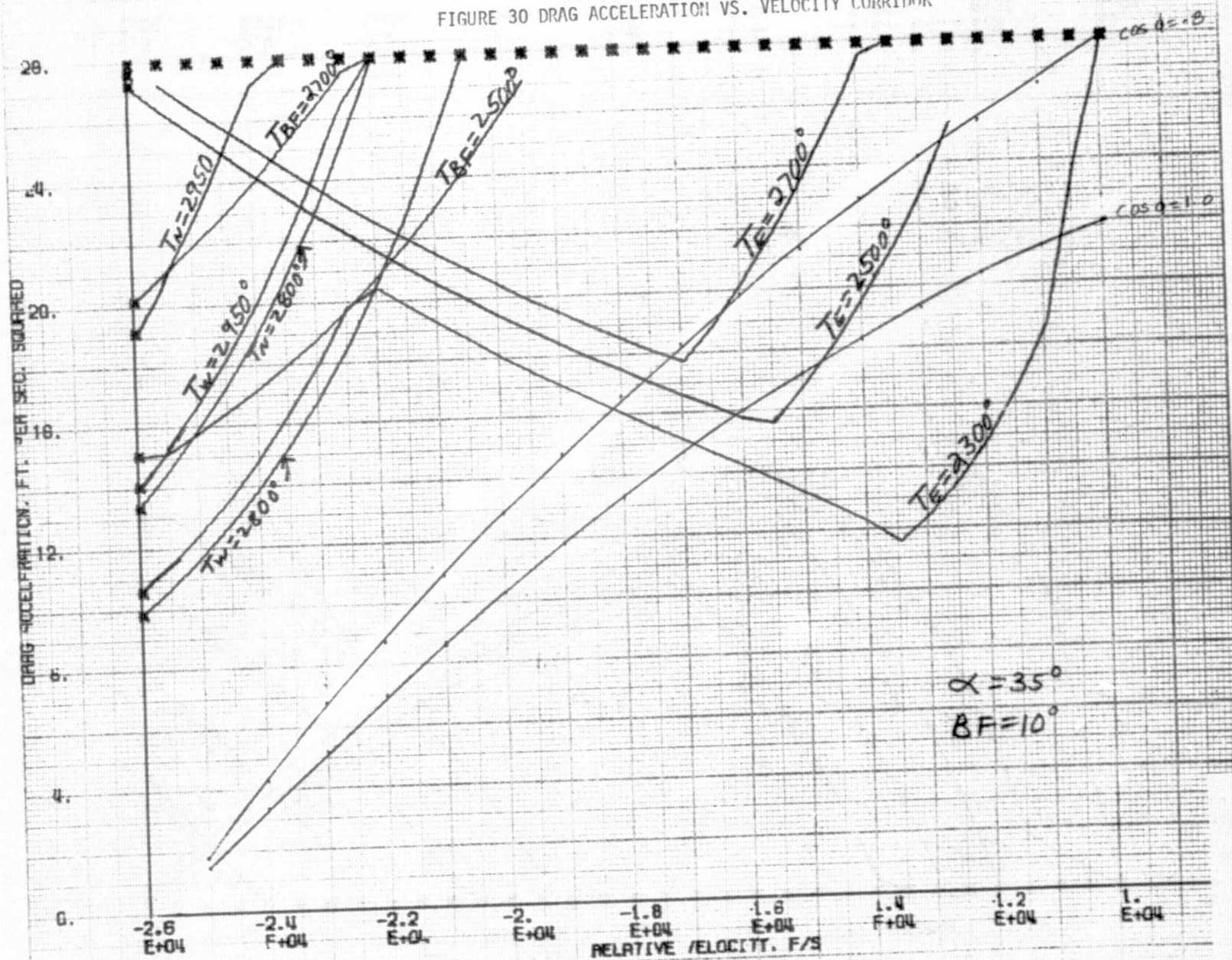


FIGURE 31 DRAG ACCELERATION VS. VELOCITY CORRIDOR

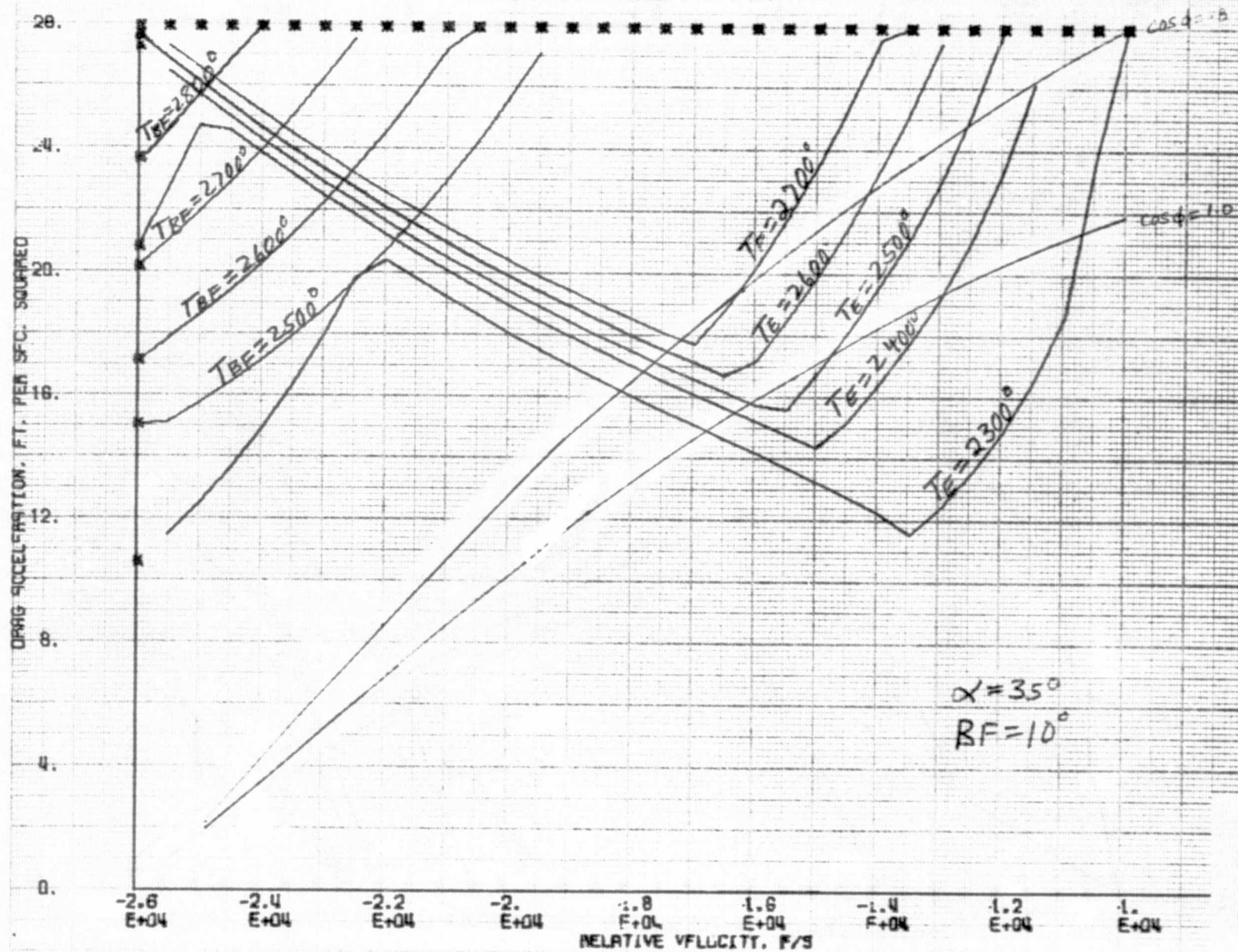




FIGURE 32 DRAG ACCELERATION VS. VELOCITY CORRIDOR

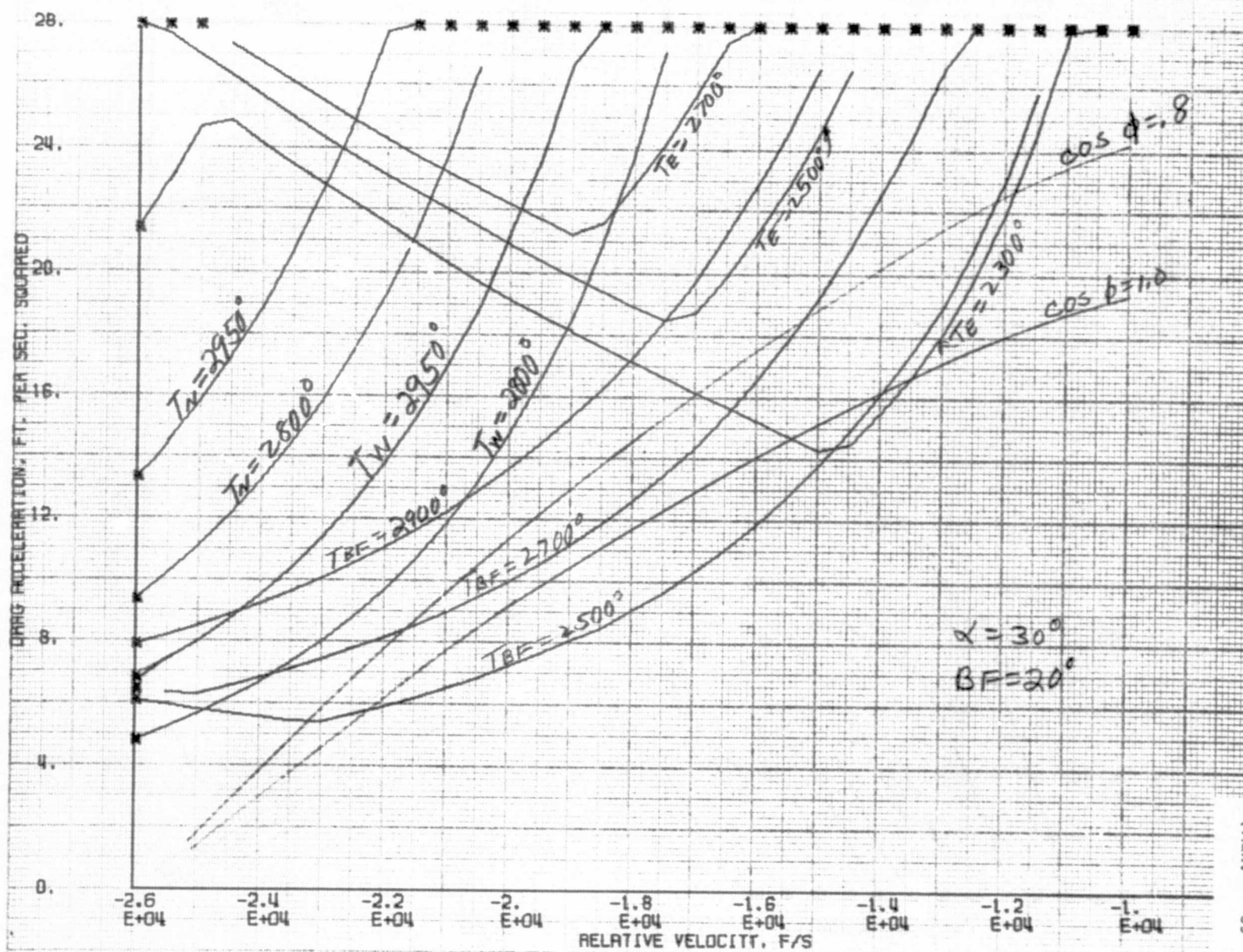


FIGURE 33 DRAG ACCELERATION VS. VELOCITY CORRIDOR

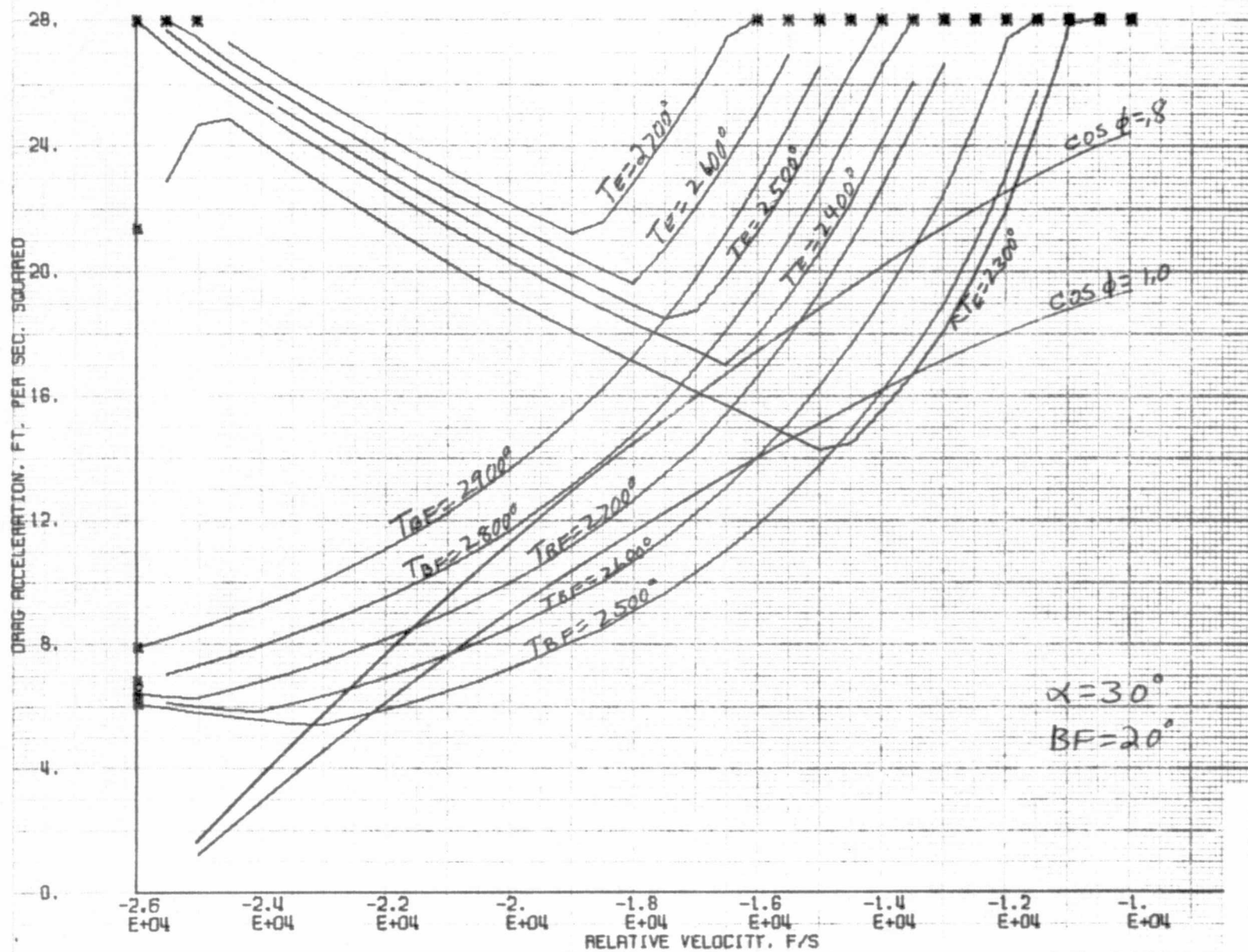




FIGURE 34 DRAG ACCELERATION VS. VELOCITY CORRIDOR

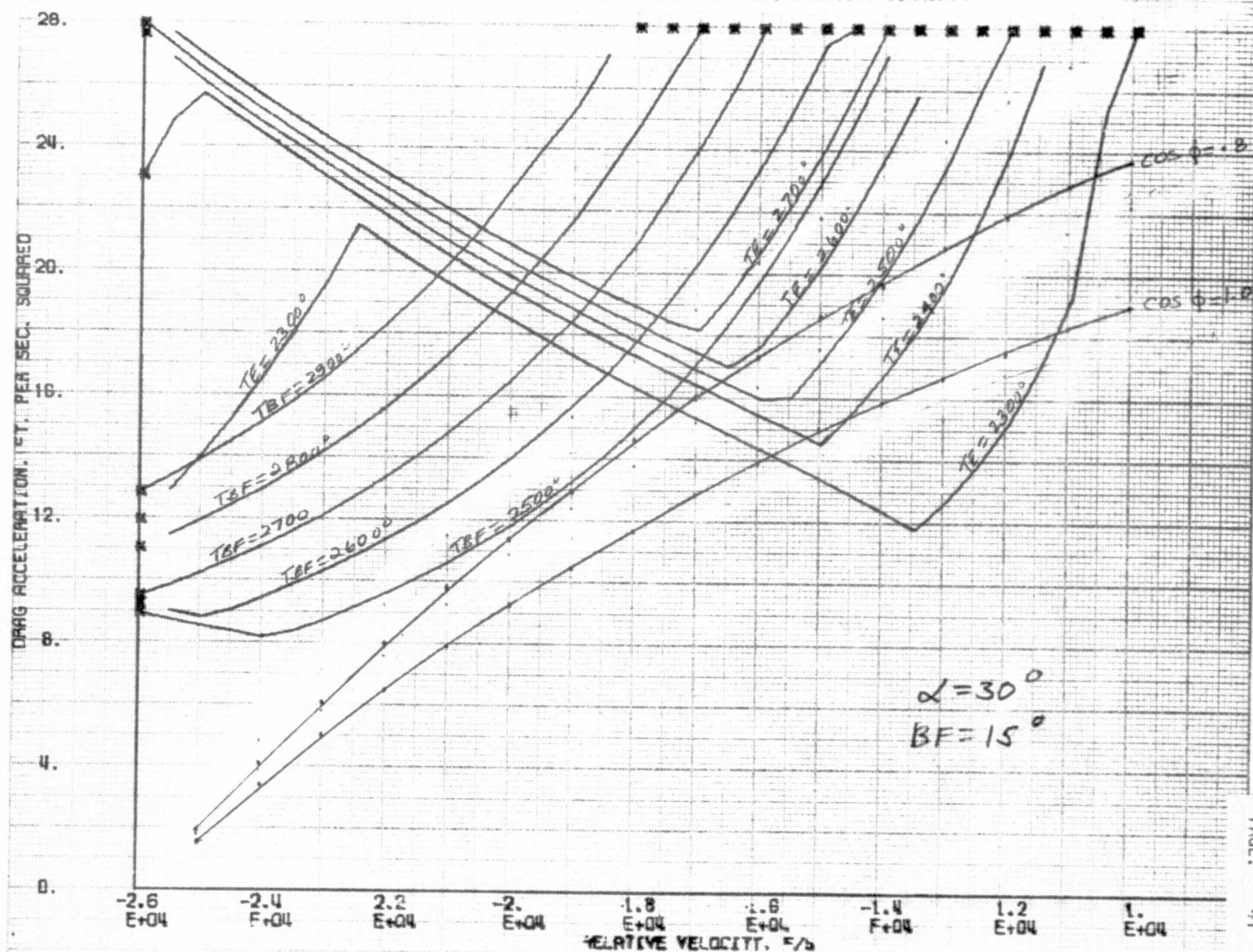


FIGURE 35 DRAG ACCELERATION VS. VELOCITY CORRIDOR

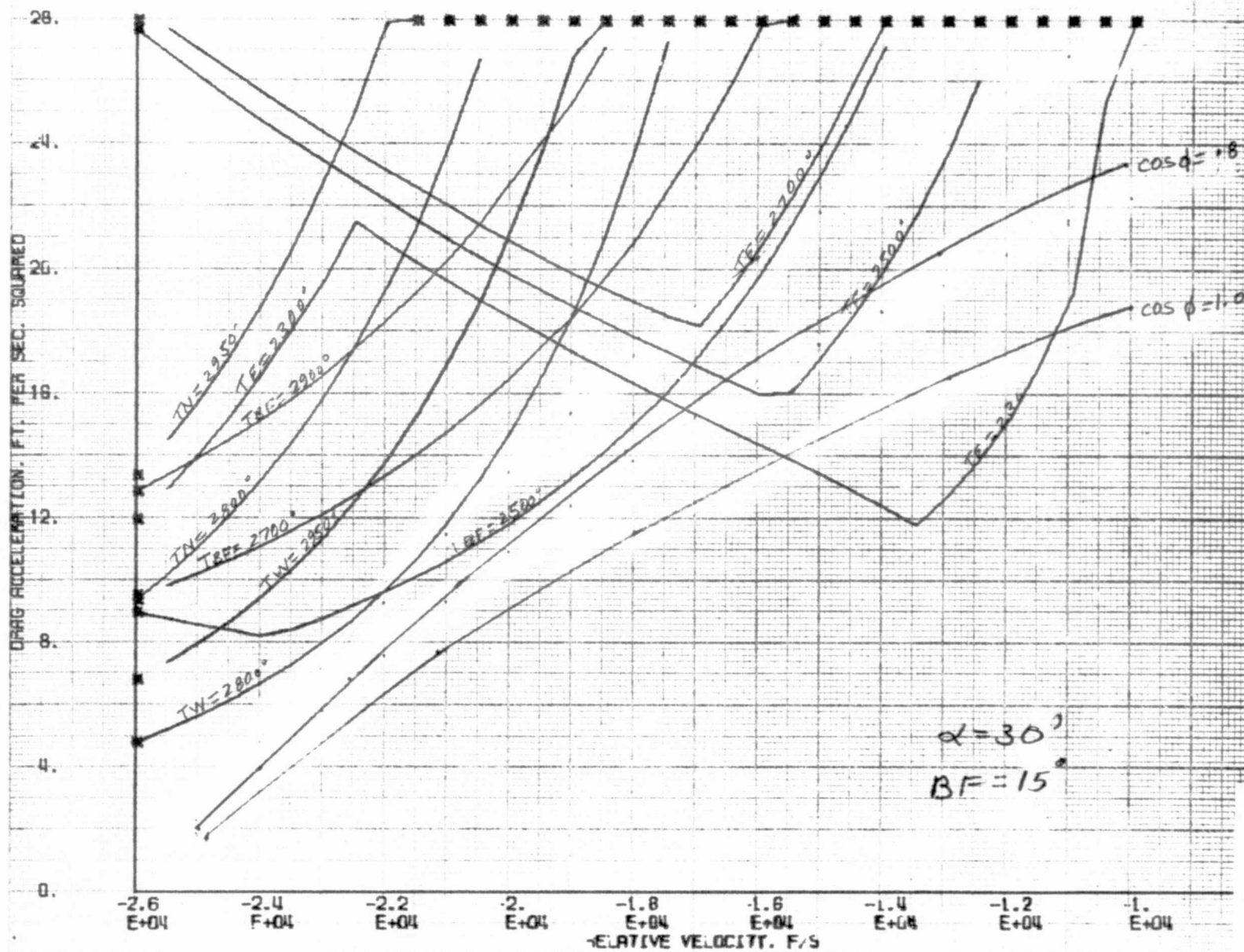






FIGURE 37 DRAG ACCELERATION VS. VELOCITY CORRIDOR

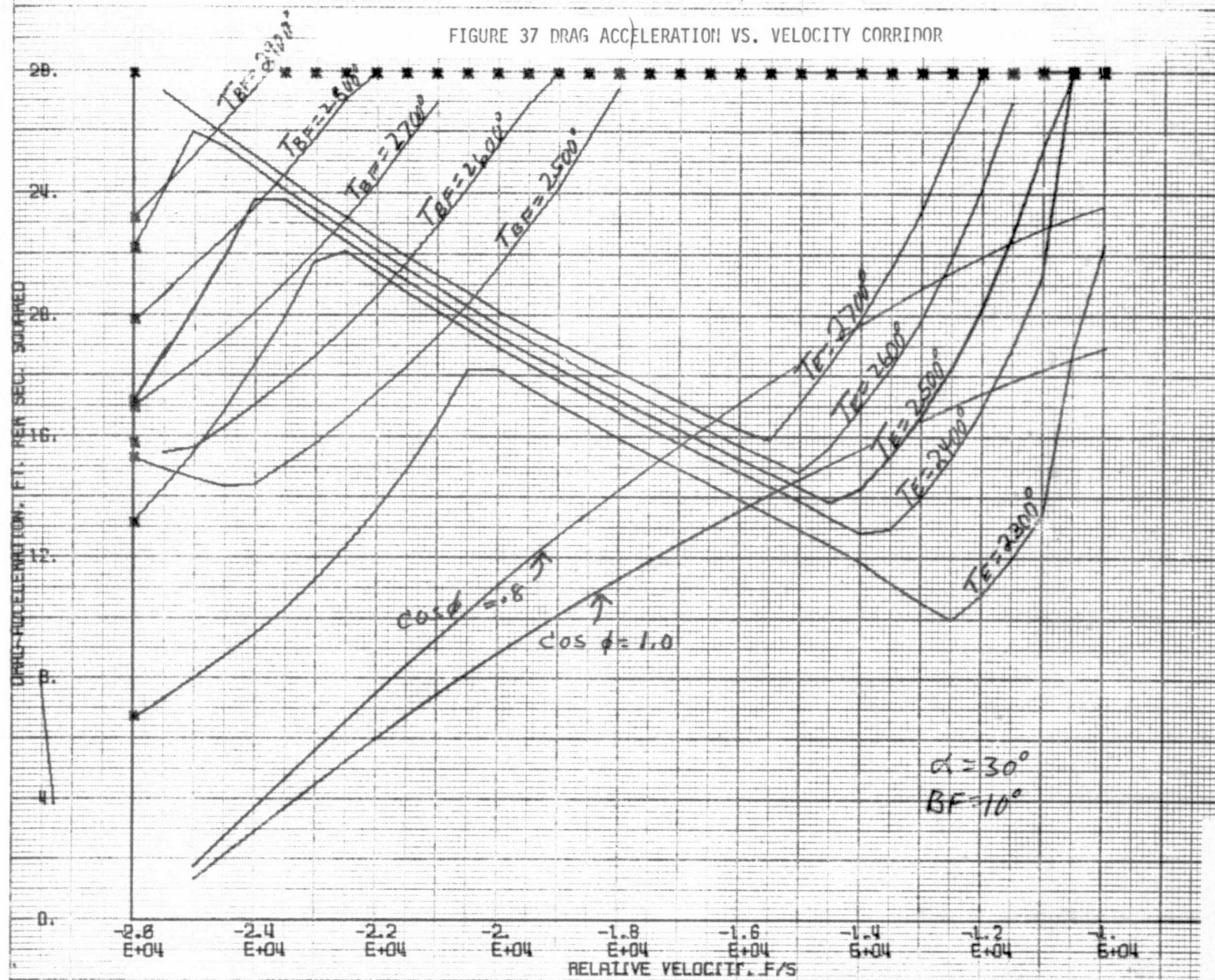


FIGURE 38 DRAG ACCELERATION VS. VELOCITY CORRIDOR

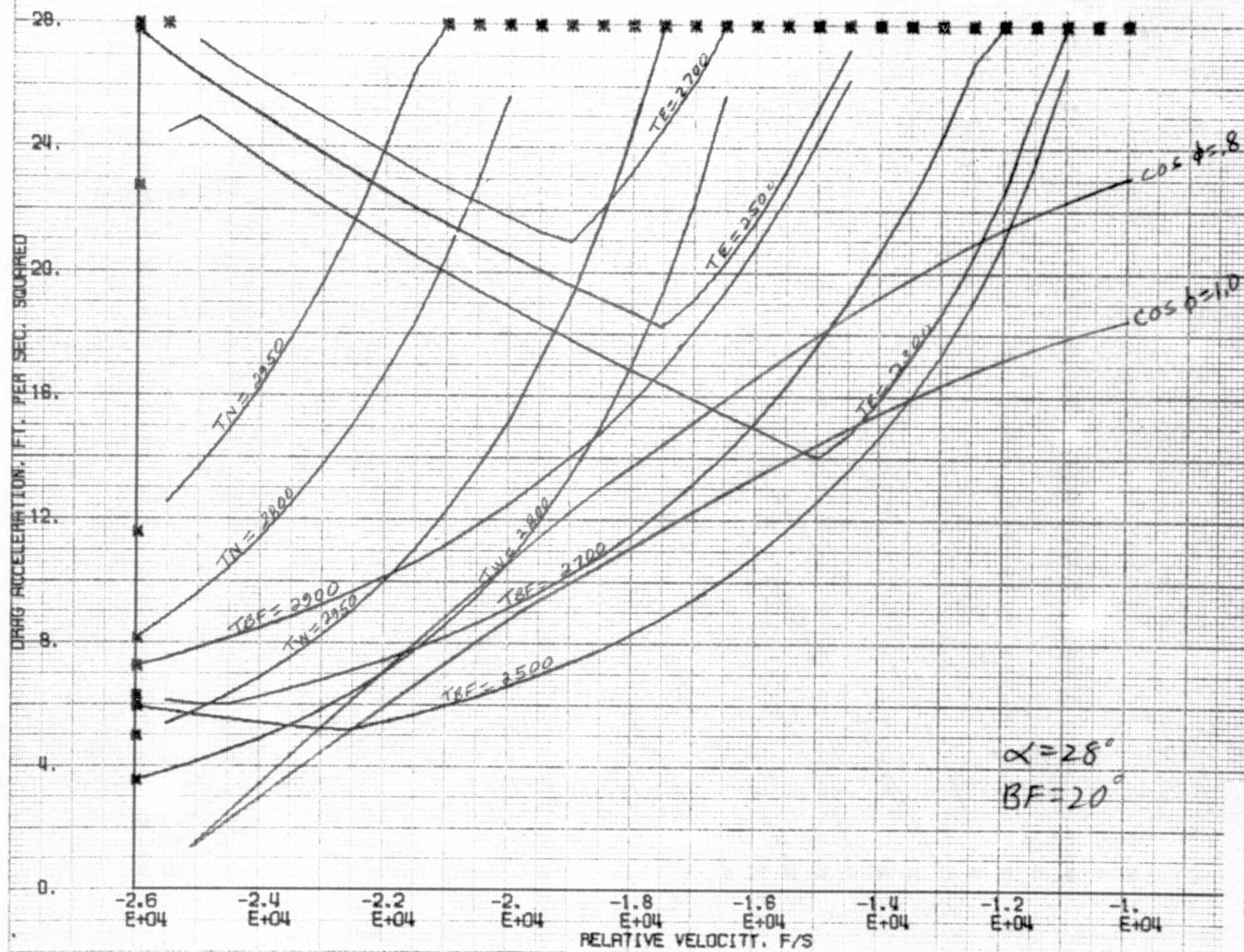




FIGURE 39 DRAG ACCELERATION VS. VELOCITY CORRIDOR

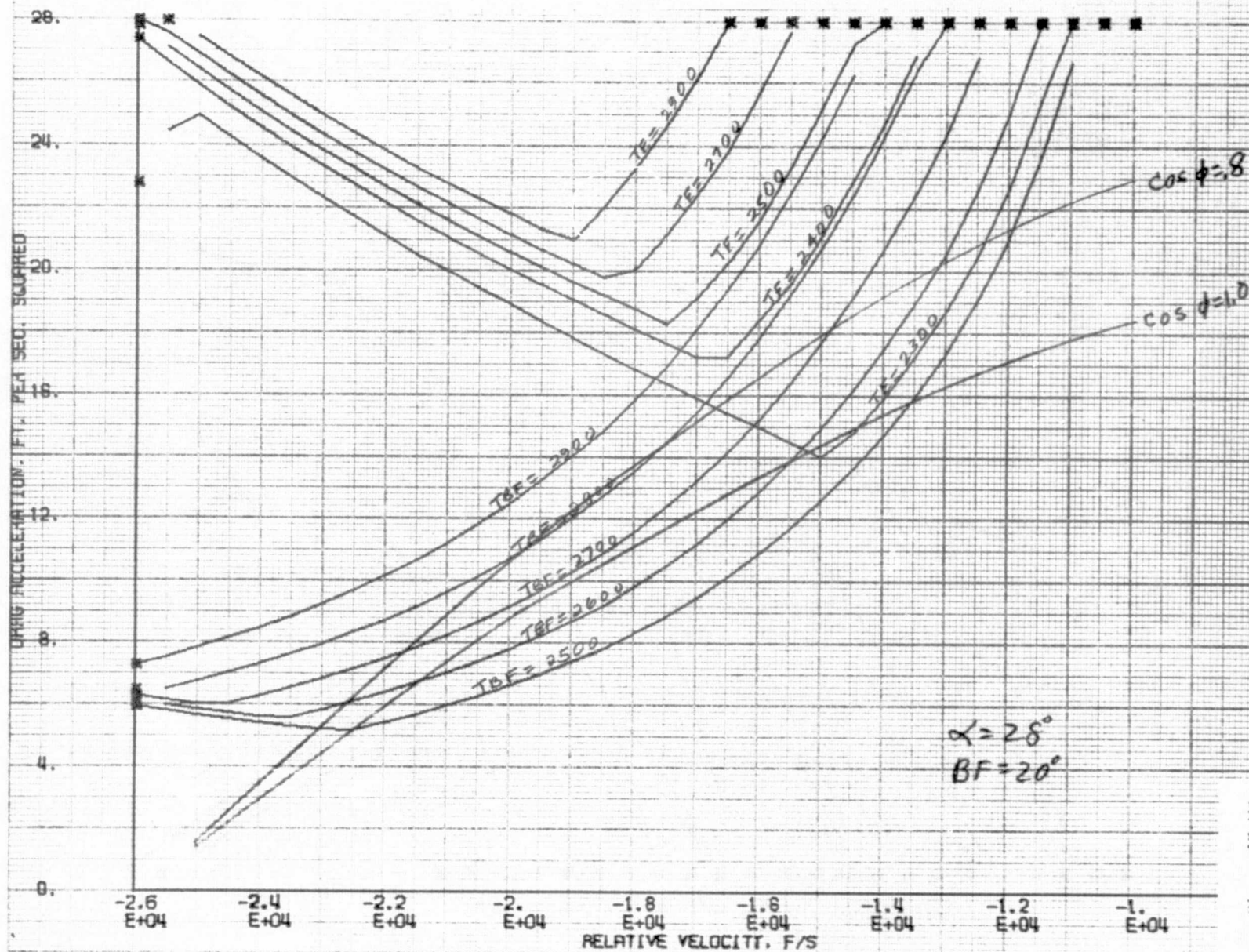




FIGURE 40 DRAG ACCELERATION VS. VELOCITY COPRIDOR

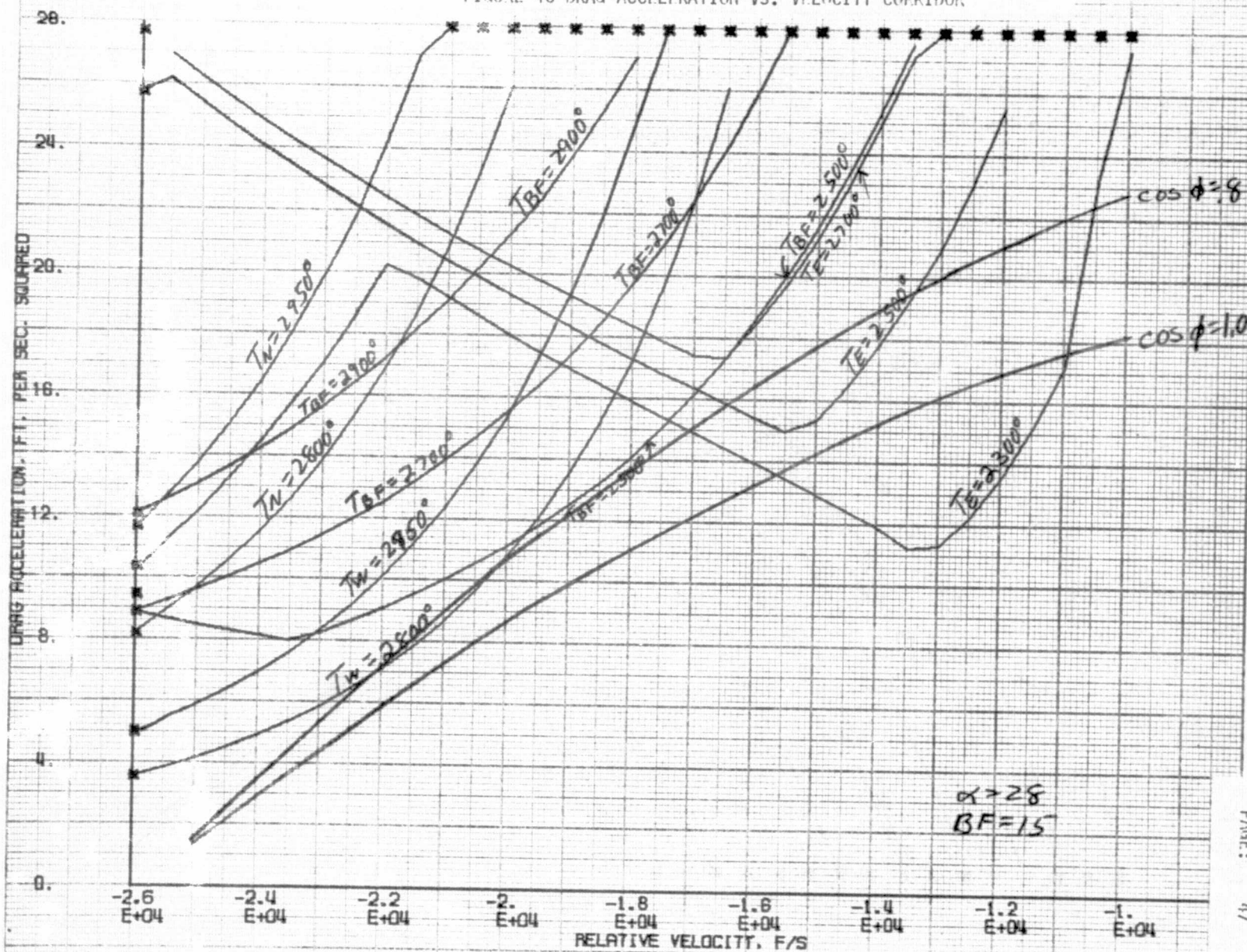


FIGURE 41 DRAG ACCELERATION VS. VELOCITY CORRIDOR

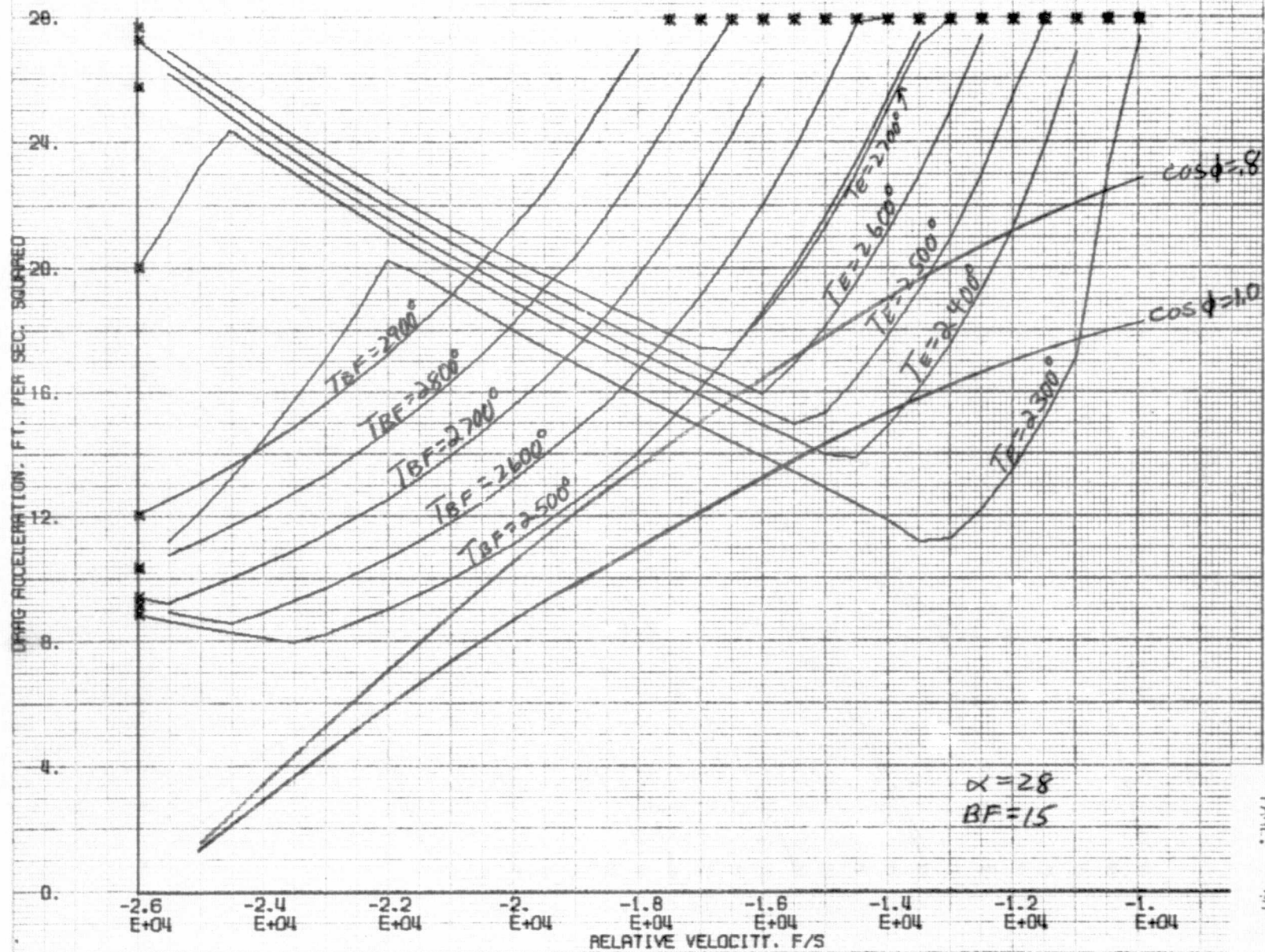




FIGURE 42 DRAG ACCELERATION VS. VELOCITY CORRIDOR

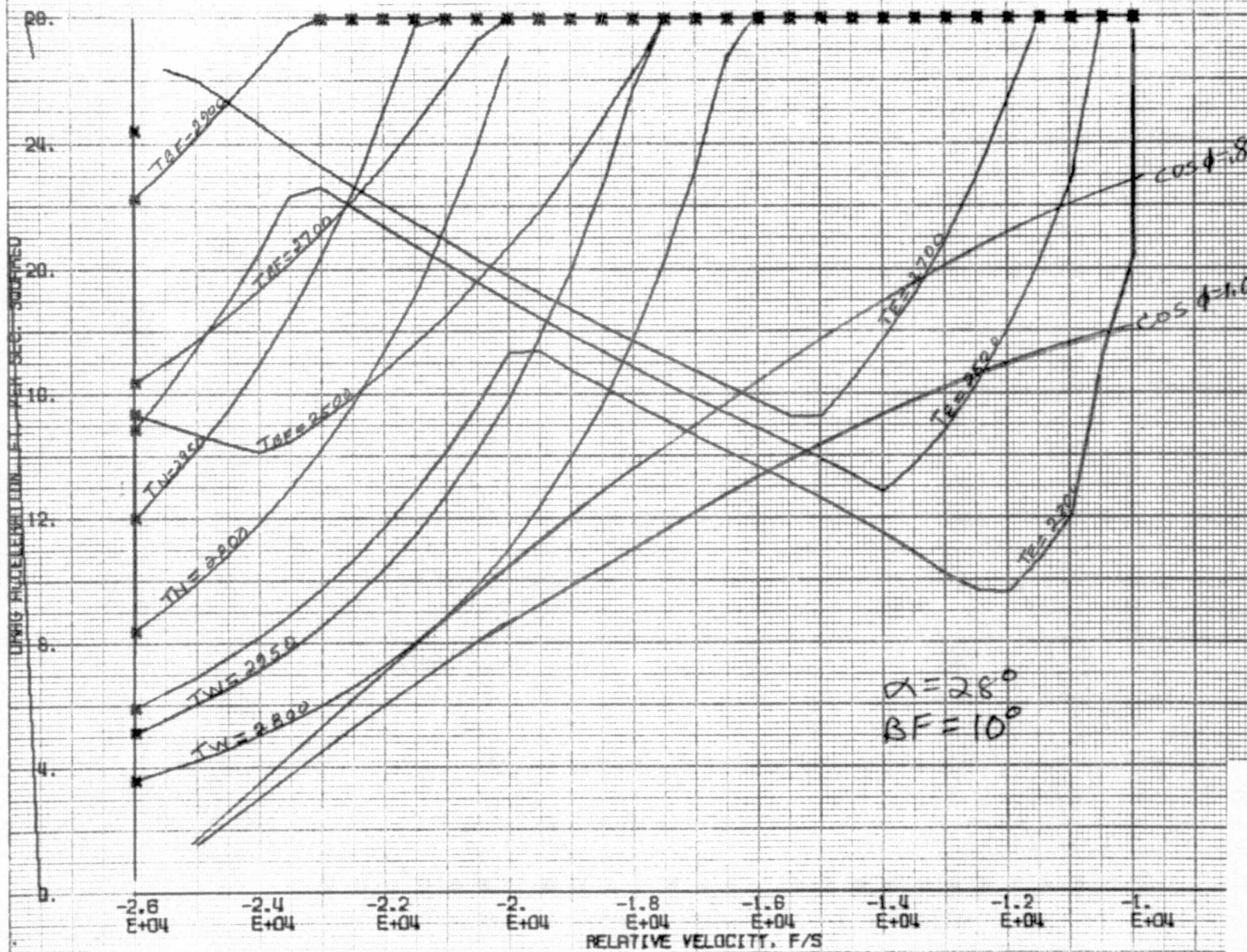
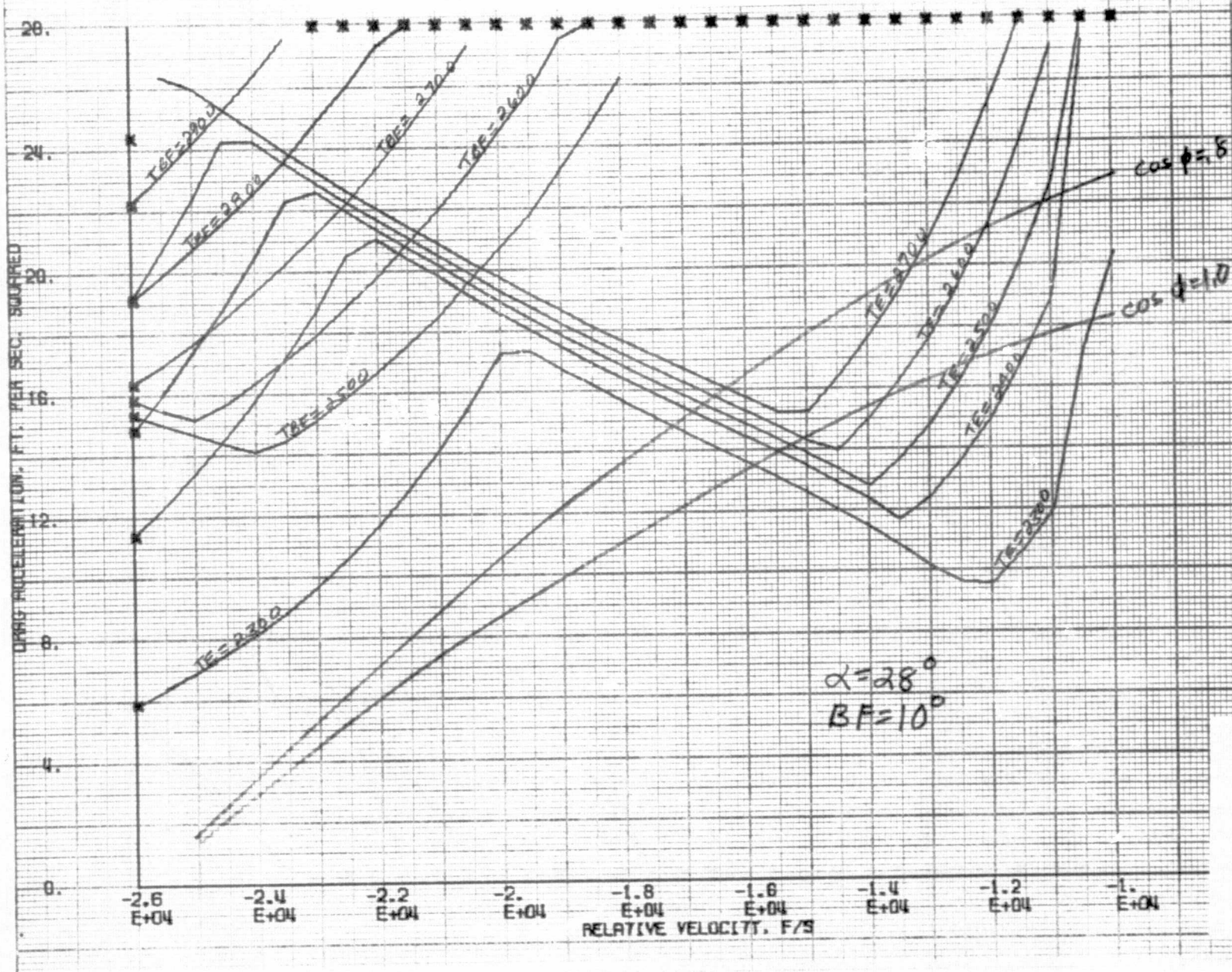




FIGURE 43 DRAG ACCELERATION VS. VELOCITY CORRIDOR



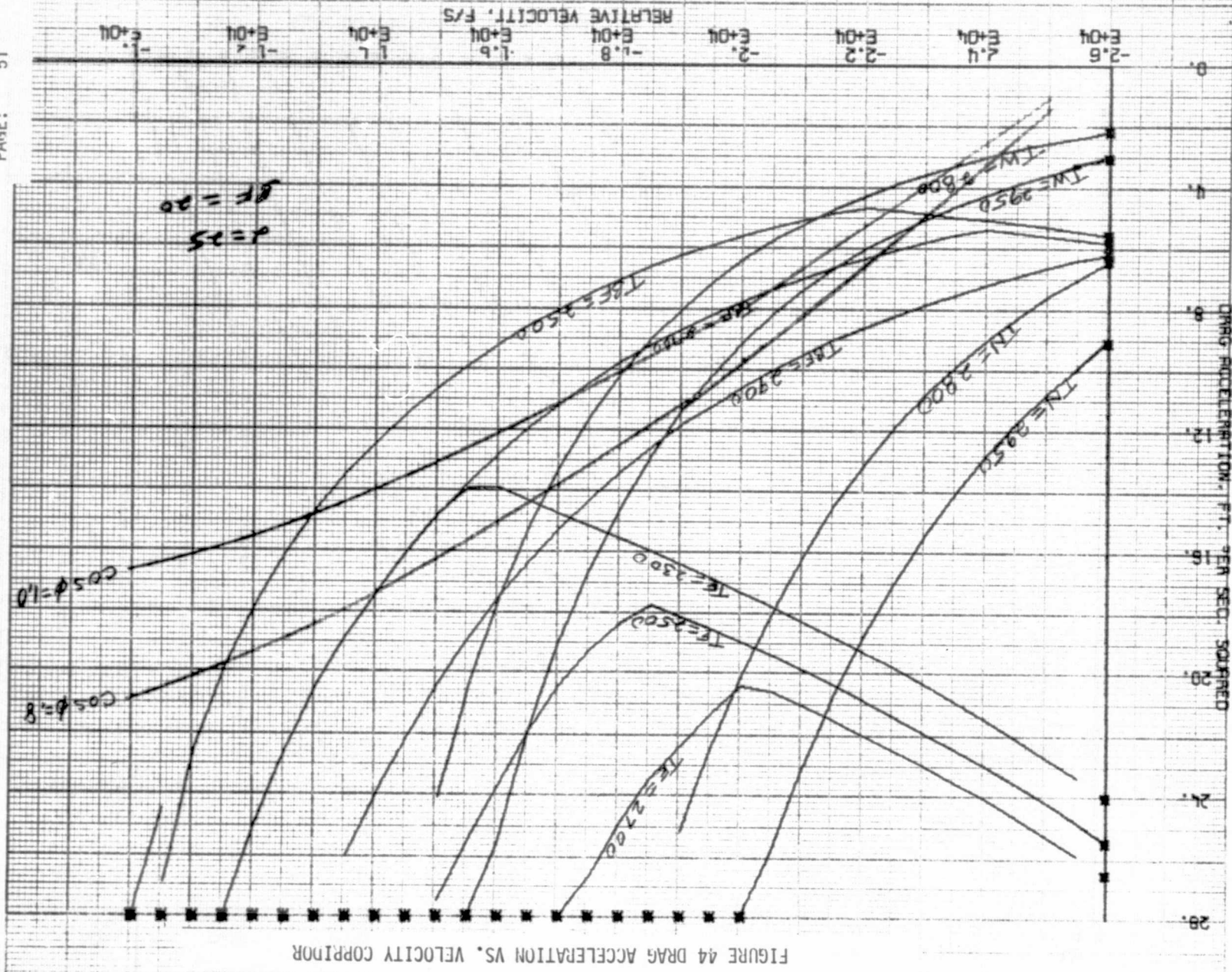




FIGURE 45 DRAG ACCELERATION VS. VELOCITY CORRIDOR

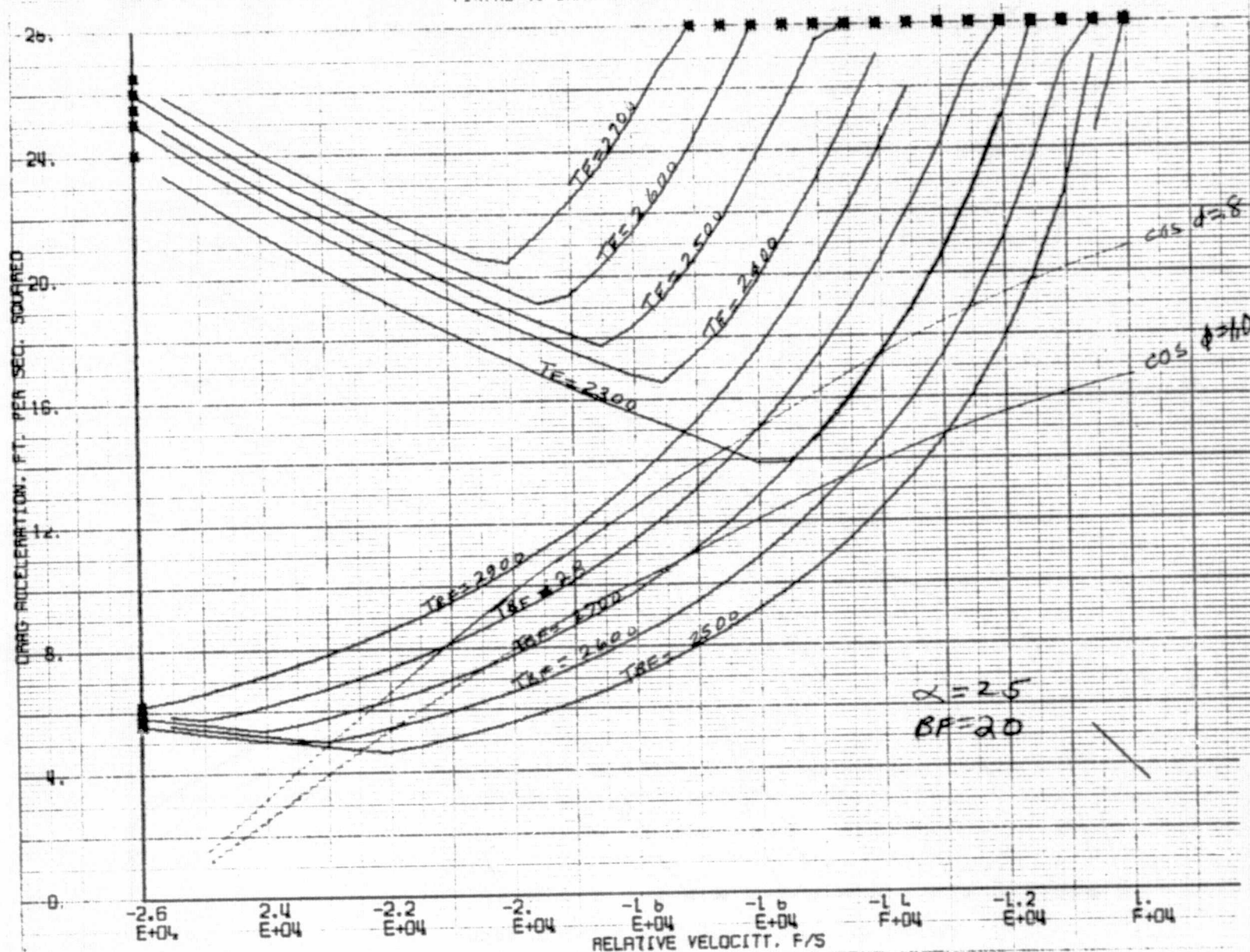




FIGURE 46 DRAG ACCELERATION VS. VELOCITY CORRIDOR

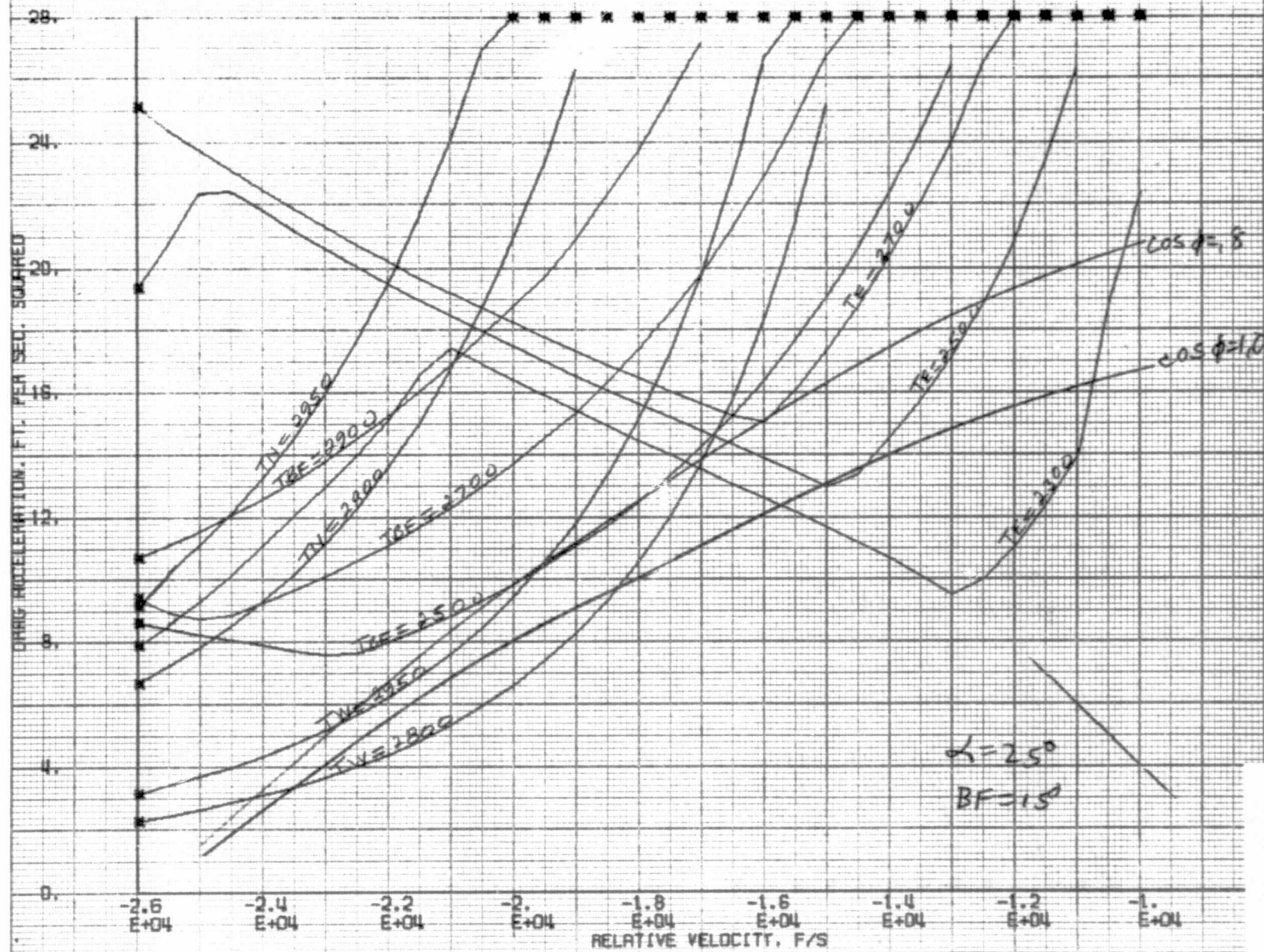


FIGURE 47 DRAG ACCELERATION VS. VELOCITY CORRIDOR

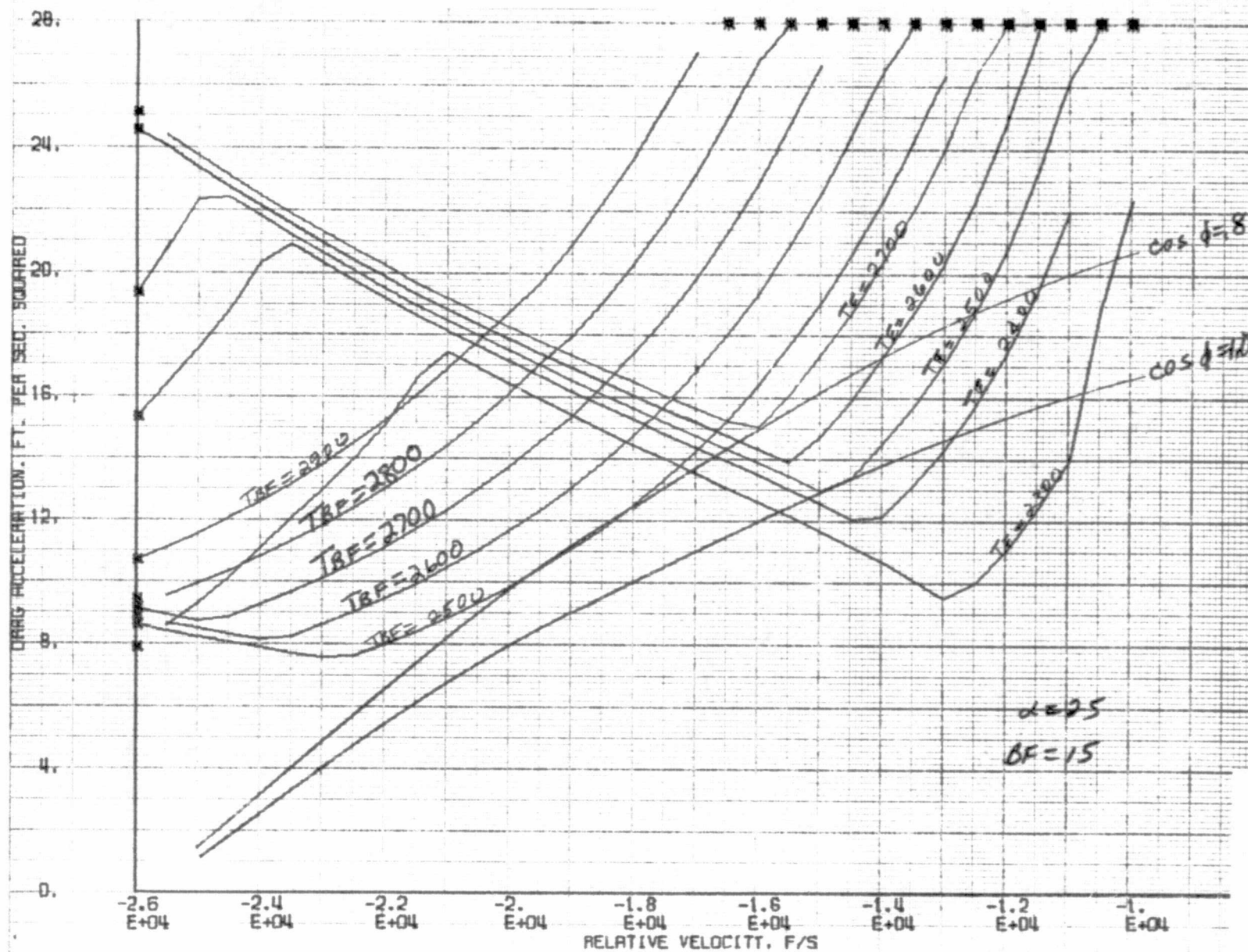






FIGURE 49 DRAG ACCELERATION VS. VELOCITY CORRIDOR

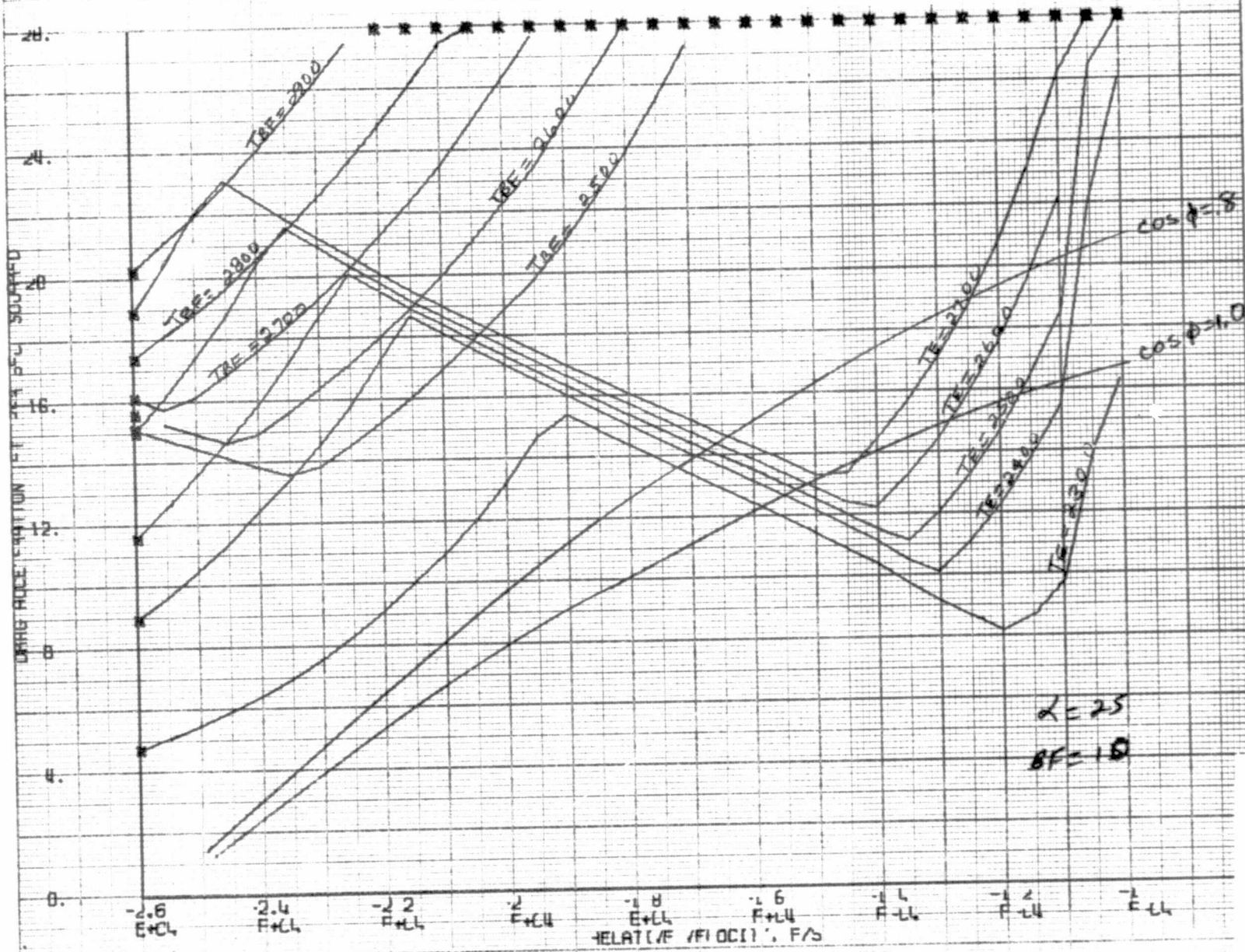


FIGURE 50 DYNAMIC PRESSURE VS. VELOCITY CORRIDOR

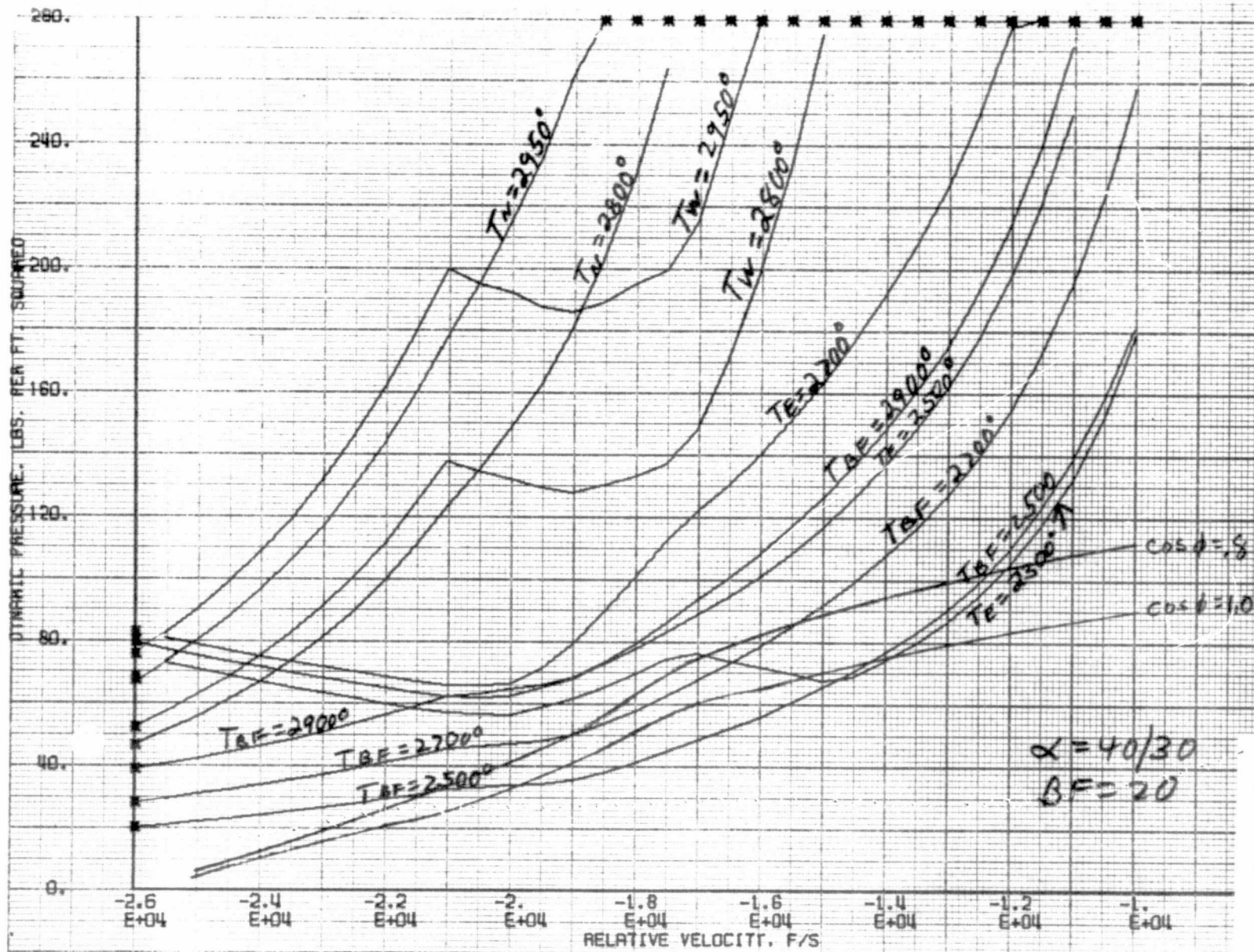


FIGURE 51 DYNAMIC PRESSURE VS. VELOCITY CORRIDOR

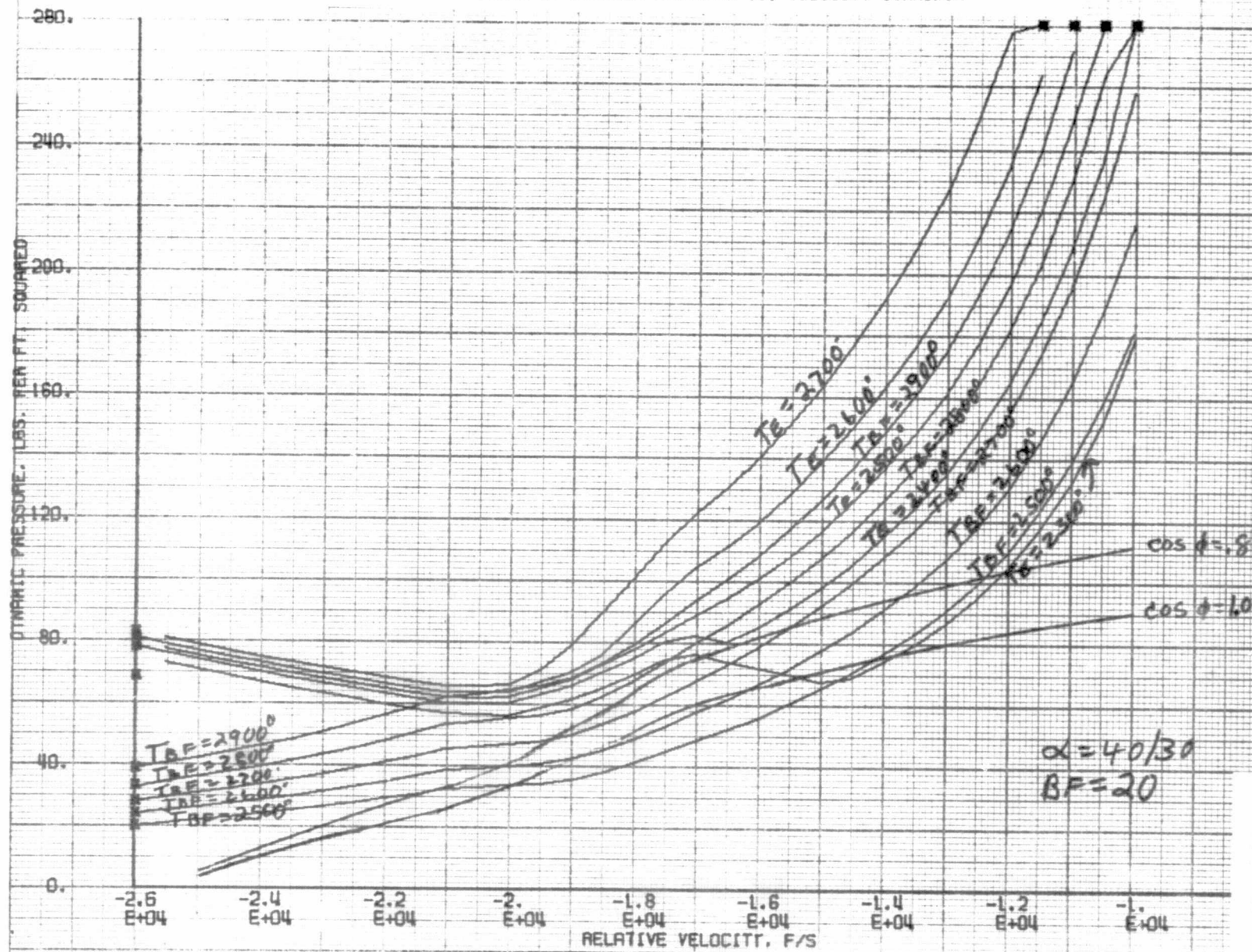




FIGURE 52 DYNAMIC PRESSURE VS. VELOCITY CORRIDOR

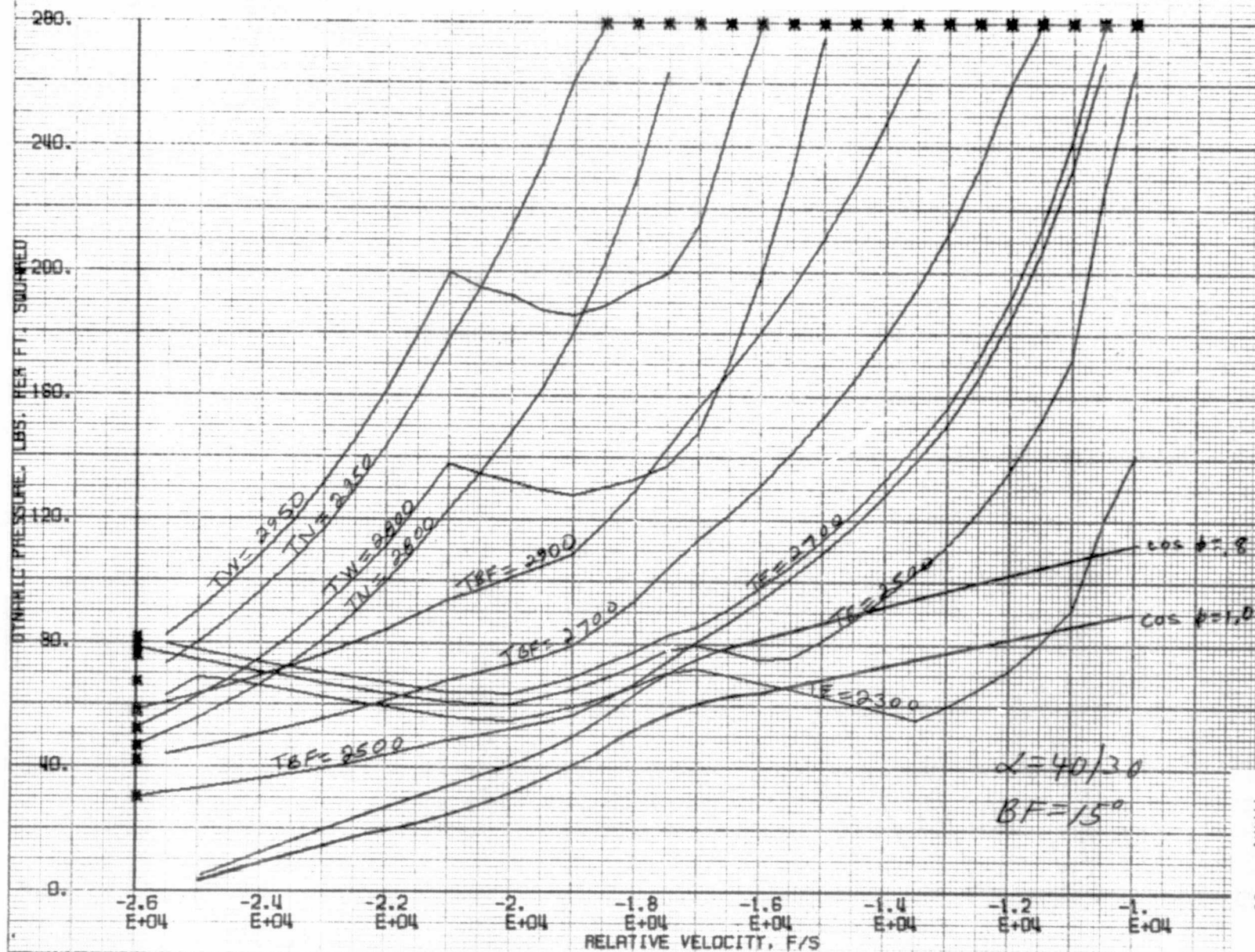


FIGURE 53 DYNAMIC PRESSURE VS. VELOCITY CORRIDOR

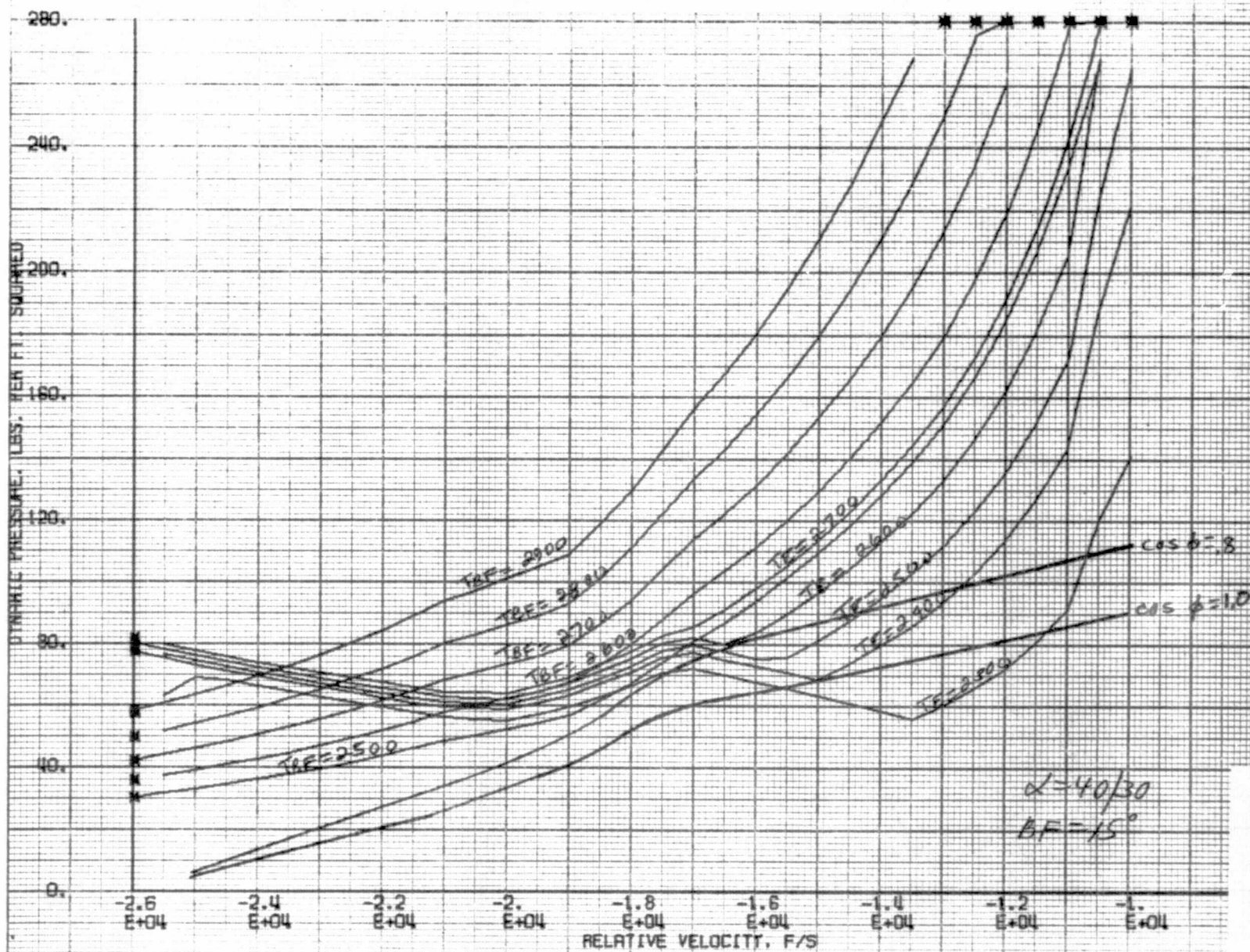




FIGURE 54 DYNAMIC PRESSURE VS. VELOCITY CORRIDOR

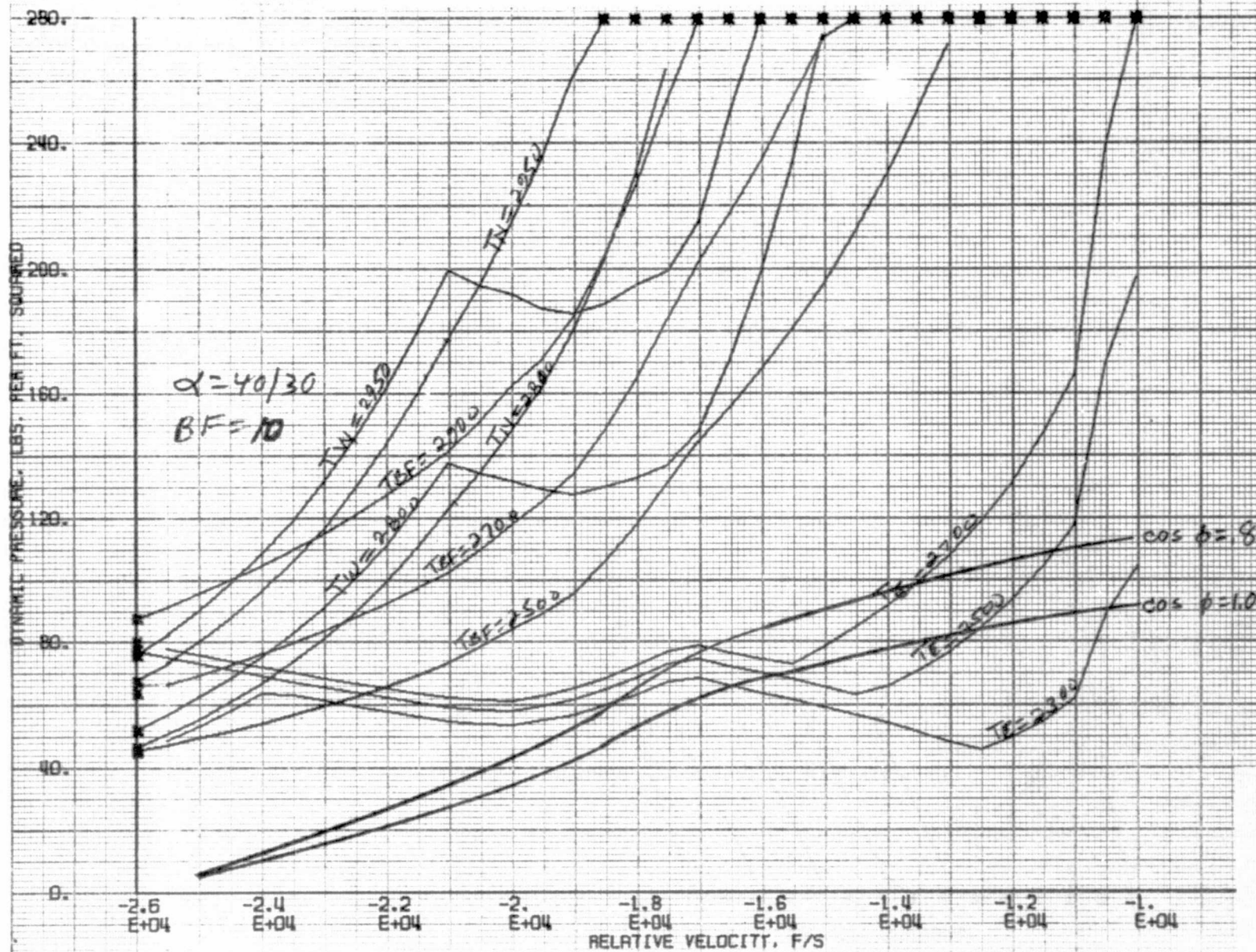




FIGURE 55 DYNAMIC PRESSURE VS. VELOCITY CORRIDOR

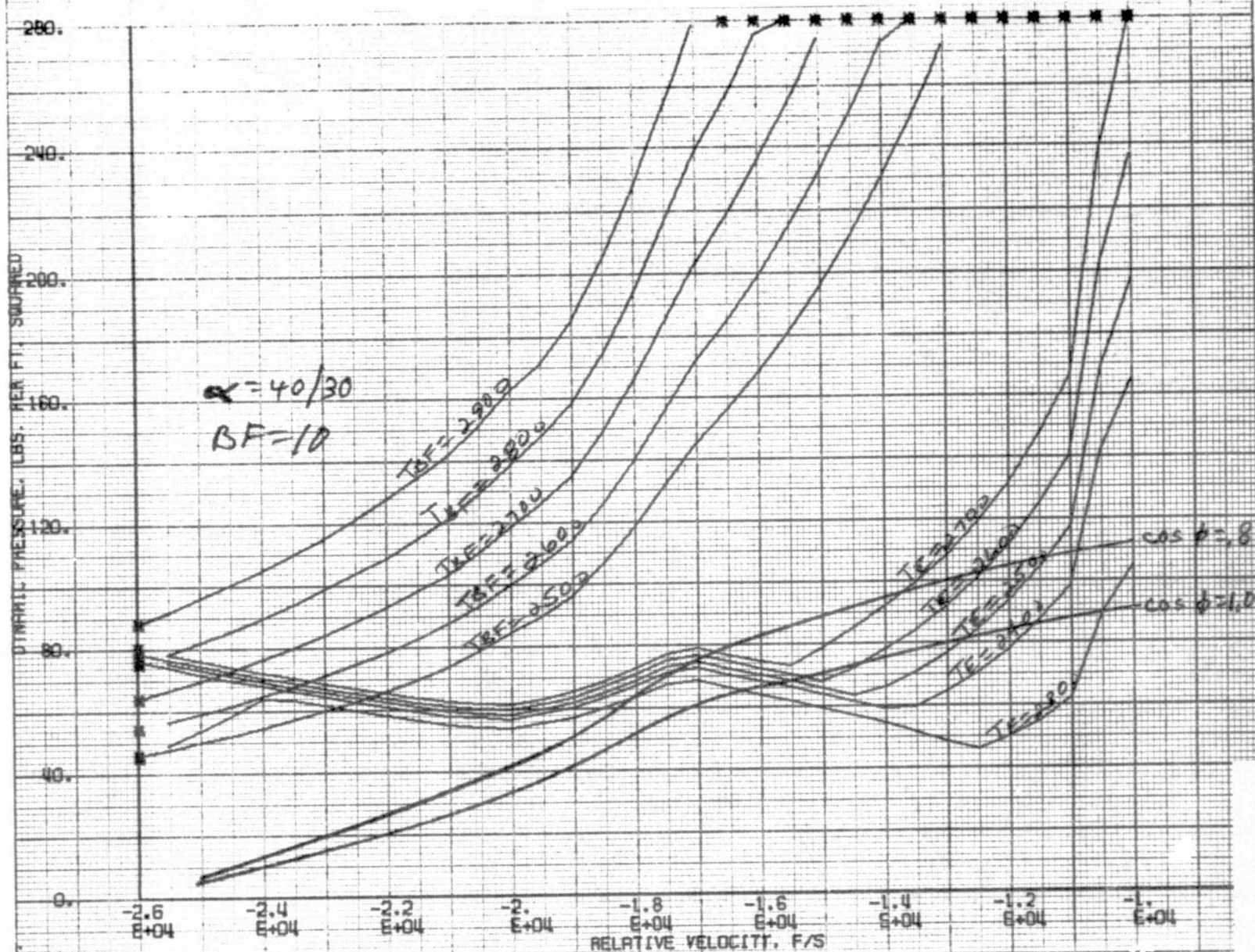


FIGURE 56 DYNAMIC PRESSURE VS. VELOCITY CORRIDOR

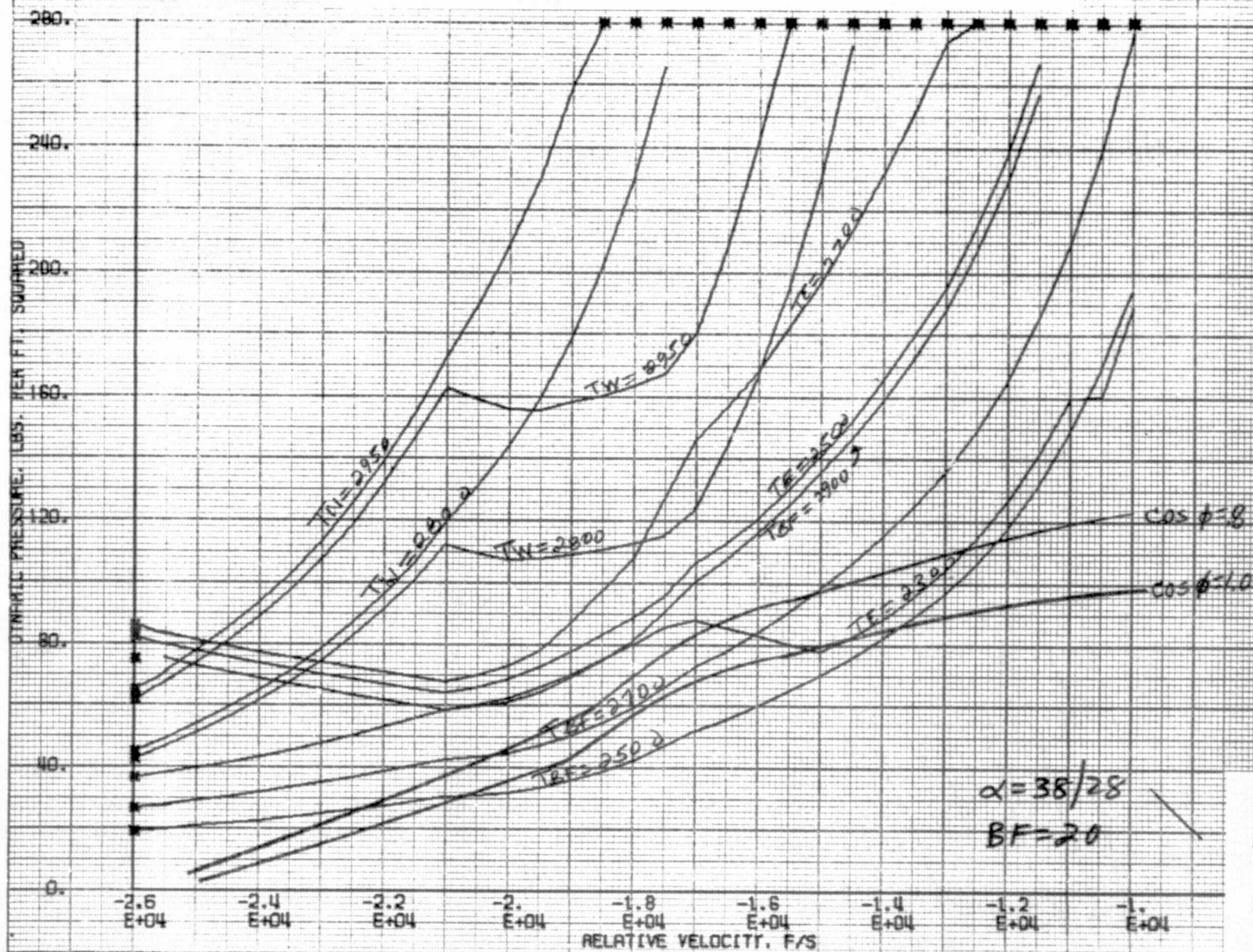




FIGURE 57 DYNAMIC PRESSURE VS. VELOCITY CORRIDOR

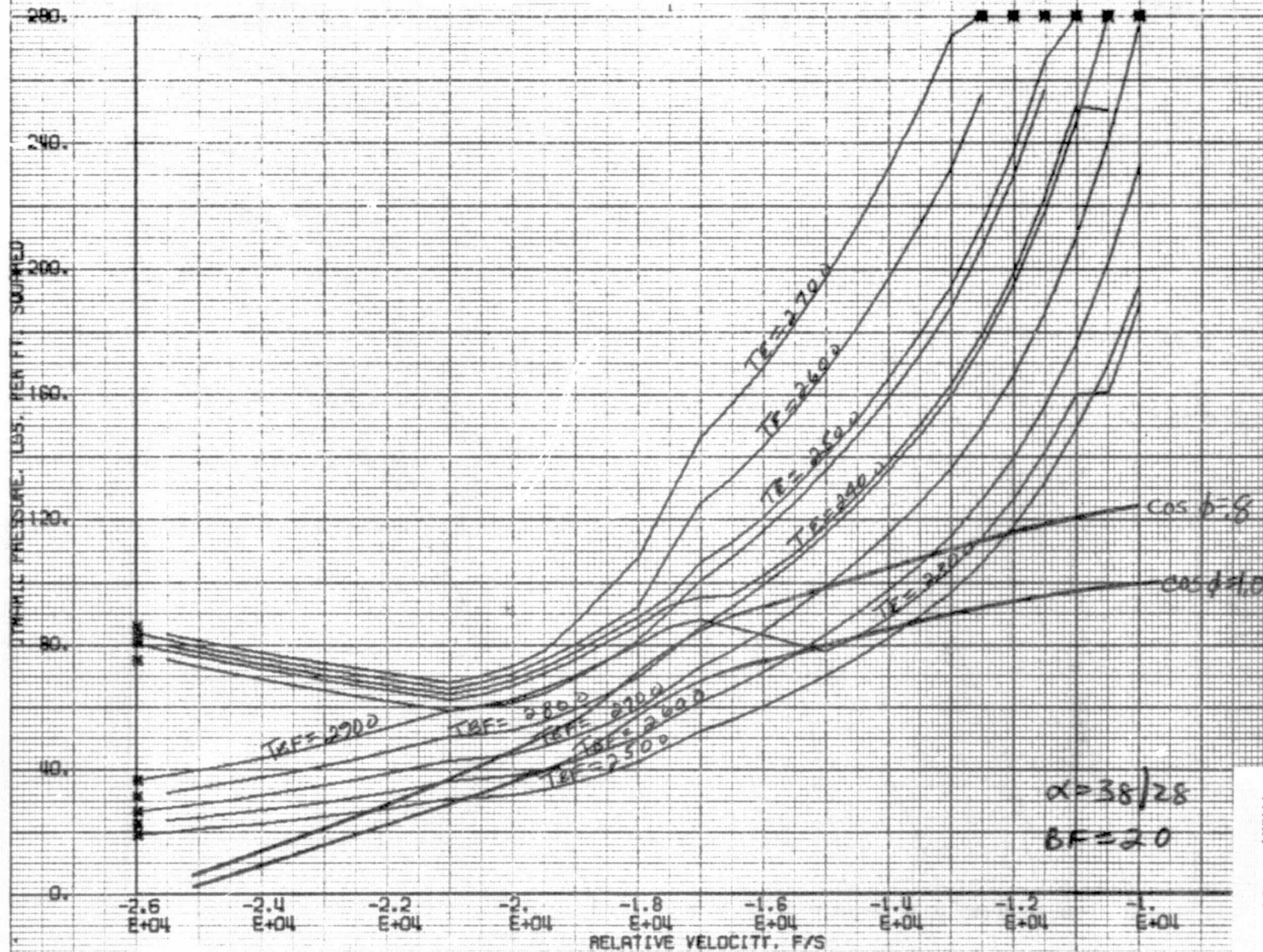




FIGURE 58 DYNAMIC PRESSURE VS. VELOCITY CORRIDOR

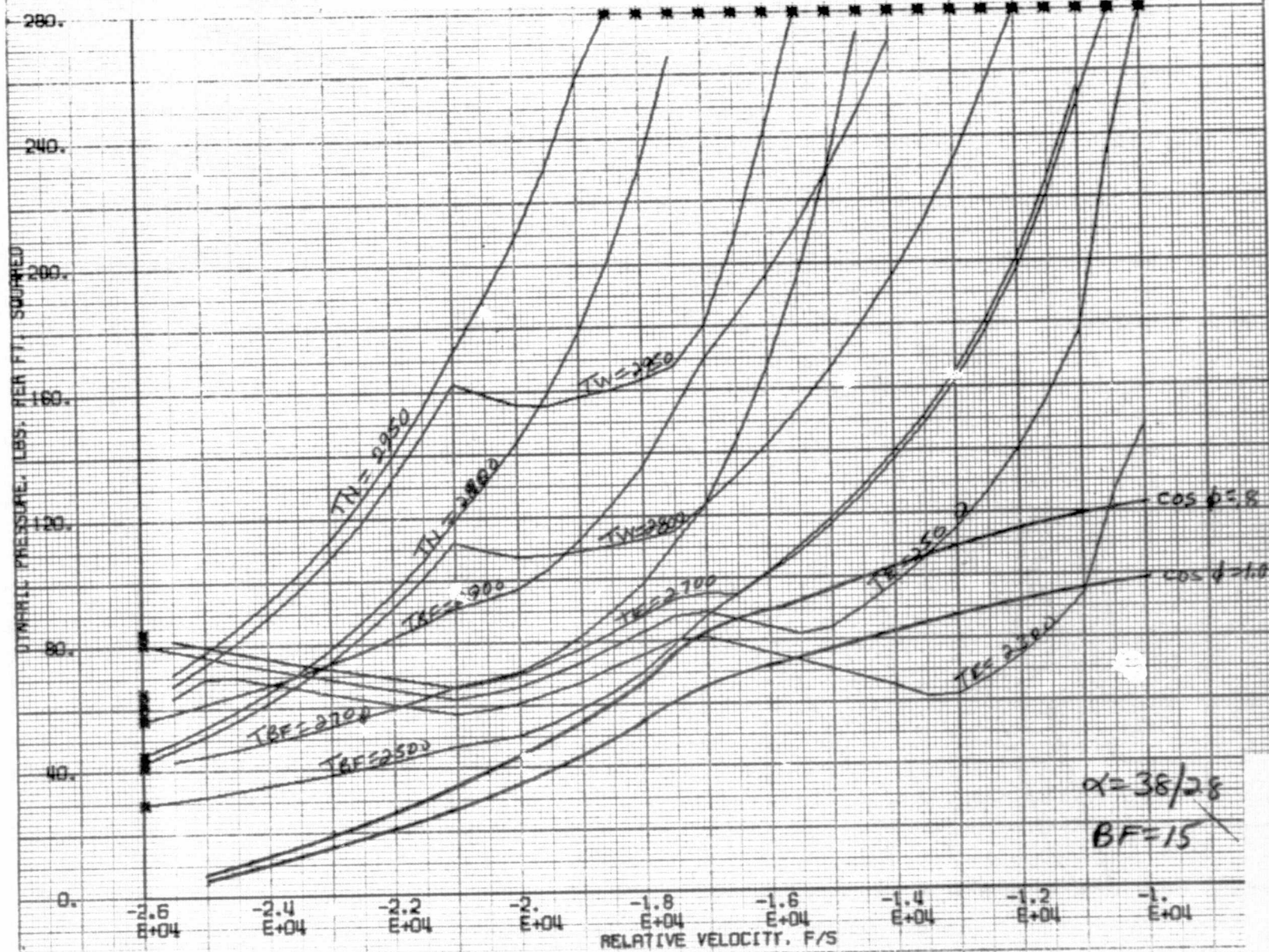


FIGURE 59 DYNAMIC PRESSURE VS. VELOCITY CORRIDOR

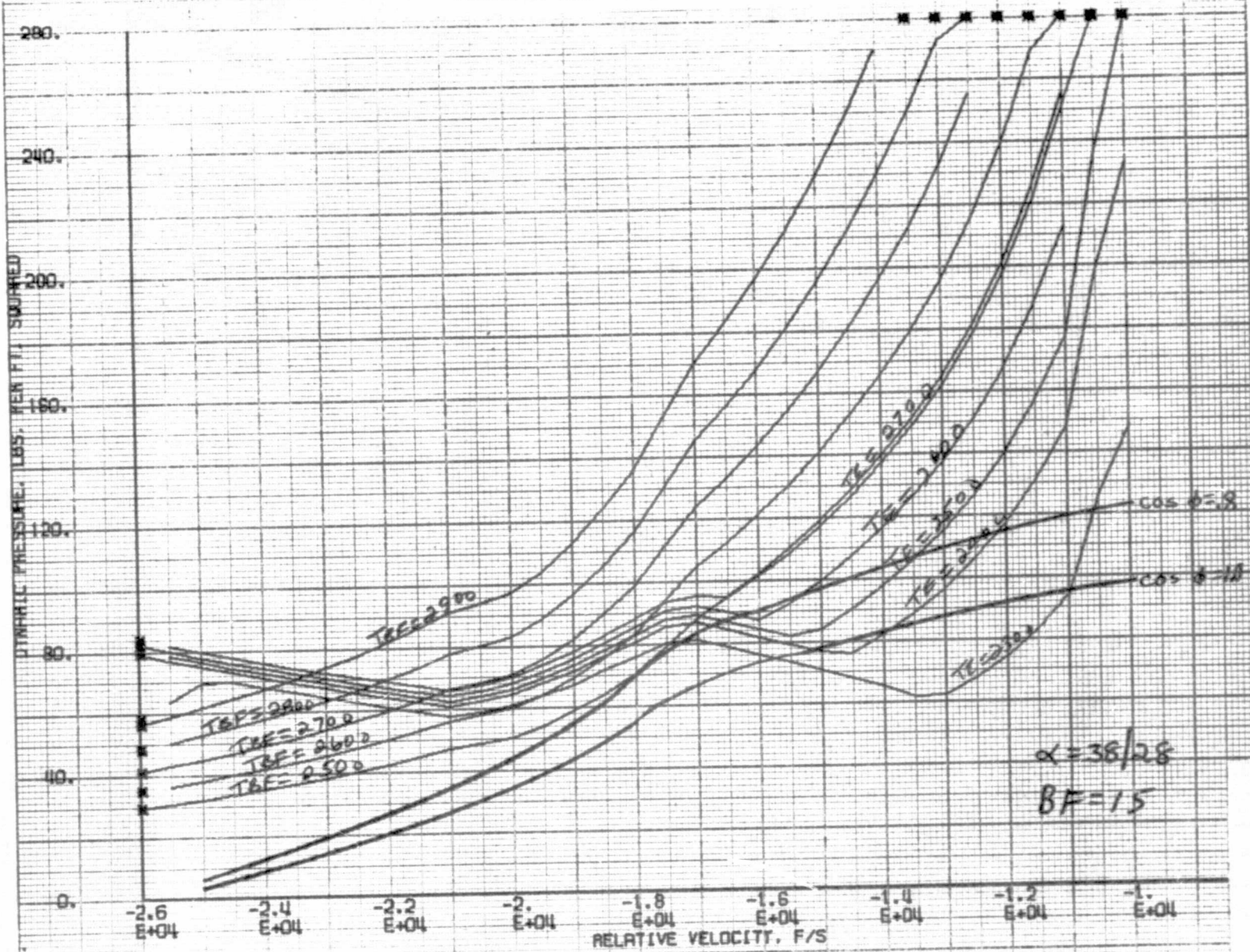


FIGURE 60 DYNAMIC PRESSURE VS. VELOCITY CORRIDOR

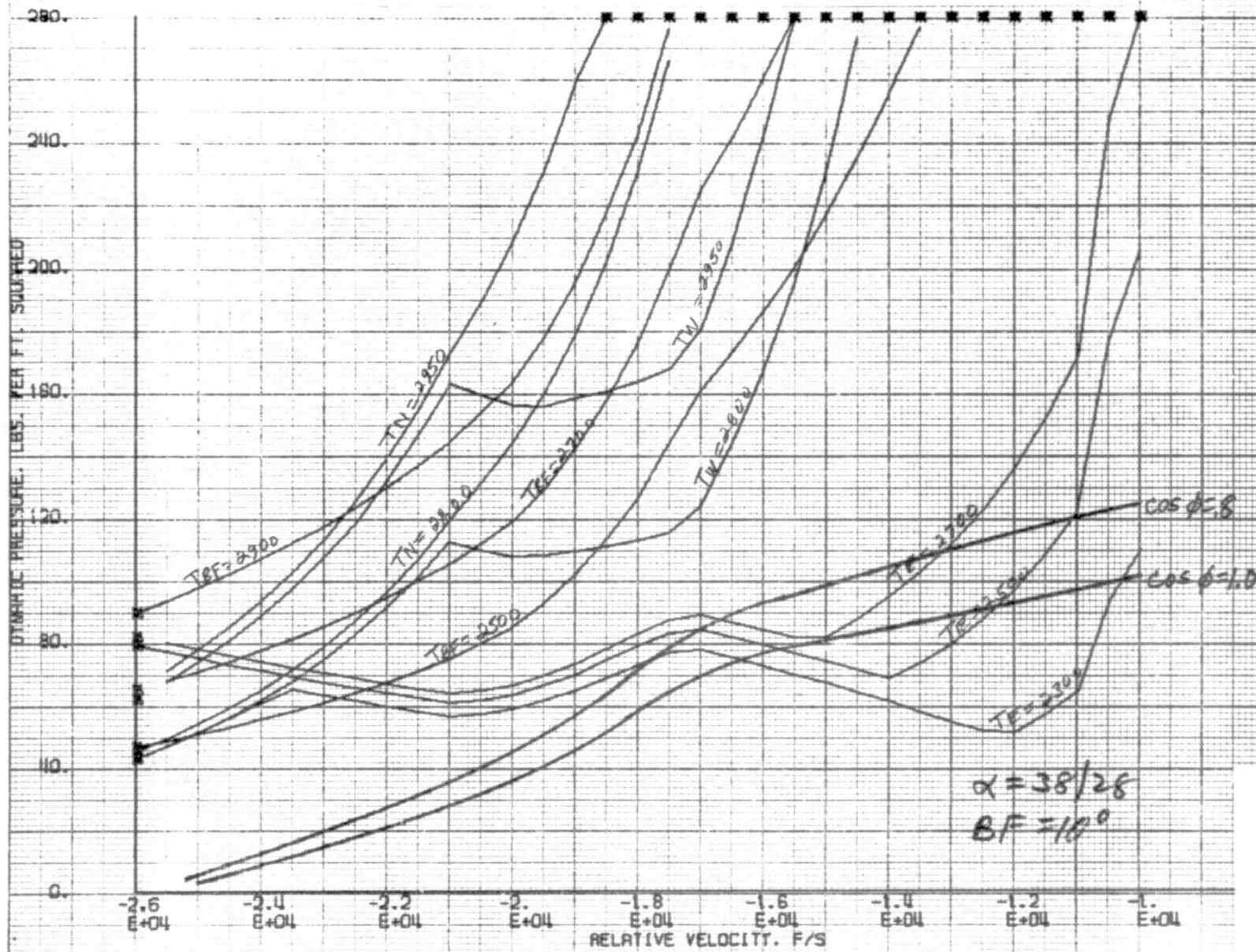




FIGURE 61 DYNAMIC PRESSURE VS. VELOCITY CORRIDOR

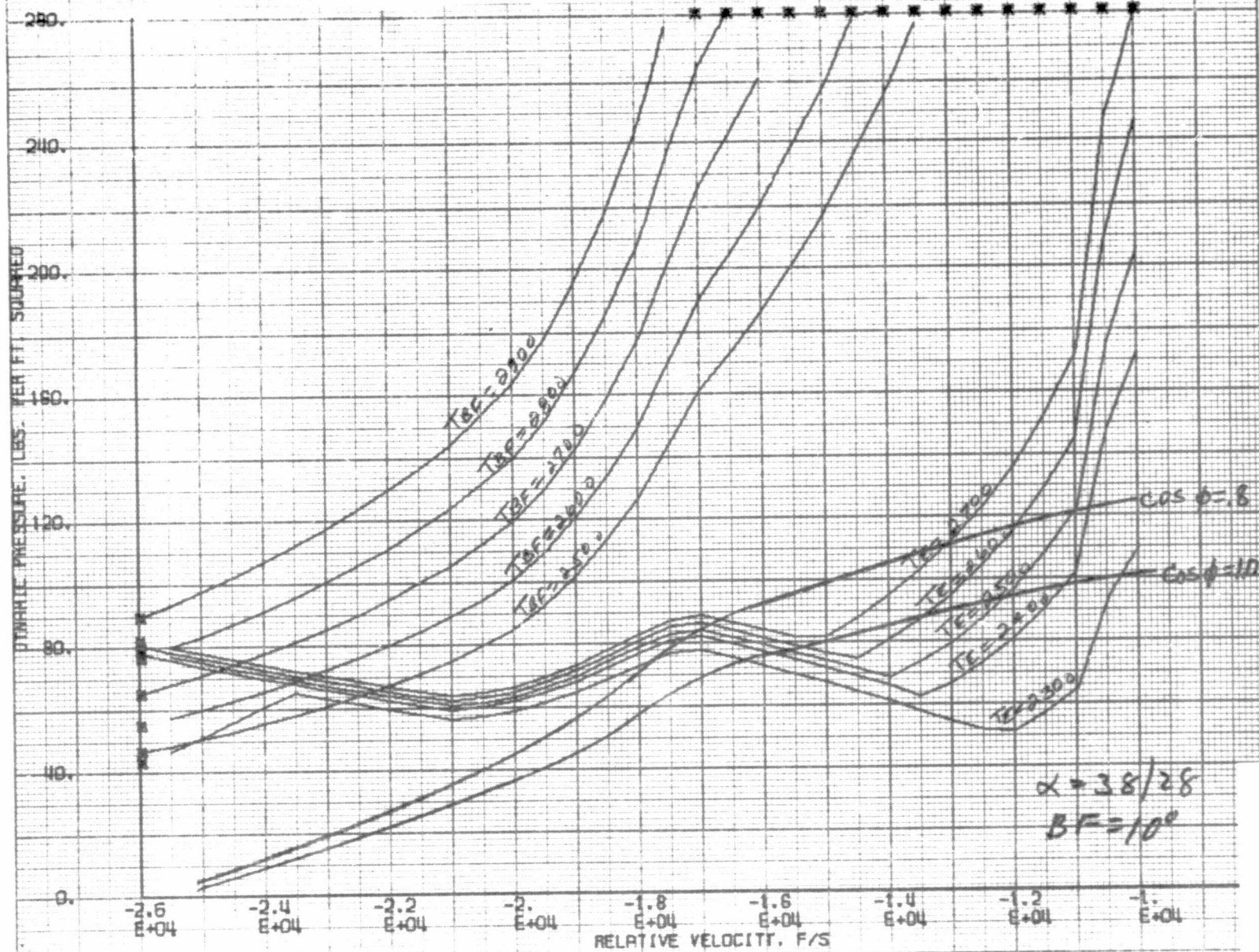


FIGURE 62 DYNAMIC PRESSURE VS. VELOCITY CORRIDOR

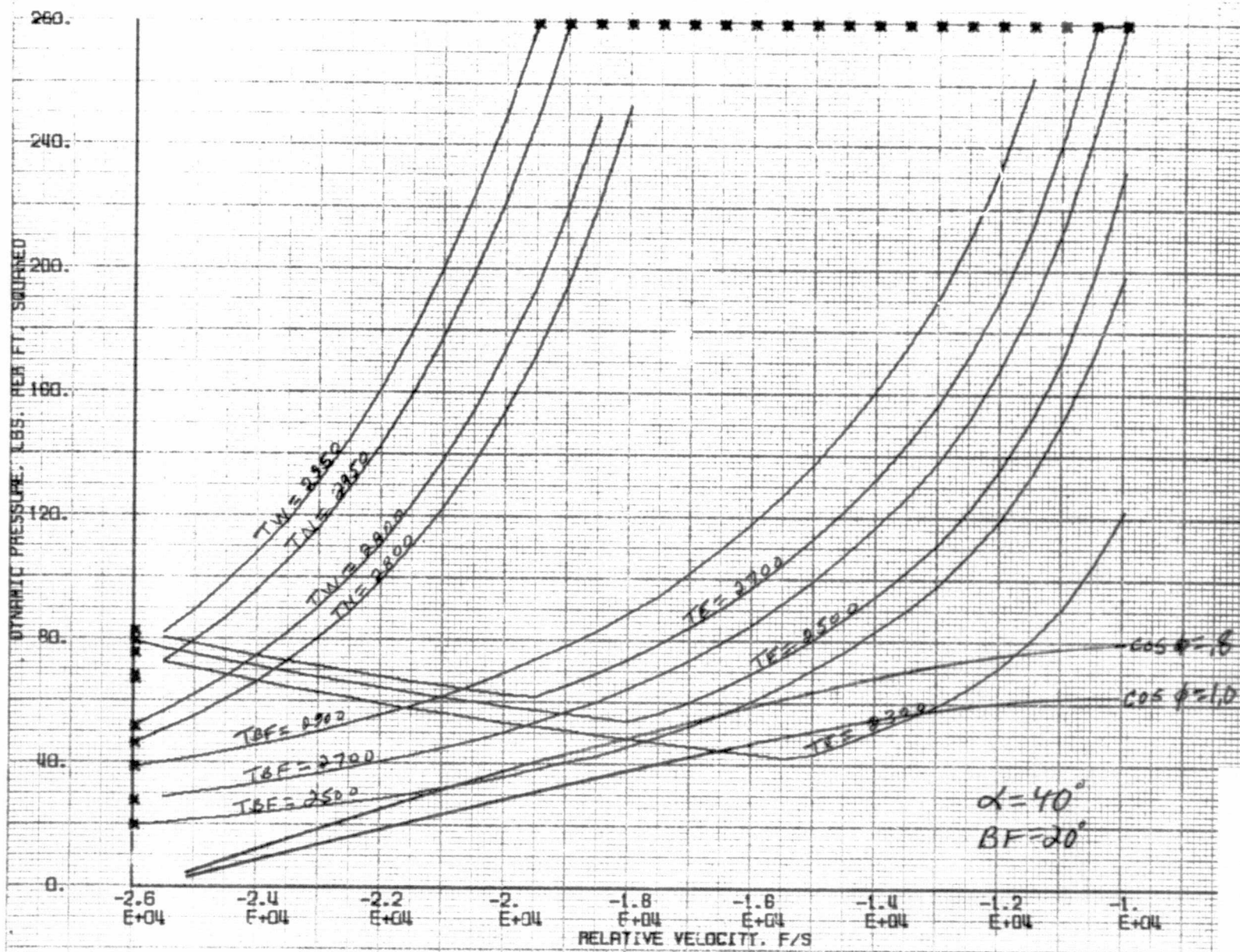


FIGURE 63 DYNAMIC PRESSURE VS. VELOCITY CORRIDOR

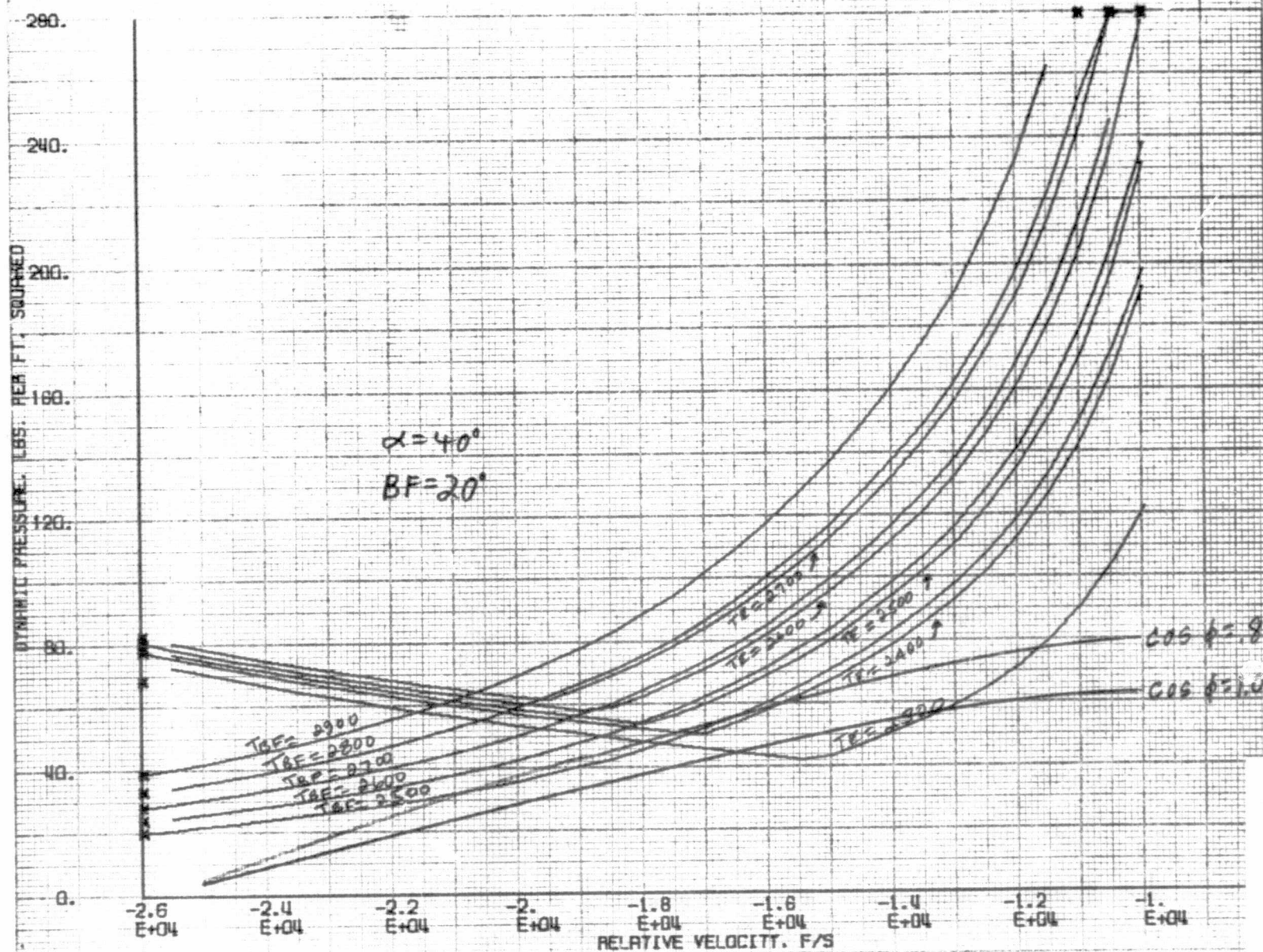




FIGURE 64 DYNAMIC PRESSURE VS. VELOCITY CORRIDOR

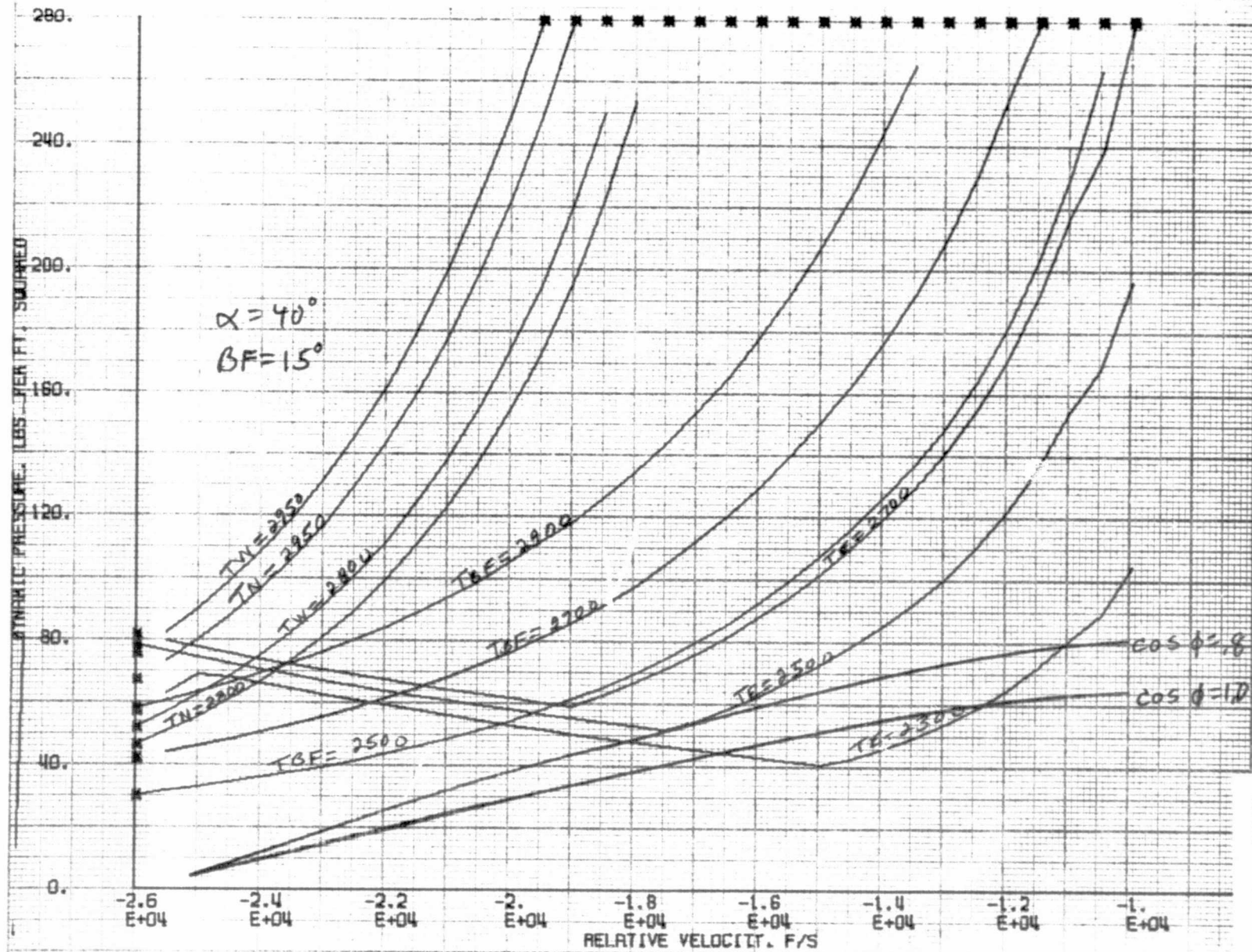
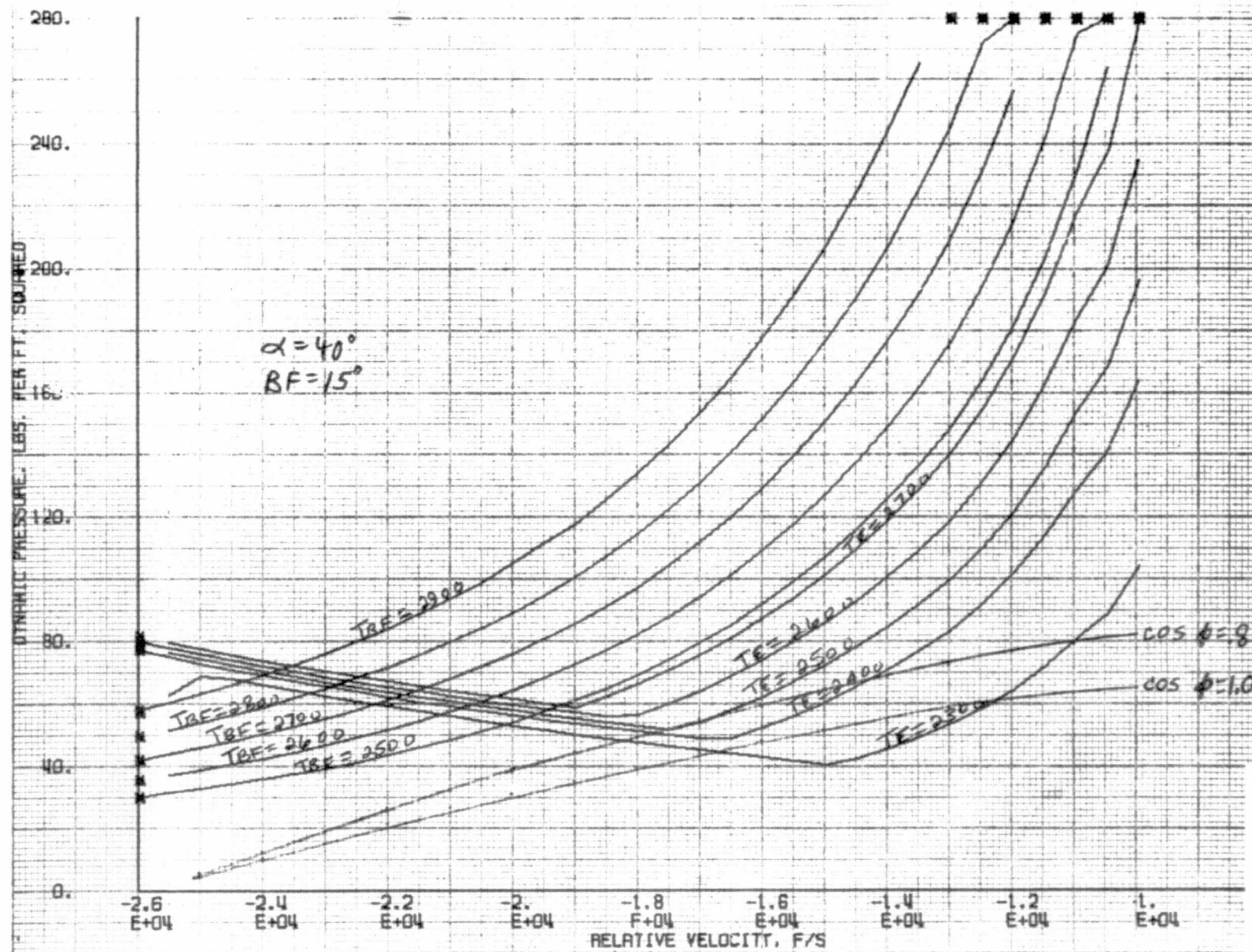


FIGURE 65 DYNAMIC PRESSURE VS. VELOCITY CORRIDOR



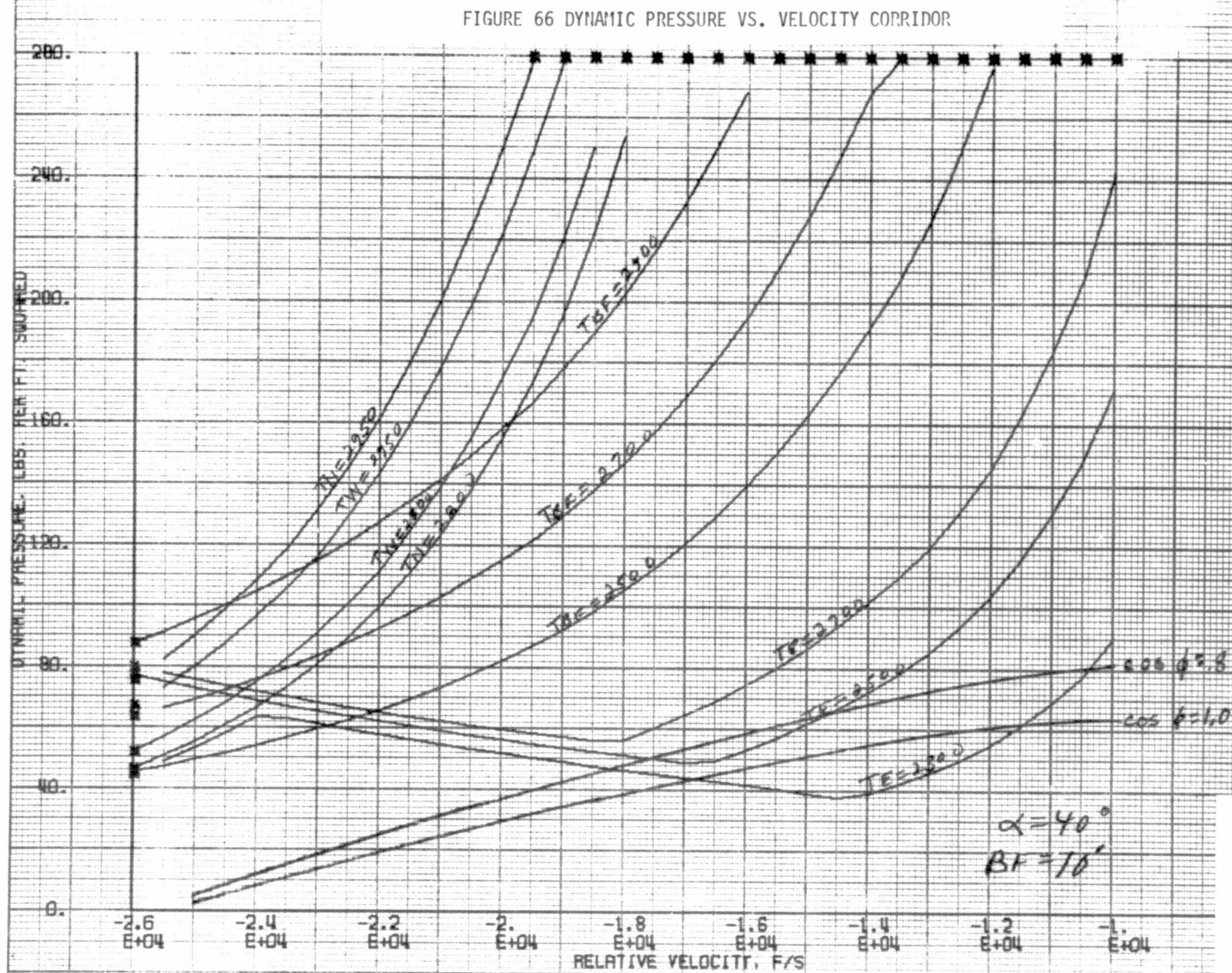




FIGURE 67 DYNAMIC PRESSURE VS. VELOCITY CORRIDOR

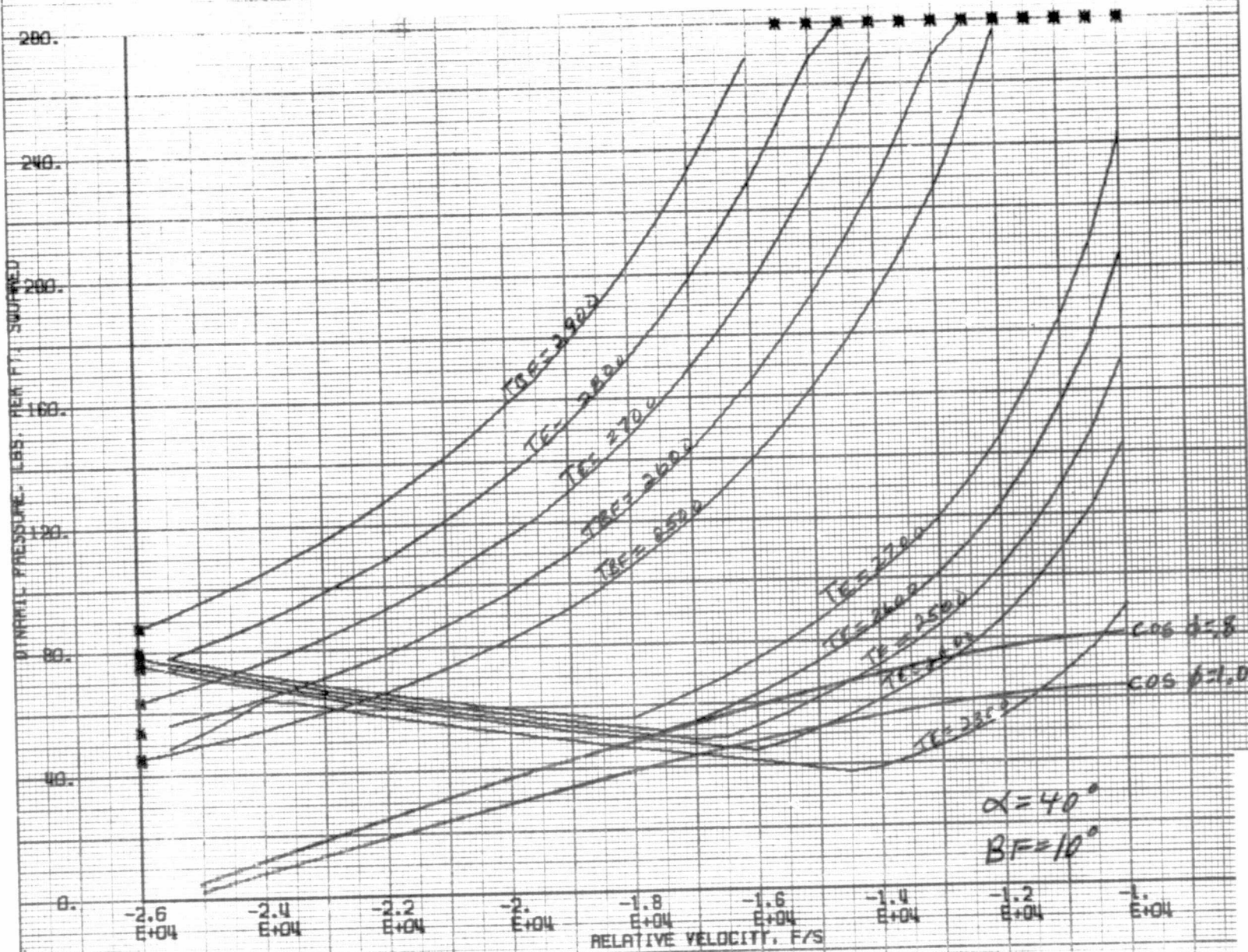


FIGURE 68 DYNAMIC PRESSURE VS. VELOCITY CORRIDOR

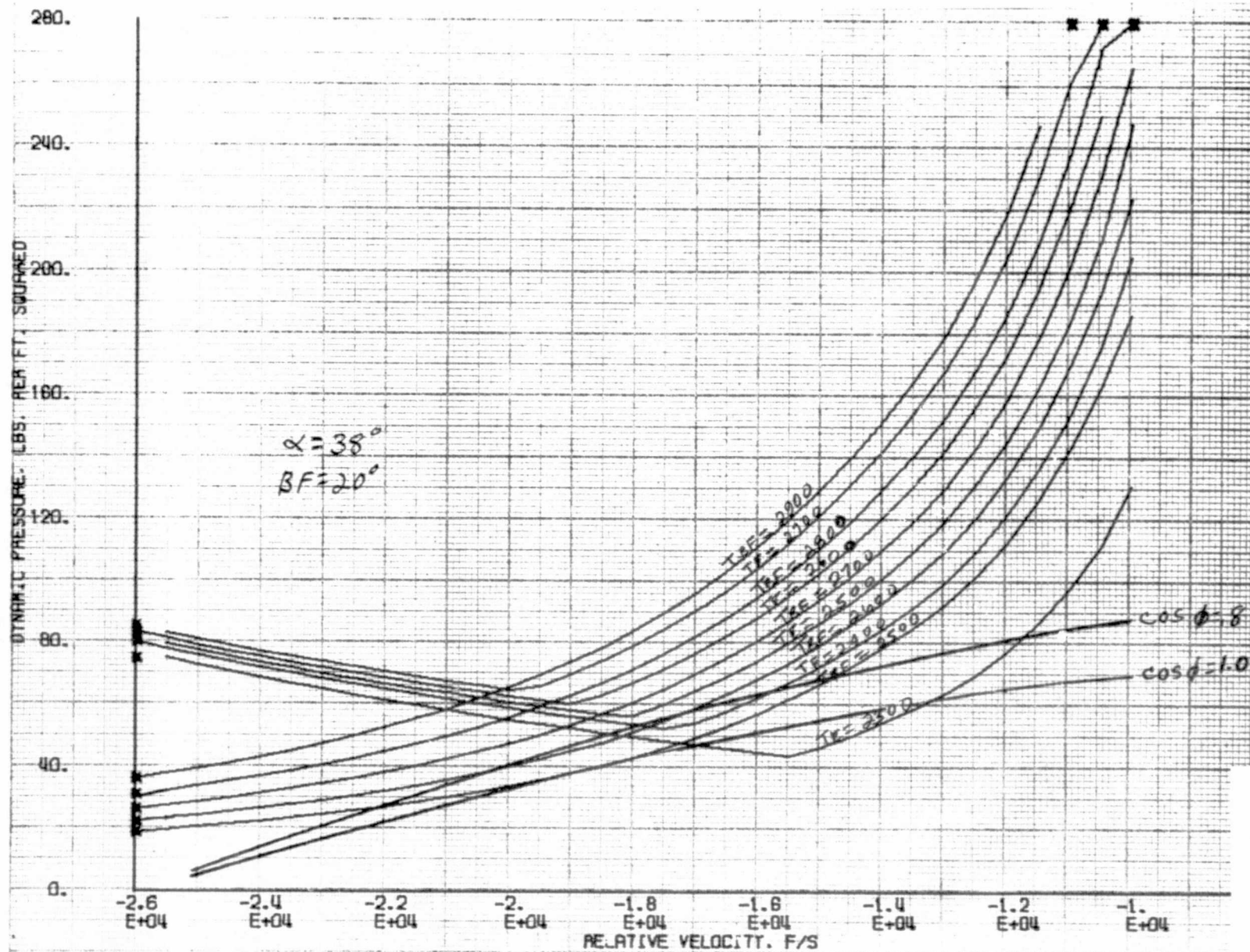


FIGURE 69 DYNAMIC PRESSURE VS. VELOCITY CORRIDOR

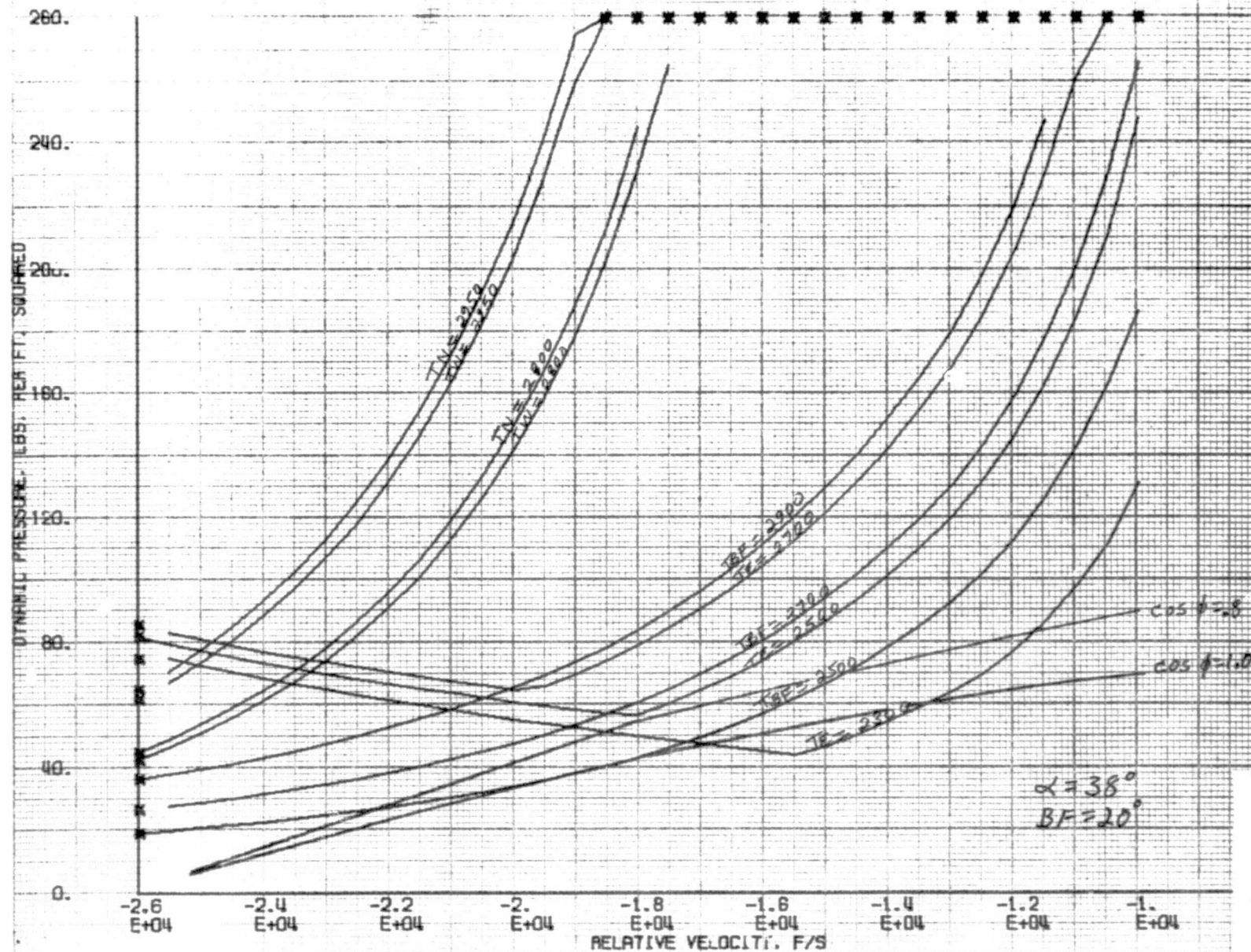




FIGURE 70 DYNAMIC PRESSURE VS. VELOCITY CORRIDOR

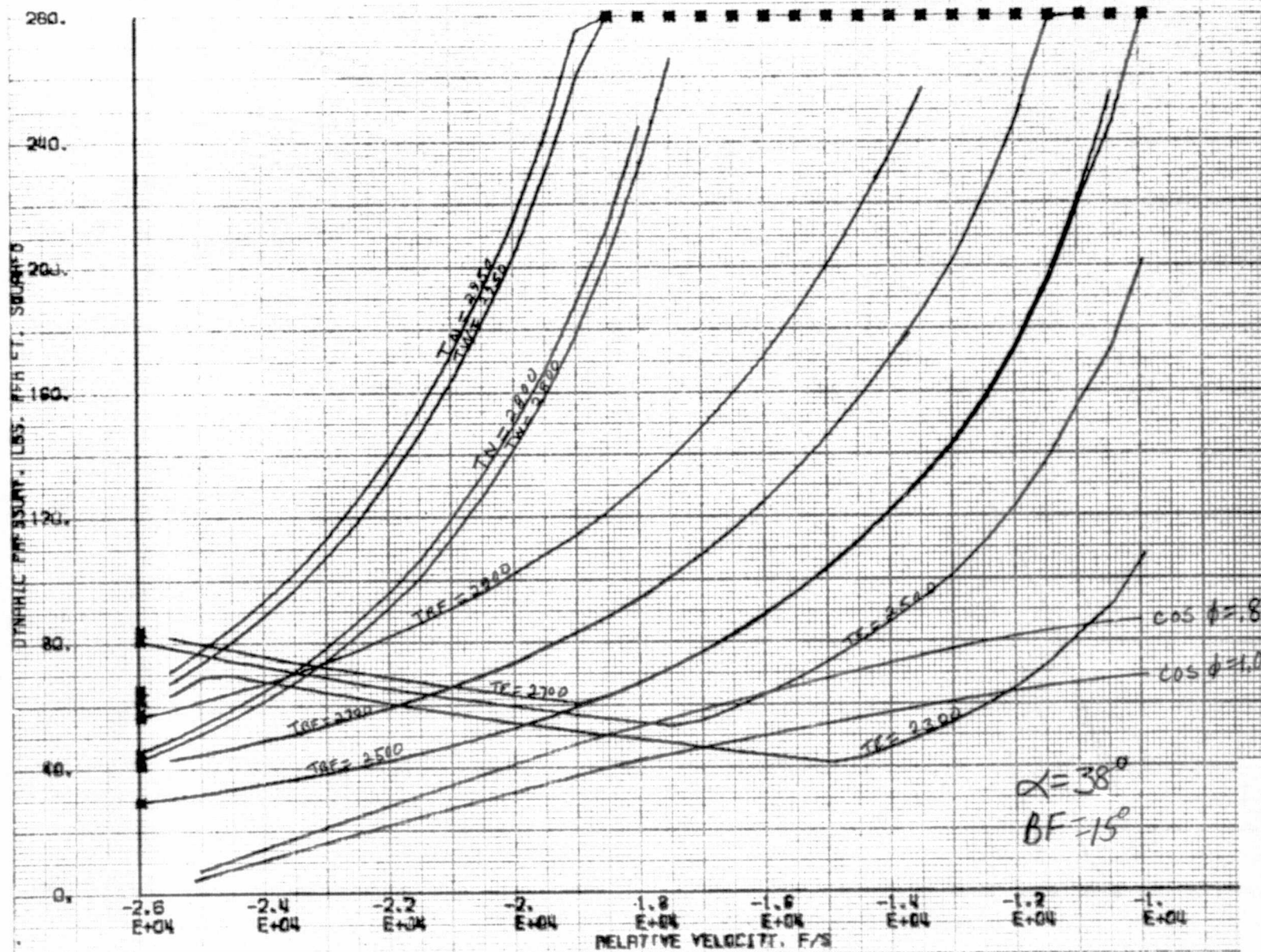


FIGURE 71 DYNAMIC PRESSURE VS. VELOCITY CORRIDOR

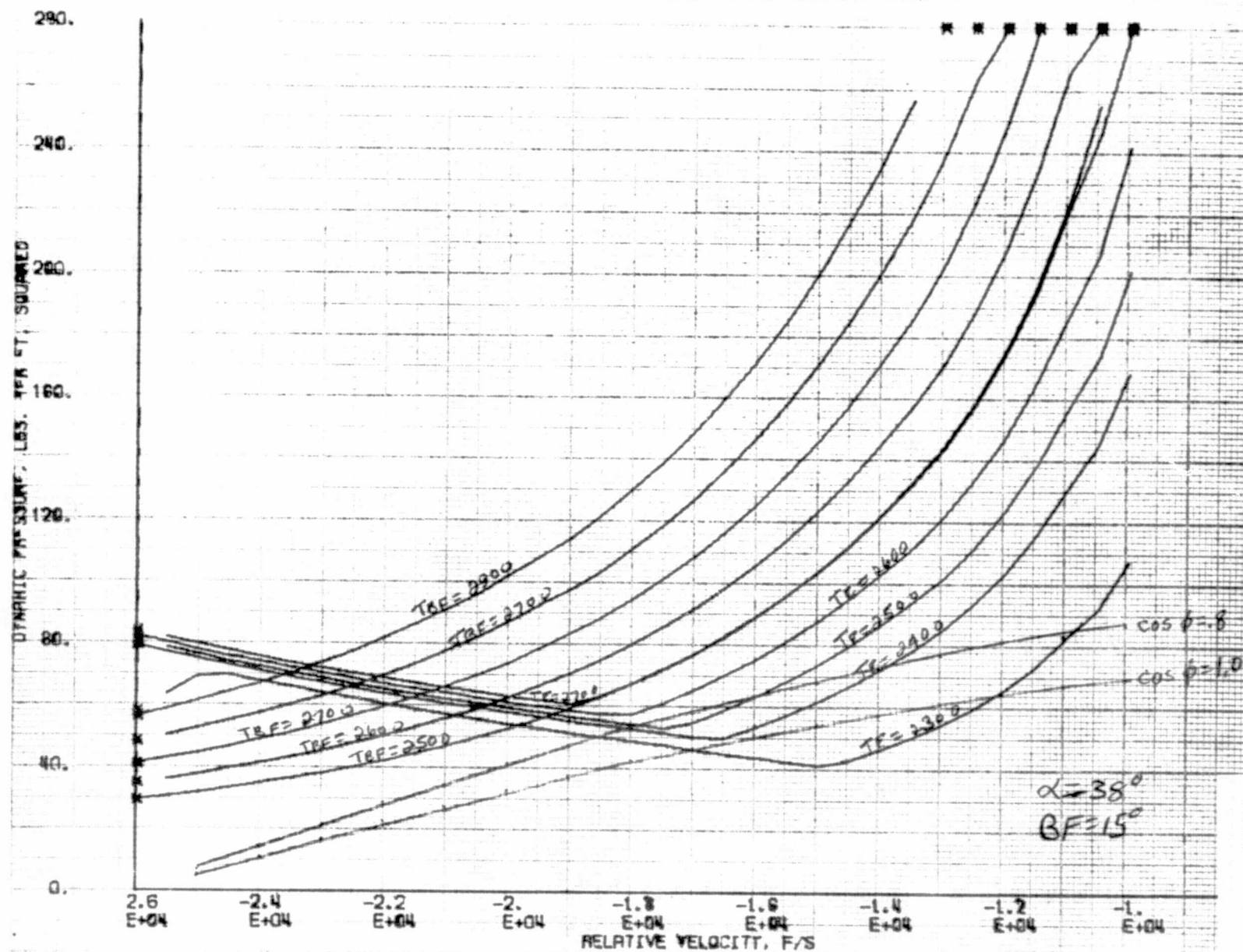


FIGURE 72 DYNAMIC PRESSURE VS. VELOCITY CORRIDOR

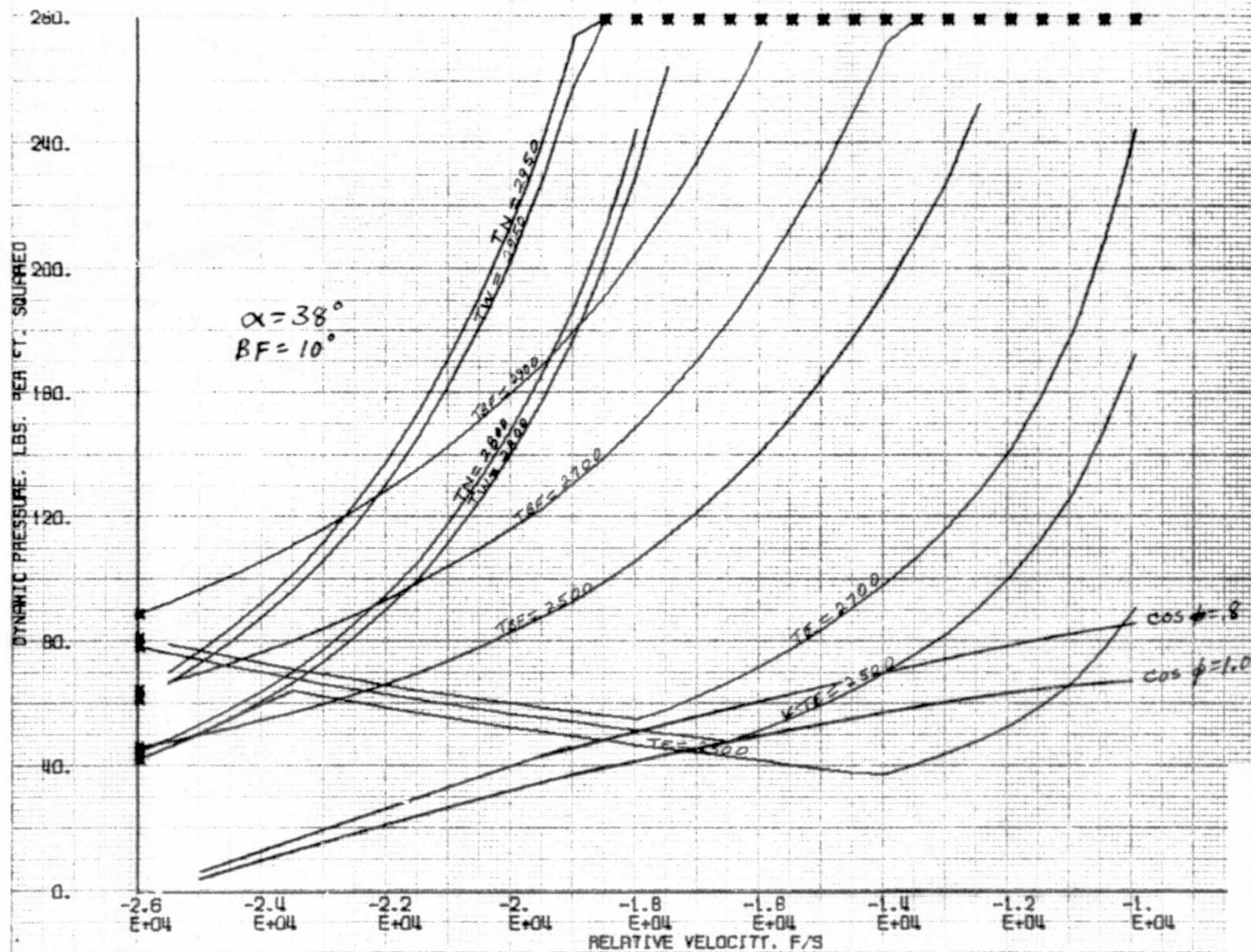




FIGURE 73 DYNAMIC PRESSURE VS. VELOCITY CORRIDOR

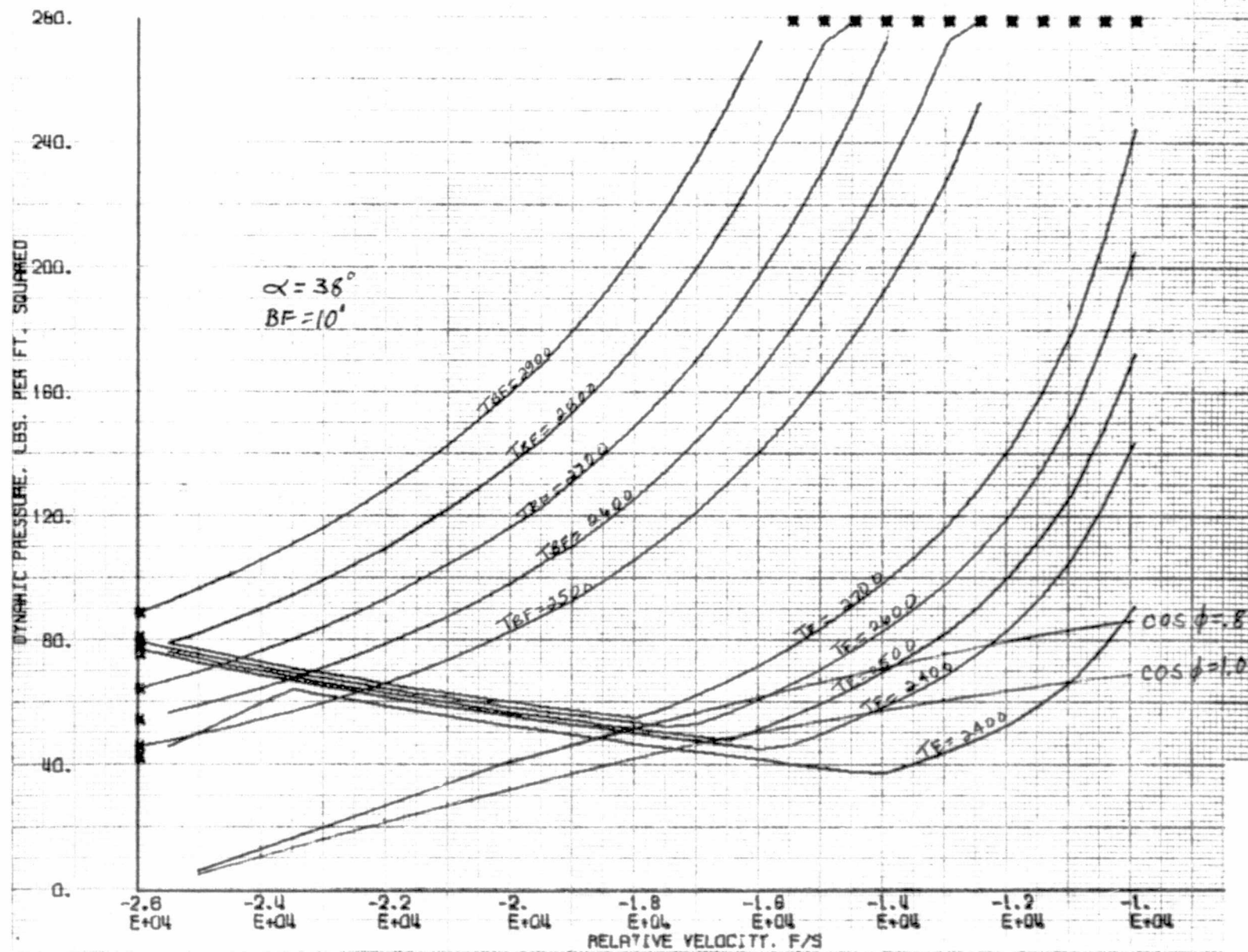


FIGURE 74 DYNAMIC PRESSURE VS. VELOCITY CORRIDOR

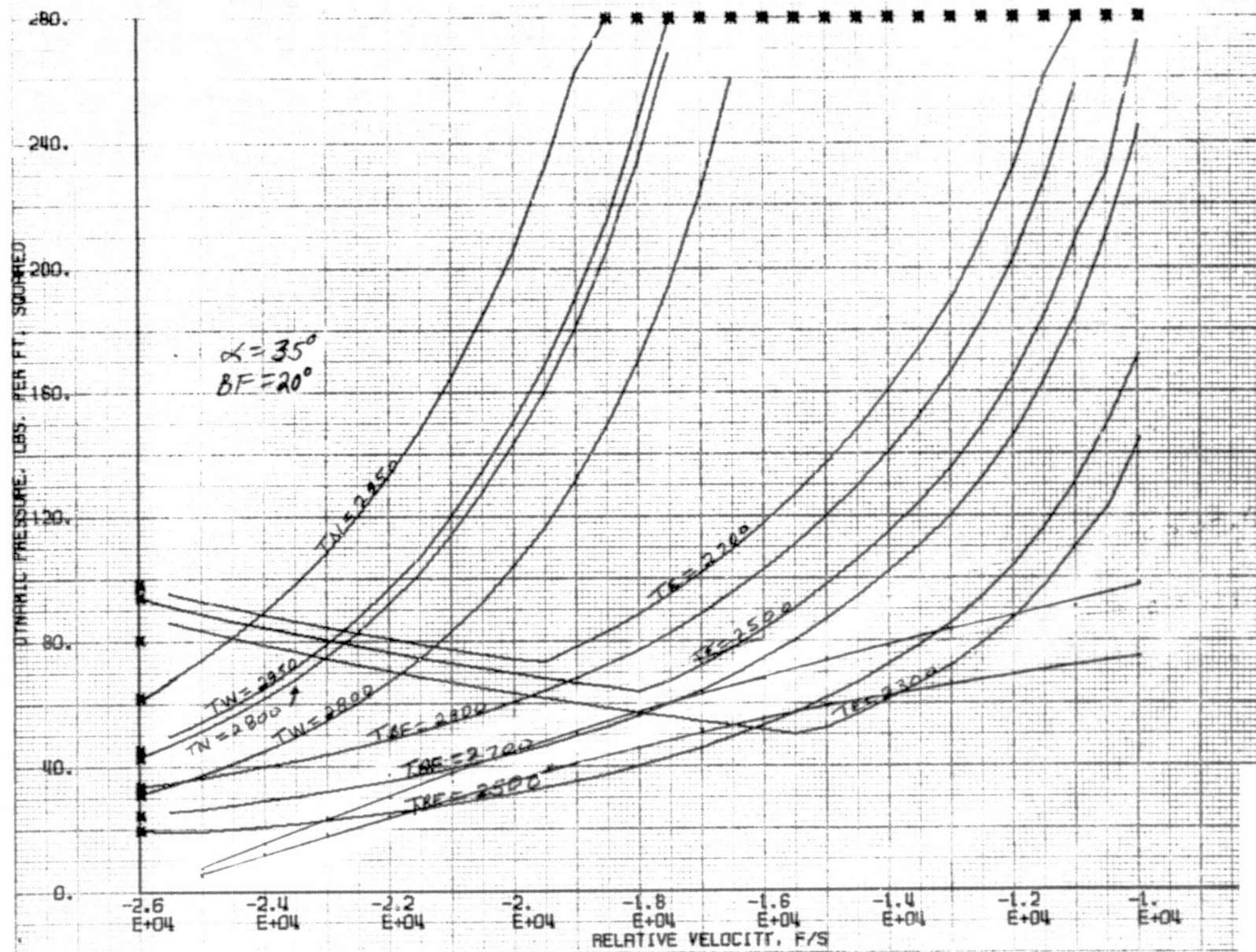
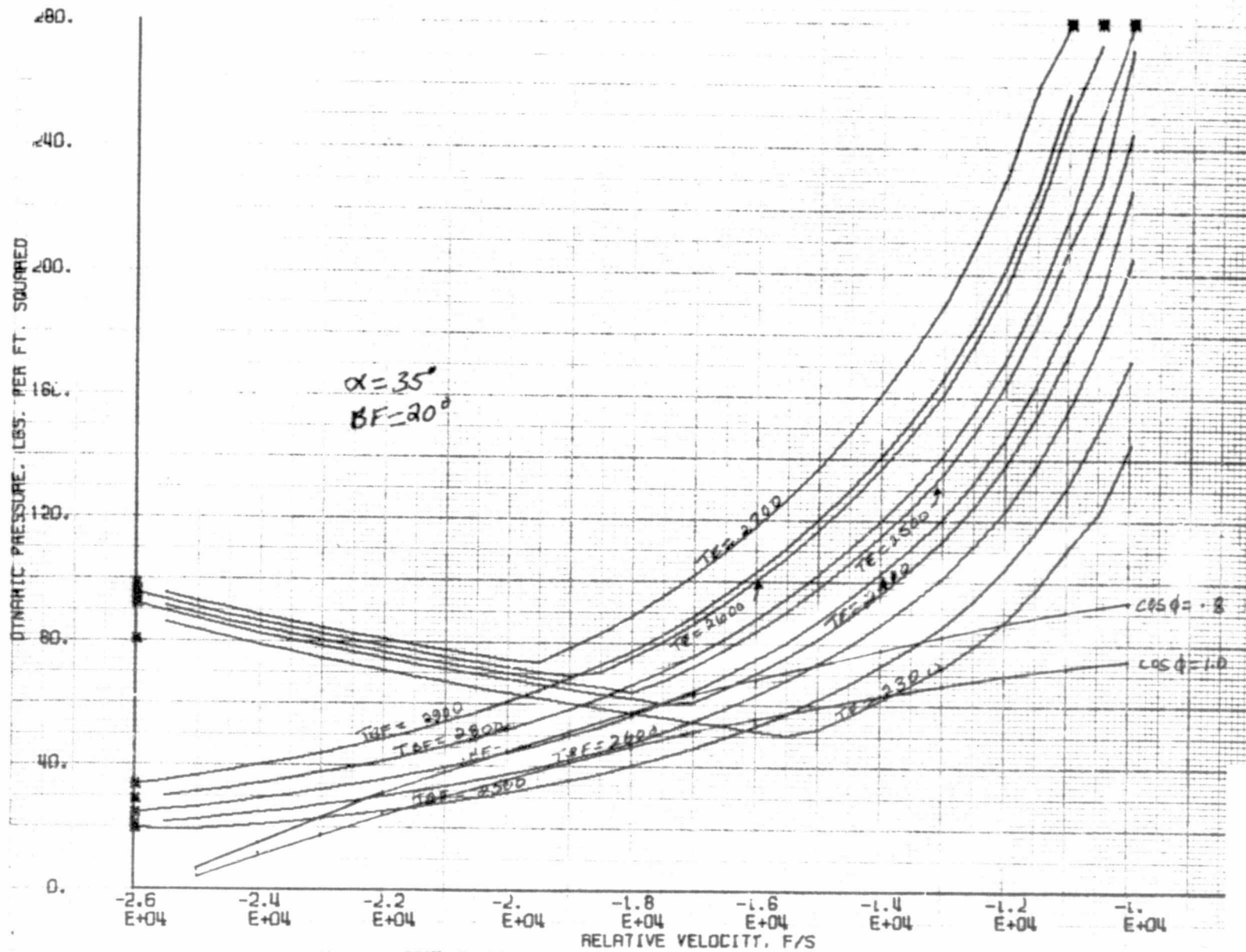


FIGURE 75 DYNAMIC PRESSURE VS. VELOCITY CORRIDOR





REPRODUCIBILITY OF THE ORIGINAL PAGE IS POOR

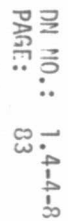


FIGURE 77 DYNAMIC PRESSURE VS. VELOCITY CORRIDOR

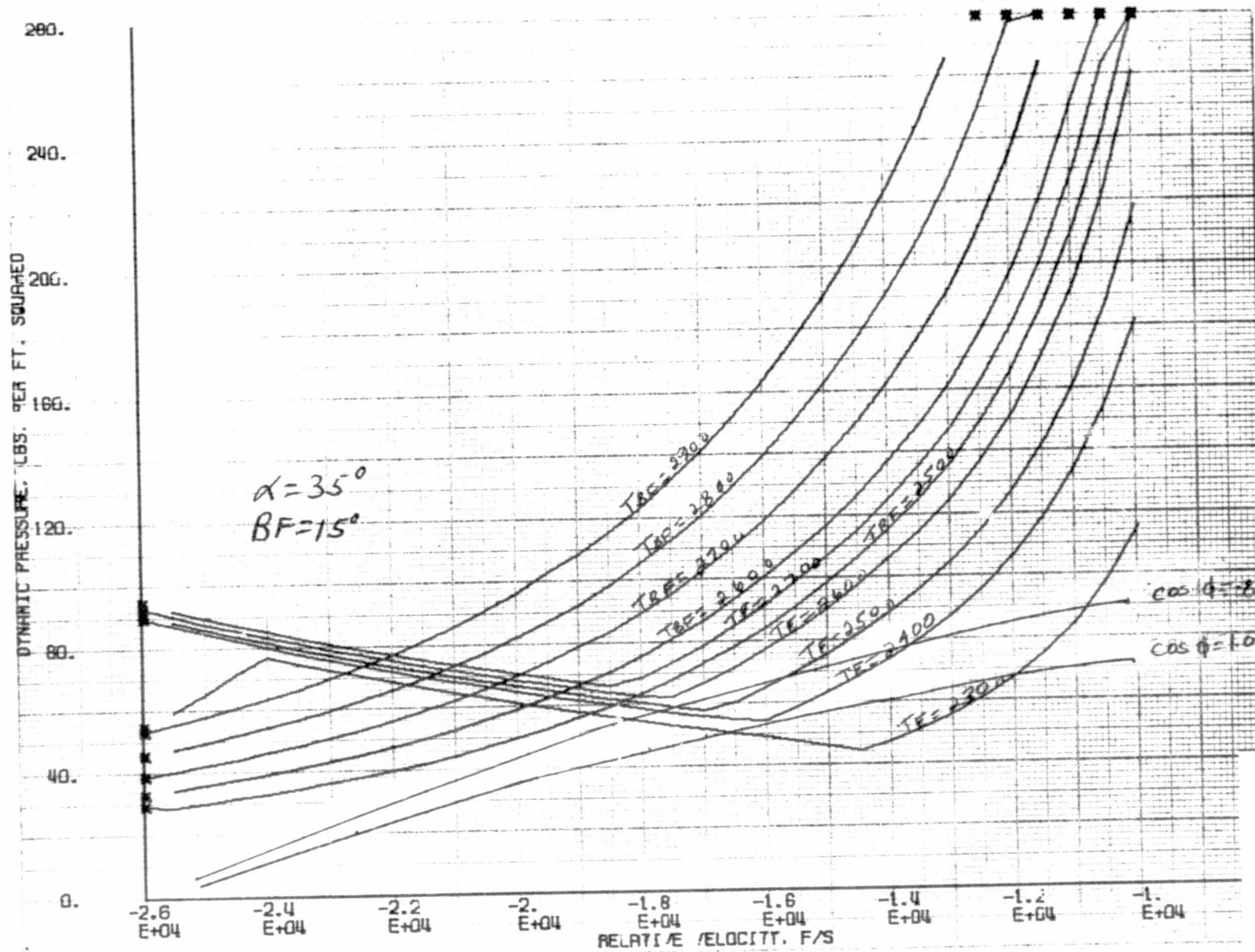


FIGURE 78 DYNAMIC PRESSURE VS. VELOCITY CORRIDOR

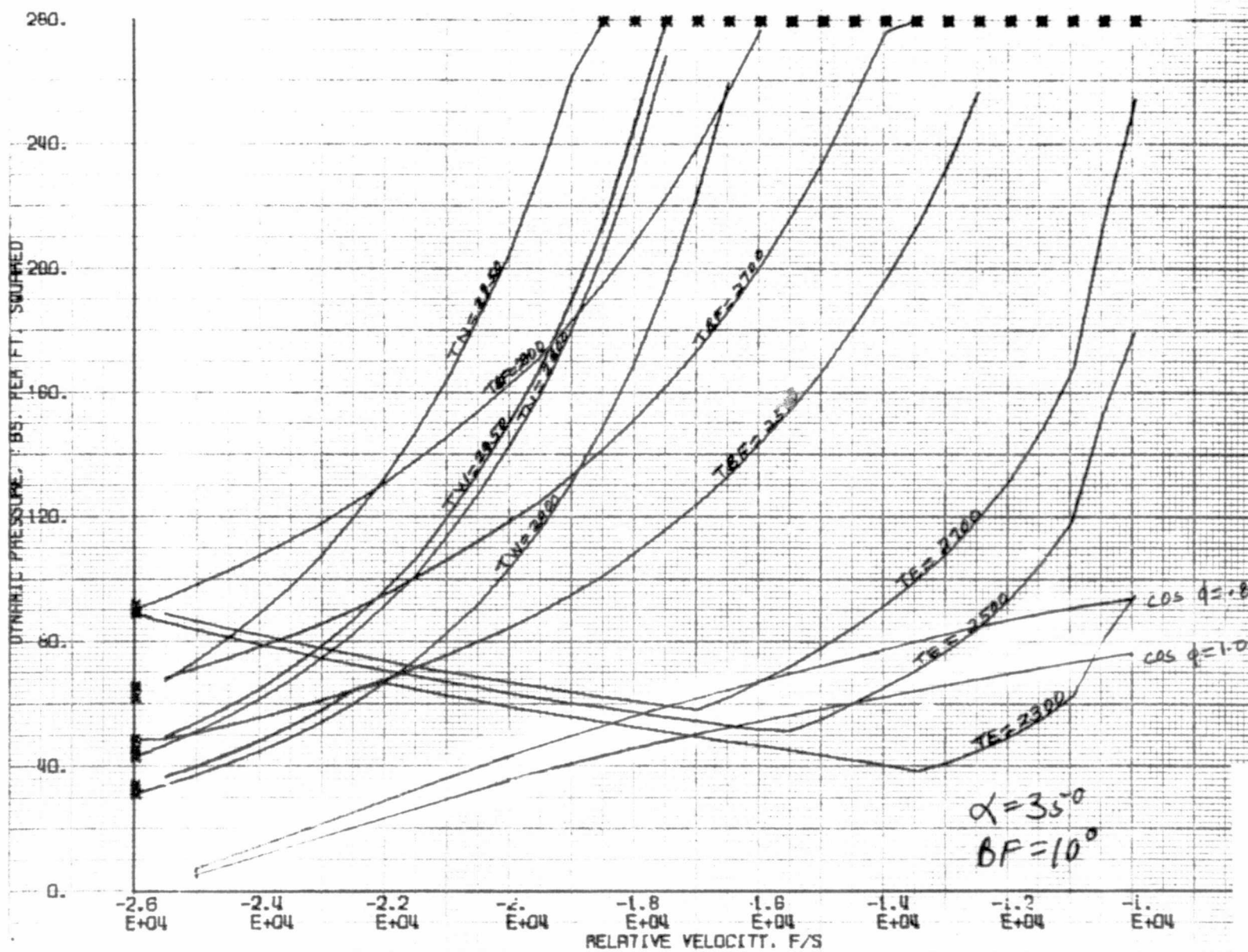




FIGURE 79 DYNAMIC PRESSURE VS. VELOCITY CORRIDOR

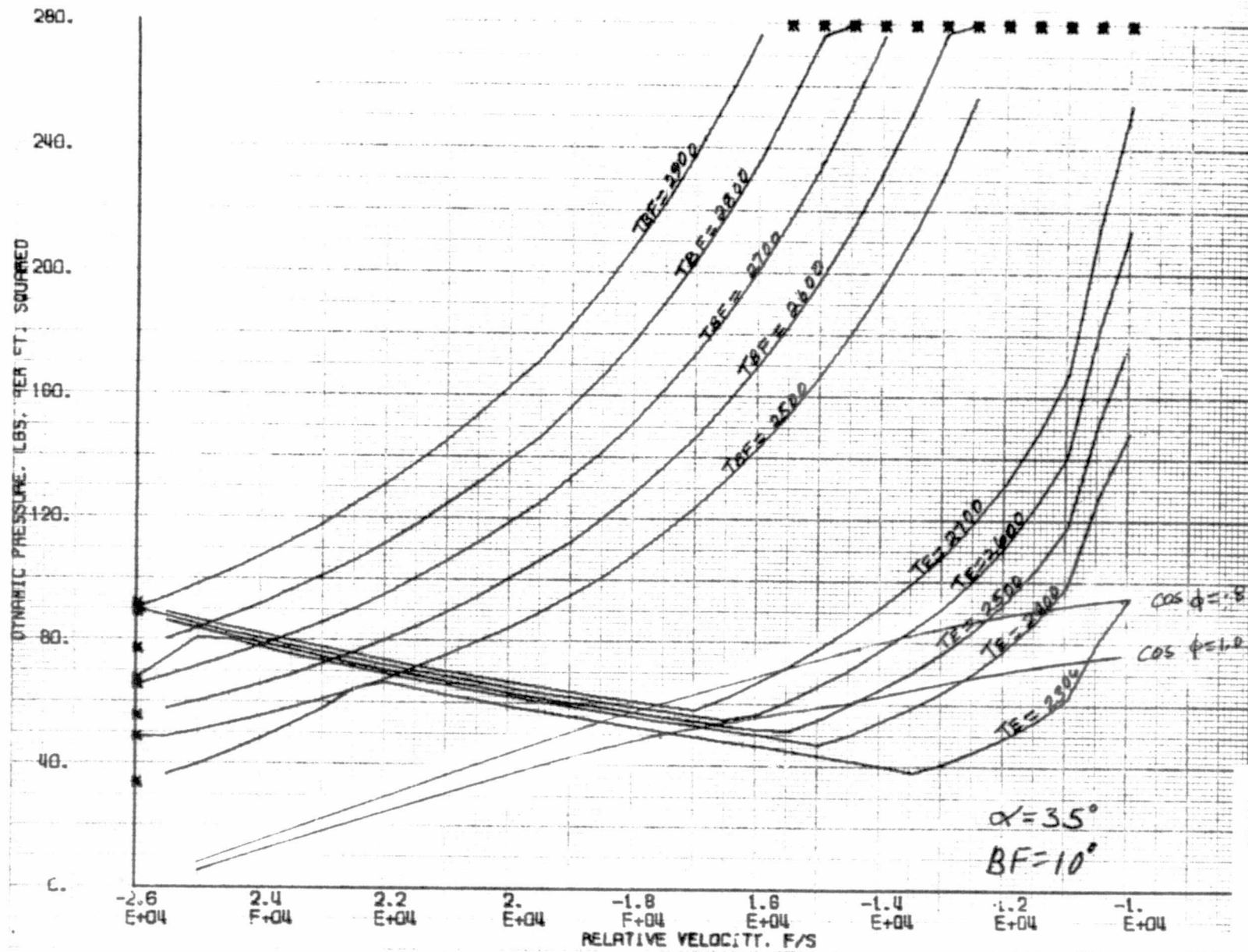


FIGURE 80 DYNAMIC PRESSURE VS. VELOCITY CORRIDOR

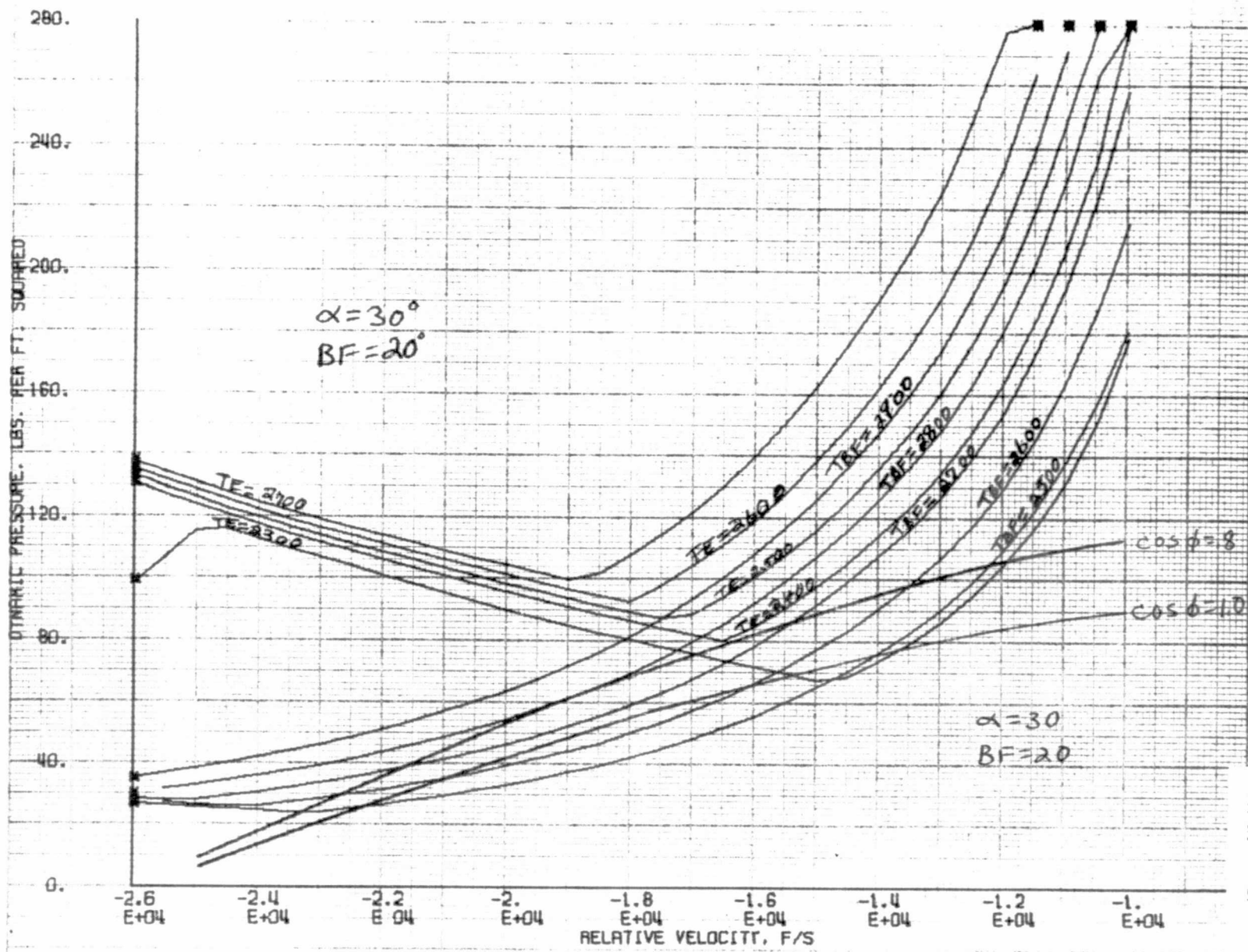


FIGURE 81 DYNAMIC PRESSURE VS. VELOCITY CORRIDOR

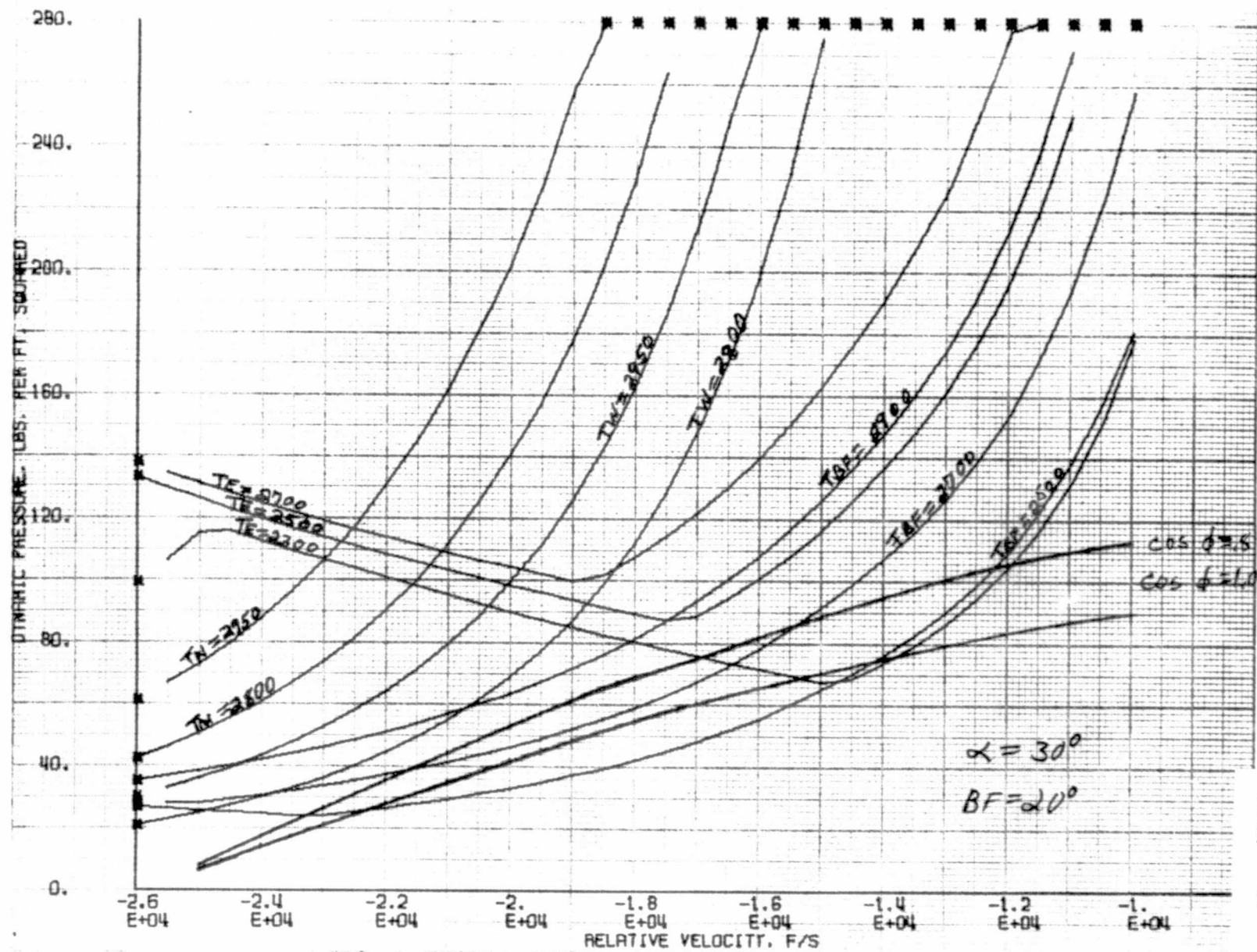




FIGURE 82 DYNAMIC PRESSURE VS. VELOCITY CORRIDOR

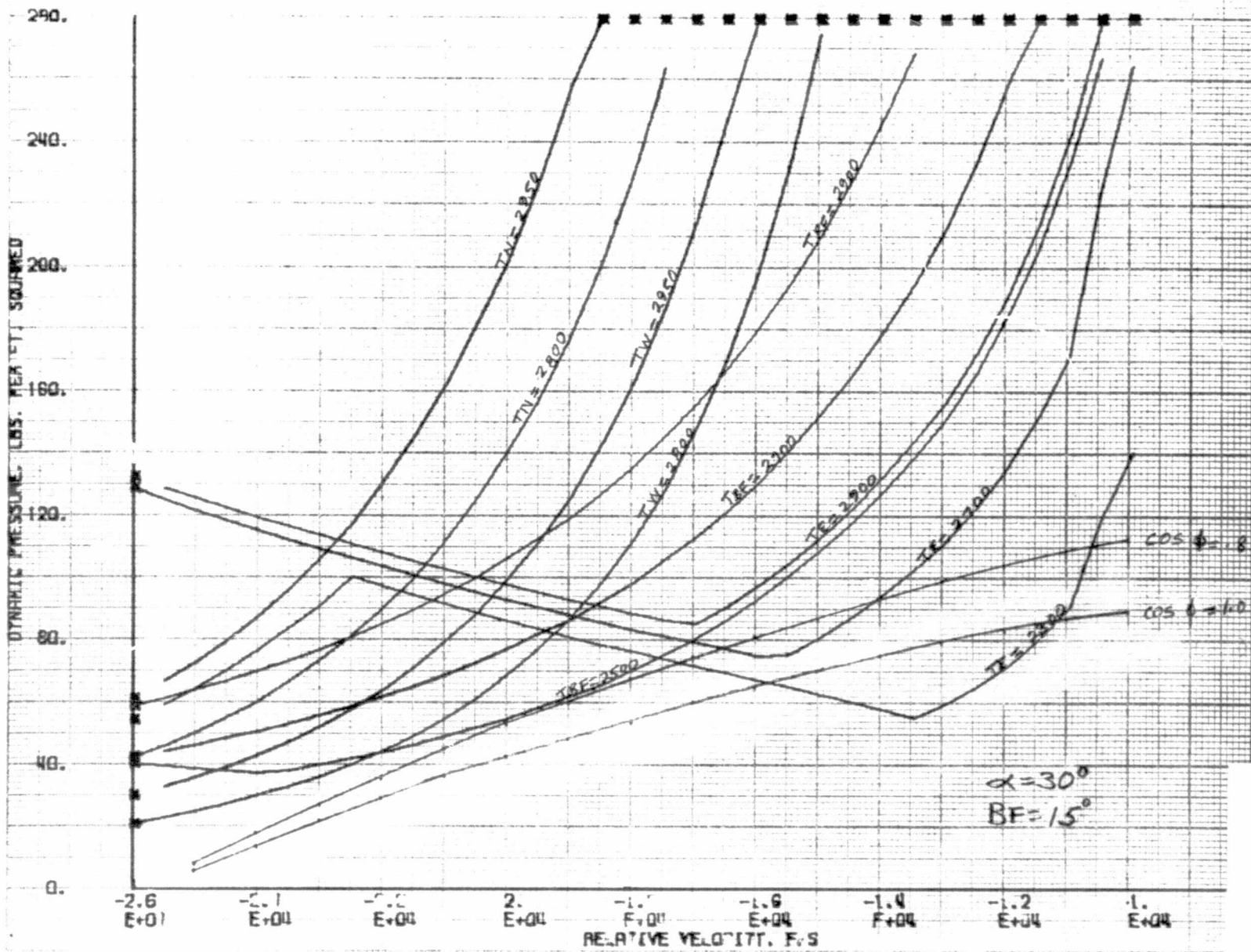


FIGURE 83 DYNAMIC PRESSURE VS. VELOCITY CORRIDOR

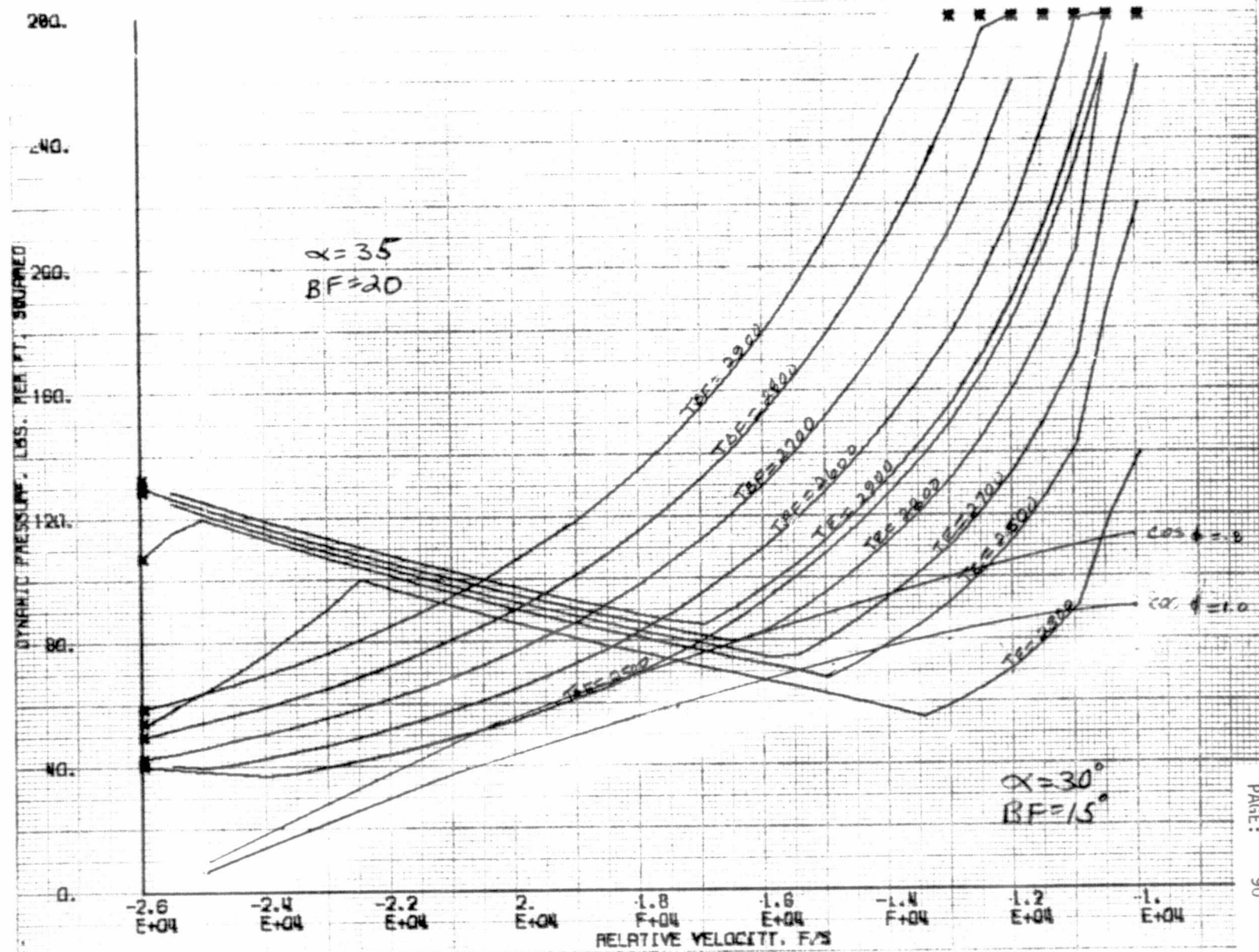


FIGURE 84 DYNAMIC PRESSURE VS. VELOCITY CORRIDOR

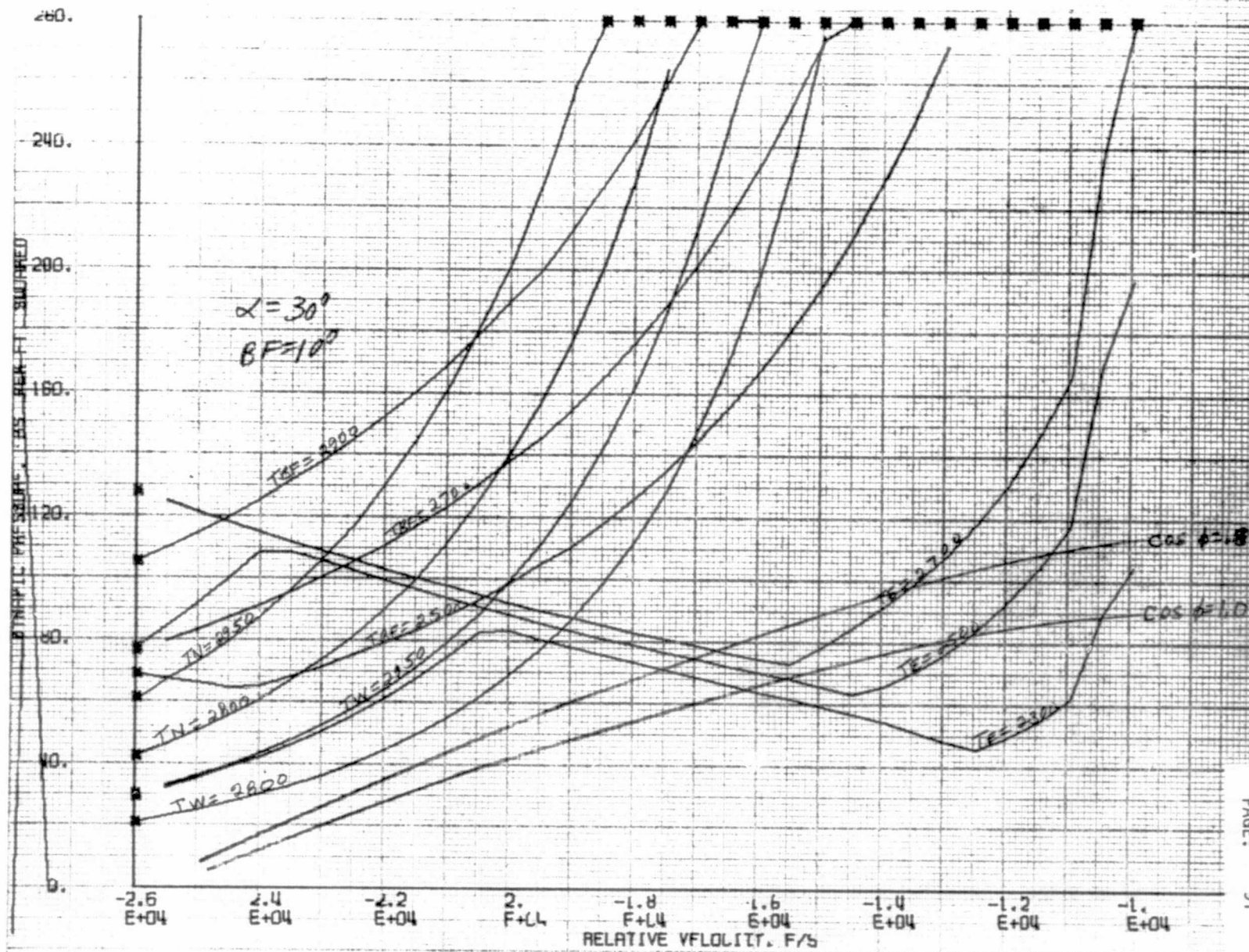
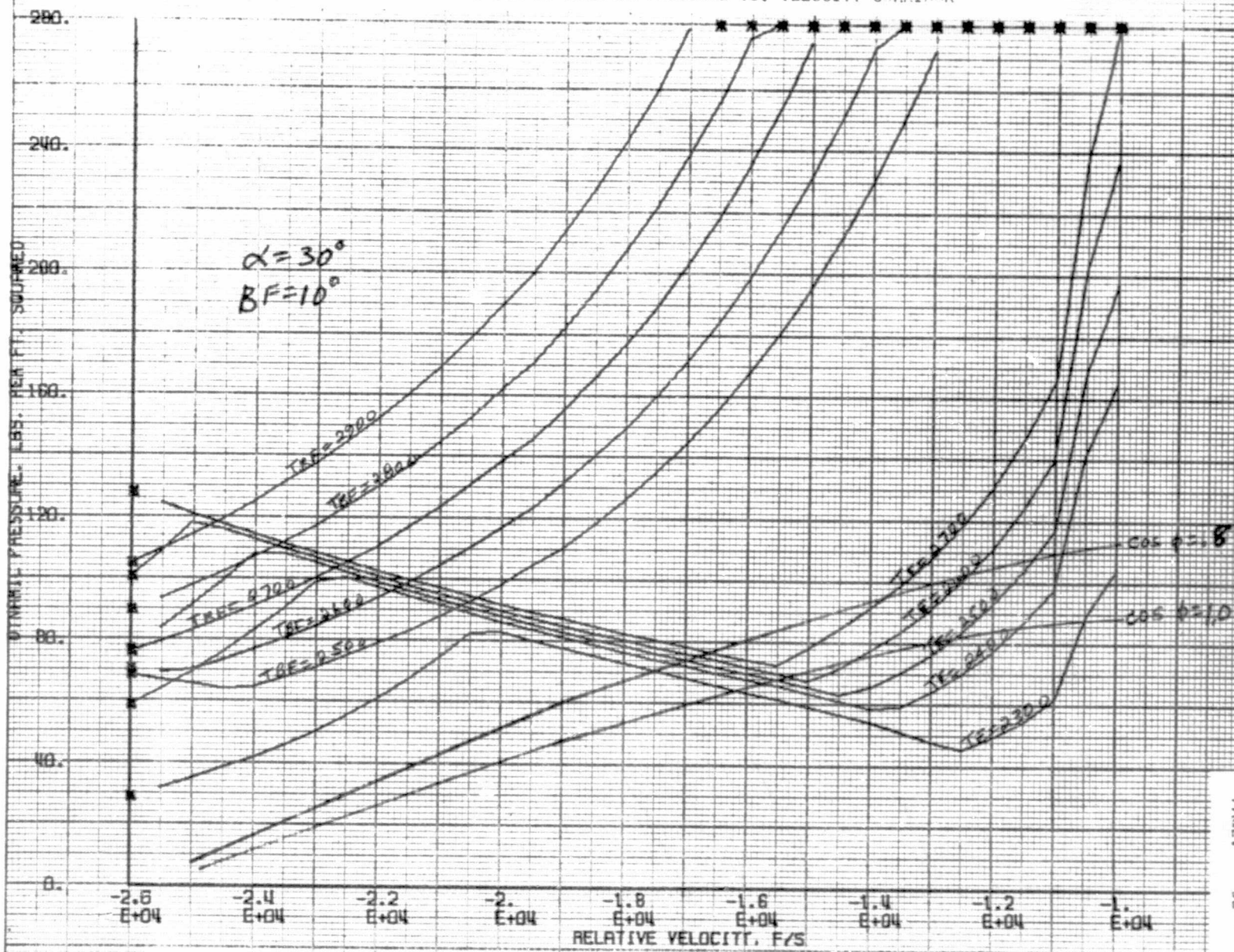




FIGURE 85 DYNAMIC PRESSURE VS. VELOCITY CORRIDOR



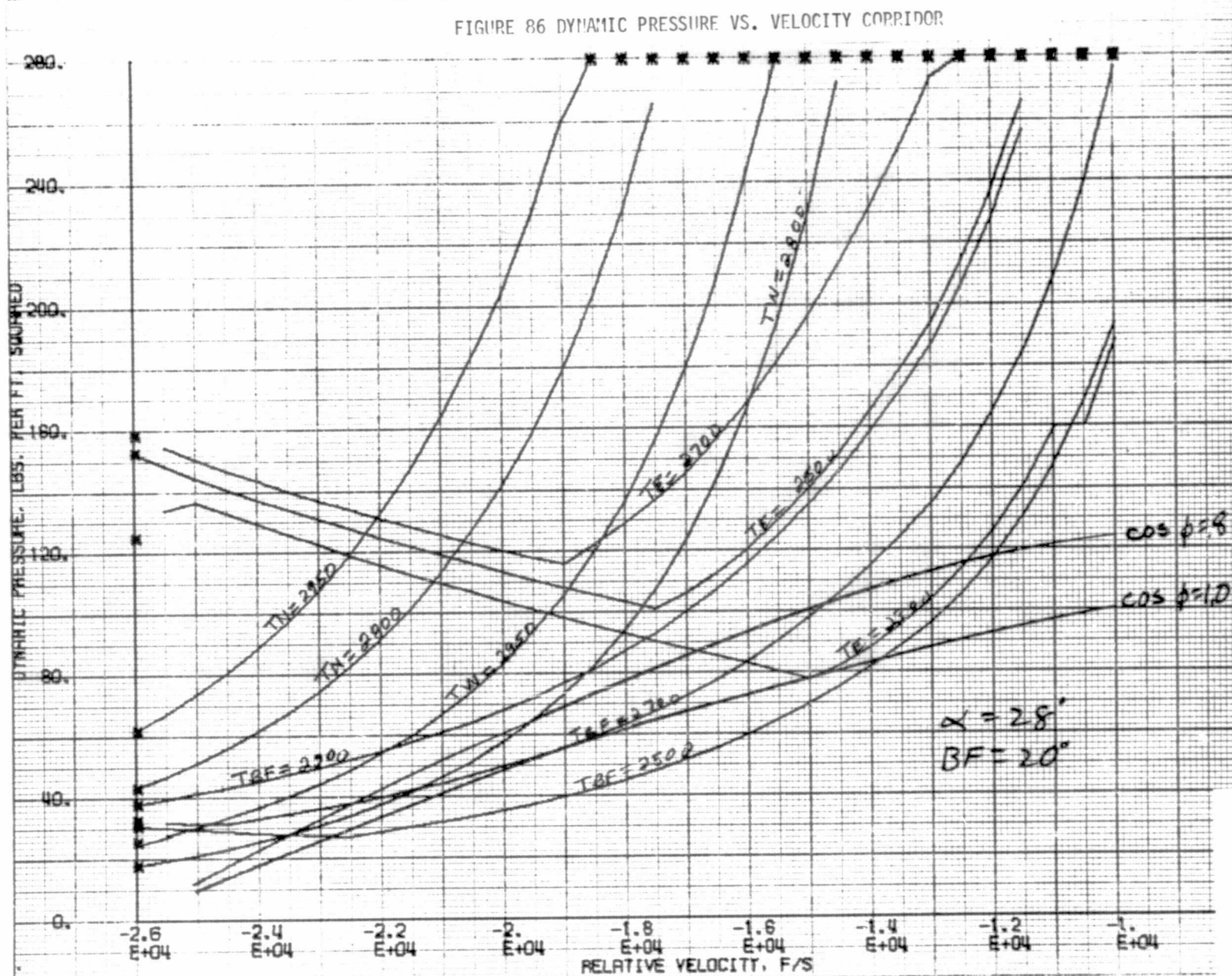


FIGURE 87 DYNAMIC PRESSURE VS. VELOCITY CORRIDOR

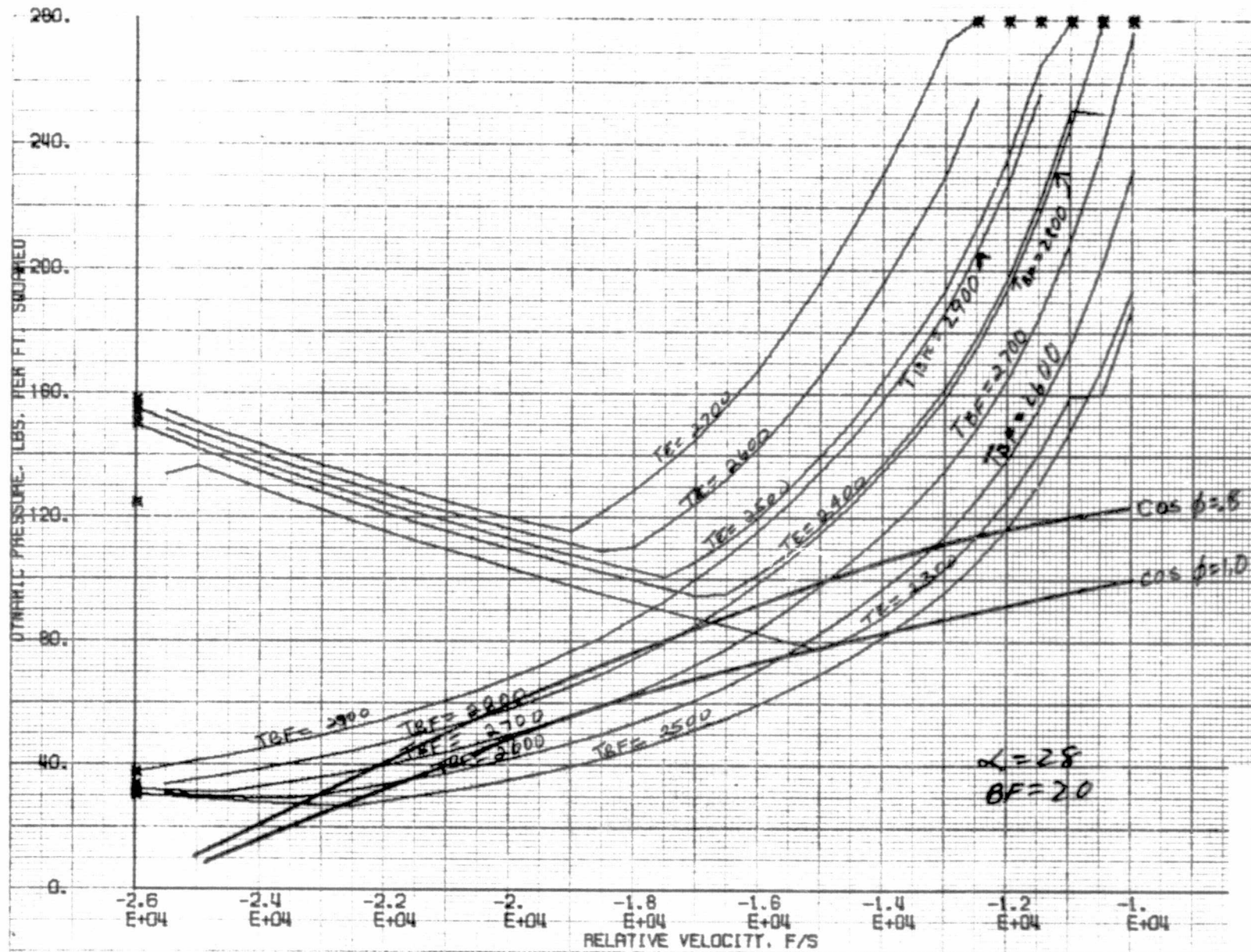




FIGURE 88 DYNAMIC PRESSURE VS. VELOCITY CORRIDOR

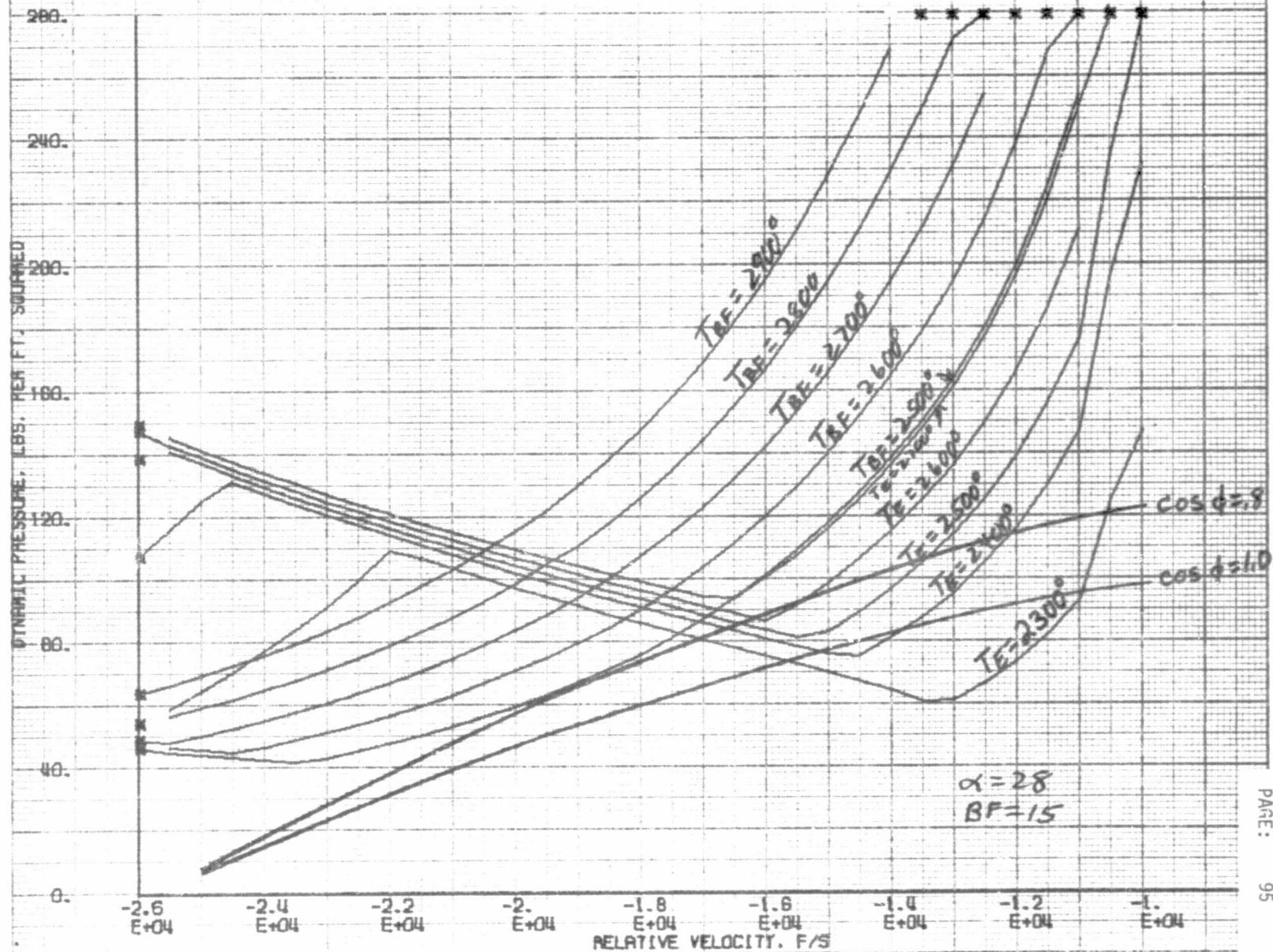


FIGURE 09 DYNAMIC PRESSURE VS. RELATIVE VELOCITY

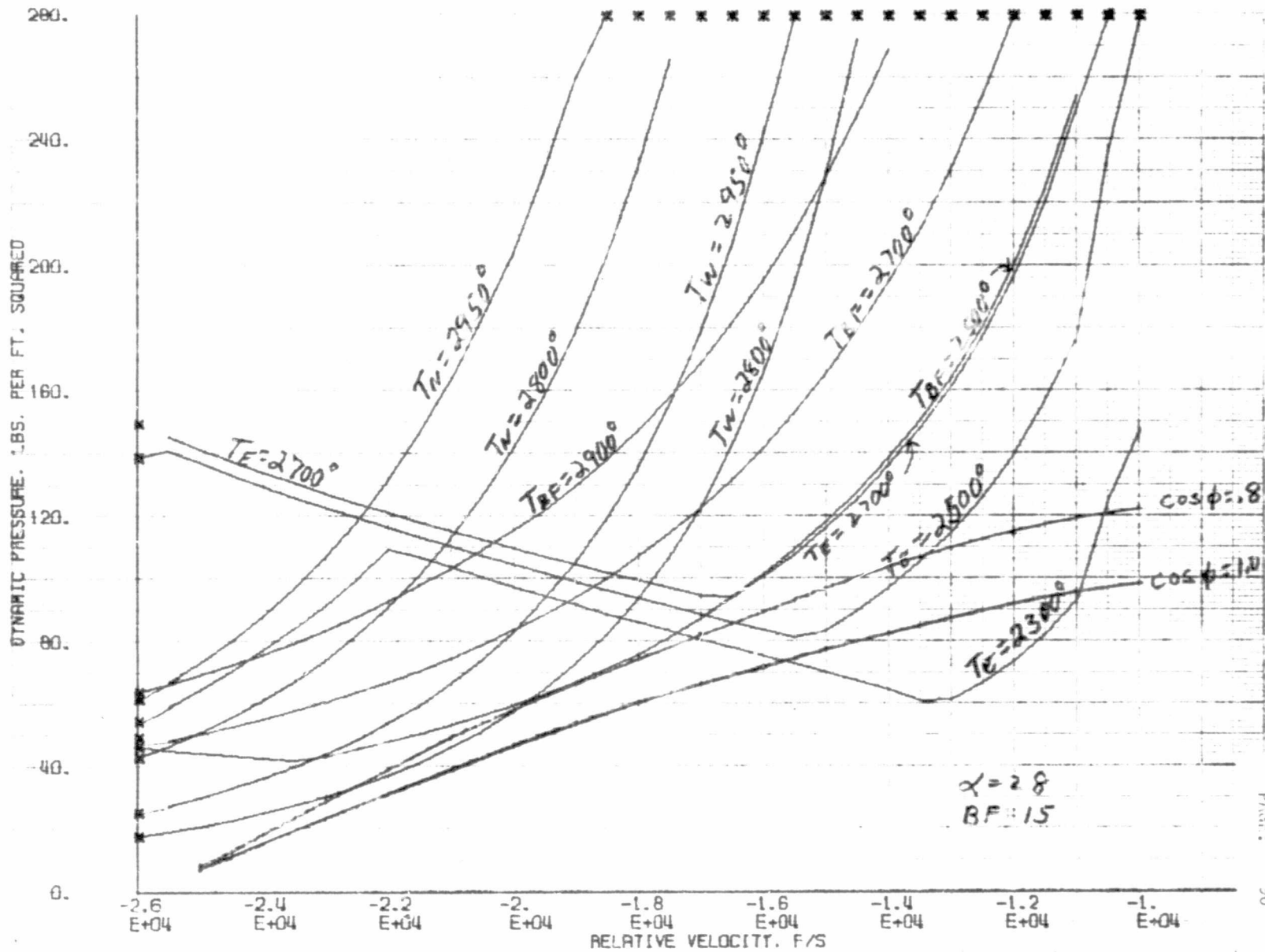


FIGURE 90 DYNAMIC PRESSURE VS. VELOCITY CORRIDOR

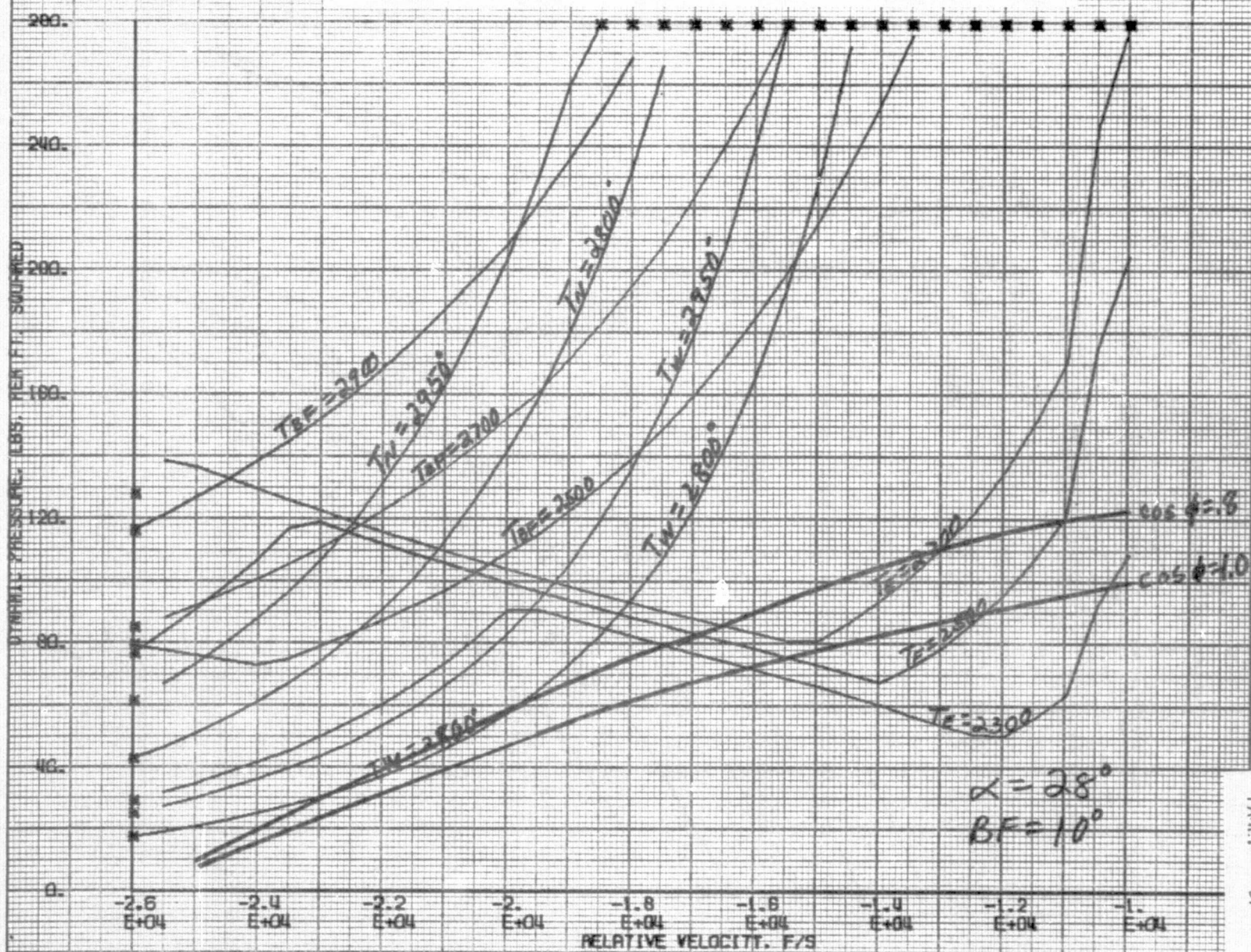




FIGURE 91 DYNAMIC PRESSURE VS. VELOCITY CORRIDOR

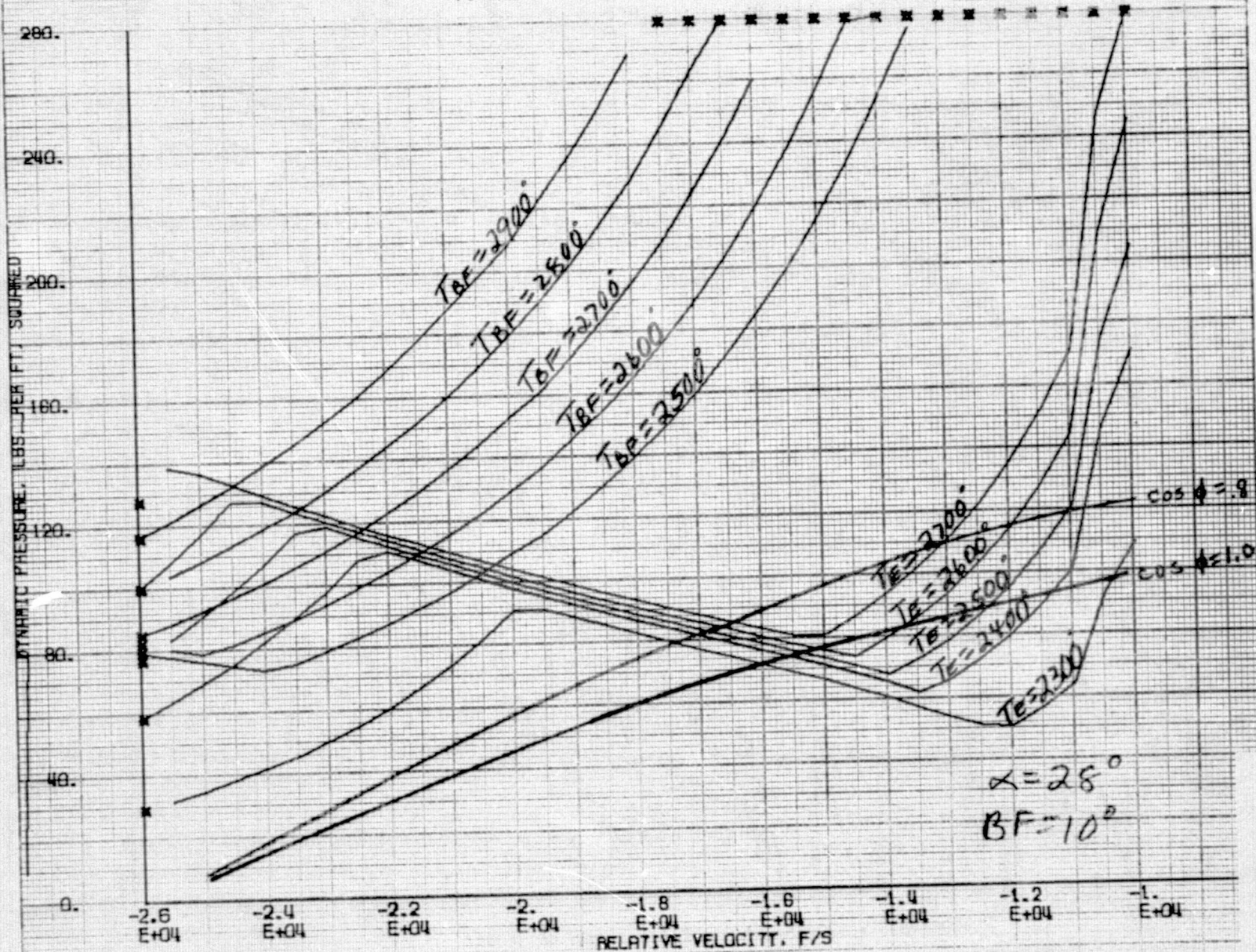


FIGURE 92 DYNAMIC PRESSURE VS. VELOCITY CORRIDOR

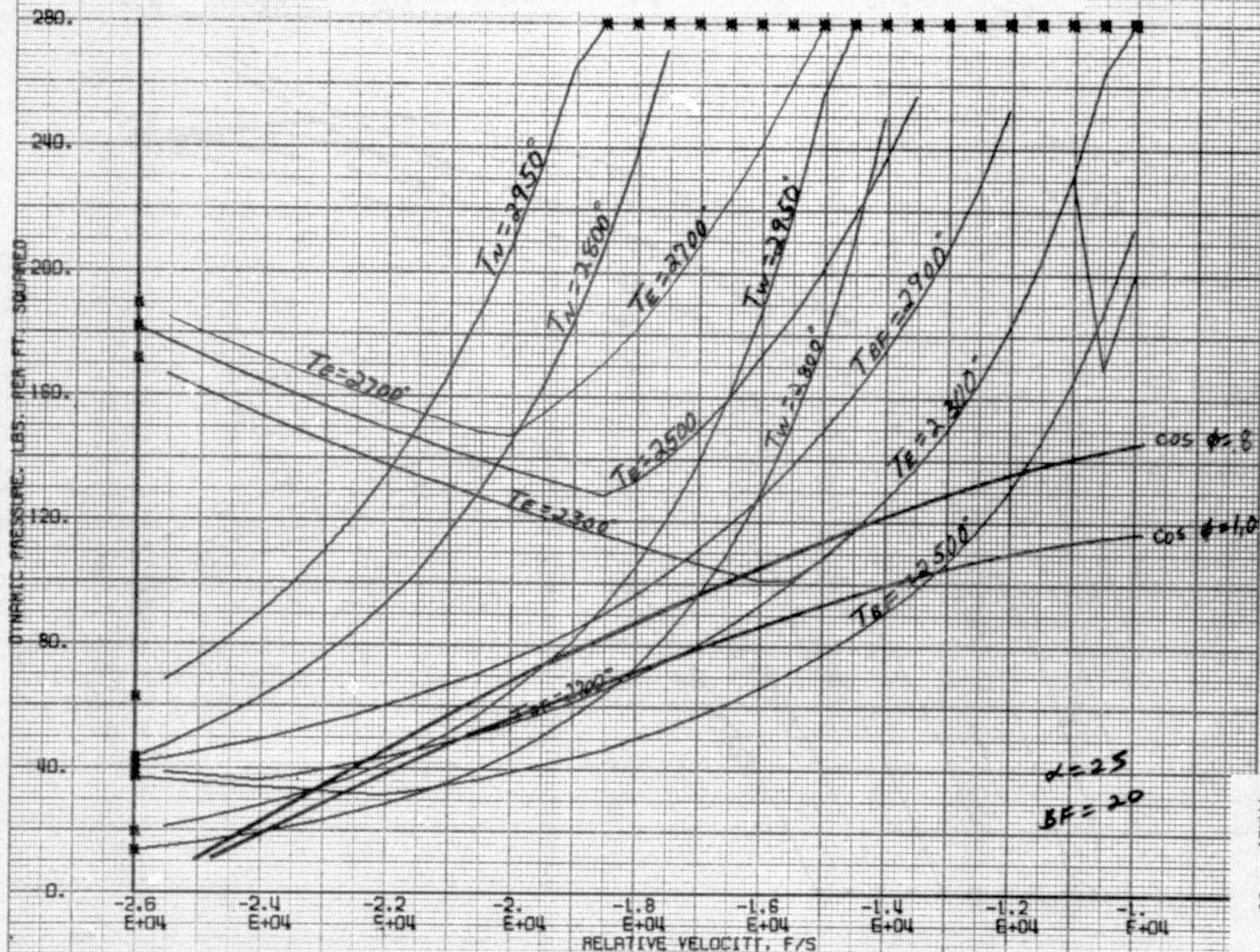




FIGURE 93 DYNAMIC PRESSURE VS. VELOCITY CORRIDOR

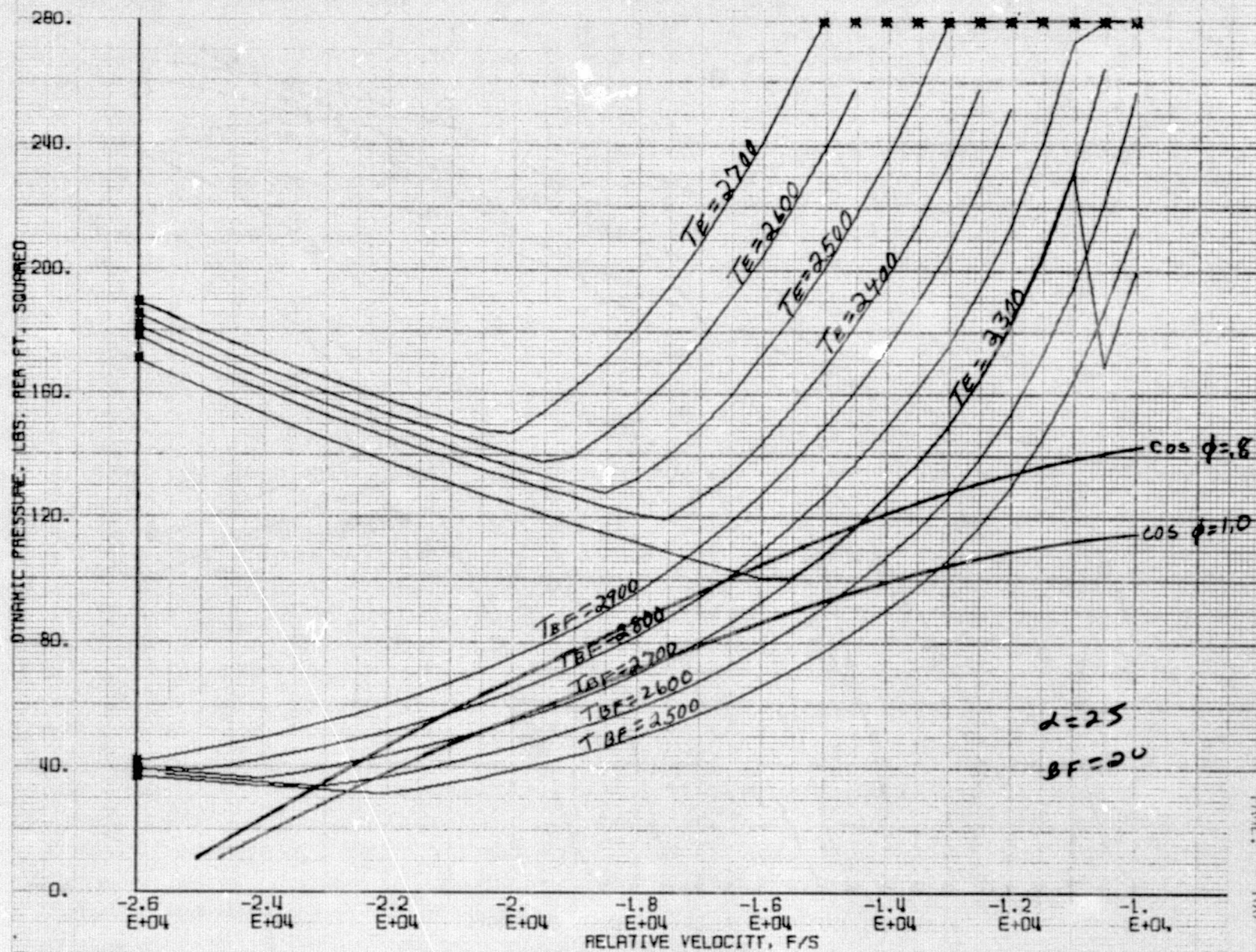




FIGURE 94 DYNAMIC PRESSURE VS. VELOCITY CORRIDOR

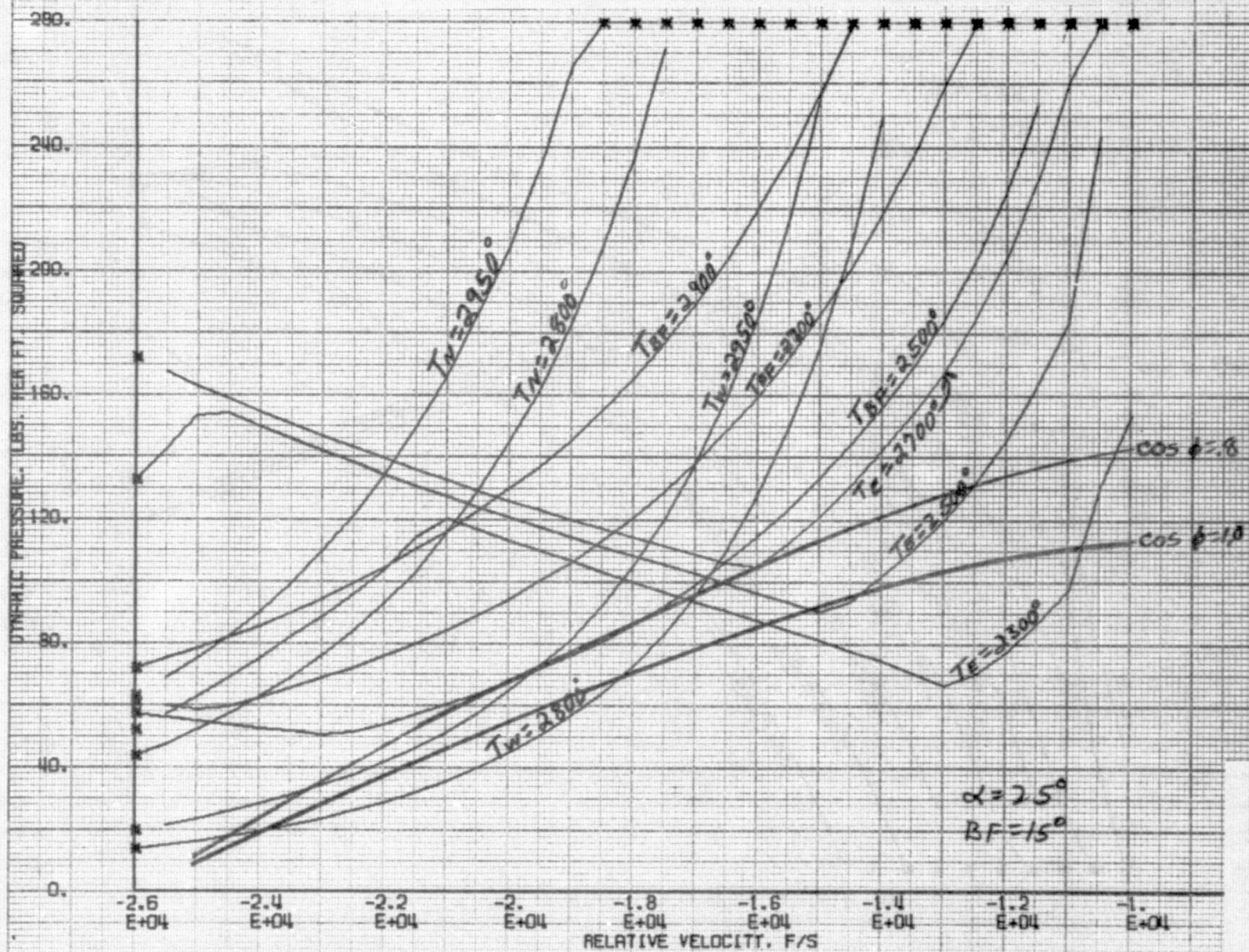


FIGURE 95 DYNAMIC PRESSURE VS. VELOCITY CORRIDOR

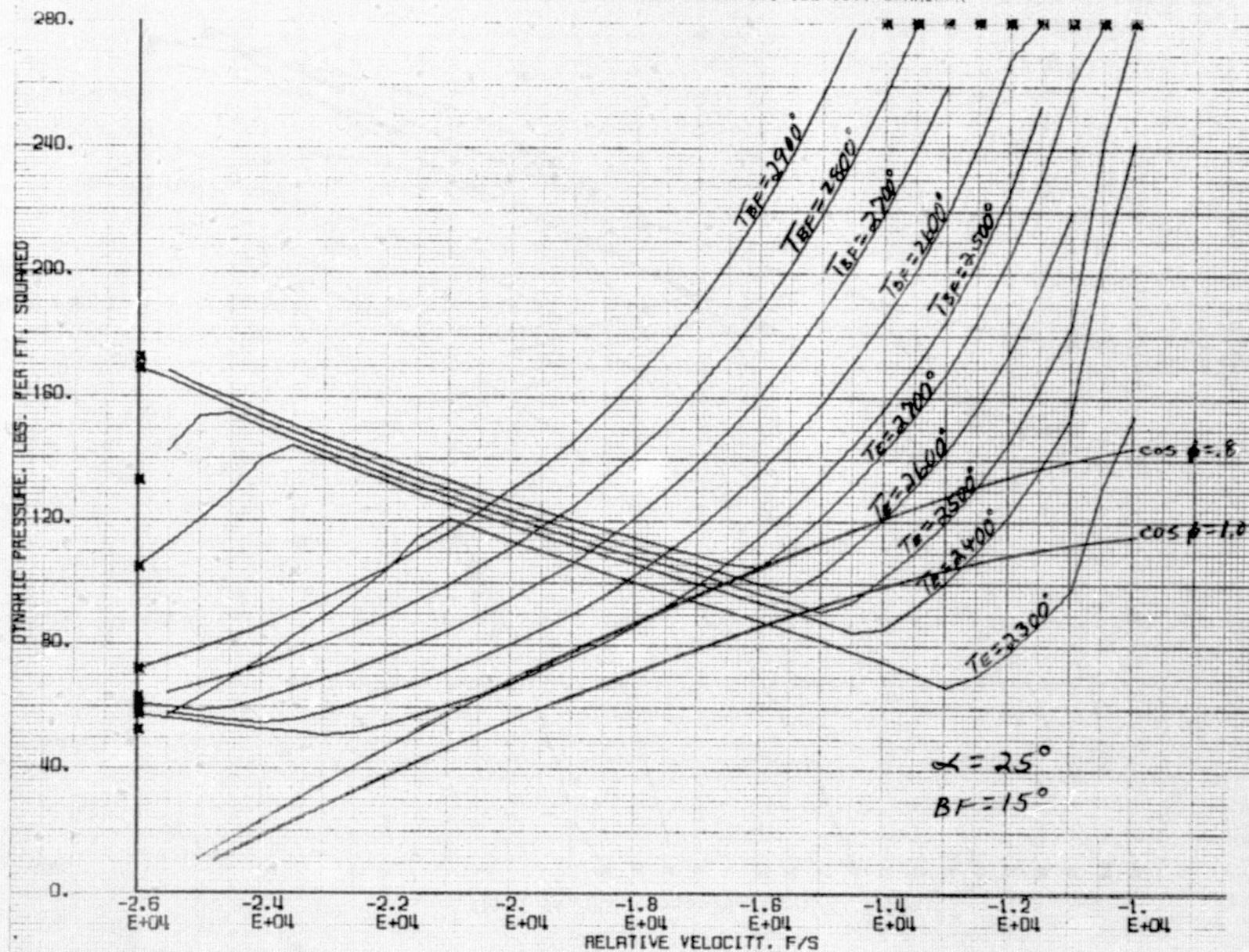




FIGURE 96 DYNAMIC PRESSURE VS. VELOCITY CORRIDOR

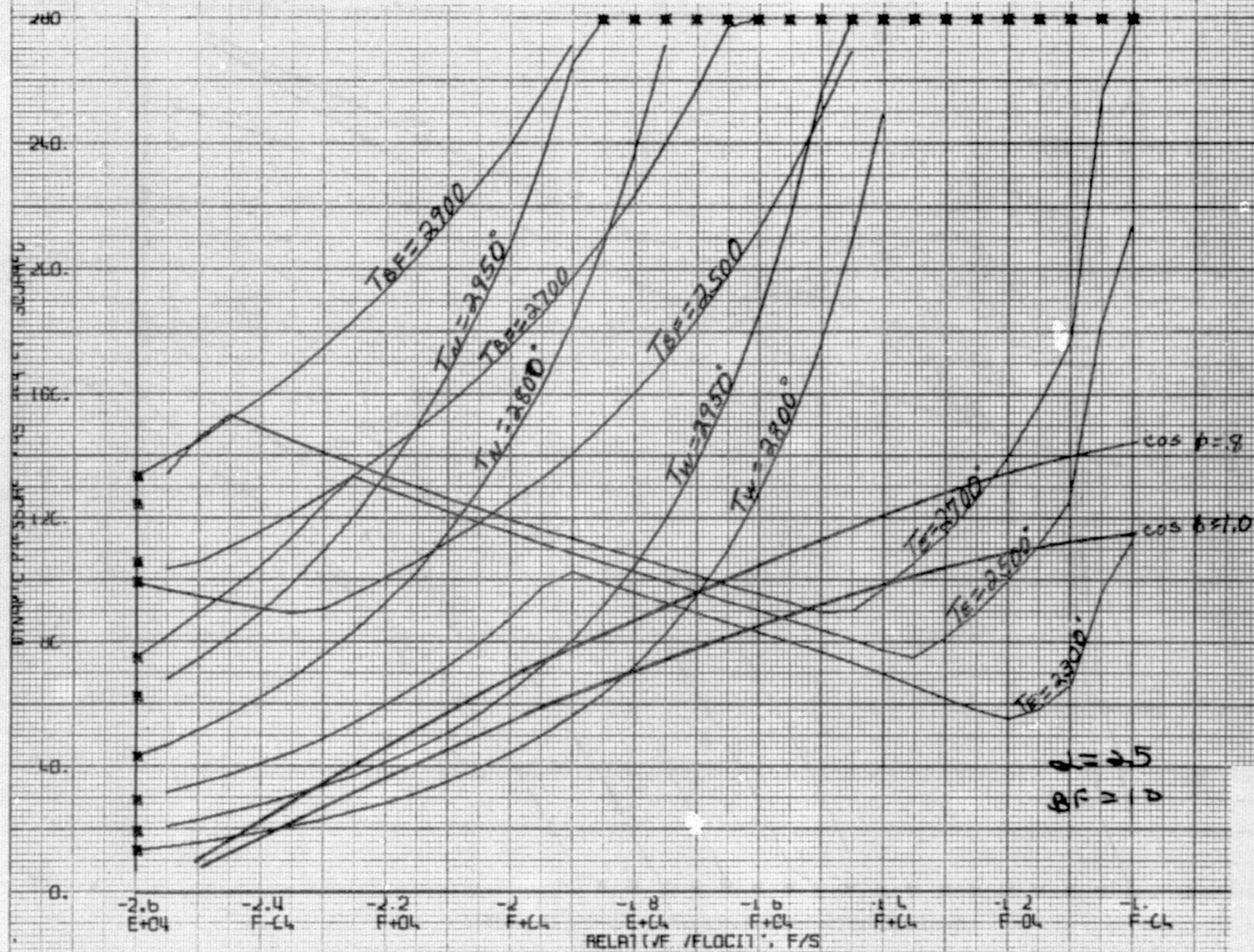




FIGURE 97 DYNAMIC PRESSURE VS. VELOCITY CORRIDOR

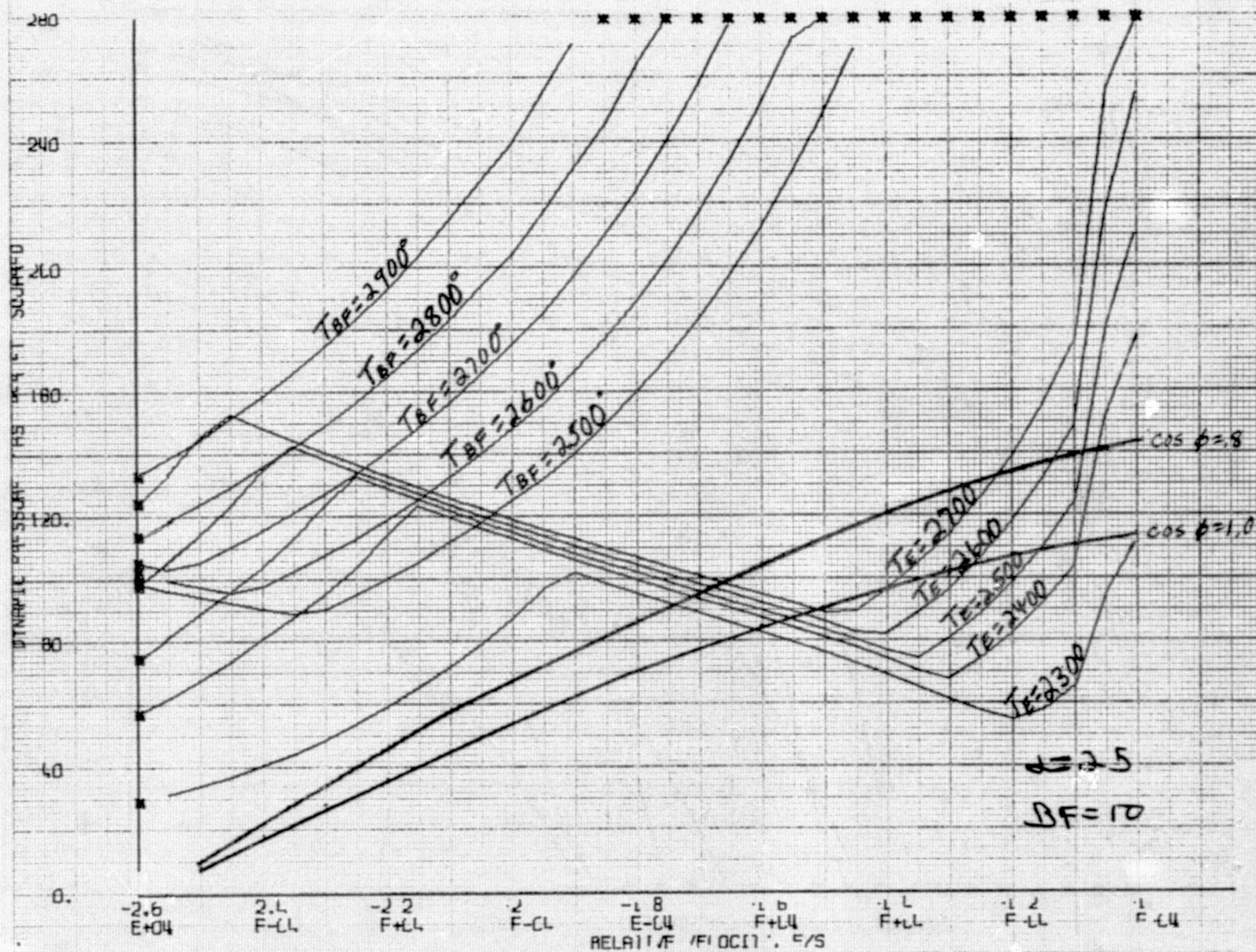


FIGURE 98 ALTITUDE VS. VELOCITY CORRIDOR

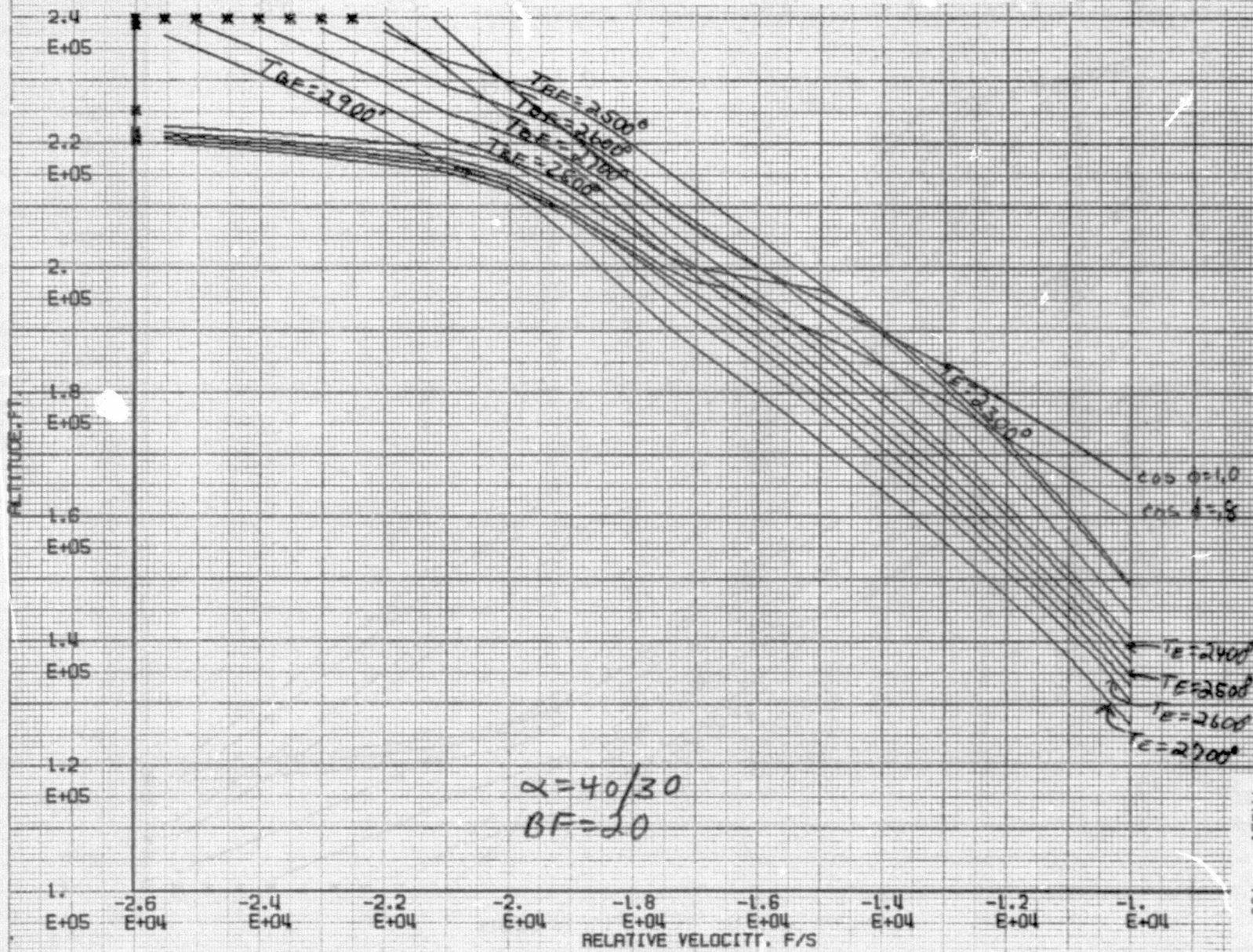




FIGURE 99 ALTITUDE VS. VELOCITY CORRIDOR

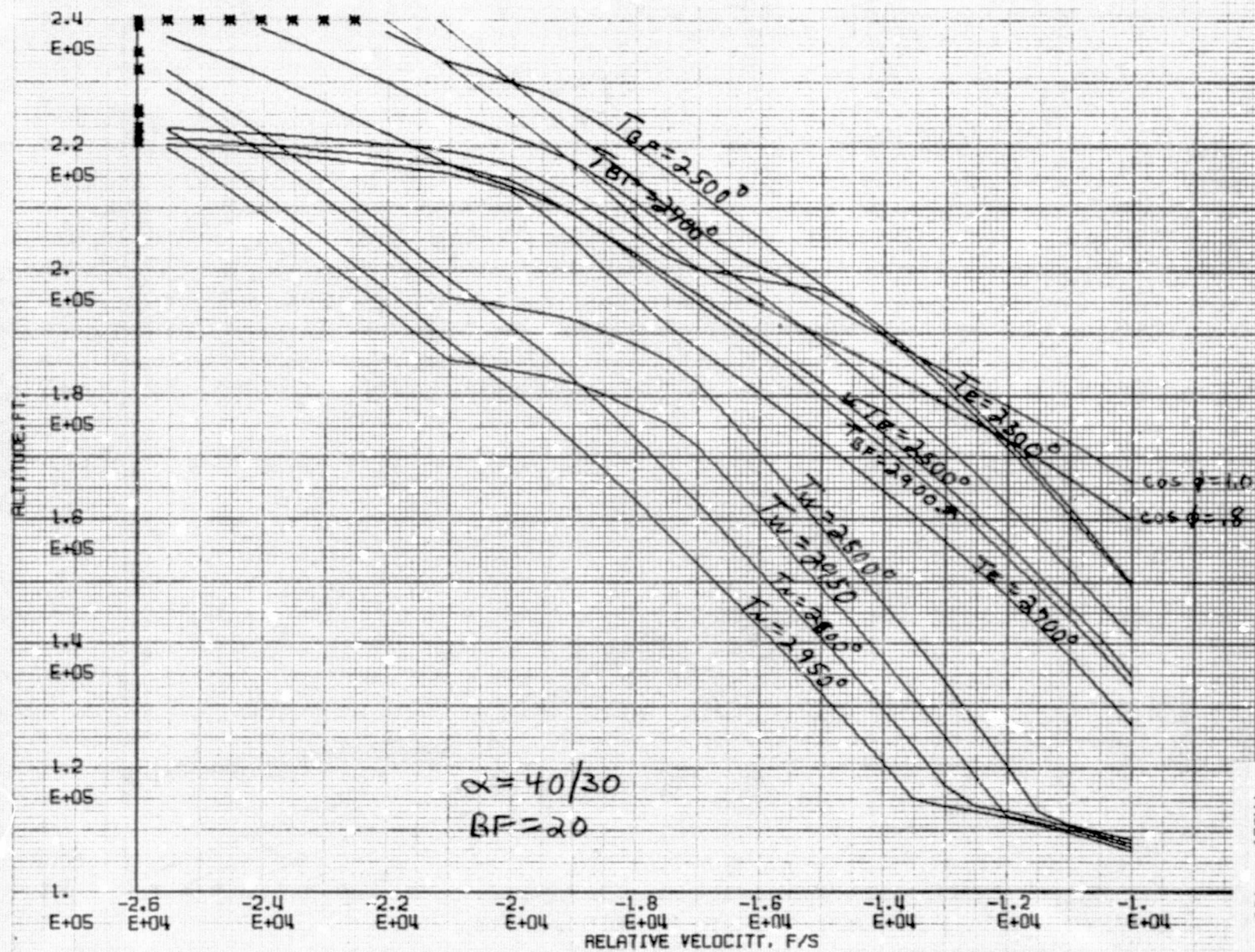




FIGURE 100 ALTITUDE VS. VELOCITY CORRIDOR

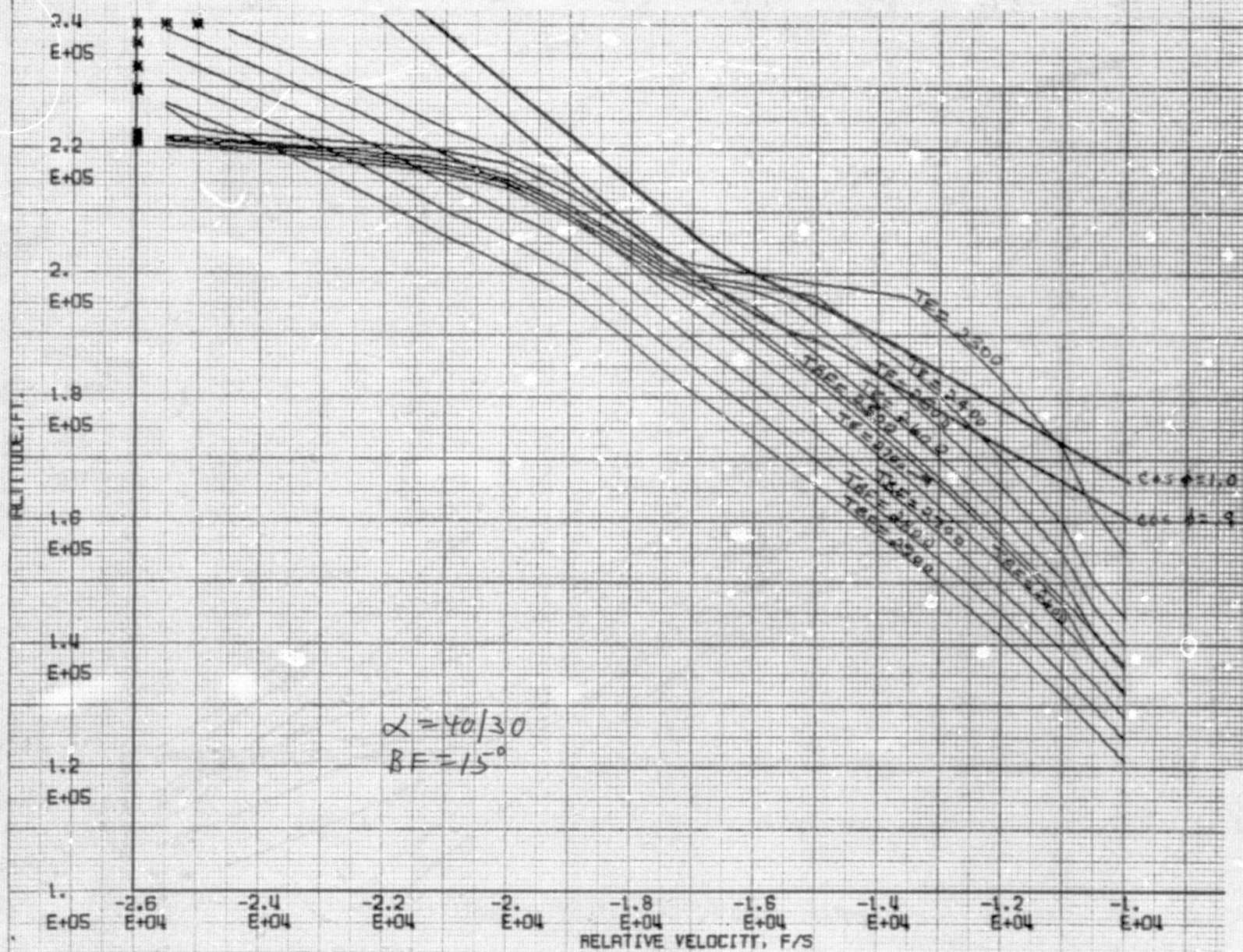


FIGURE 101 ALTITUDE VS. VELOCITY CORRIDOR

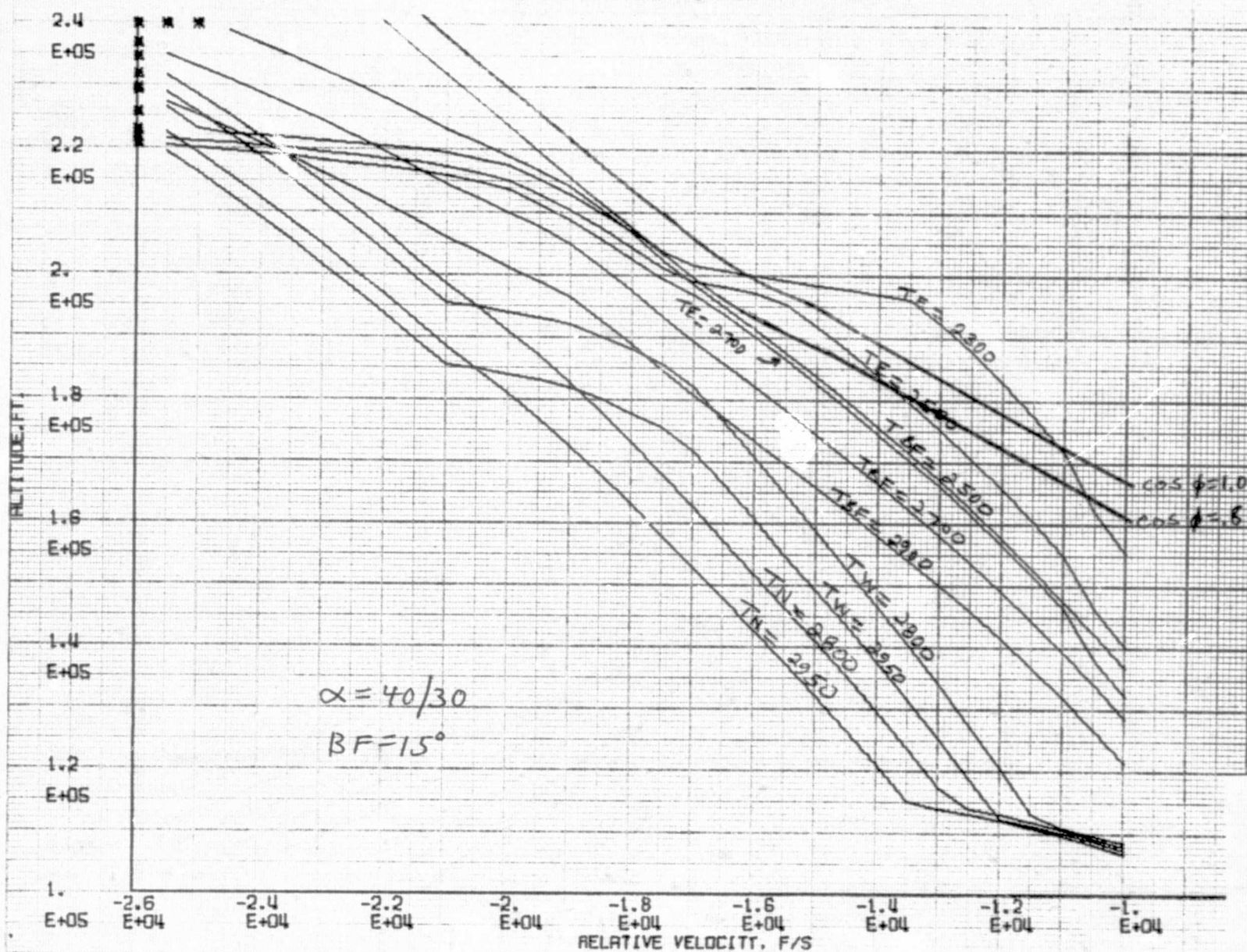




FIGURE 102 ALTITUDE VS. VELOCITY CORRIDOR

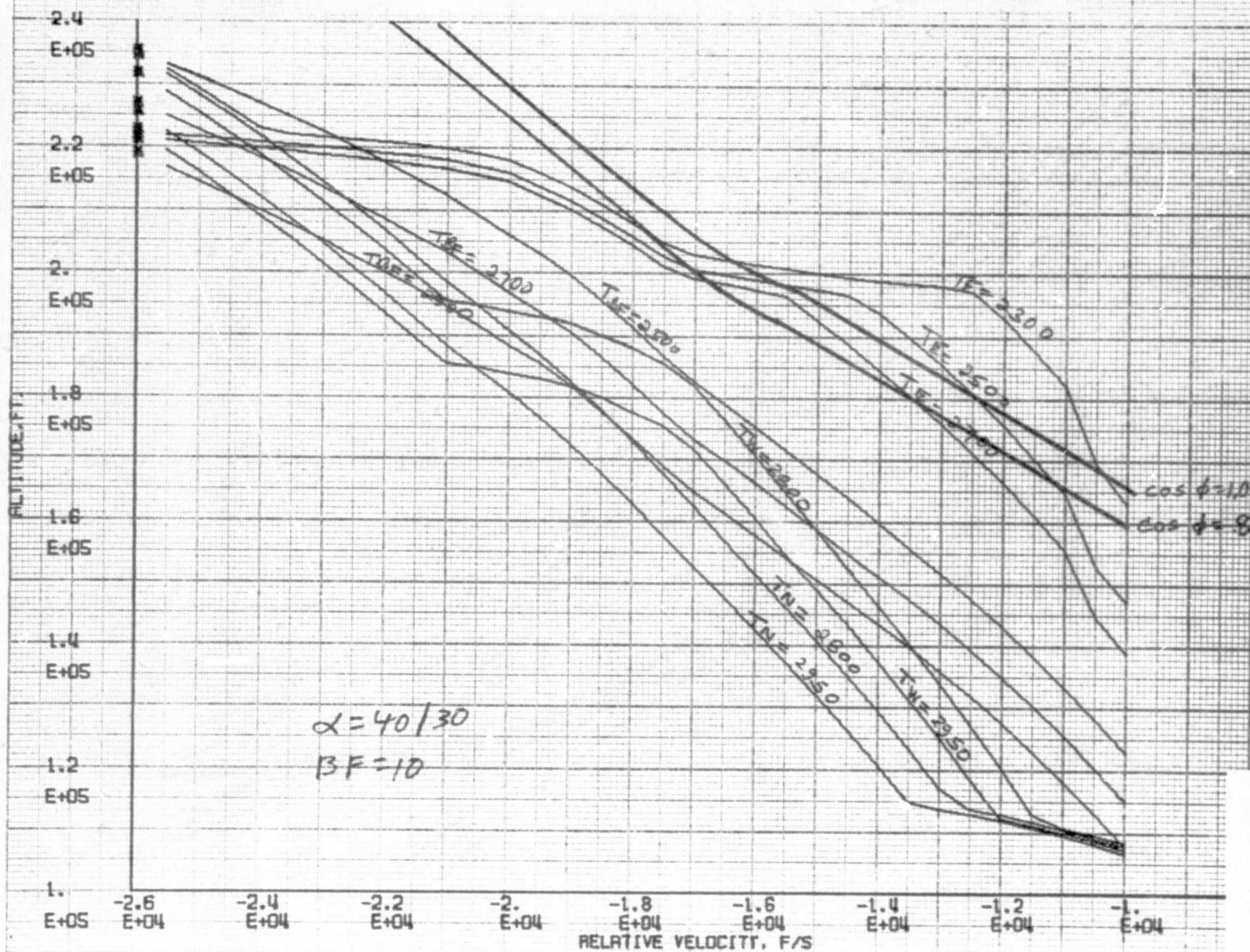




FIGURE 103 ALTITUDE VS. VELOCITY CORRIDOR

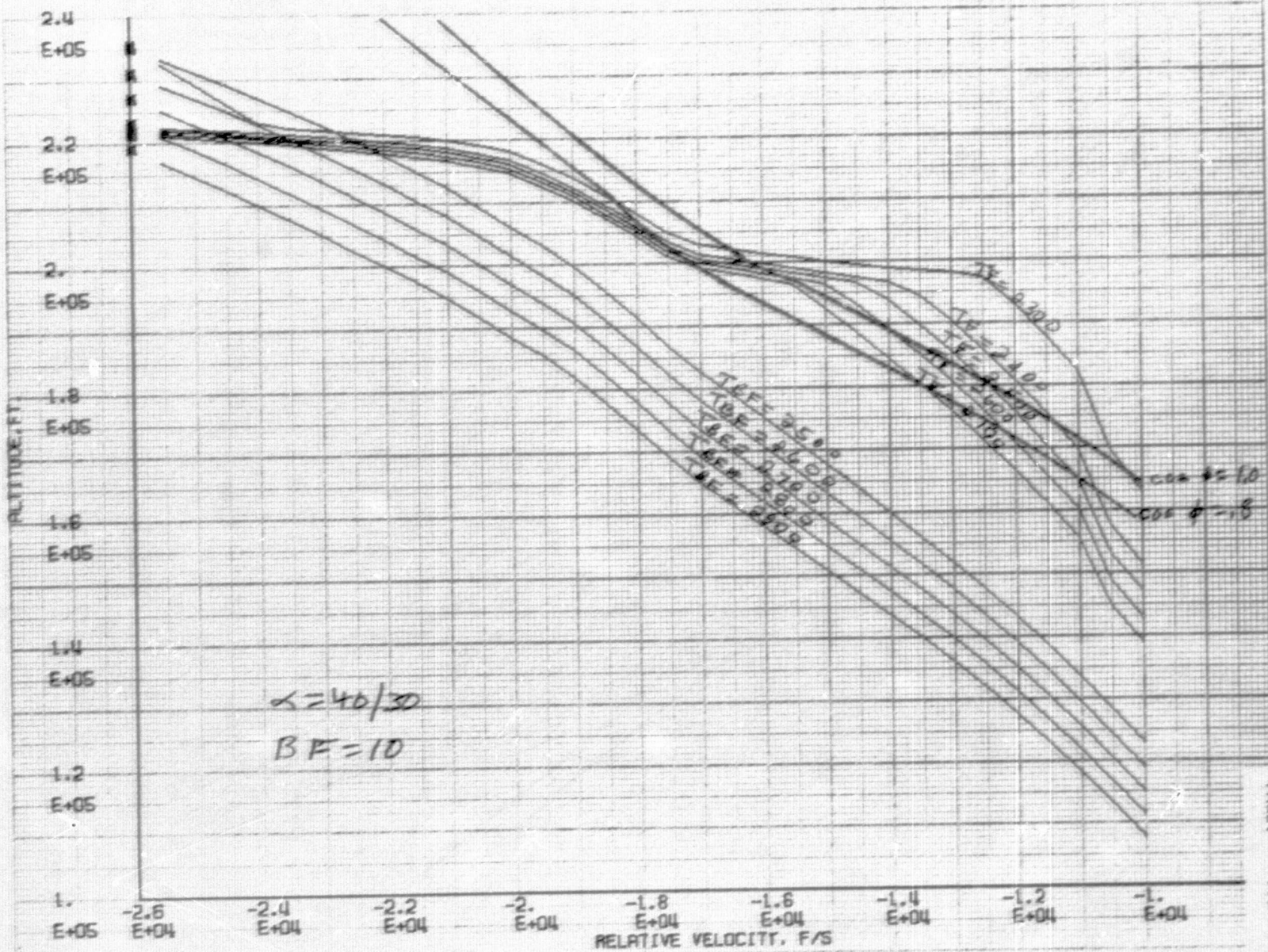


FIGURE 104 ALTITUDE VS. VELOCITY CORRIDOR

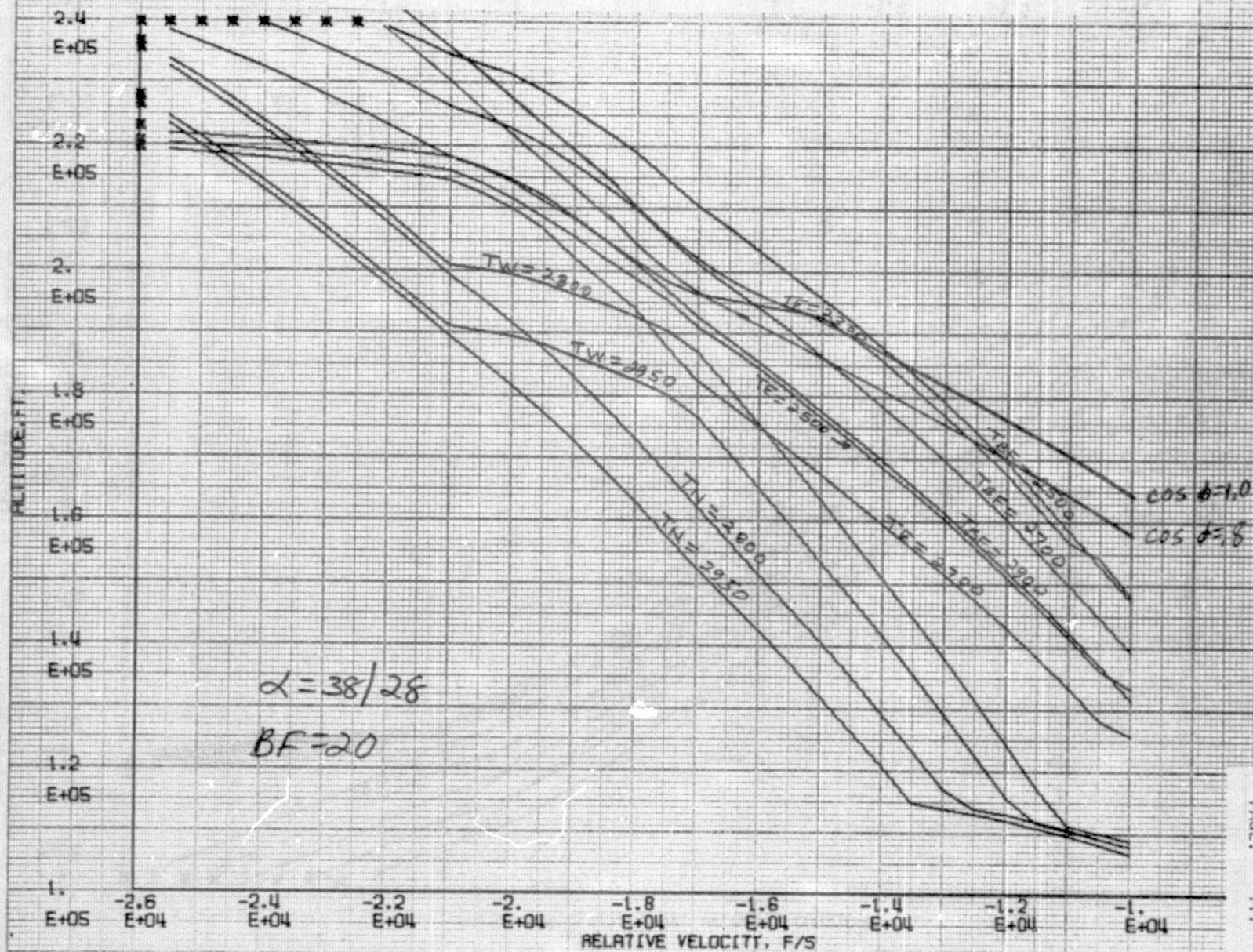




FIGURE 105 ALTITUDE VS. VELOCITY CORRIDOR

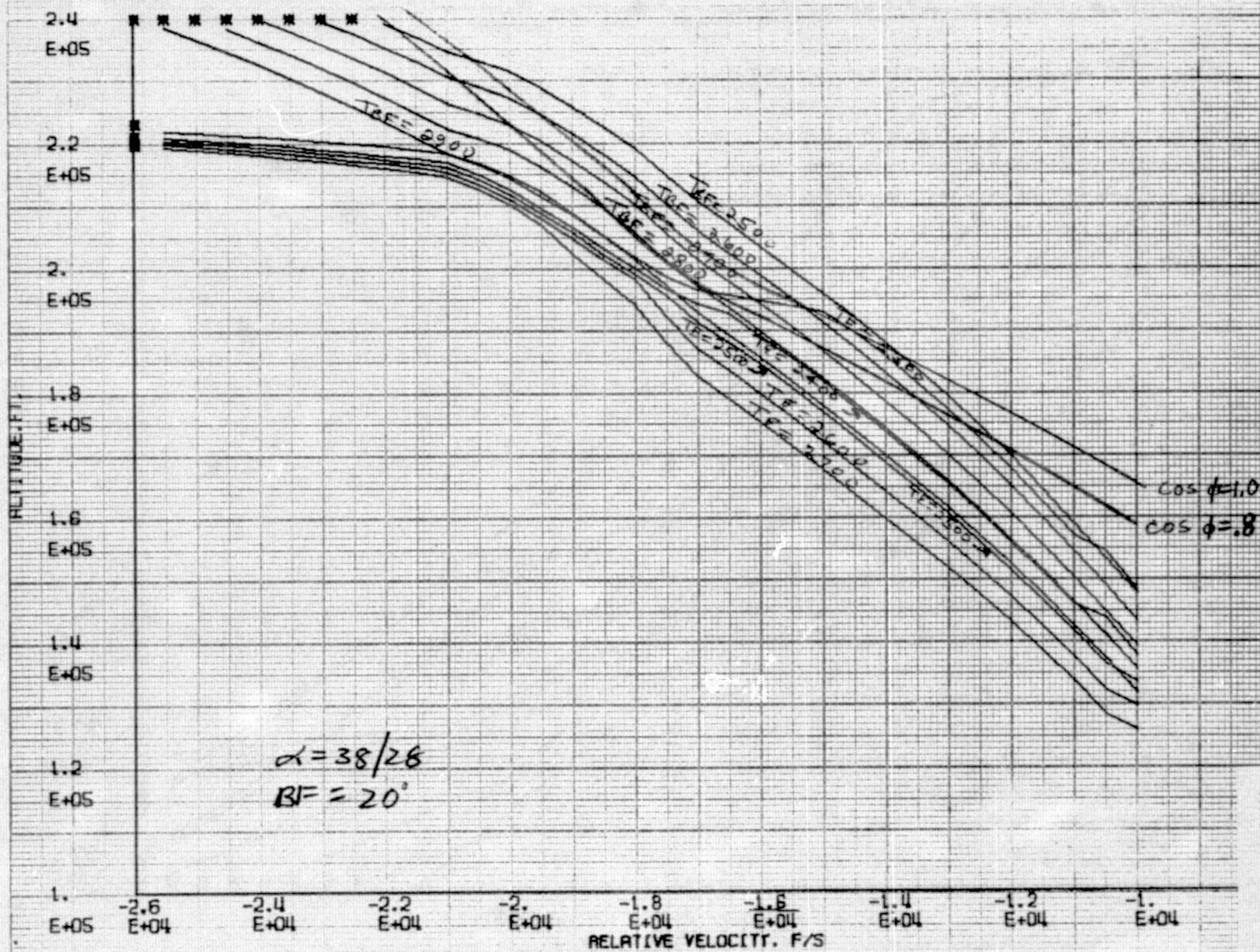




FIGURE 106 ALTITUDE VS. VELOCITY CORRIDOR

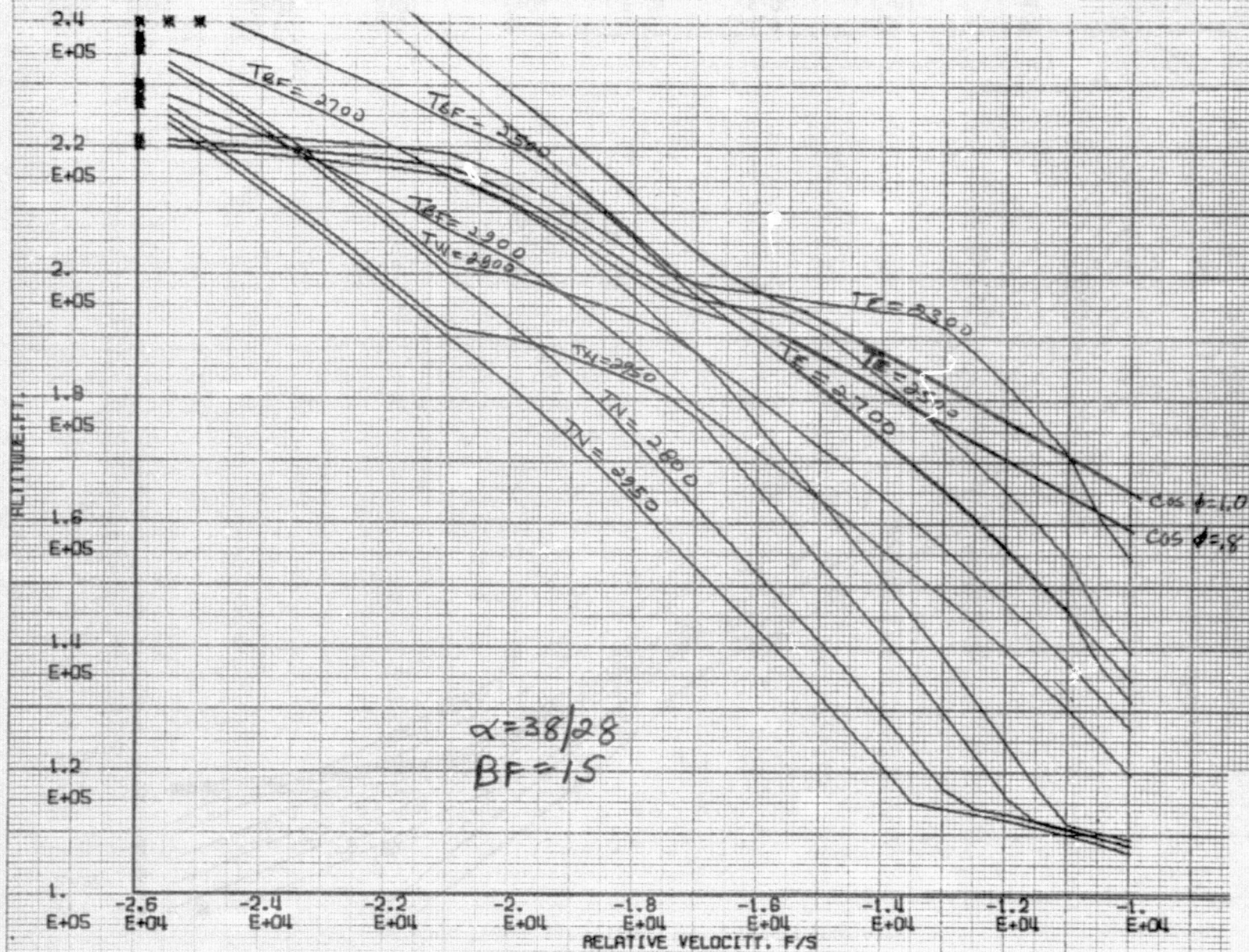


FIGURE 107 ALTITUDE VS. VELOCITY CORRIDOR.

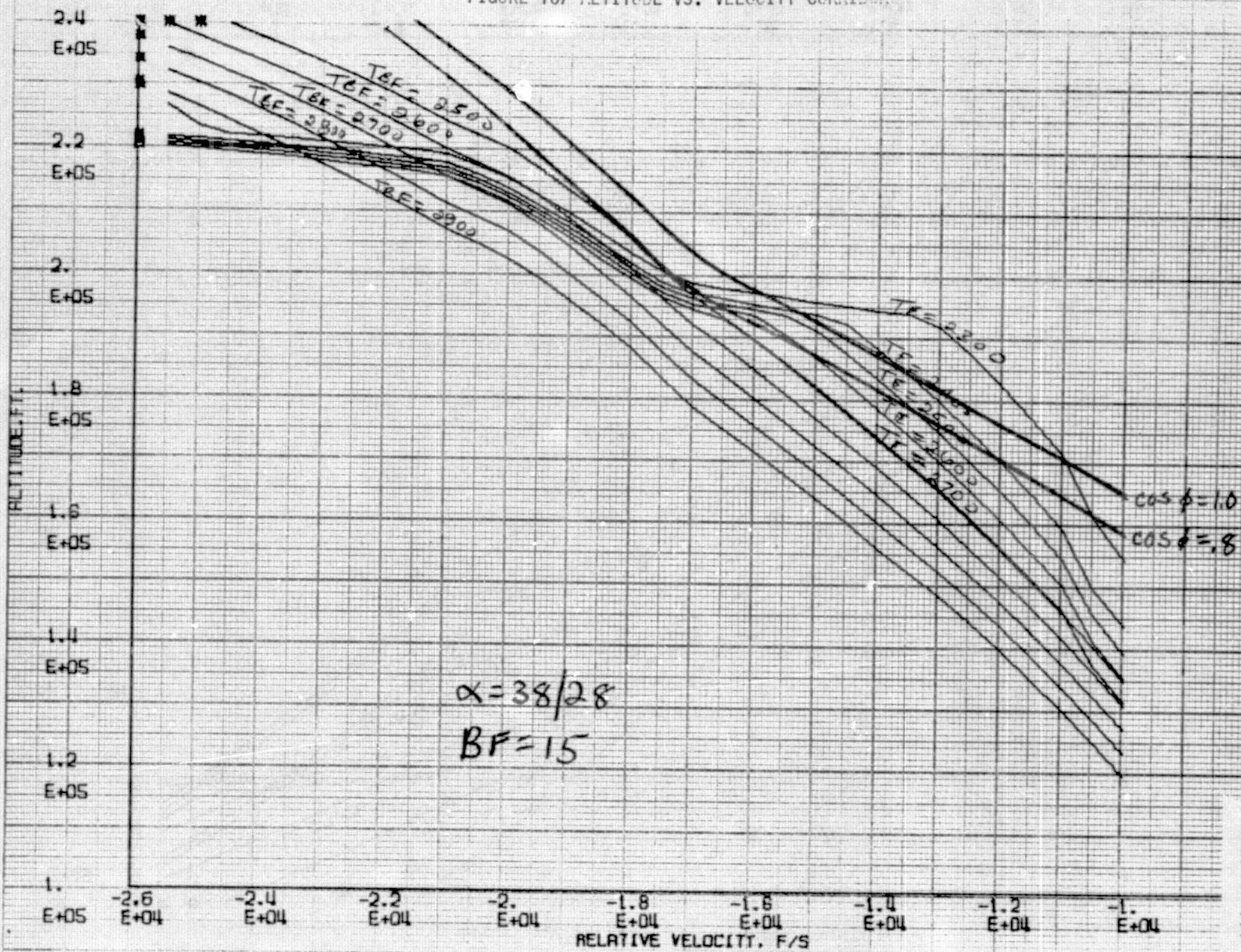




FIGURE 108 ALTITUDE VS. VELOCITY CORRIDOR

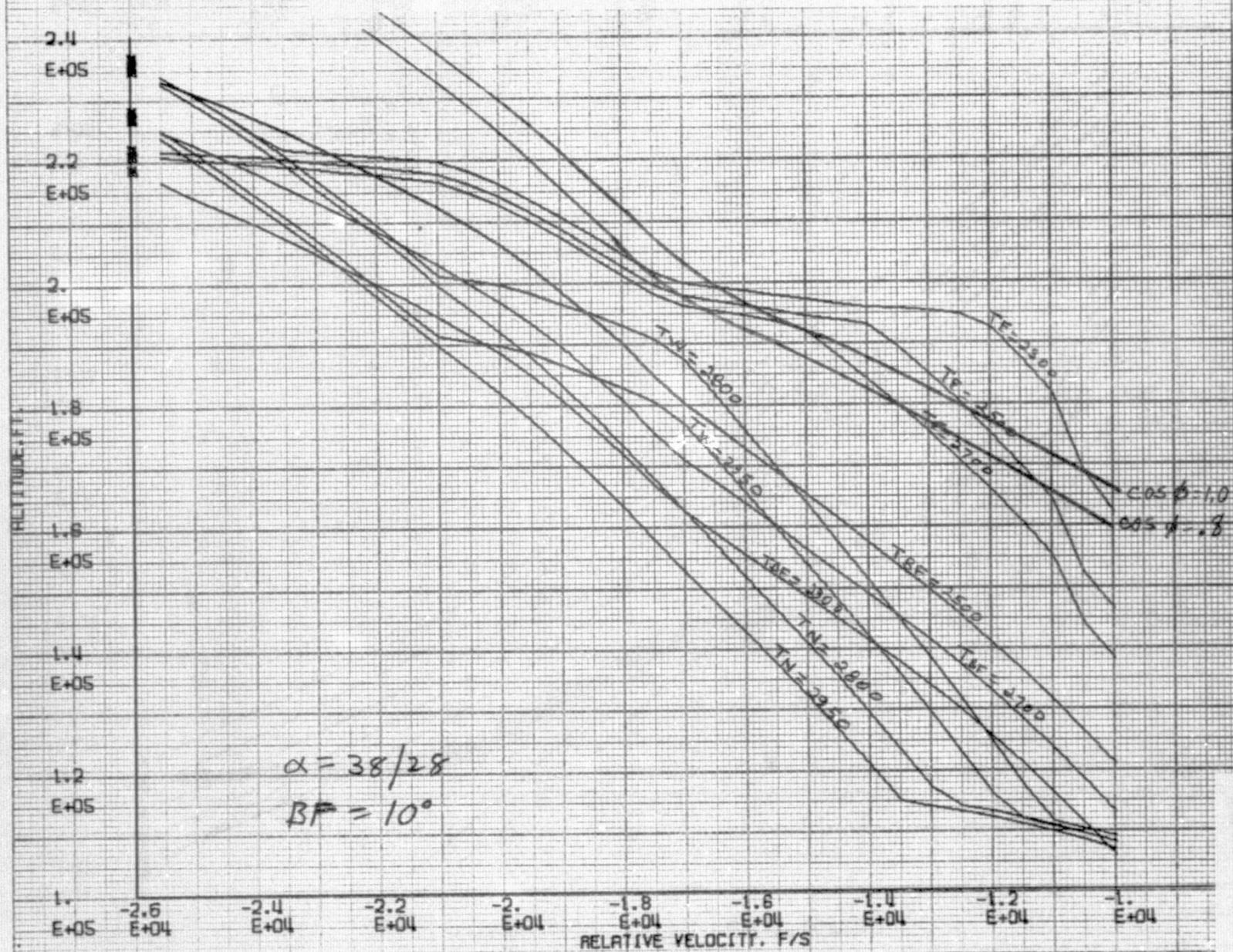




FIGURE 109 ALTITUDE VS. VELOCITY CORRIDOR

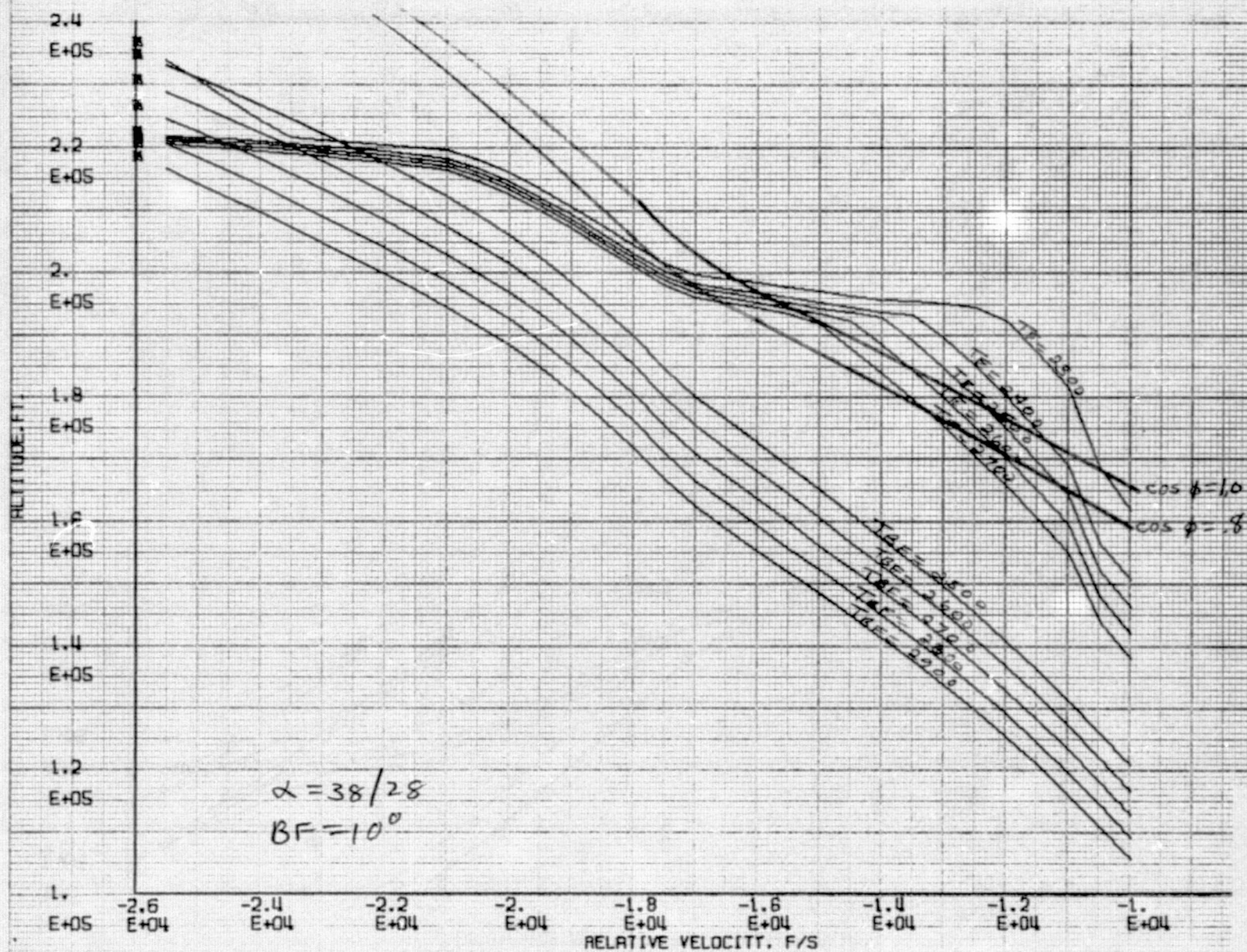


FIGURE 110 ALTITUDE VS. VELOCITY CORRIDOR

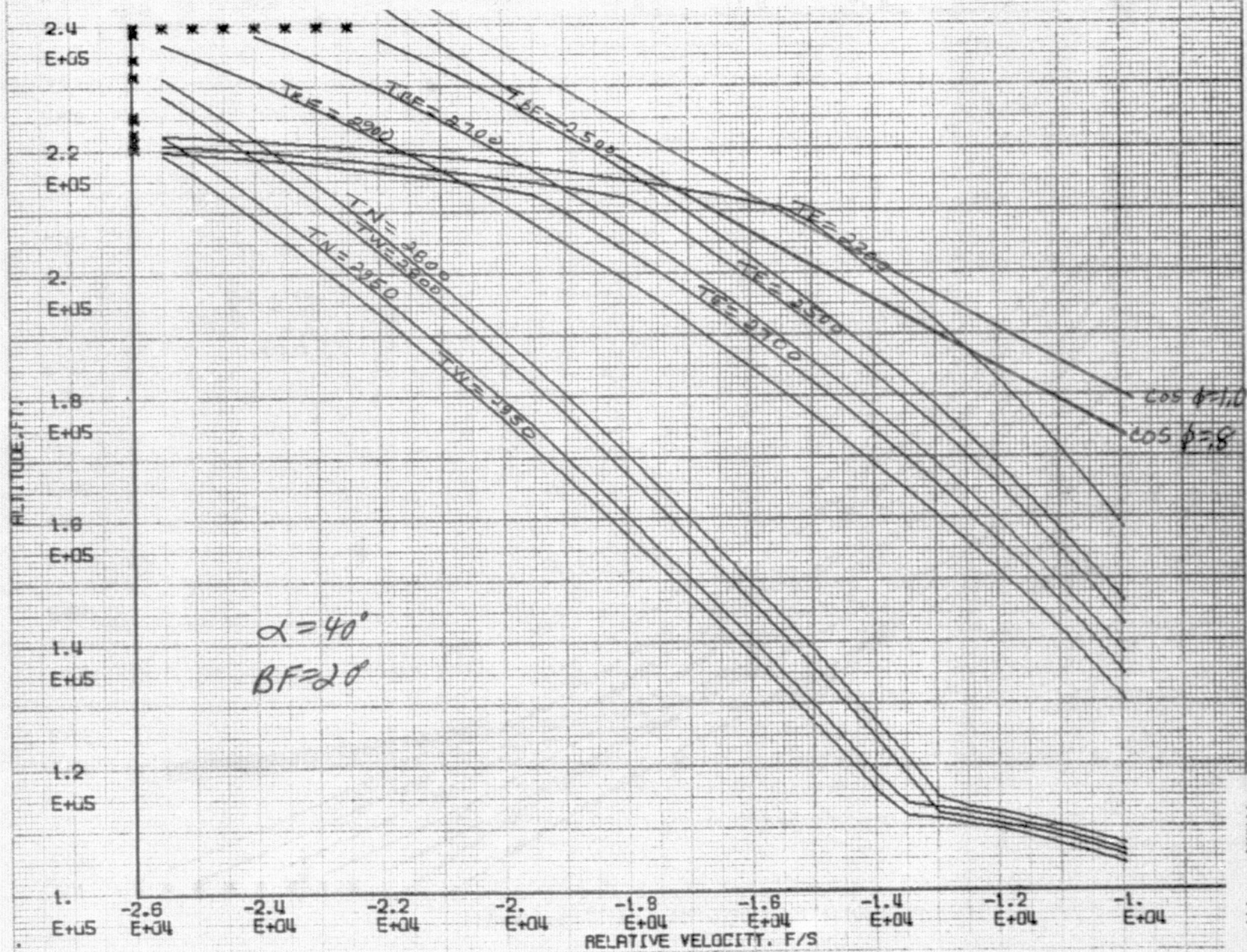




FIGURE 111 ALTITUDE VS. VELOCITY CORRIDOR

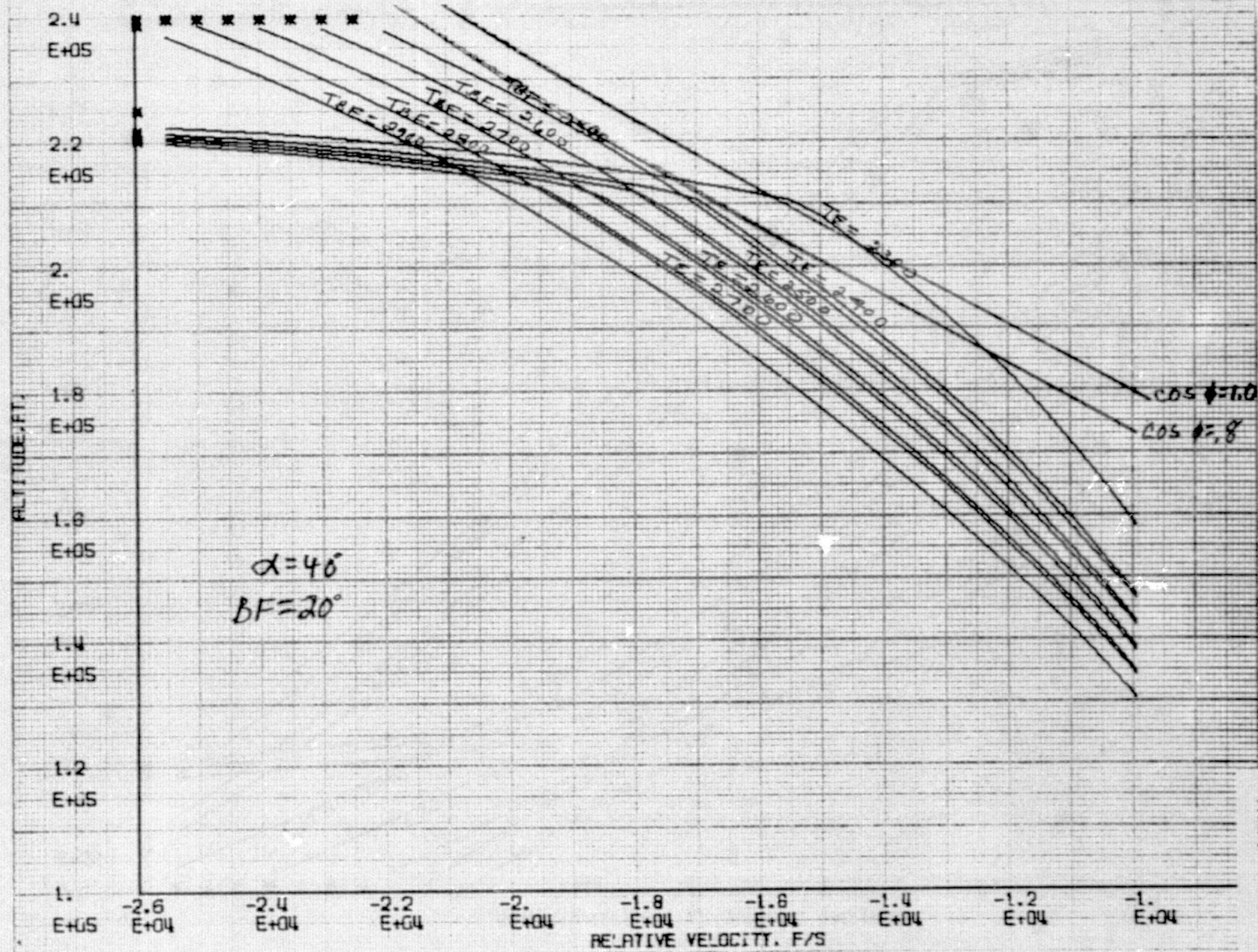




FIGURE 112 ALTITUDE VS. VELOCITY CORRIDOR

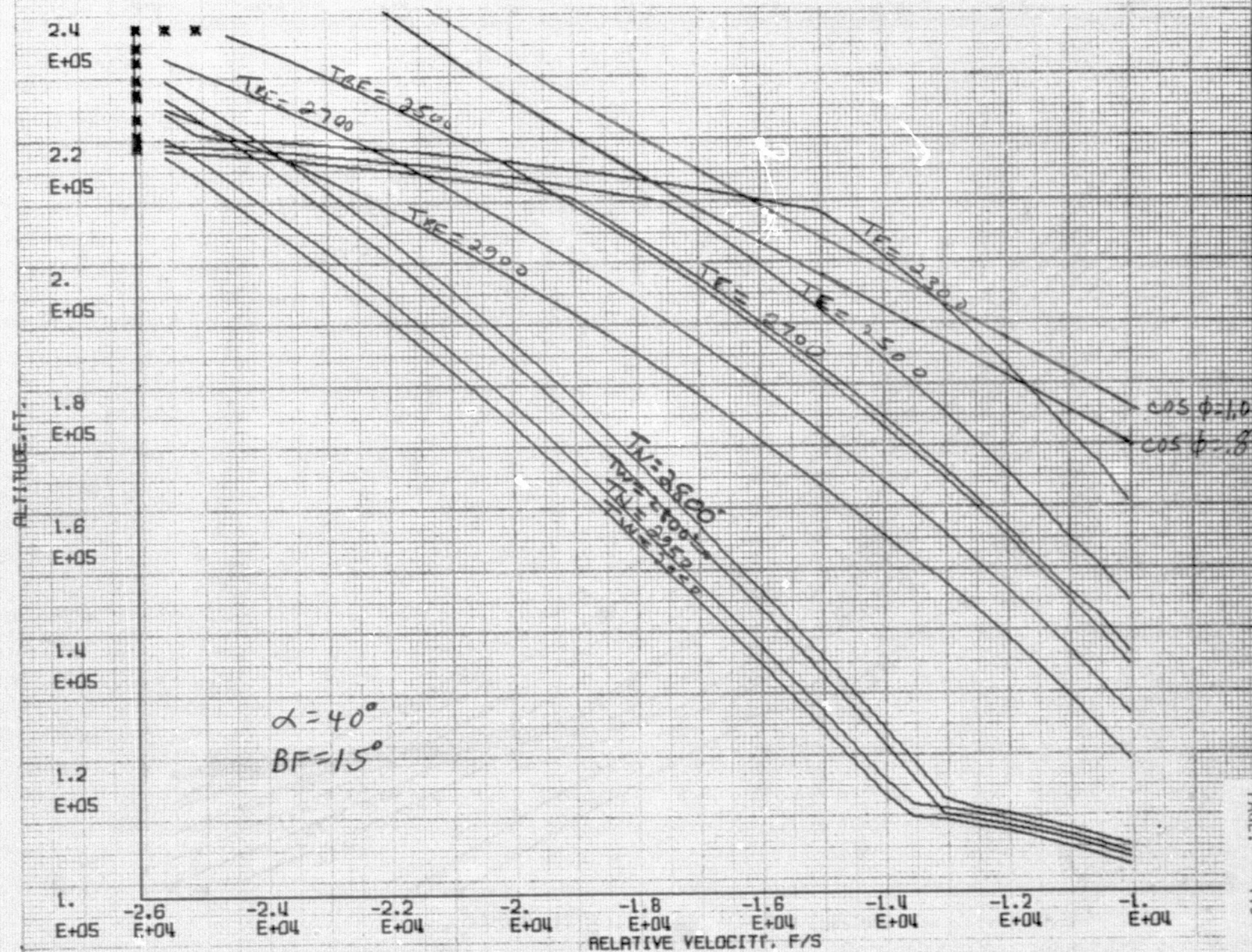


FIGURE 113 ALTITUDE VS. VELOCITY CORRIDOR

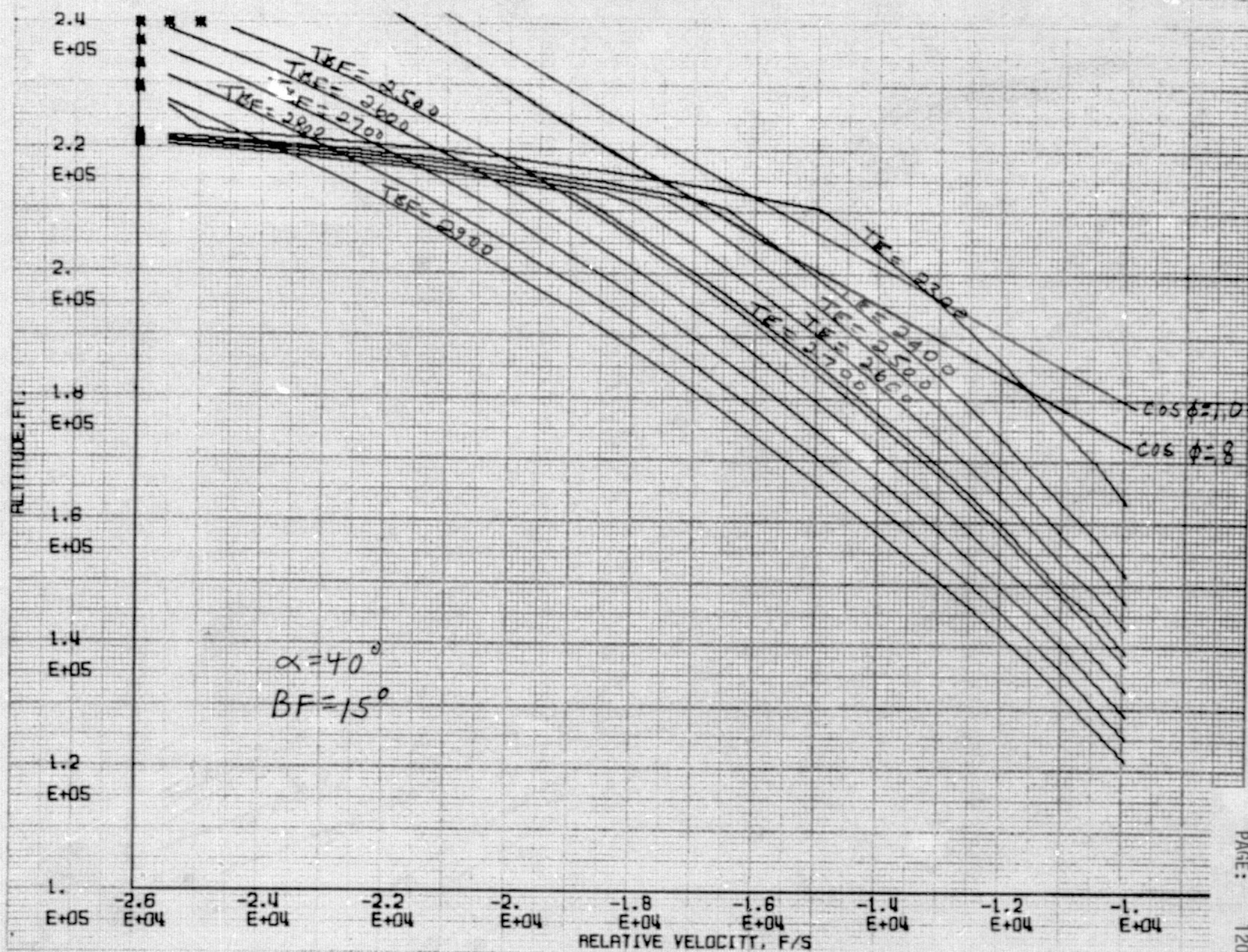




FIGURE 114 ALTITUDE VS. VELOCITY CORRIDOR

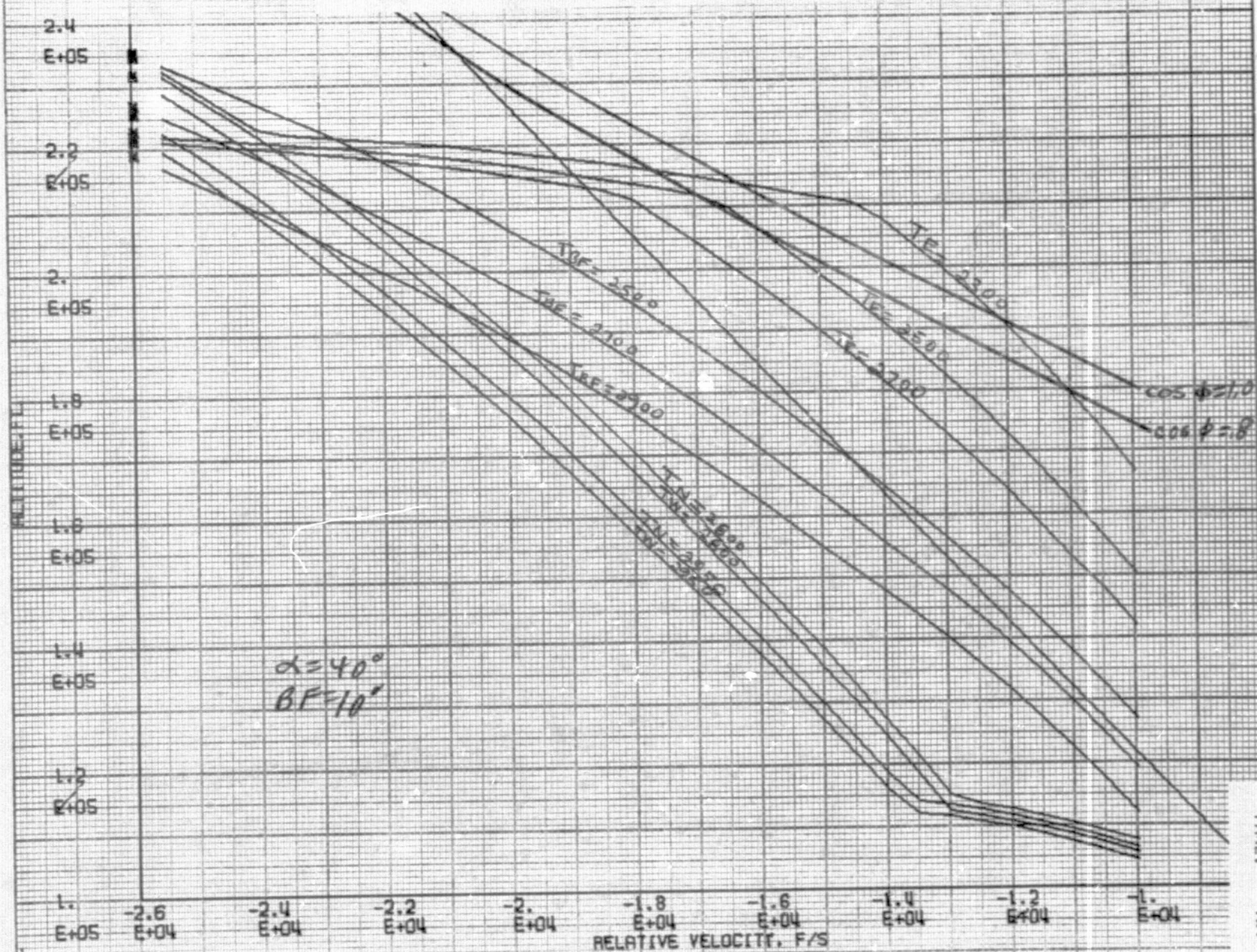




FIGURE 115 ALTITUDE VS. VELOCITY CORRIDOR

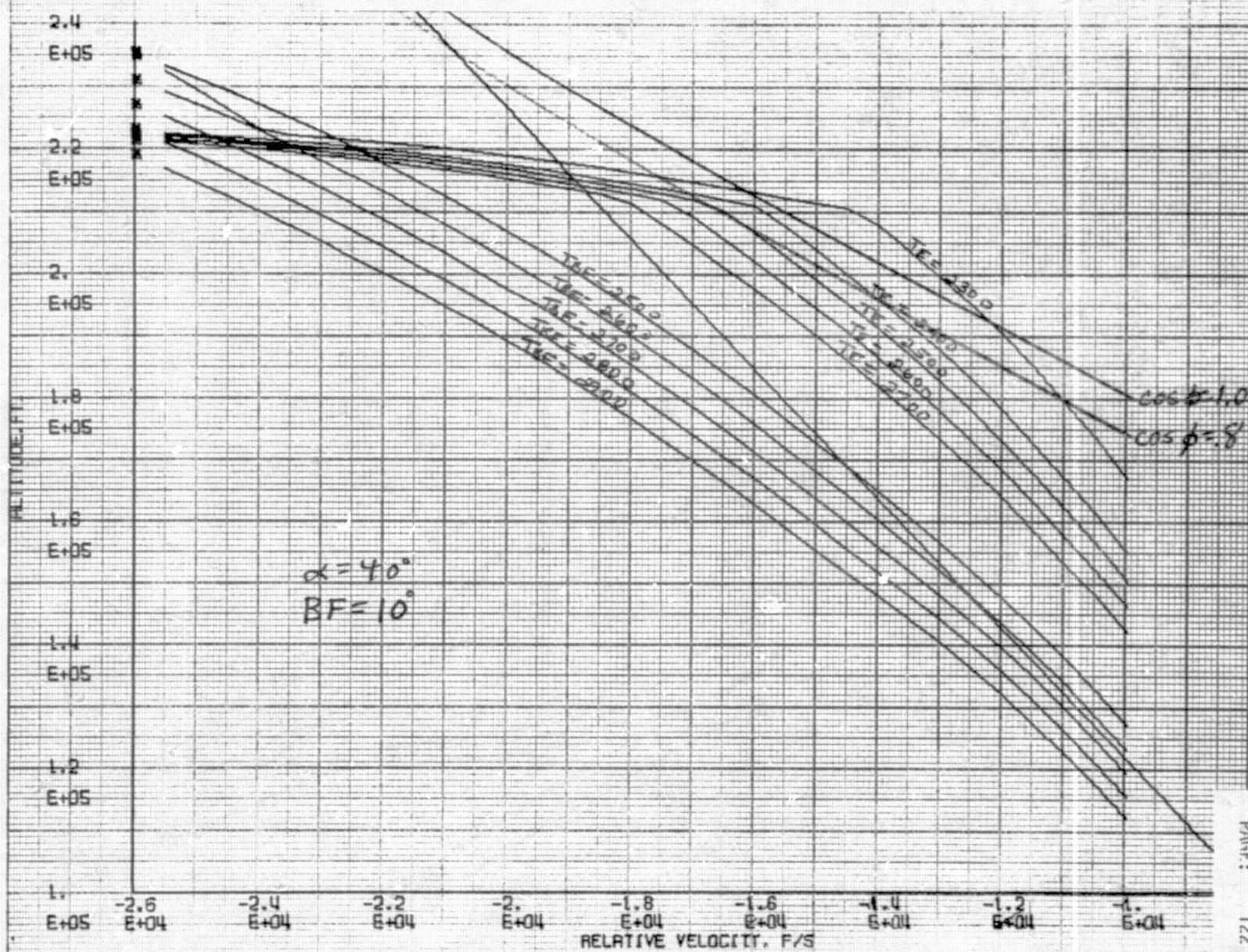


FIGURE 116 ALTITUDE VS. VELOCITY CORRIDOR

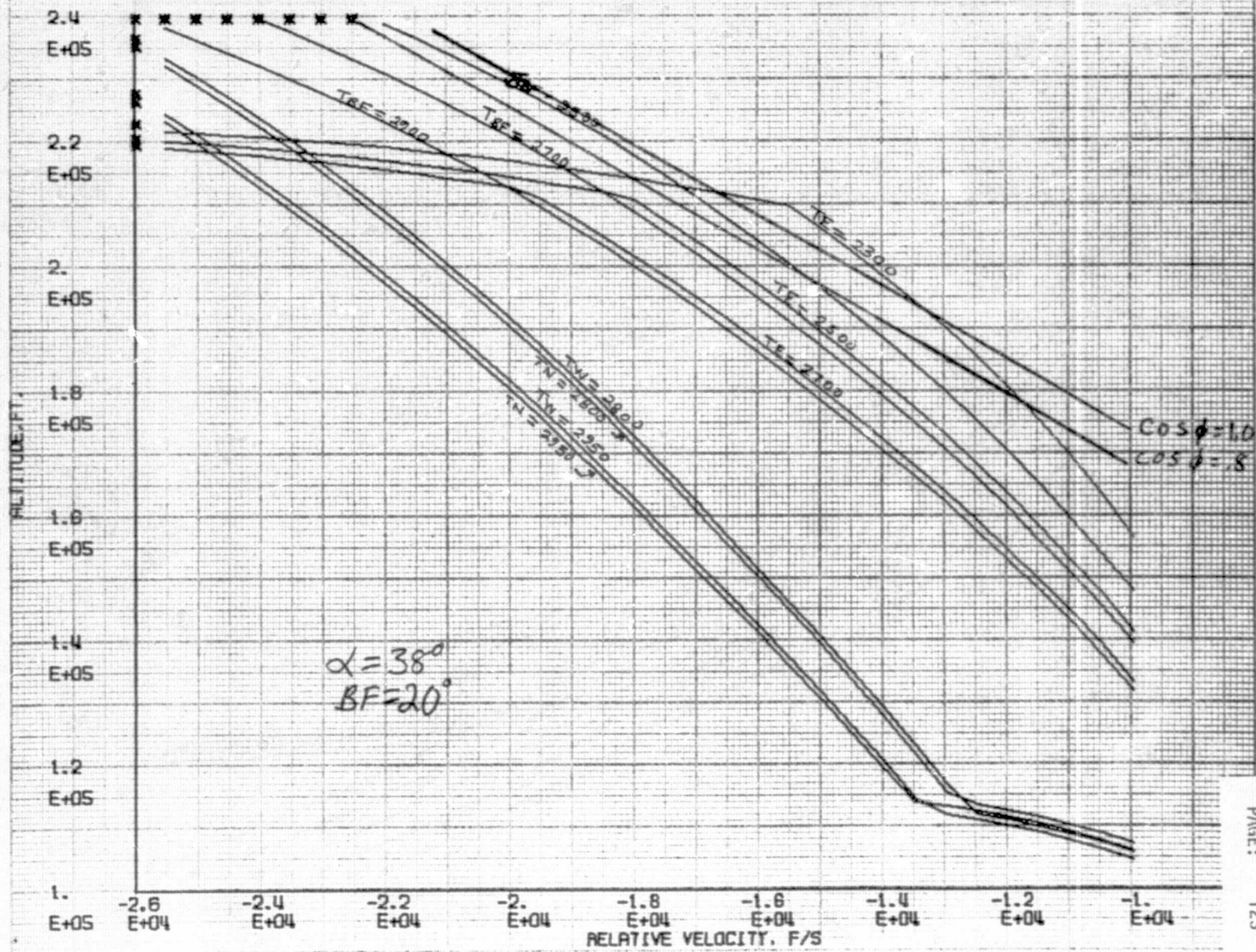
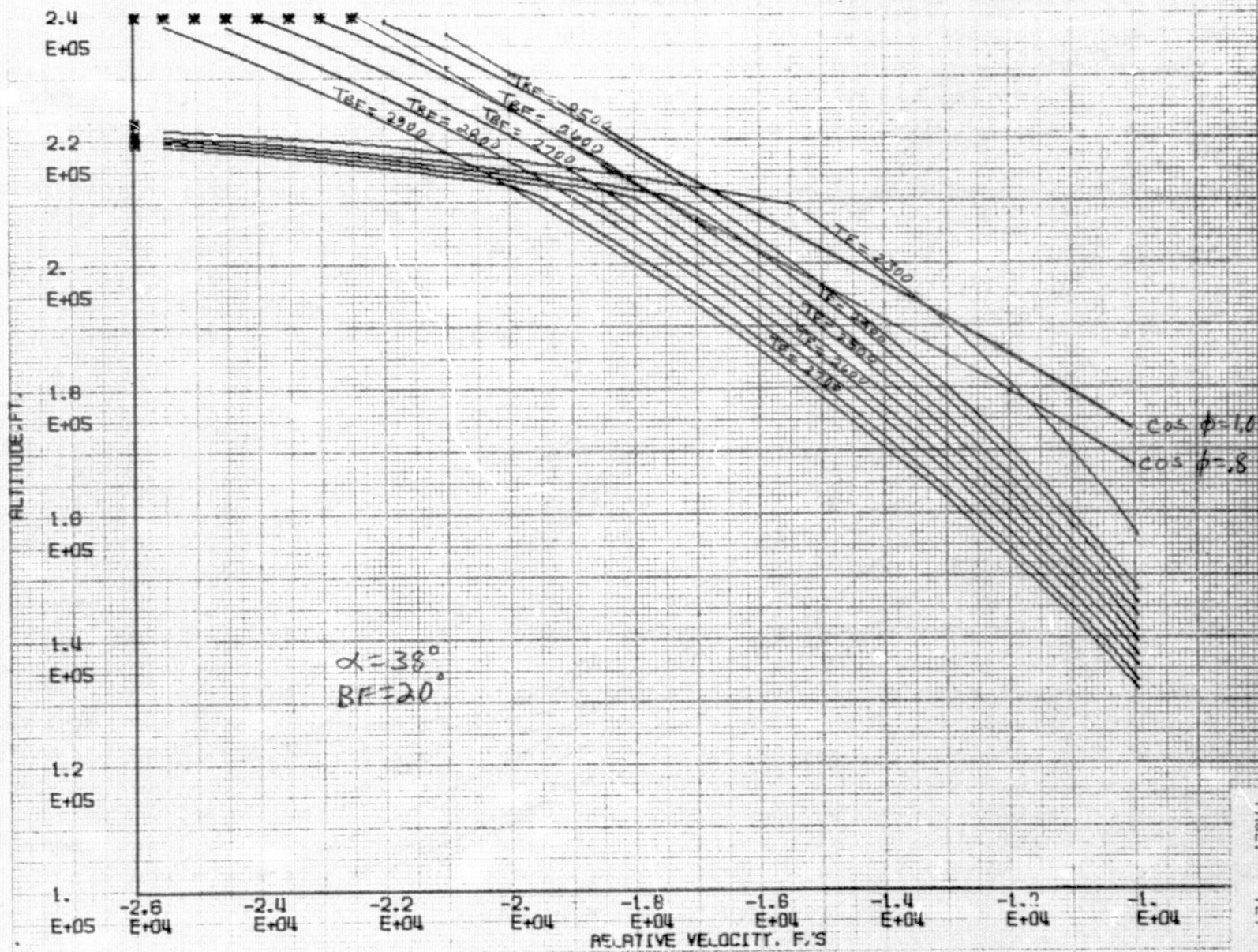




FIGURE 117 ALTITUDE VS. VELOCITY CORRIDOR





REPRODUCIBILITY OF THE  
ORIGINAL PAGE IS POOR

FIGURE 118 ALTITUDE VS. VELOCITY CORRIDOR

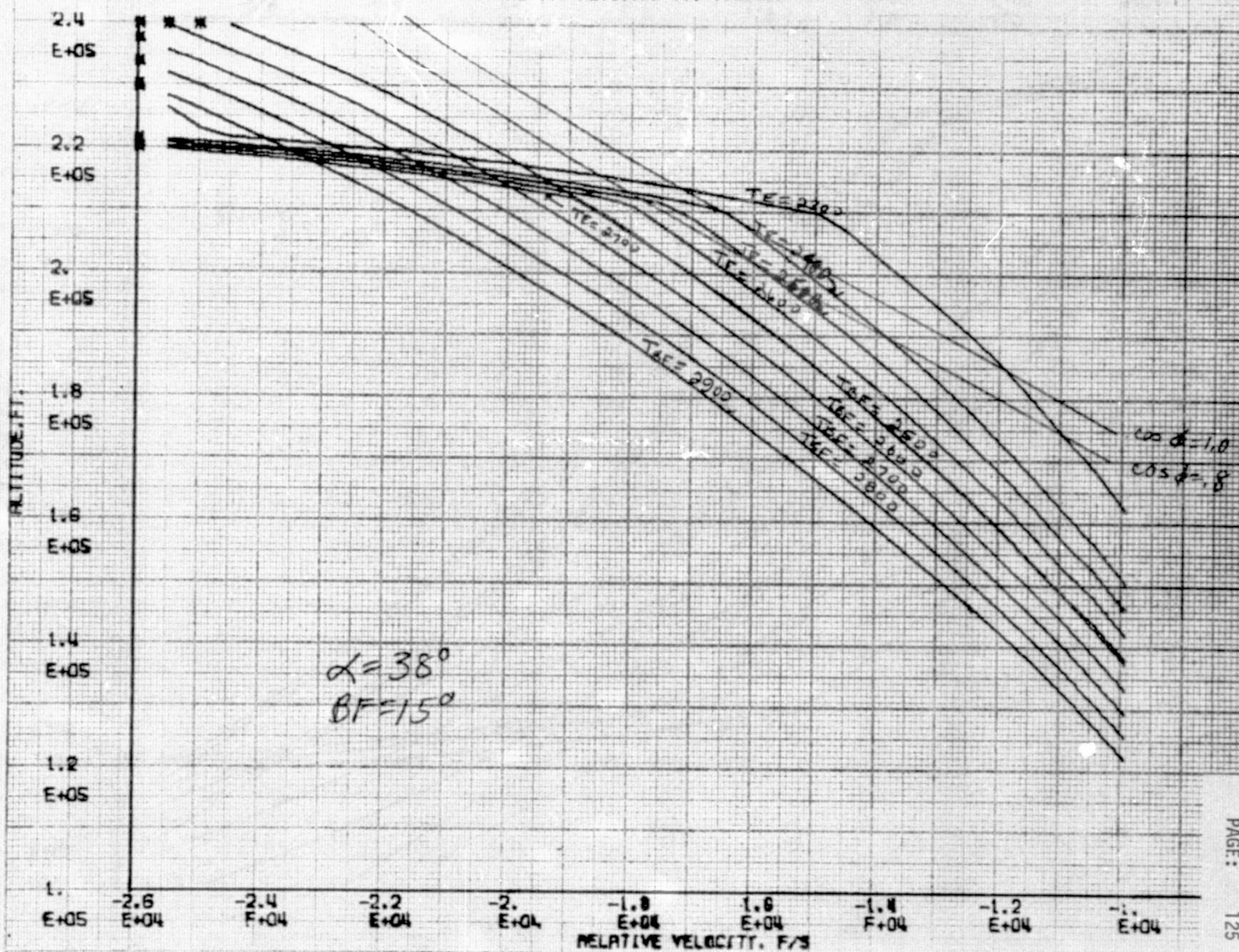


FIGURE 119 ALTITUDE VS. VELOCITY CORRIDOR

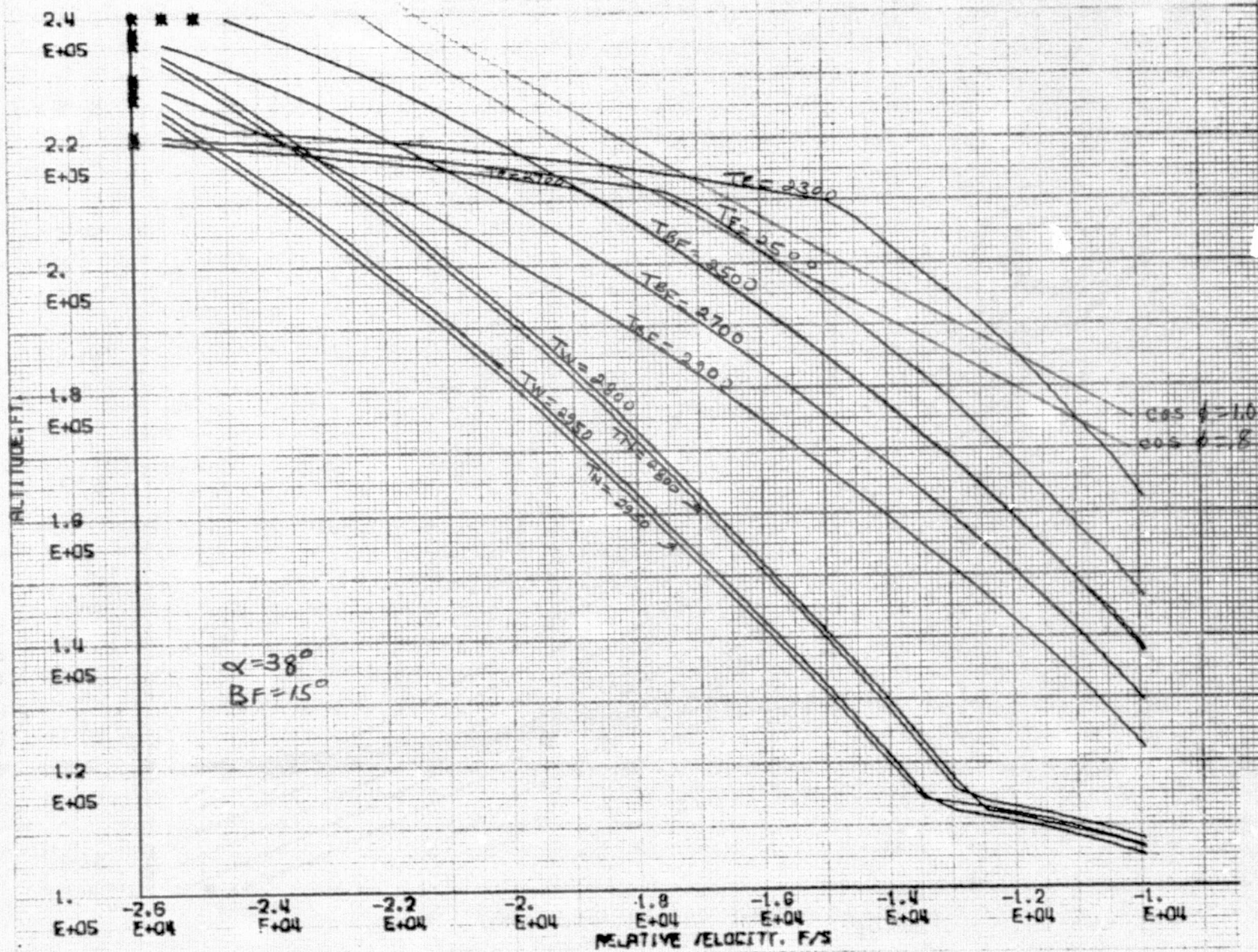




FIGURE 120 ALTITUDE VS. VELOCITY CORRIDOR

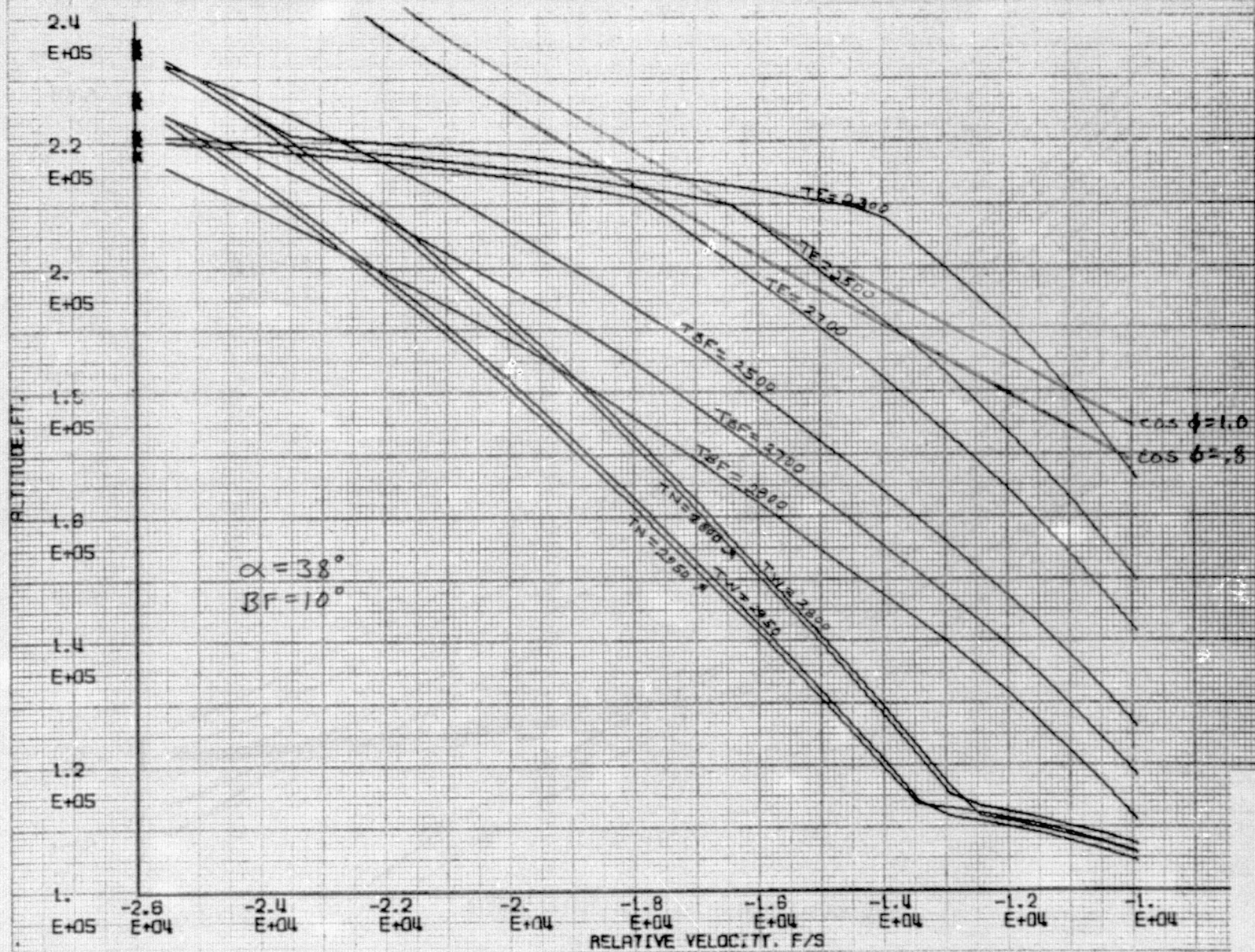




FIGURE 121 ALTITUDE VS. VELOCITY CORRIDOR

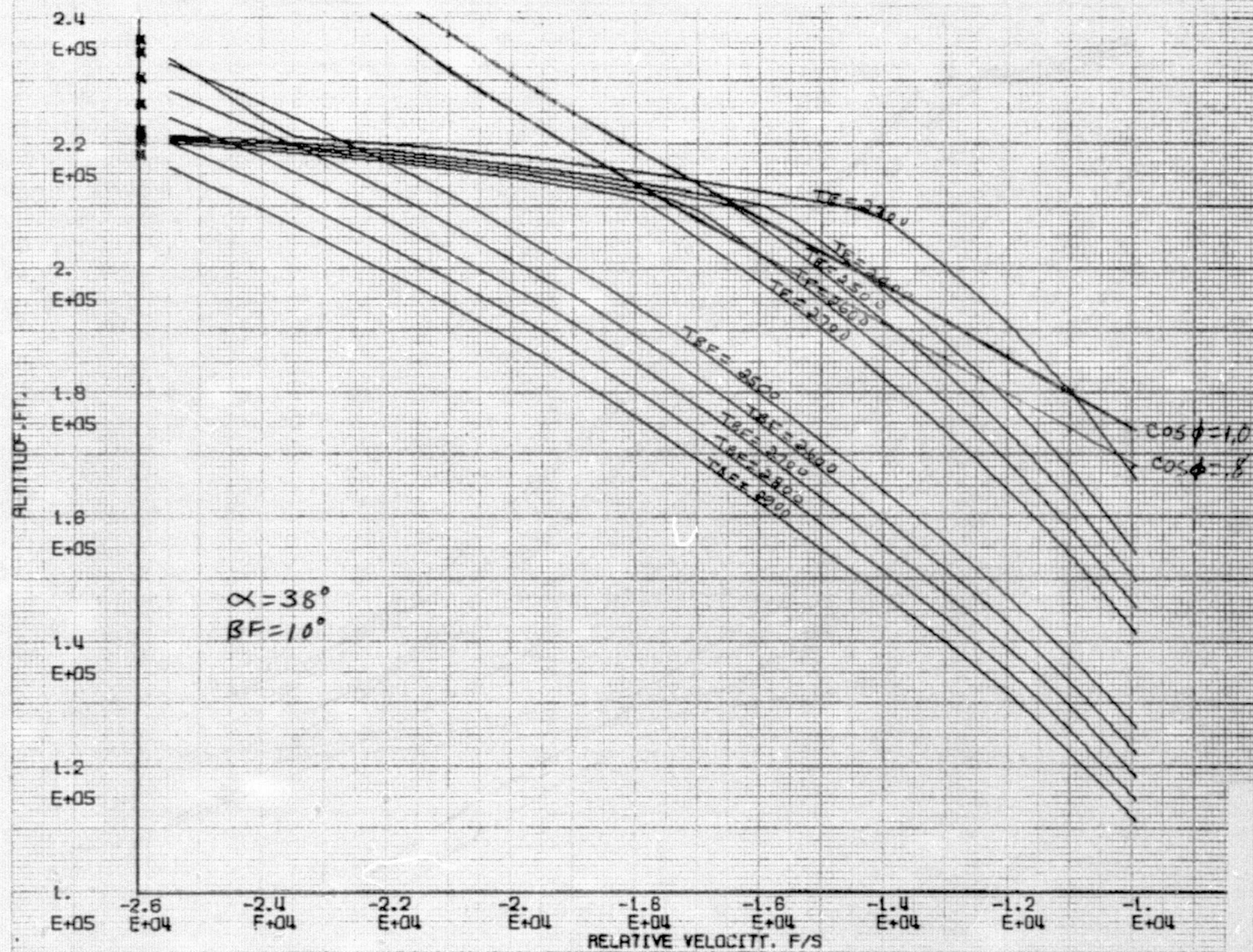


FIGURE 122 ALTITUDE VS. VELOCITY CORRIDOR

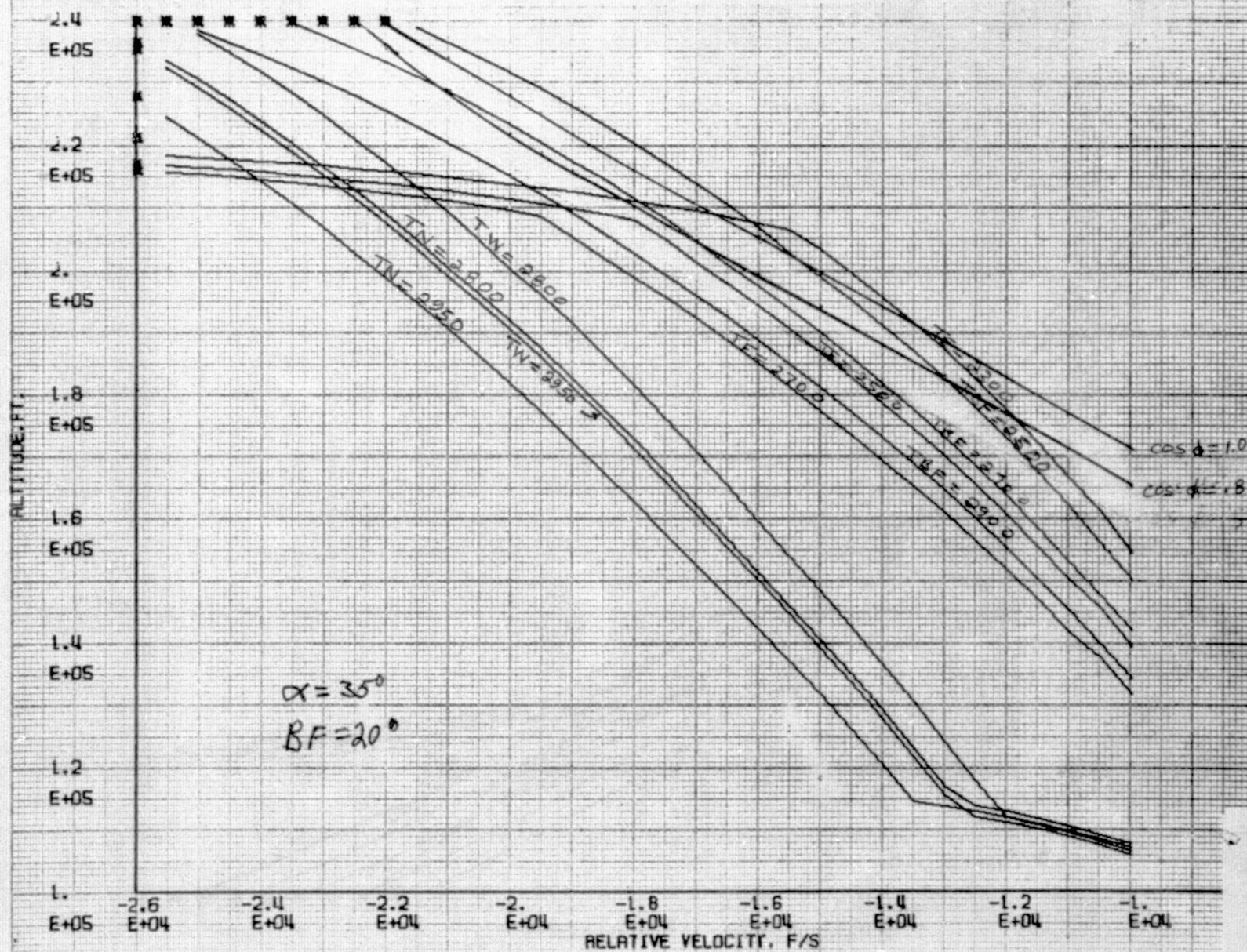




FIGURE 123 ALTITUDE VS. VELOCITY CORRIDOR

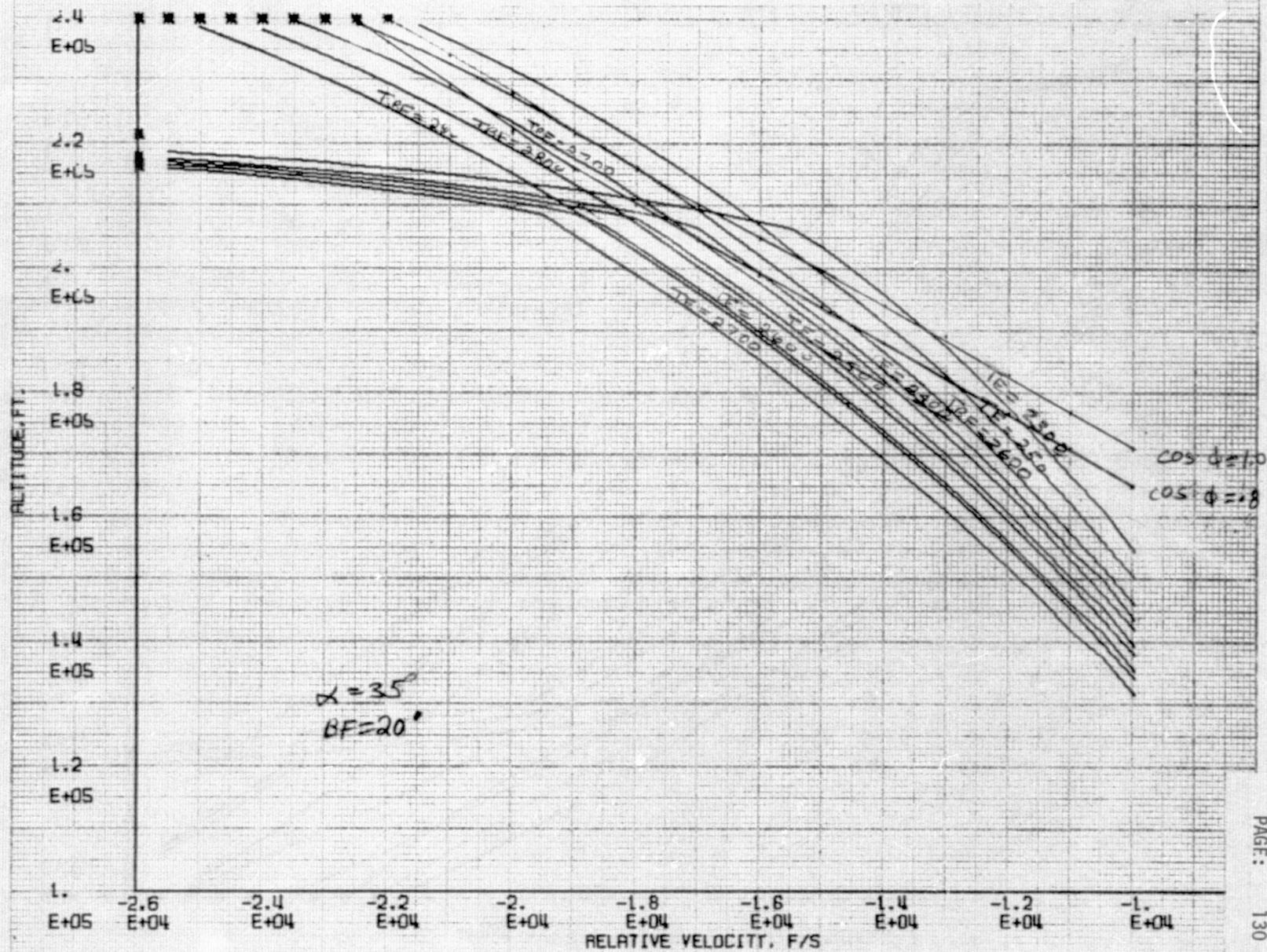




FIGURE 124 ALTITUDE VS. VELOCITY CORRIDOR

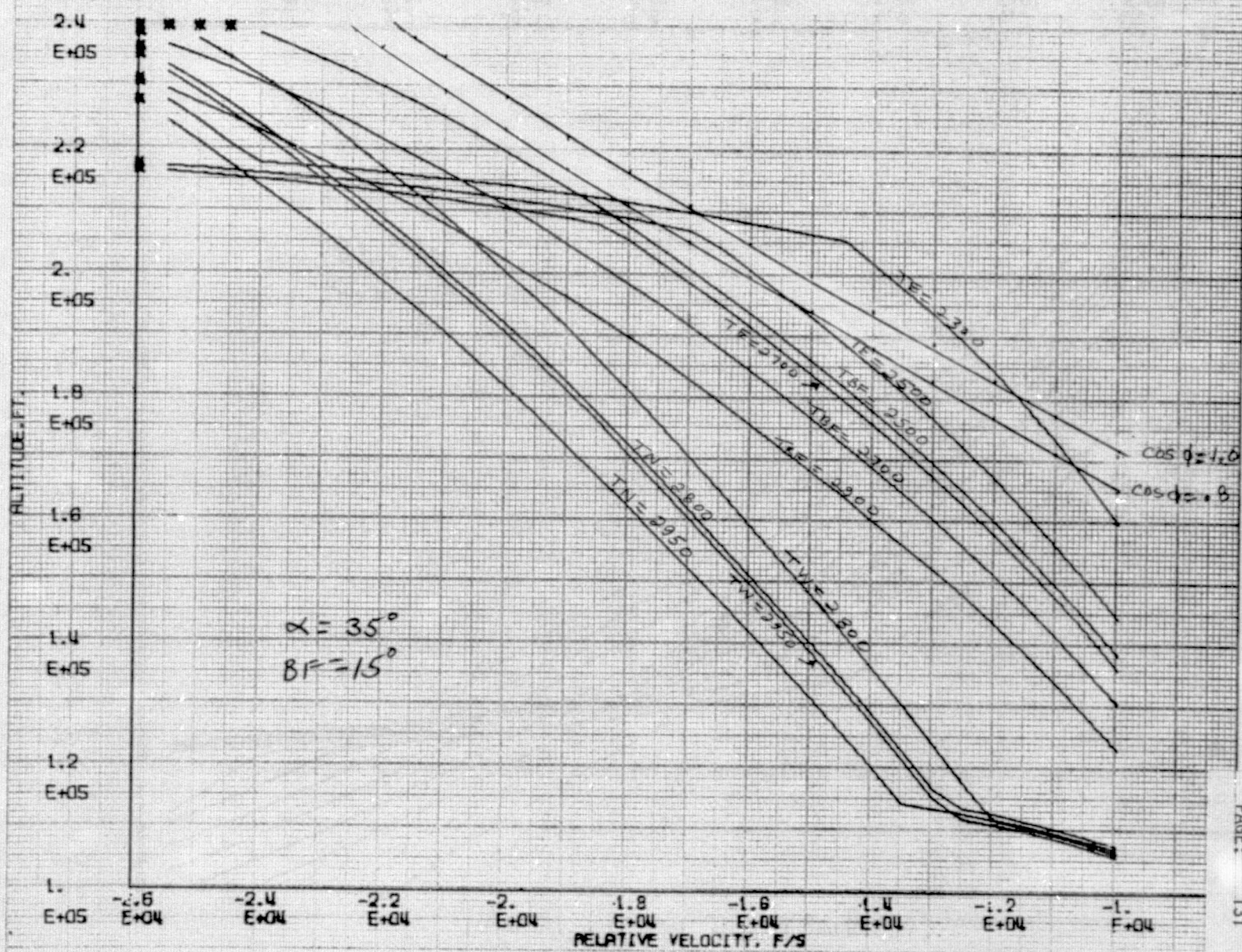


FIGURE 125 ALTITUDE VS. VELOCITY CORRIDOR

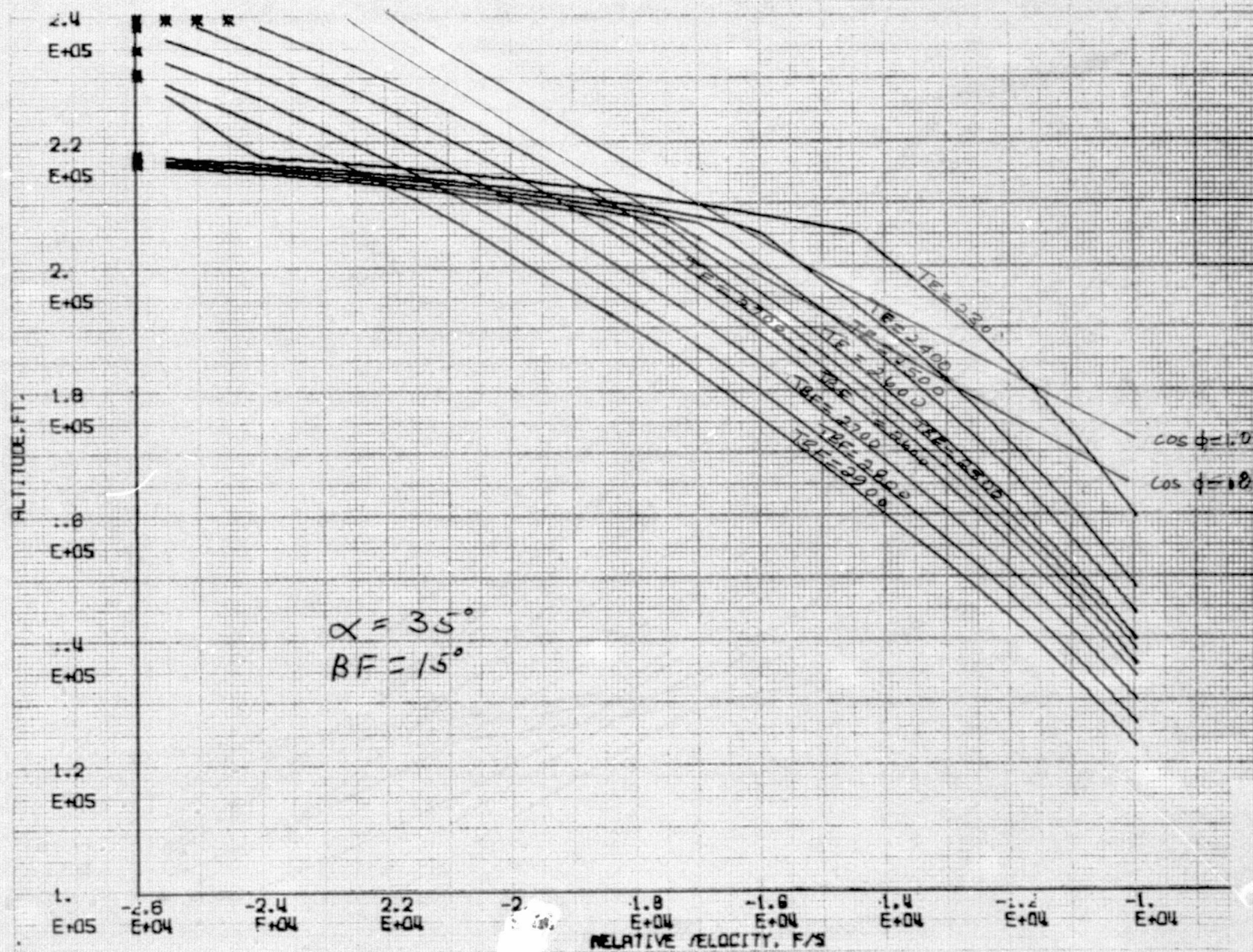




FIGURE 126 ALTITUDE VS. VELOCITY CORRIDOR

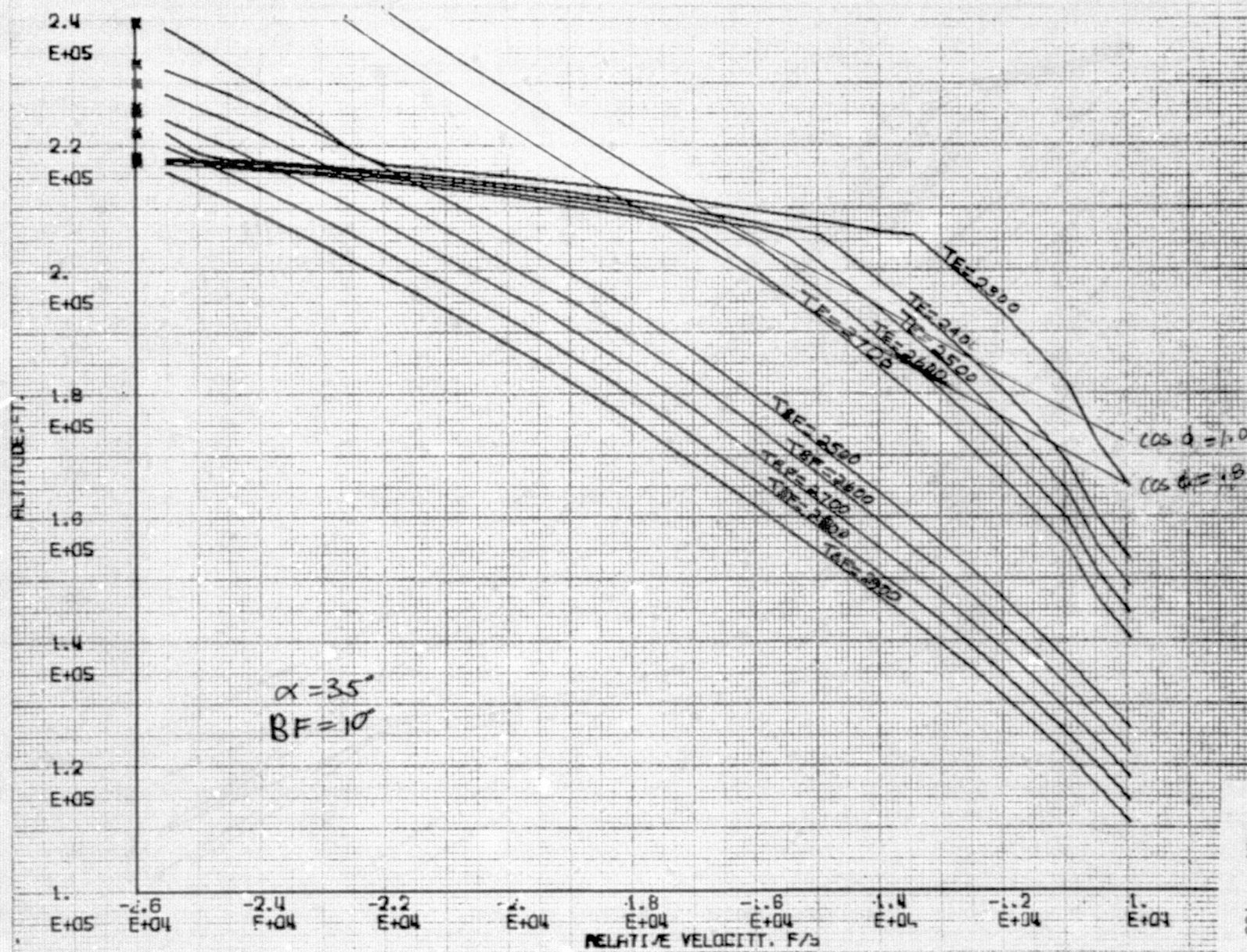


FIGURE 127 ALTITUDE VS. VELOCITY CORRIDOR

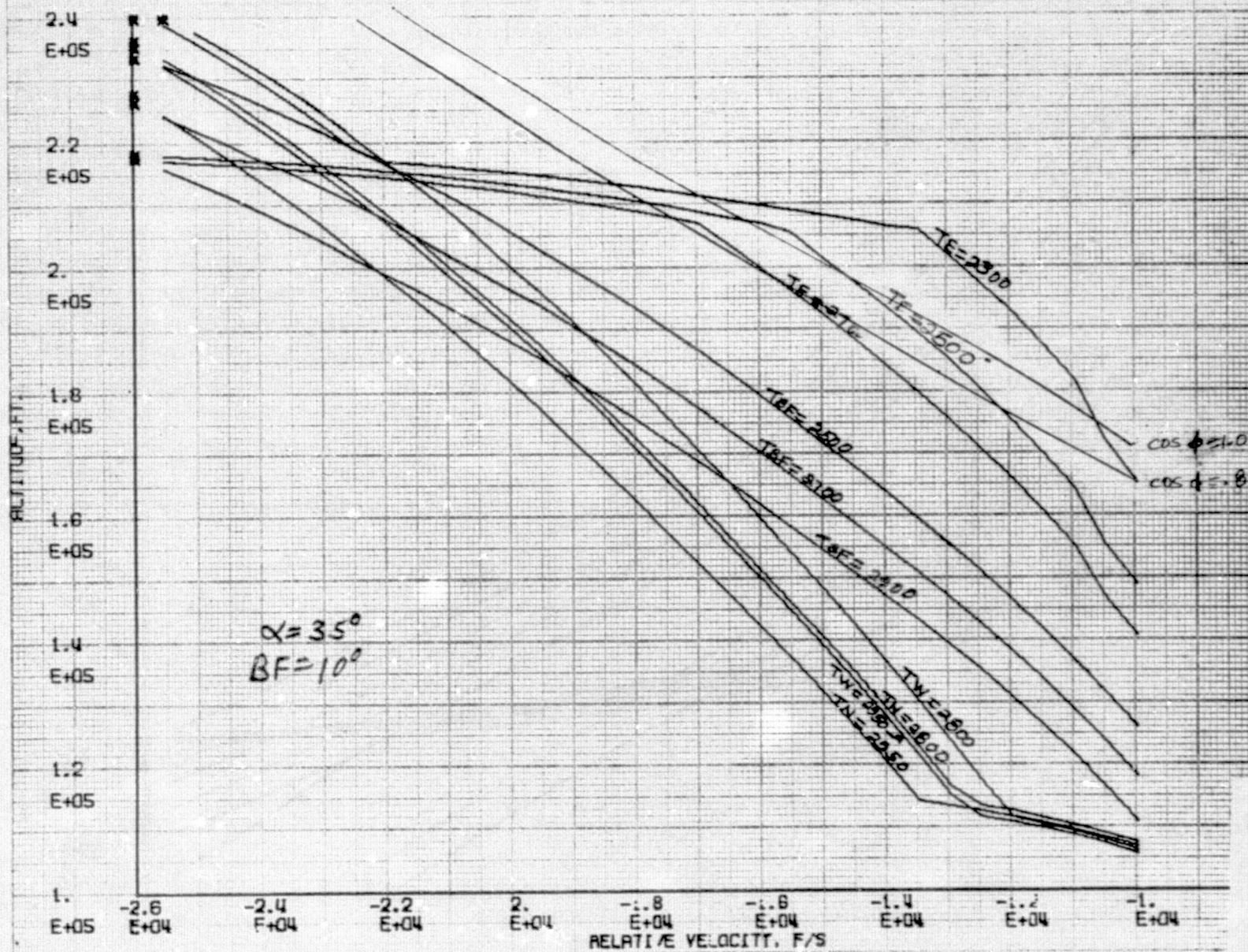




FIGURE 128 ALTITUDE VS. VELOCITY CORRIDOR

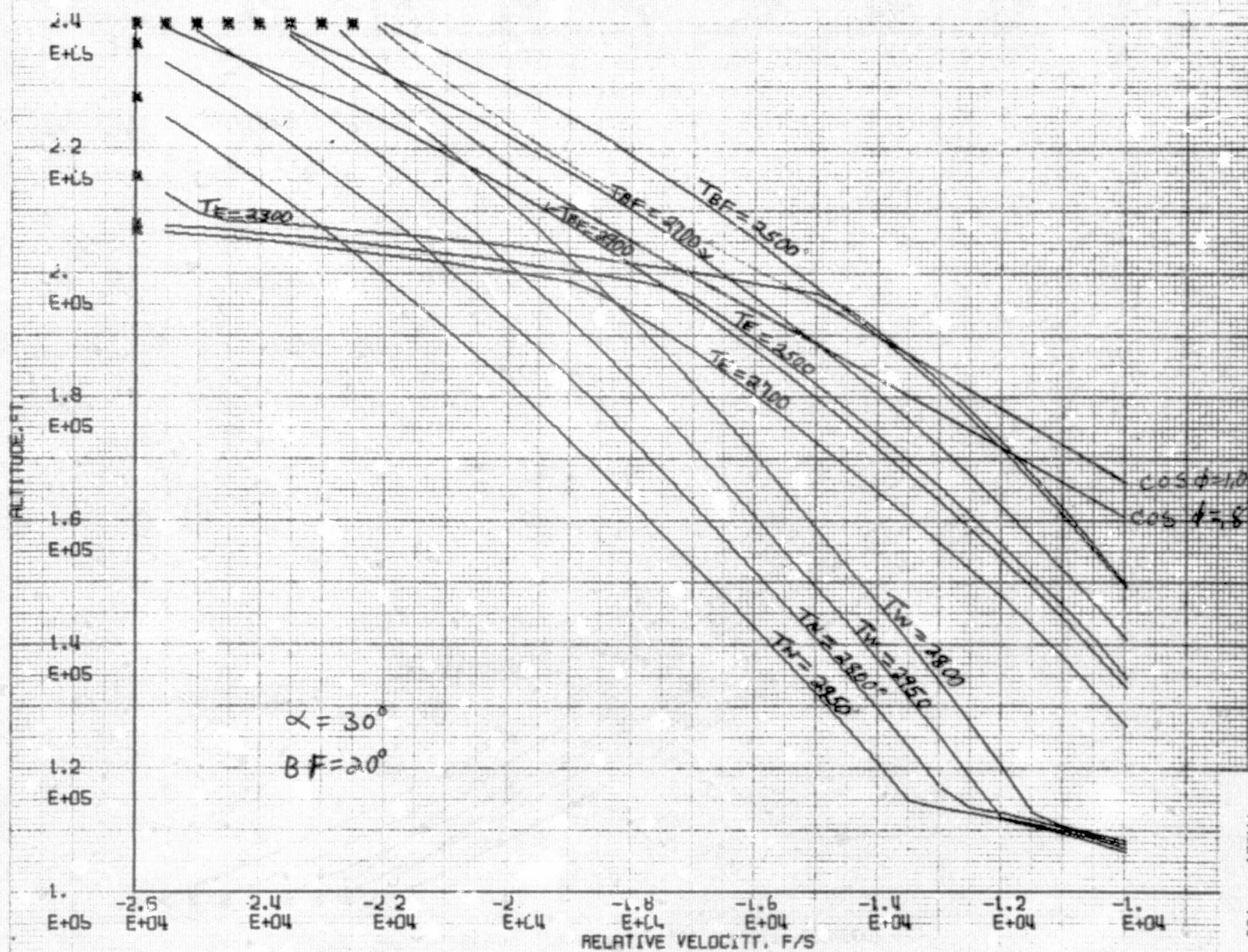


FIGURE 129 ALTITUDE VS. VELOCITY CORRIDOR

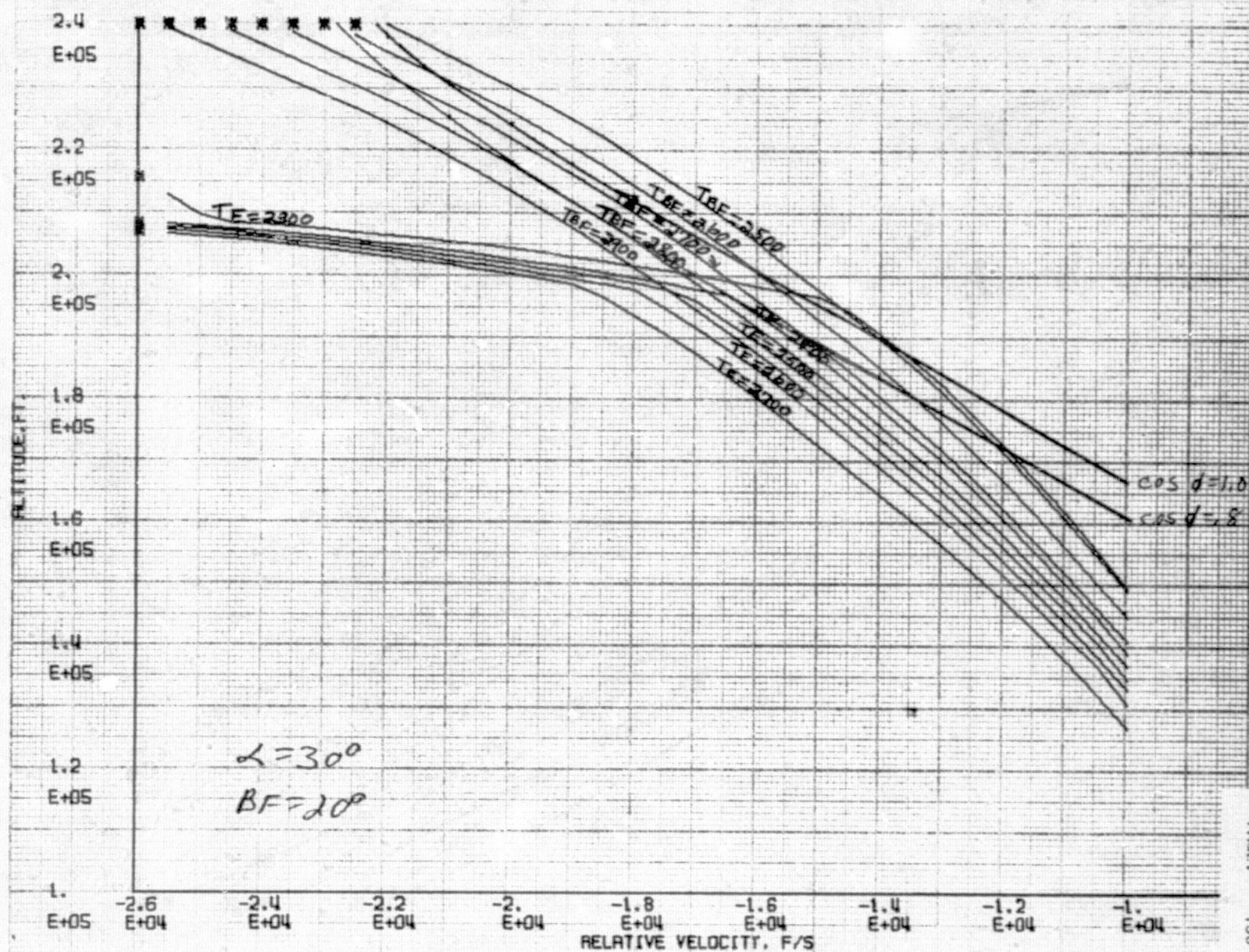




FIGURE 130 ALTITUDE VS. VELOCITY CORRIDOR

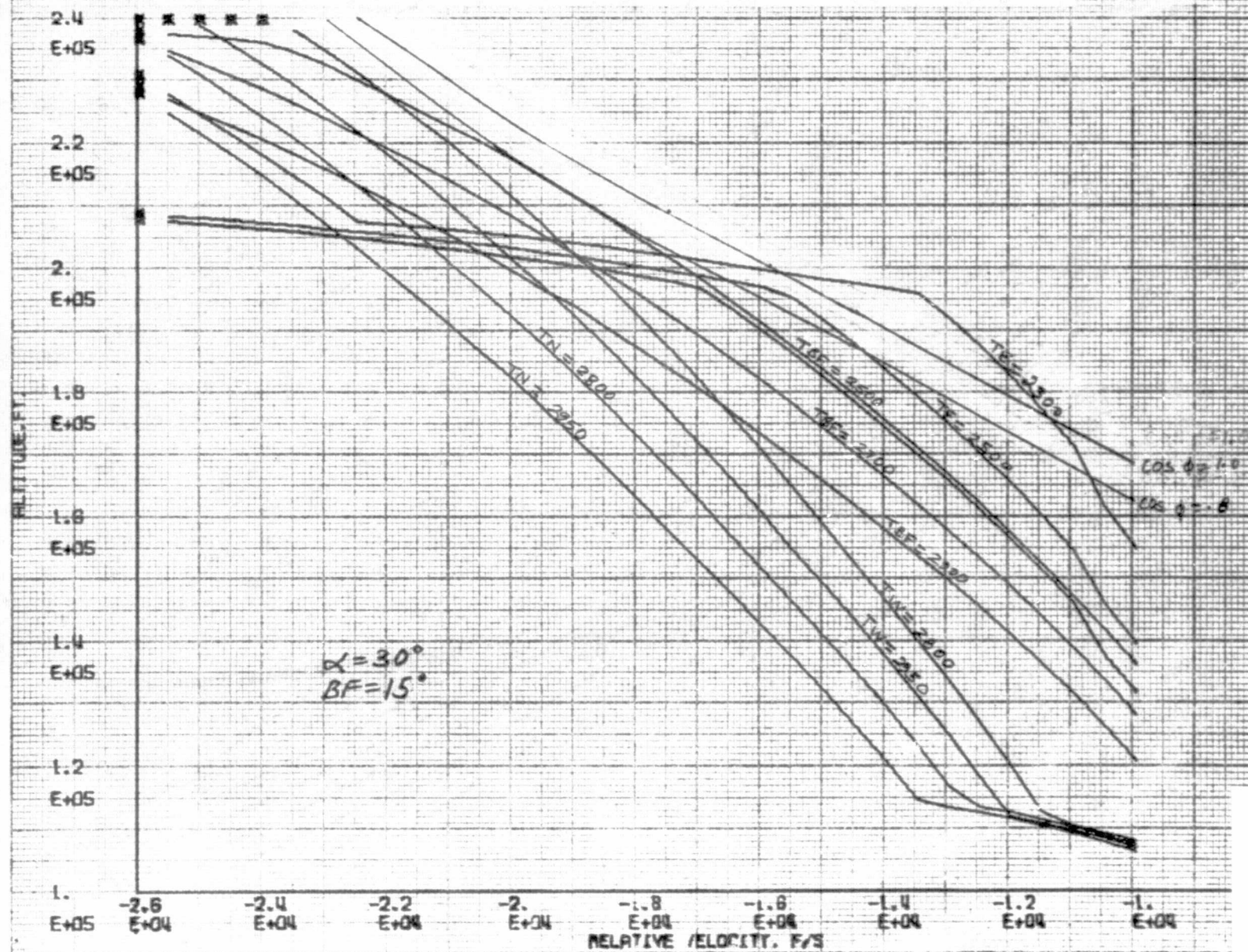


FIGURE 131 ALTITUDE VS. VELOCITY CORRIDOR

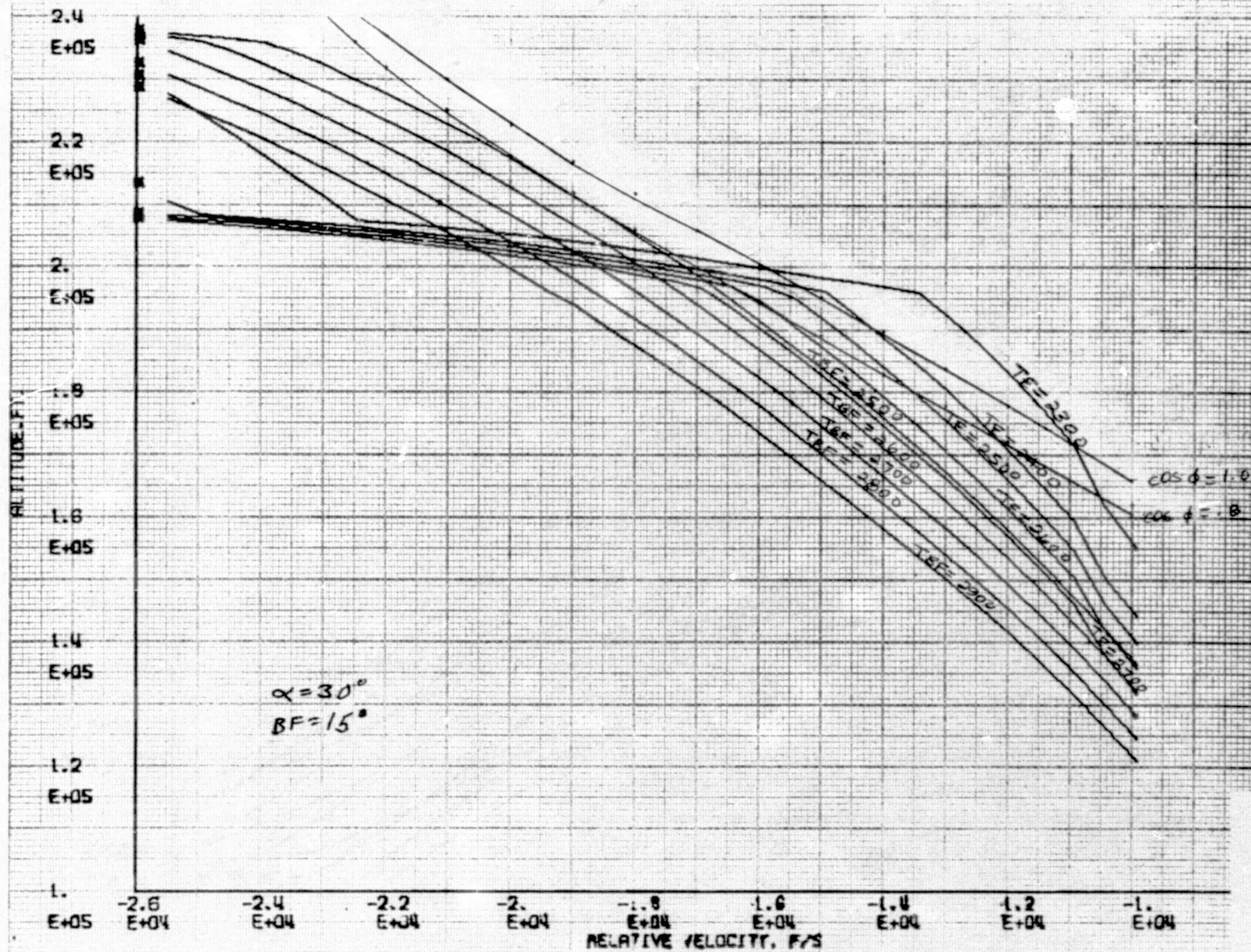




FIGURE 132 ALTITUDE VS. VELOCITY CORRIDOR

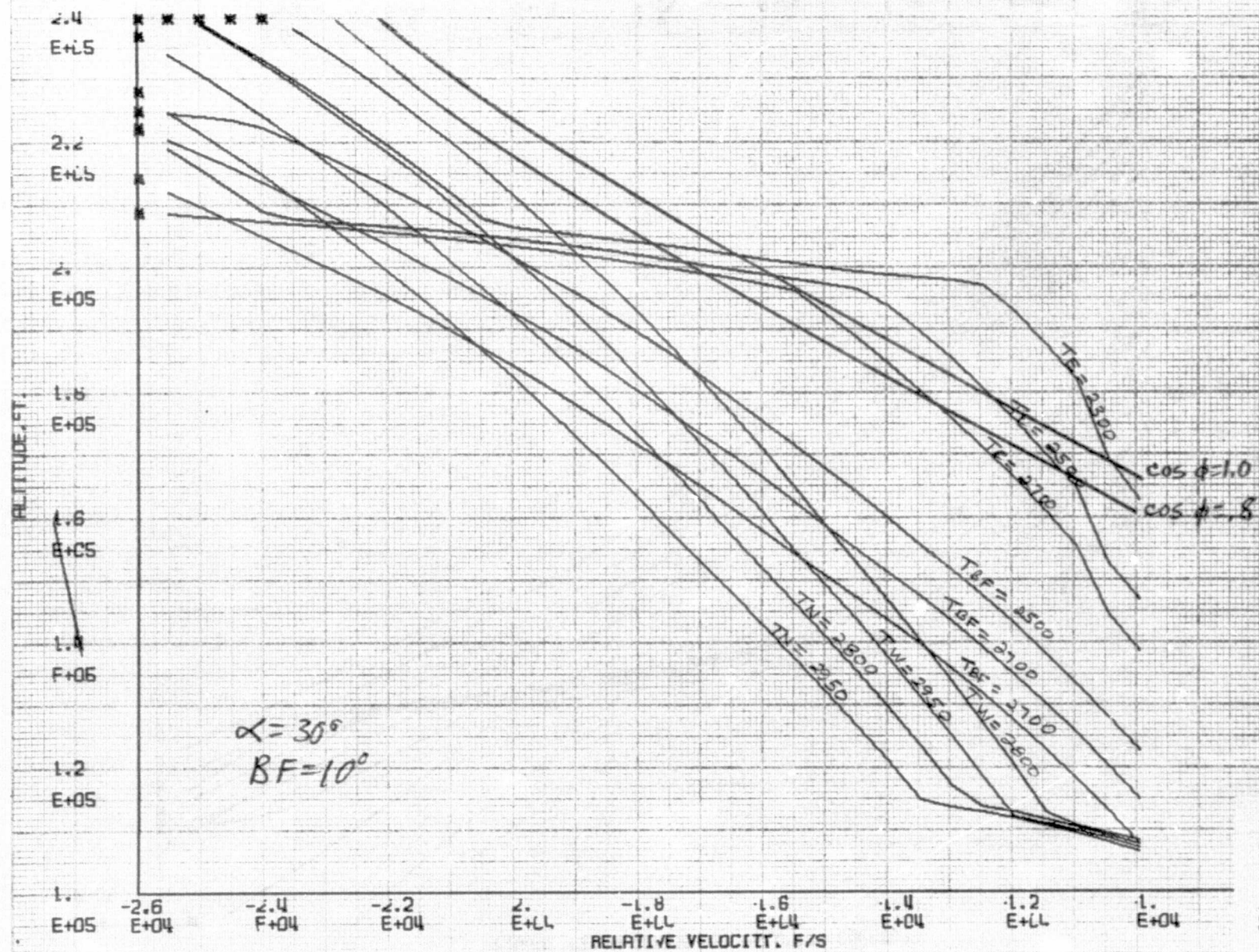
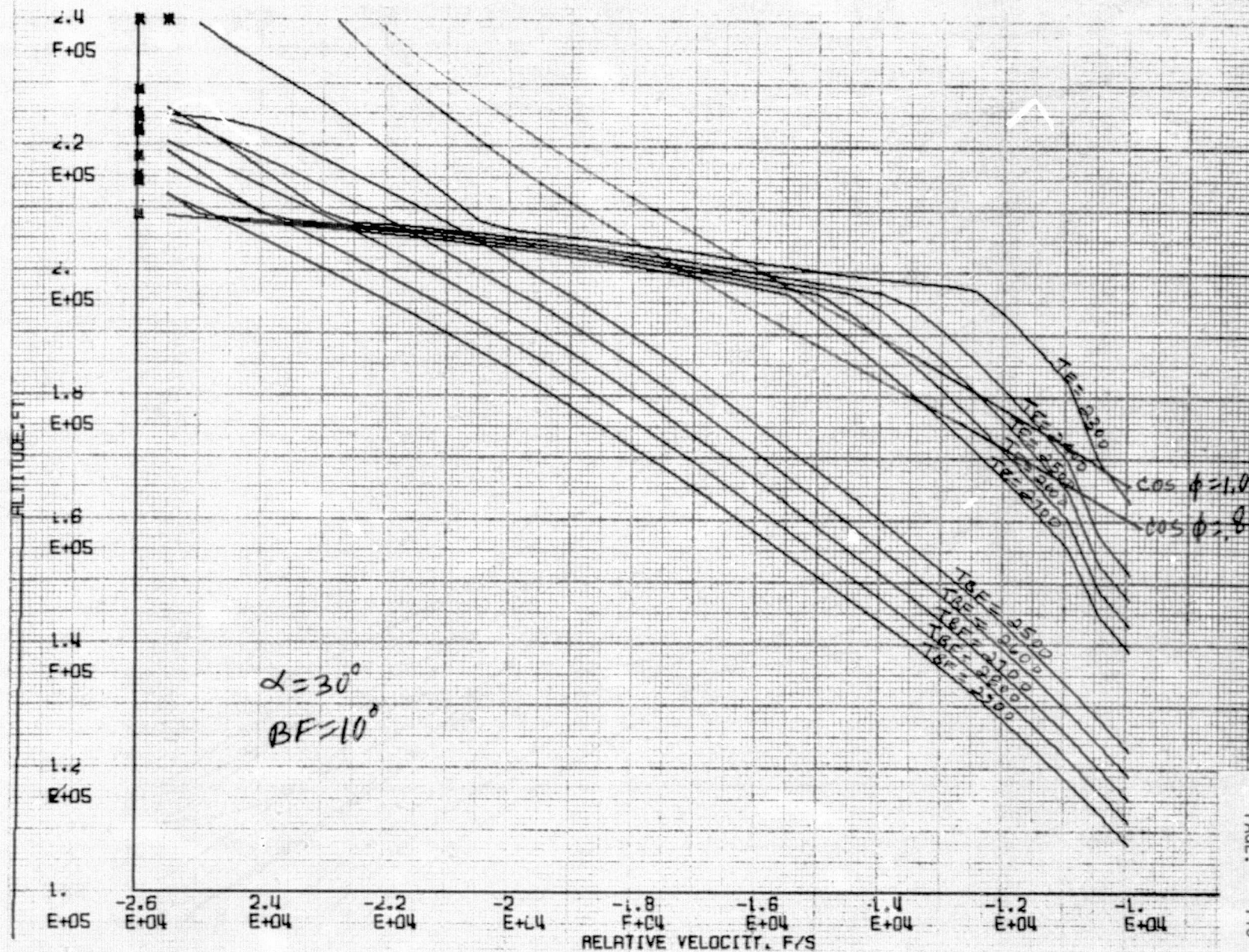


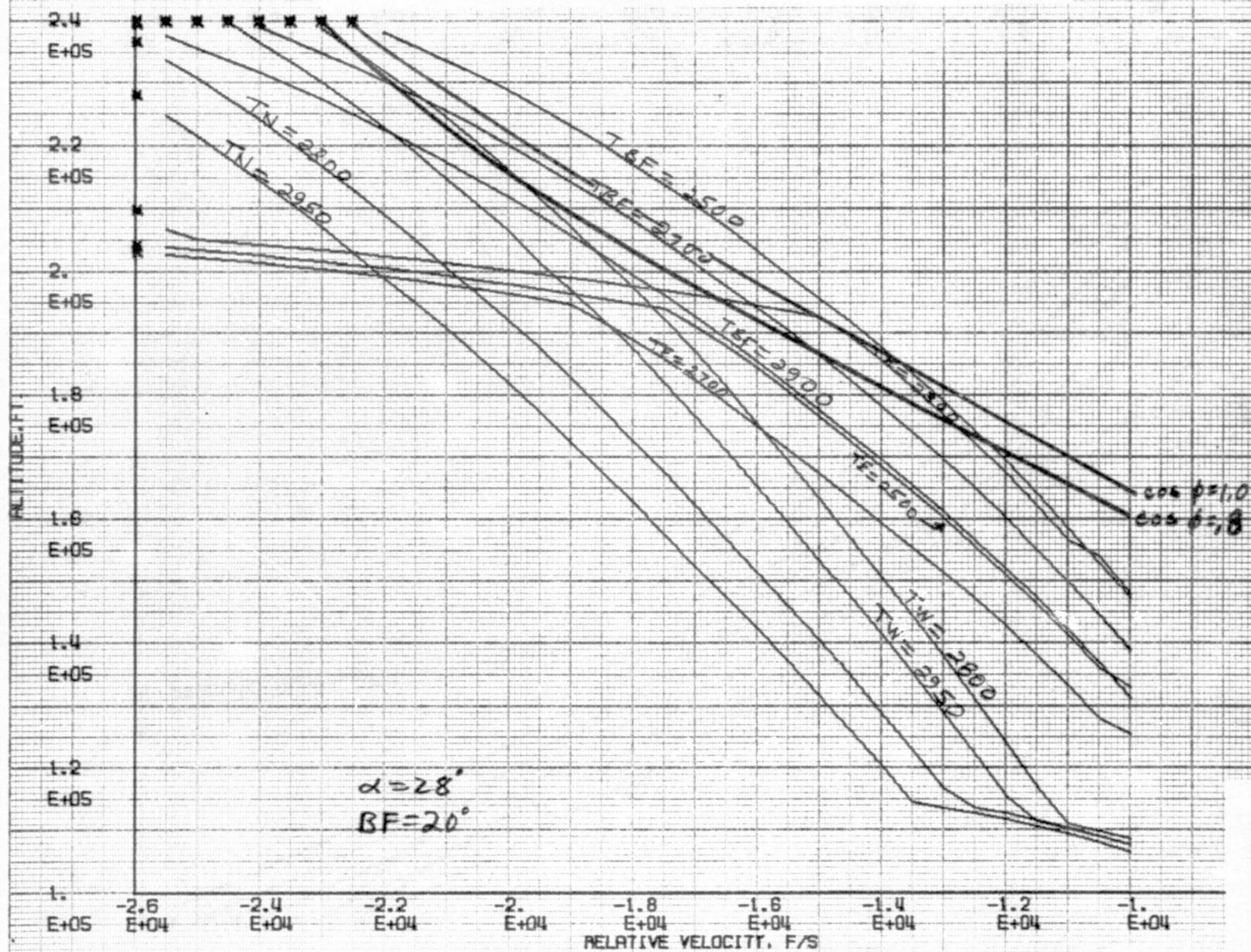
FIGURE 133 ALTITUDE VS. VELOCITY CORRIDOR





REPRODUCIBILITY OF THE  
ORIGINAL PAGE IS POOR

FIGURE 134 ALTITUDE VS. VELOCITY CORRIDOR



DN NO.: 1.A-4-8  
PAGE: 141

FIGURE 135 ALTITUDE VS. VELOCITY CORRIDOR

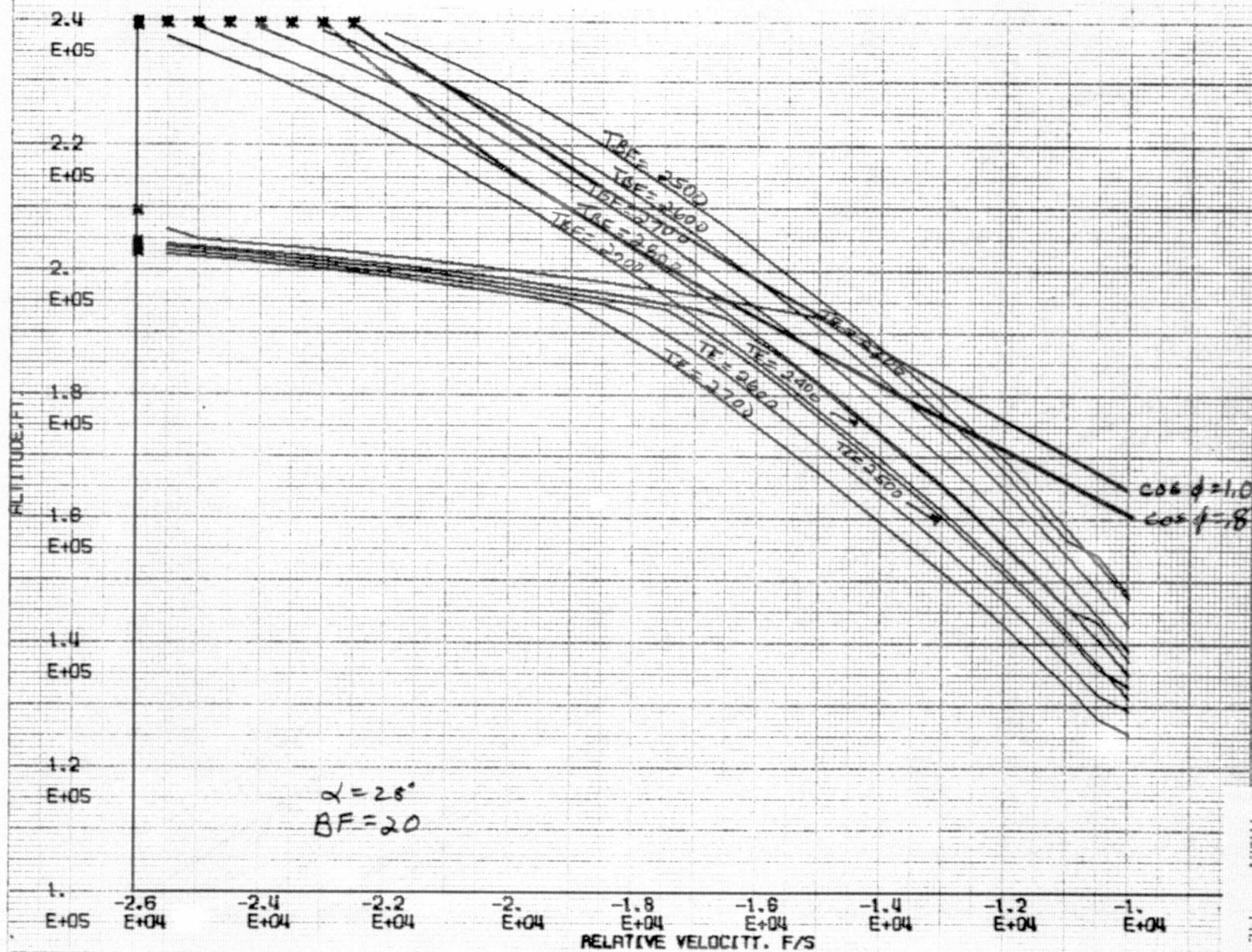




FIGURE 136 ALTITUDE VS. VELOCITY CORRIDOR

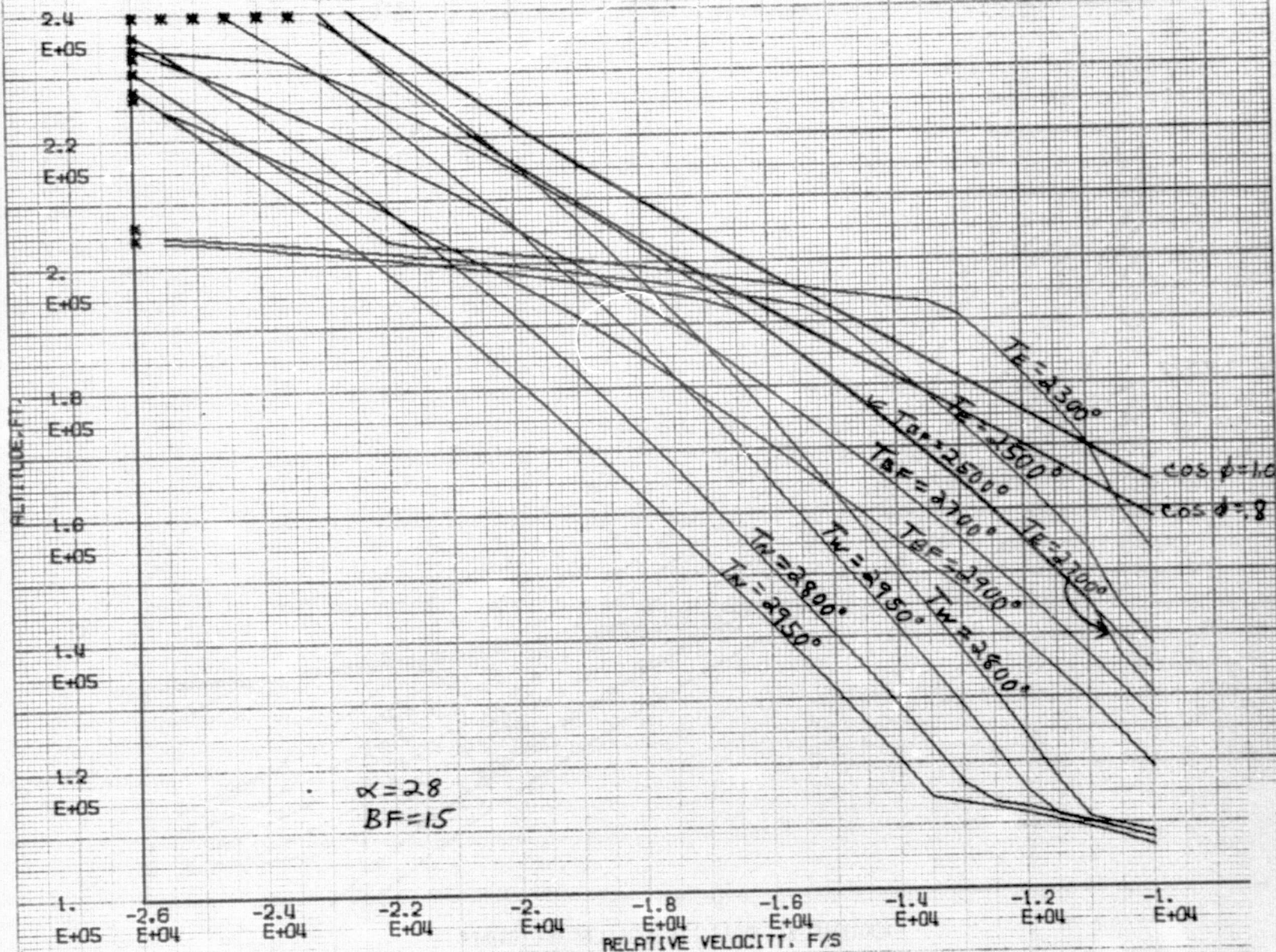


FIGURE 137 ALTITUDE VS. VELOCITY CORRIDOR

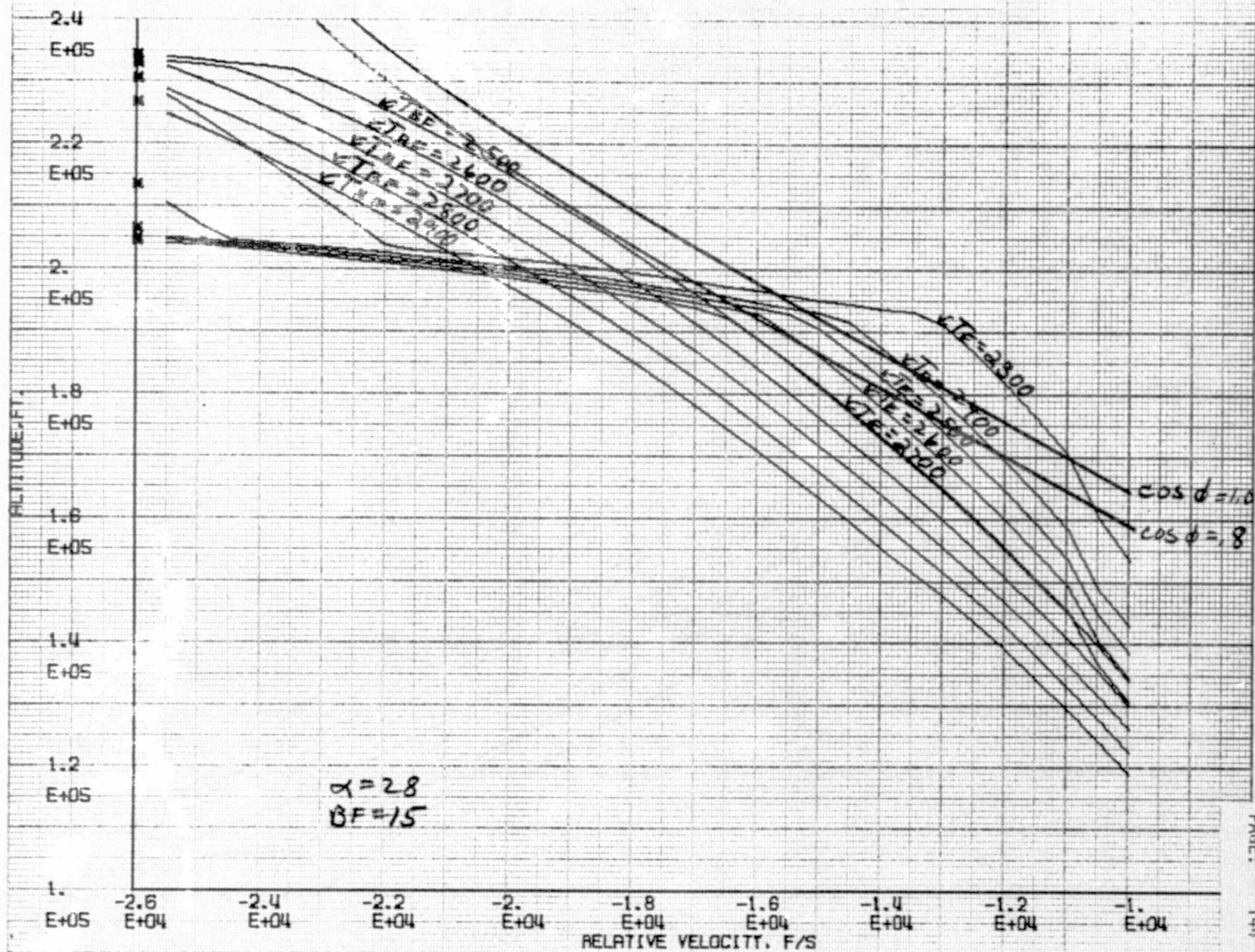




FIGURE 138 ALTITUDE VS. VELOCITY CORRIDOR

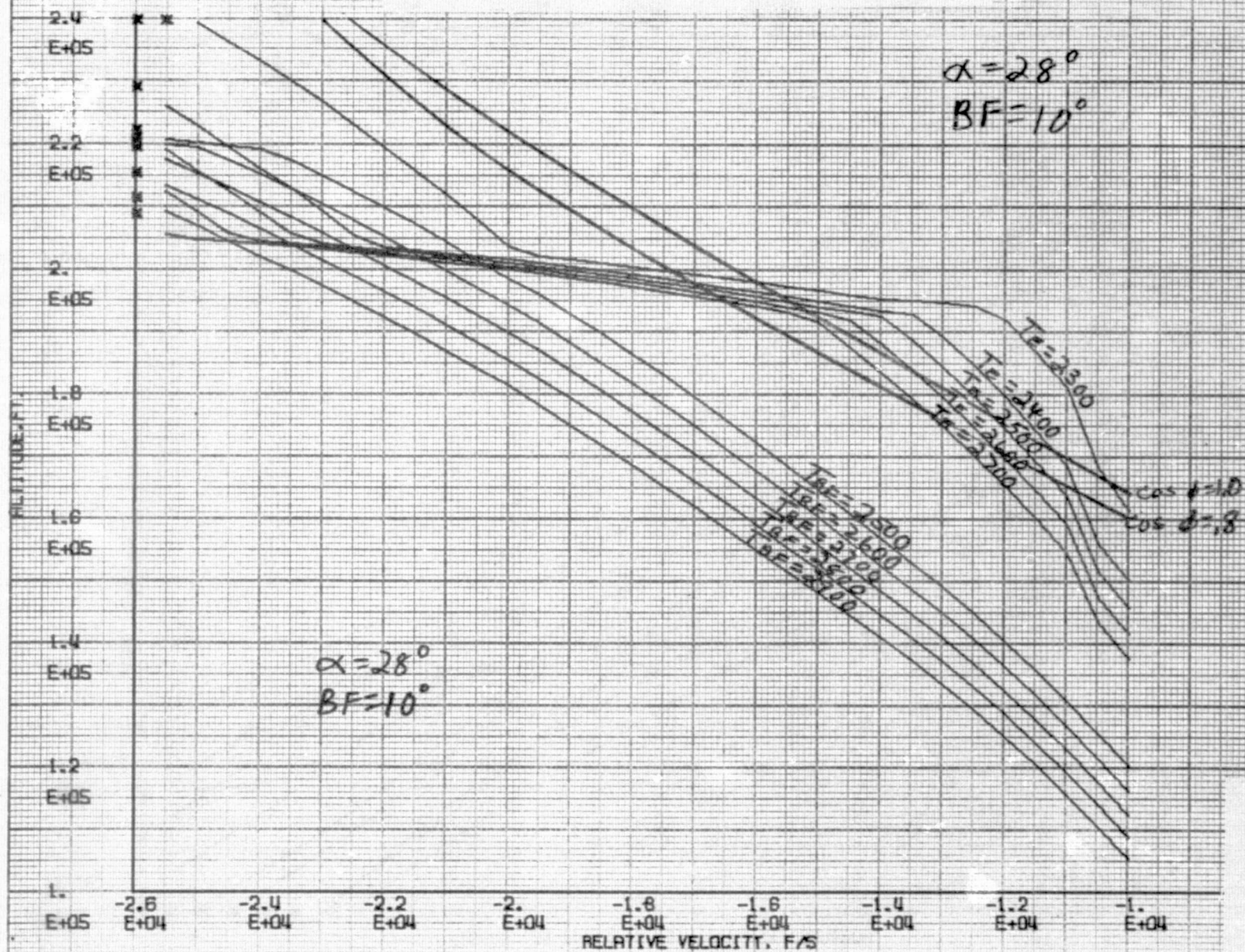


FIGURE 139 ALTITUDE VS. VELOCITY CORRIDOR

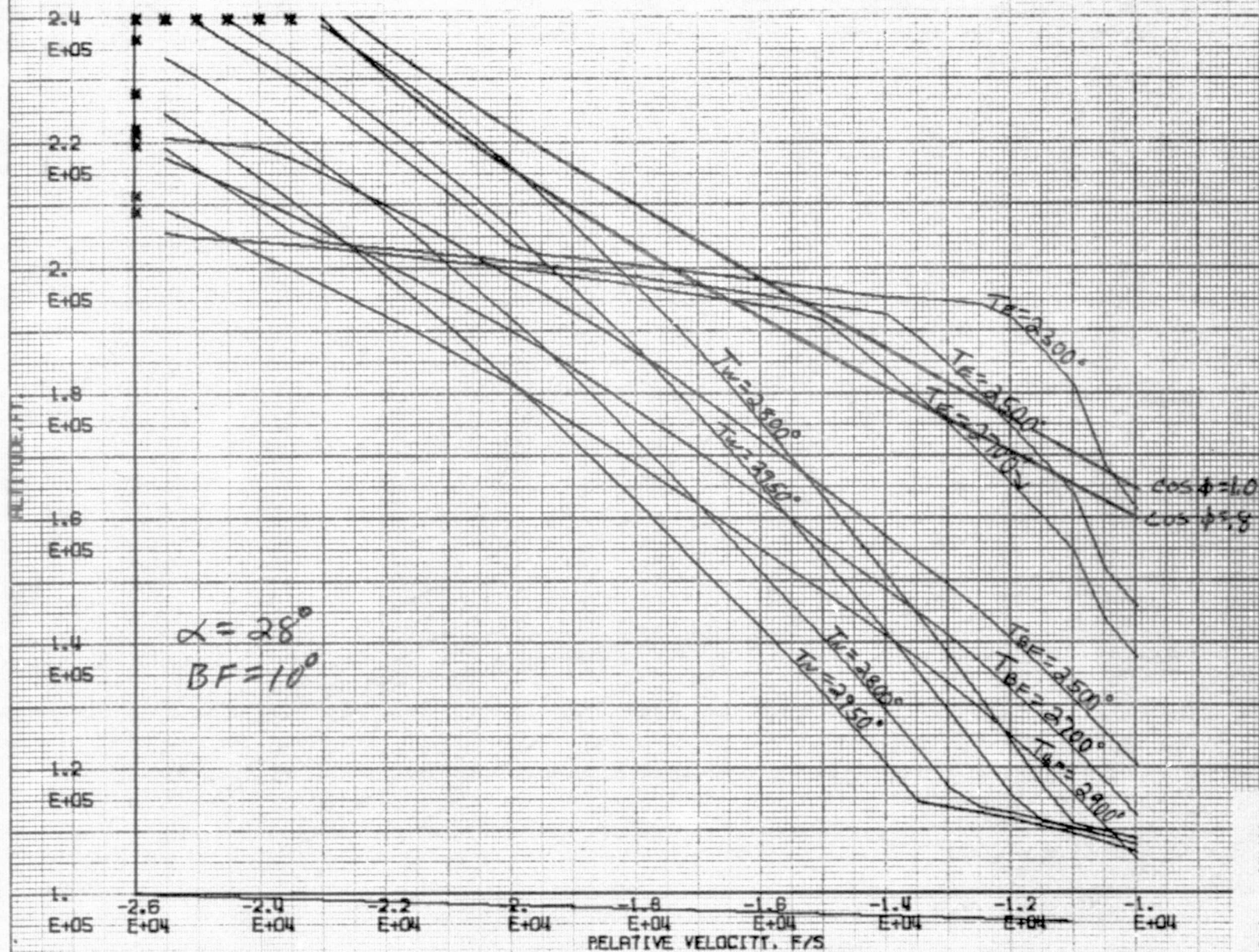




FIGURE 140 ALTITUDE VS. VELOCITY CORRIDOR

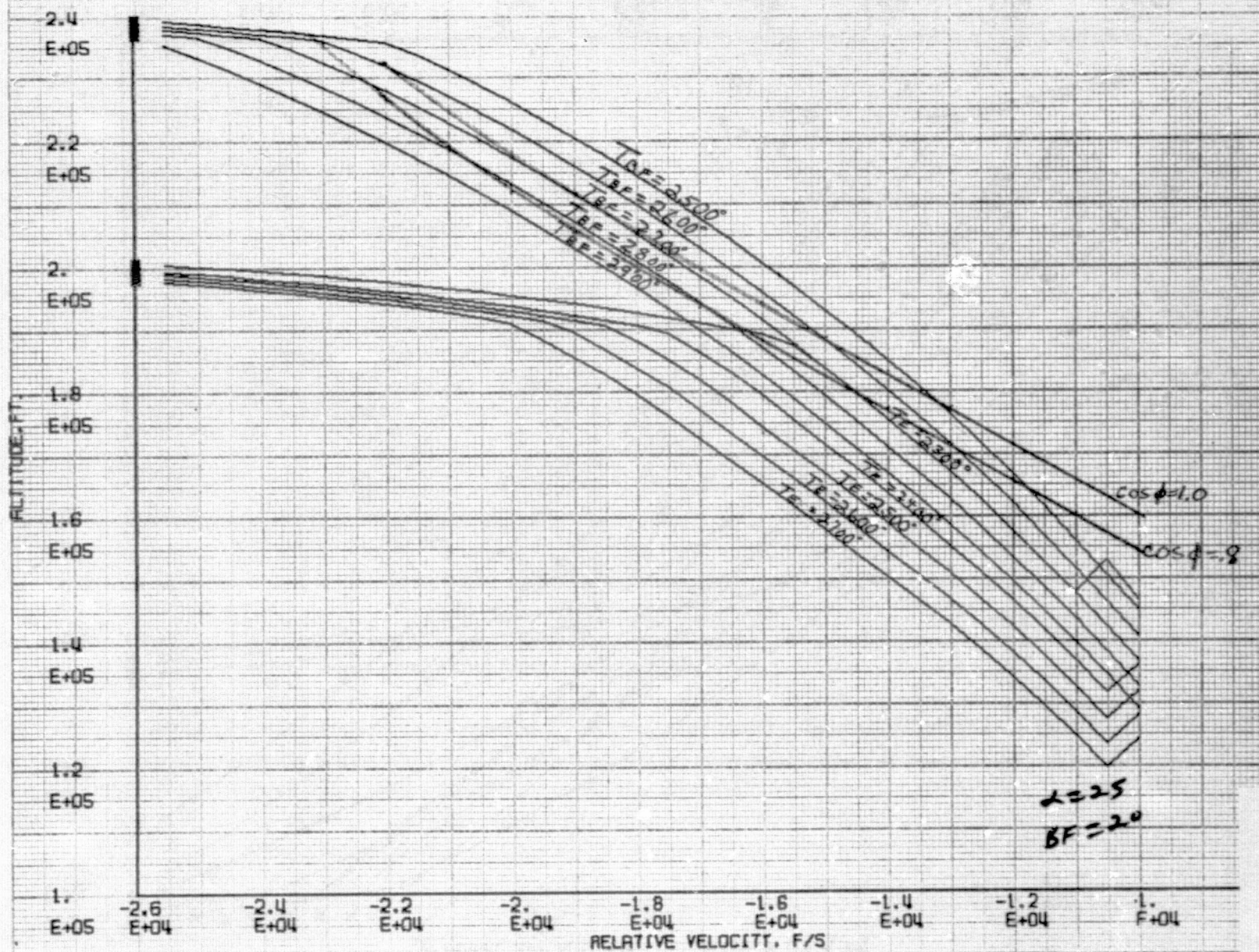






FIGURE 142 ALTITUDE VS. VELOCITY CORRIDOR

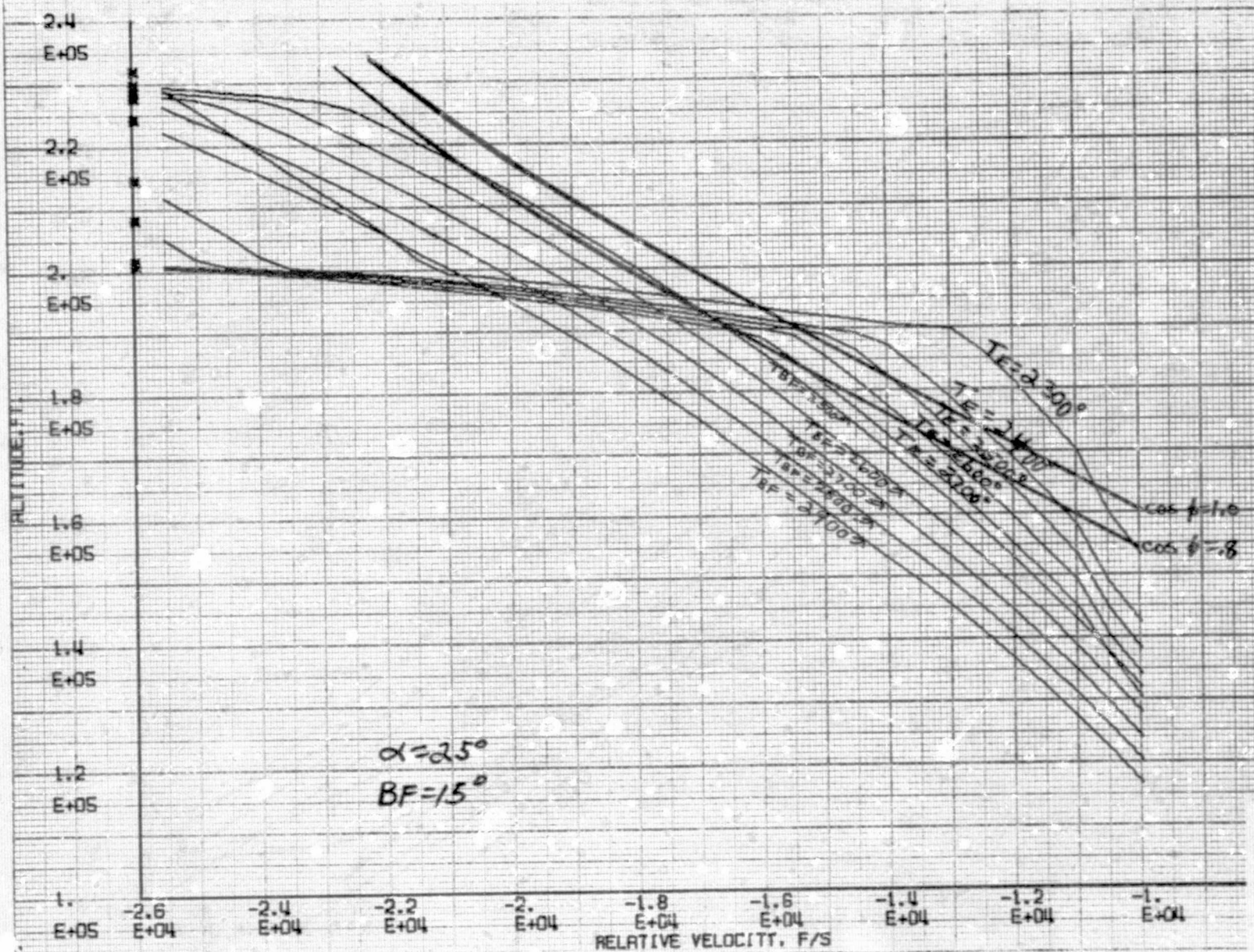


FIGURE 143 ALTITUDE VS. VELOCITY CORRIDOR

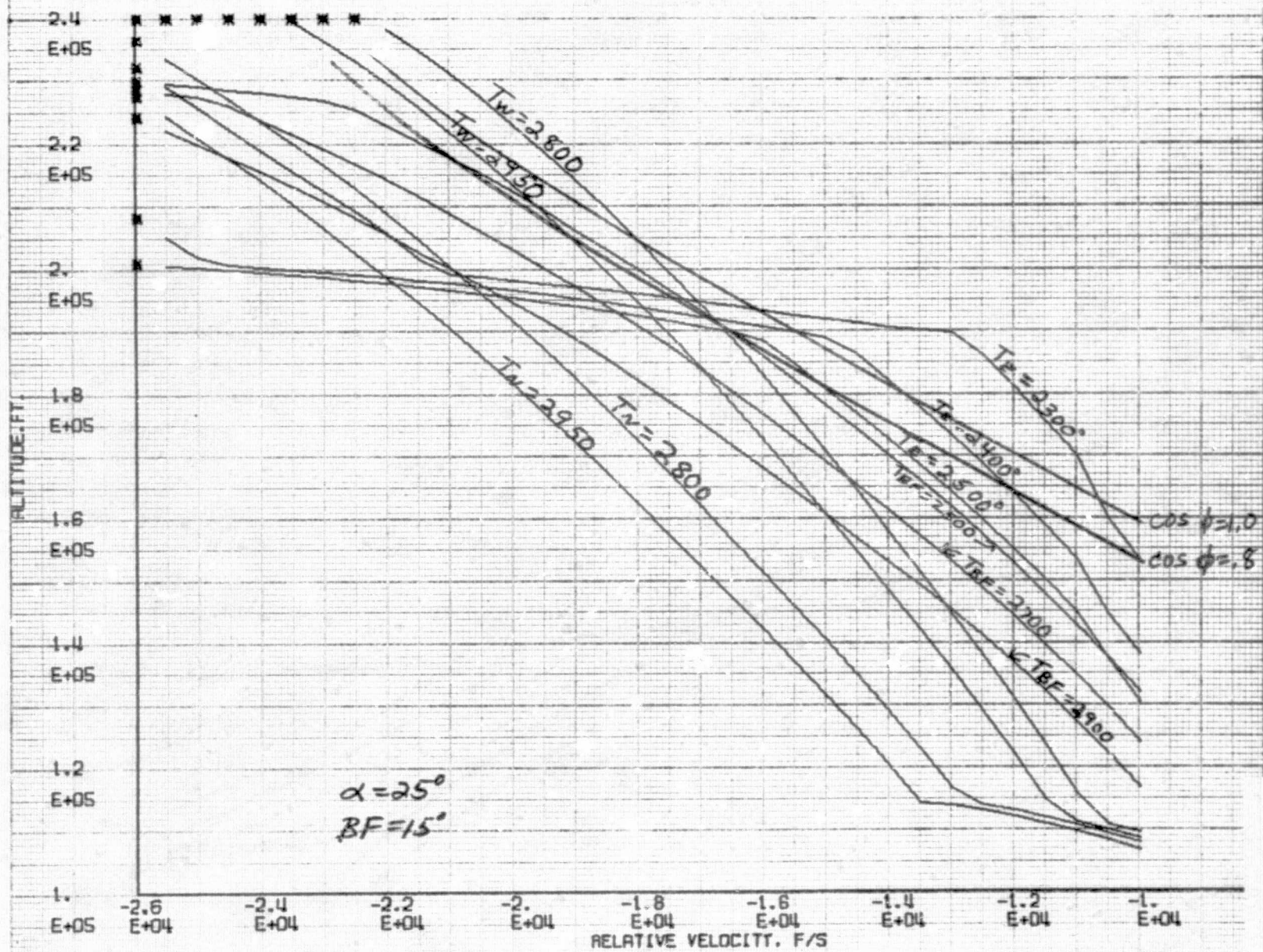




FIGURE 144 ALTITUDE VS. VELOCITY CORRIDOR

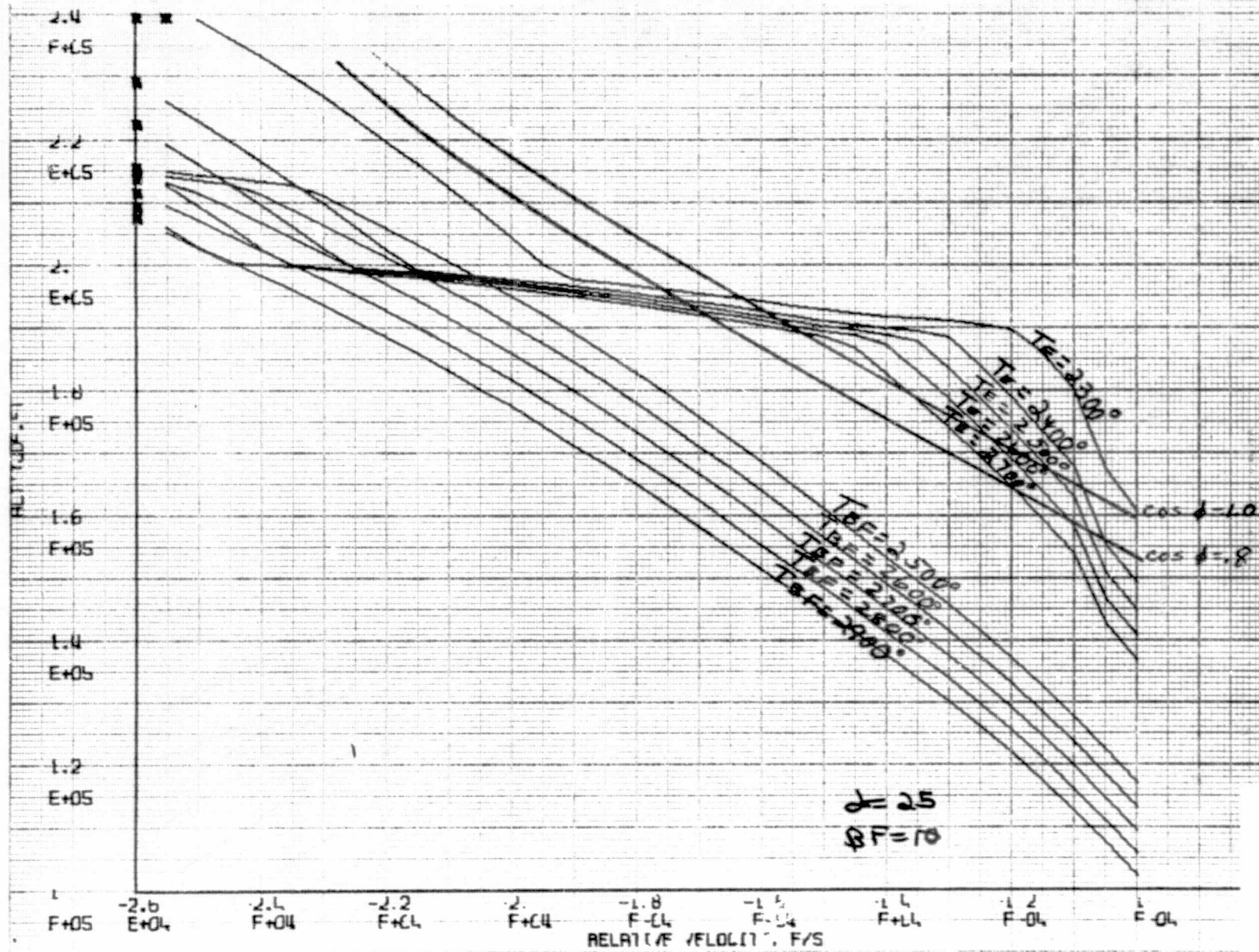
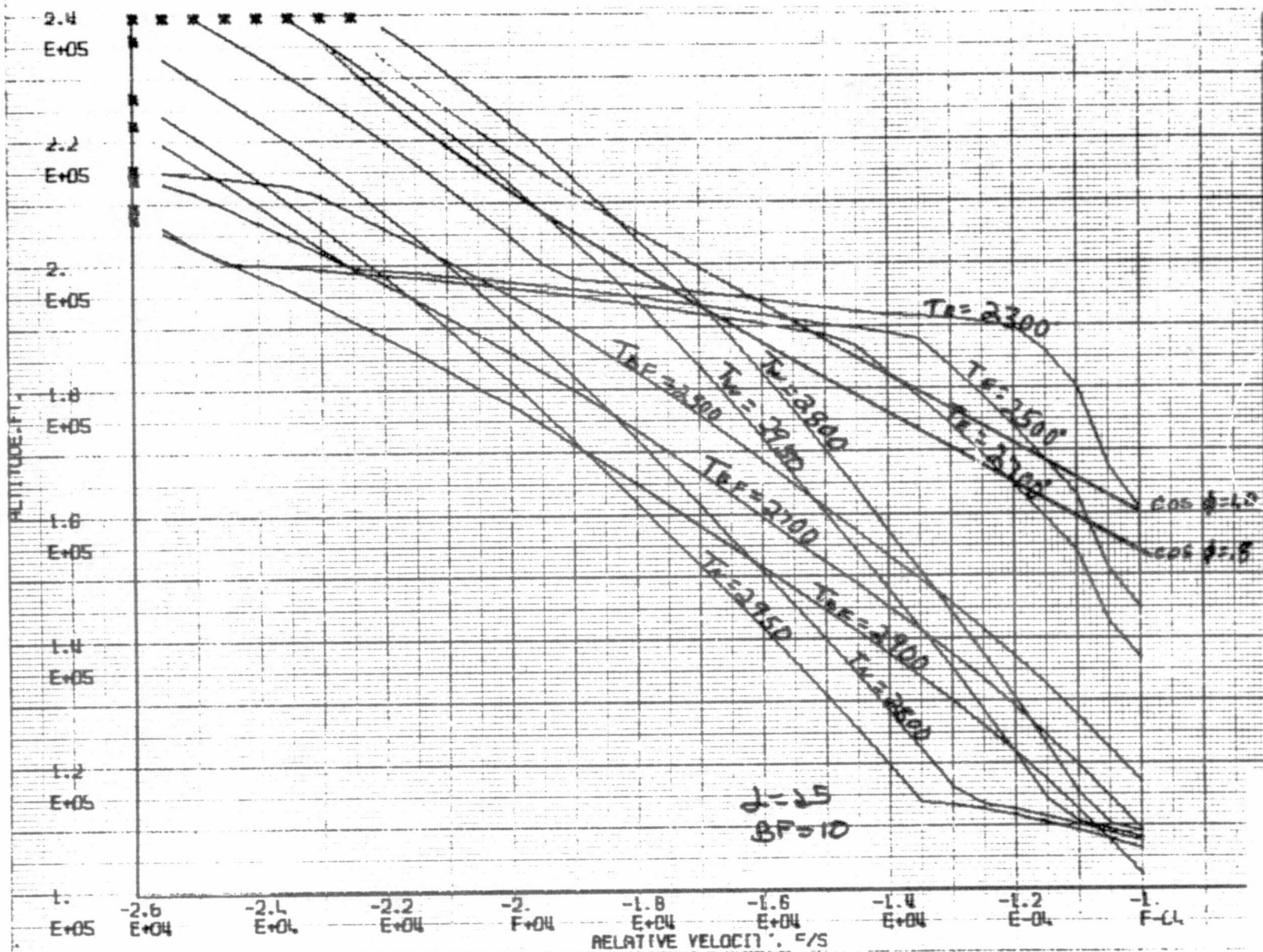


FIGURE 145 ALTITUDE VS. VELOCITY CORRIDOR



D#1 NO.: 1.4-4-8  
 PAGE: 152